This is to certify that the

dissertation entitled

INHIBITORY EFFECTS OF ZINC ON GLUCOCORTICOID - APOPTOSIS IN MOUSE THYMOCYTES

presented by

William George Telford

has been accepted towards fulfillment
of the requirements for

Ph.D. degree in Microbiology

Major professor

Date 6/1/94

INHIBITORY EFFECTS OF ZINC ON GLUCOCORTICOID-INDUCED APOPTOSIS IN MOUSE THYMOCYTES

By

William George Telford

A DISSERTATION

Submitted to
Michigan State University
in partial fulfillment of the requirements
for the degree of

DOCTOR OF PHILOSOPHY

Department of Microbiology

1994

ABSTRACT

INHIBITORY EFFECTS OF ZINC ON GLUCOCORTICOID-INDUCED APOPTOSIS IN MOUSE THYMOCYTES

By

William George Telford

Mouse thymocytes undergo apoptosis or physiological cell death when incubated *in vitro* with physiologically relevant concentrations of glucocorticoids. High concentrations of zinc (500 to 5000 μM) have been previously found to inhibit hormone-induced thymocyte death, and many other types of apoptotic death as well. Although the mechanism by which zinc inhibits apoptotic death has been the subject of considerable speculation, no definitive mechanism or mechanisms have been found to explain this phenomenon. This project investigated an important aspect of hormone-induced cell death as a potential target for zinc, namely the early steps of the glucocorticoid receptor (GR) signal transduction pathway. A flow cytometric assay for apoptotic death was used to confirm that high concentrations of zinc inhibited glucocorticoid-induced apoptosis in mouse thymocytes and to more clearly define the extracellular and intracellular zinc concentration requirements for this inhibition. These concentrations of zinc were subsequently found to inhibit binding of radiolabeled dexamethasone to cytosolic receptor in mouse thymocytes and subsequent translocation of ligand-bound receptor to the nucleus, implicating initial receptor-ligand binding and/or receptor transformation as possible targets of the observed inhibition. *In vitro* studies confirmed that zinc reversibly inhibited GR binding to ligand, and suggested that thiol amino acid residues in the steroid binding domain of the receptor were involved. Taken together, these results indicate that zinc effects of GR signalling at the level of ligand binding represents a valid potential mechanism of apoptotic inhibition in hormone-treated mouse thymocytes.

TABLE OF CONTENTS

LIST OF TABLES

LIST OF FIGURES

Figure 5-1. Presence of thymocytes in the apoptotic region of the PI DNA cell cycle following incubation without (no treatment) or with corticosterone at 1 μM (CS 1 μM) for eight hours. Apoptotic regions are indicated with arrows.

Figure 5-2. Presence of apoptotic thymocytes with reduced forward light scatter following incubation without (no treatment) or with corticosterone at 1 μM (CS 1 μM) for eight hours. Apoptotic cells are indicated by the outlined regions.

Figure 5-3. Electron micrograph of unfixed mouse thymocytes treated with corticosterone at 1 μM for eight hours. Representative apoptotic cells are indicated with arrows.

Figure 5-4. Densitometric tracings from agarose electrophoresis of purified DNA lysates from corticosterone-treated mouse thymocytes, either unsorted (top densitometric trace) or sorted by fluorescence activated cell sorting for G_0/G_1 cells (middle trace) or apoptotic cells (bottom trace) from the subpopulations indicated in the DNA histogram (top illustration) as described in Materials and Methods. Lambda phage HindIII molecular weight markers of 200, 400, 600, 800, 2000, 2300 and 4400 bp markers and fragments are shown.

Figure 5-5. Time-response curves for mouse thymocytes incubated without (open circles) or with corticosterone at 1 μM (closed circles). Percentage apoptotic cells was calculated as the percentage of cells in the apoptotic region of the PI DNA cell cycle. Data is the mean plus or minus standard deviation of duplicate samples (error bars are not visible).

Figure 5-6. Induction of apoptosis in mouse thymocytes by brief treatment with corticosterone at 1 μM. Cells were incubated with corticosterone for indicated periods (30 minutes to 4 hours) followed by removal of steroid and continued incubation to eight hours. Cells were then analyzed for the presence of apoptotic cells by flow cytometry (filled circles). Cell samples incubated with steroid, washed and reincubated with steroid (top dotted line, CS 1 μM) or incubated without steroid, washed and reincubated without steroid (bottom dotted line, No CS) were carried out simultaneously as controls for effects of the washing process on resulting cell death. Data is the mean plus or minus standard deviation of duplicate samples.

Figure 5-7. Corticosterone-induced apoptosis in CD4/CD8 subsets of mouse thymocytes. Fresh thymocytes (no incubation) or thymocytes incubated without (no treatment) or with corticosterone (CS 1 μM), for eight hours were immunophenotypically labeled for CD4 and CD8 expression (FITC and PE respectively), ethanol fixed, stained for cell cycle with DAPI, and flow cytometrically analyzed for all three fluorochromes as described in the text. Top panels show cytograms for FITC-CD4 versus PE-CD8. Arrows mark the division between negative and positive staining for both CD4 and CD8. Negative control fluorescence in fresh thymocytes is illustrated in the upper right corner of the no incubation cytogram. $CD4^+$ and $CD8^+$ subpopulations were then gated into CD8 or CD4 versus DNA content (DAPI) cytograms (middle and bottom rows respectively). Percentage apoptotic cells was then calculated for the total population and $CD4^+CD8^+$, $CD4^+CD8^-$ and $CD4^-CD8^+$ subsets directly from the cytograms based on the percentage

of cells in the apoptotic region of the phenotype-specific cell cycles (marked with arrows as in the top panels). Apoptotic percentages for the total population and three subpopulations are given in Table 5-2. Data is representative of two separate experiments.

Figure 5-8. Corticosterone-induced apoptosis in $\alpha\beta$TCR or CD3ϵ subsets of mouse thymocytes. Thymocytes were incubated without (no treatment) or with corticosterone (CS 1 μM) for eight hours. Cells were then immunophenotypically labeled for either $\alpha\beta$TCR or CD3ϵ (FITC), ethanol-fixed, stained for DNA content with PI as described in the text and flow cytometrically analyzed for both fluorochromes as described in the text. Top and bottom panels show $\alpha\beta$TCR or CD3ϵ expression versus DNA content (PI) cytograms respectively, with corresponding histograms showing distribution of $\alpha\beta$TCR or CD3ϵ expression subsets and DNA content (including the apoptotic region as indicated). Negative control fluorescence in untreated samples is shown in the no treatment phenotypic histograms. Percentage apoptotic cells in the $\alpha\beta TCR^{lo}$ (low), $\alpha\beta TCR^{int}$ (intermediate), $\alpha\beta TCR^{hi}$ (high) and the $CD3\epsilon^{lo}$ and $CD3\epsilon^{hi}$ subsets were calculated directly from marker expression versus DNA content cytograms based on the percentage of cells in the apoptotic region of each phenotype-specific cell cycle (marked with arrows). Apoptotic percentages for the total population and three subpopulations are given in Table 5-3. Data is representative of two experiments.

Figure 6-1. Inhibitory effects of zinc sulfate on corticosterone-induced apoptosis in mouse thymocytes based on internucleosomal DNA fragmentation. Thymocytes were incubated without or with corticosterone at 1 μM in the presence or absence of zinc sulfate heptahydrate at 500 μM for 8 hours. Cells were then lysed followed by DNA extraction. Resulting DNA samples were electrophoresed on 1.8% agarose gels, followed by ethidium bromide staining for detection of DNA fragmentation patterns. **Lane 1**, no incubation; **lane 2**, no treatment for 8 hours; **lane 3**, corticosterone alone at 1 μM for 8 hours; **lane 4**, zinc alone at 500 μM; **lane 5**, corticosterone at 1 μM and zinc at 500 μM for 8 hours; λ, lambda phage HindIII molecular weight markers. Arrow indicates 600 bp fragment.

Figure 6-2. Inhibitory effects of zinc sulfate on corticosterone-induced apoptosis in mouse thymocytes based on reduced flow cytometric PI fluorescence. Untreated thymocytes (no treatment) or thymocytes treated with corticosterone at 1 μM (CS 1 μM) and/or zinc sulfate (Zn 500 μM) were incubated for eight hours followed by fixation, PI staining and flow cytometric PI cell cycle analysis as described in the text. Data is expressed as DNA content histograms. The apoptotic subpopulation is indicated by the bracketed region, with the percentage of apoptotic cells given.

Figure 6-3. Inhibitory effects of zinc sulfate on corticosterone-induced apoptosis in mouse thymocytes based on reduced flow cytometric forward light scatter. Untreated thymocytes (no treatment) or thymocytes treated with corticosterone at 1 μM (CS 1 μM) and/or zinc sulfate (Zn 500 μM) were incubated for eight hours followed by fixation and flow cytometric analysis for forward scatter (cell size) versus side scatter (cell density) as described in the text. Percentages of apoptotic cells are derived from the percentage cells

in the apoptotic region of the PI DNA cell cycle. Data is expressed as forward versus side scatter cytograms. The apoptotic subpopulation is indicated by the outlined region, with the percentage of apoptotic cells given.

Figure 6-4. Inhibitory effects of zinc sulfate on radiation-induced apoptosis in mouse thymocytes based on reduced flow cytometric PI fluorescence. Untreated thymocytes (no treatment) or thymocytes irradiated at 0.5 gray (0.5 Gy) and/or treated with zinc sulfate (Zn 500 μM) were incubated for eight hours followed by fixation, PI staining and flow cytometric PI cell cycle analysis as described in the text. Data is expressed as DNA content histograms. The apoptotic subpopulation is indicated by the bracketed region, with the percentage of apoptotic cells given.

Figure 6-5. Inhibitory effects of zinc sulfate on radiation-induced apoptosis in mouse thymocytes based on reduced flow cytometric forward light scatter. Untreated thymocytes (no treatment) or thymocytes irradiated at 0.5 gray (0.5 Gy) and/or zinc sulfate (Zn 500 μM) were incubated for eight hours followed by fixation and flow cytometric analysis for forward scatter (cell size) versus side scatter (cell density) as described in the text. Percentages of apoptotic cells are derived from the percentage cells in the apoptotic region of the PI DNA cell cycle. Data is expressed as forward versus side scatter cytograms. The apoptotic subpopulation is indicated by the outlined region, with the percentage of apoptotic cells given.

Figure 6-6. Dose-response curve for the inhibitory effects of zinc sulfate on corticosterone-induced apoptosis in mouse thymocytes. Cells were incubated without (open circles) or with corticosterone at 1 μM (closed circles) for eight hours with simultaneous addition of zinc sulfate at the indicated concentration. Percentages of apoptotic cells are derived from the percentage cells in the apoptotic region of the PI DNA cell cycle. Data is expressed as the mean plus or minus standard deviation of duplicate samples.

Figure 6-7. Dose-response curve for the inhibitory effects of zinc chloride on corticosterone-induced apoptosis in mouse thymocytes. Cells were incubated without (open circles) or with corticosterone at 1 μM (closed circles) for eight hours with simultaneous addition of zinc chloride at the indicated concentration. Percentages of apoptotic cells are derived from the percentage cells in the apoptotic region of the PI DNA cell cycle. Data is expressed as the mean plus or minus standard deviation of duplicate samples.

Figure 6-8. Dose-response curves for the effects of zinc sulfate, copper sulfate and nickle sulfate on DEX-induced apoptosis in mouse thymocytes. Cells were incubated without (top panel) or with dexamethasone at 0.1 μM (bottom panel) for eight hours with simultaneous addition of indicated metal salt at the indicated concentrations. Percentages of apoptotic cells are derived from the percentage cells in the apoptotic region of the PI DNA cell cycle. Data is expressed as the mean plus or minus standard deviation of duplicate samples.

Figure 6-9. Standard curve for acetylene/air flame atomic absorption spectroscopy of zinc at 213.9 nm absorption wavelength with deuterium background correction. Concentrations range from 0.02 to 0.2 ppm (μg/ml). Values are expressed as the mean plus or minus standard deviation of triplicate samples.

Figure 6-10. Zinc content of mouse thymocytes incubated without (open circles) or with zinc sulfate at 500 μM (filled circles) for 2, 4 or 8 hours as analyzed by atomic absorption spectroscopy. Data is expressed as the mean plus or minus standard error of μg $Zn/10^9$ cells.

Figure 7-1. *In vivo* cytosolic ^{3}H-DEX binding assay **(left panel)** and nuclear localization assay **(right panel)** showing total (TOTAL, with no unlabeled competitor), non-specific (NON, with a 500-fold excess of unlabeled competitor) and specific (SPEC) ^{3}H-DEX binding for 10^6 cells incubated with ^{3}H-DEX at 50 nM for 60 minutes. Specific binding equals the difference between total and non-specific binding. Data is expressed as the mean plus or minus standard deviation of triplicate samples.

Figure 7-2. GR-specific ^{3}H-DEX binding activity in the mouse thymocyte cytoplasm. Mouse thymocytes were incubated with ^{3}H-DEX, lysed to obtain cytosol and immunoabsorbed with either BUGR2 (anti-GR) or MAR18.5 (negative control) followed by Sepharose-protein A. The Sepharose pellets were then removed and the cytosol counted for ^{3}H. Values are expressed as percentages of total cytoplasmic binding with no immunoabsorption.

Figure 7-3. Western blotting of mouse thymocyte cytosolic GR in comparison with liver cytosolic GR. SEPH-BUGR2 and SEPH-MAR18.5 indicate immunoabsorption with anti-GR and negative control antibodies respectively. Immunoblotting was done with BUGR2 and/or HRP-conjugated sheep-anti-mouse IgG (G-anti-MIg).

Figure 7-4. Effect of zinc preincubation (500 μM for 0, 2 and 4 hour preincubation) on cytosolic ^{3}H-DEX binding in mouse thymocytes. Data is expressed as percentages of specific binding in control samples.

Figure 7-5. Effect of zinc preincubation (4 hours) on cytosolic ^{3}H-DEX binding in mouse thymocytes. Data is expressed as percentages of specific binding in control samples.

Figure 7-6. Effect of zinc preincubation (4 hours) on nuclear localization of ^{3}H-DEX in mouse thymocytes. Data is expressed as percentages of specific binding in control samples.

Figure 8-1. Comparison of total (TOTAL, with no cold competitor), non-specific (NON, with a 500-fold excess of unlabeled DEX as competitor) and specific (SPEC) ^{3}H-DEX binding activity in the DCC absorption (left panel) and DEAE-cellulose filter (right panel) assay in mouse liver cytosol. Specific binding equals the difference between total and non-specific binding. Total protein concentration were one mg per sample. The difference between total and non-specific binding equals specific binding. Data is

Figure 8-12. Effect of zinc on specific ^{3}H-DEX binding activity of crude mouse liver cytosolic GR using DCC absorption assay. Data is expressed as the percentage of specific binding in the no zinc control.

Figure 8-13. Effect of zinc on ^{3}H-DEX binding activity of crude mouse liver cytosolic GR using DEAE-cellulose filter binding assay. Data is expressed as the percentage of specific binding of the control.

Figure 8-14. Western blot of mouse liver cytosolic GR immunoabsorbed from cytosols previously incubated without or with zinc at 100 μM. Samples without (TOTAL) and with 500-fold unlabeled DEX as competitor (NON) are included. Ig indicates immunoglobulin heavy chains.

Figure 8-15. Effect of preincubation with zinc on specific ^{3}H-DEX binding activity of crude mouse liver cytosolic GR using DCC absorption binding assay. Open circles show binding activity with two hour preincubation, filled circles with simultaneous additions. Data is expressed as the percentage of specific binding for the control.

Figure 8-16. Effect of molybdate on zinc-associated ^{3}H-DEX-GR specific binding inhibition using DCC absorption assay. Open circles show binding activity with 30 mM sodium molybdate, filled circles with none. Data is expressed as the percentage of specific binding in the no zinc control.

Figure 8-17. Effect of zinc on preformed ^{3}H-DEX-GR complexes using DCC absorption assay. Data is expressed as the percentage of specific binding for the control.

Figure 8-18. Reversibility of zinc-associated specific ^{3}H-DEX-GR binding inhibition using DCC absorption assay. Open circles show binding activity before removal of zinc, filled circles after removal of zinc by Chelex-100. Data is expressed as the percentage of specific binding in the no zinc control.

Figure 8-19. Reversibility of zinc-associated specific ^{3}H-DEX-GR binding inhibition with 10 mM DTT. Data is expressed as the percentage of specific binding in the no zinc control with 1 mM DTT.

Figure 8-20. Effect of zinc on specific ^{3}H-DEX binding to immunoabsorbed mouse liver cytosolic GR (left panel) compared with crude cytosol (right panel). Data is expressed as the percentage specific binding in the no zinc control.

Figure 8-21. Western blot of immunoabsorbed mouse liver cytosolic GR following incubation without or with zinc at 100 μM. Samples without (TOTAL) and with 500-fold unlabeled competitor (NON) are included. Ig indicates immunoglobulin heavy chains.

Figure 8-22. Effect of zinc on specific ^{3}H-DEX binding to immunoabsorbed mouse thymocyte cytosolic GR (left panel) compared with crude cytosol (right panel). Data is expressed as the percentage of specific binding in the no zinc control.

Figure 8-23. Top panel. Diagram of experimental scheme for determining effect of zinc on ligand-dependent temperature-mediated hsp90 dissociation from GR using hsp90-GR coabsorption and Western blotting. **Bottom panel.** Western blot of GR (upper blot) and coabsorbed hsp90 (lower blot) of BUGR2-immunoabsorbed ligand-bound mouse liver cytosolic GR stabilized at 4°C or transformed at 20°C, without or with zinc at 100 uM. SEPH-BUGR2 and SEPH-MAR18.5 indicate immunoabsorption with BUGR2 or MAR18.5 respectively. AC88 is the monoclonal antibody against hsp90.

Figure 8-24. Top panel. Diagram of experimental scheme for determining effect of zinc on ligand-independent hsp90 association with GR using hsp90-GR coabsorption and Western blotting. **Bottom panel.** Western blot of GR (upper blot) and coabsorbed hsp90 (lower blot) of BUGR2-immunoabsorbed "ligand-free" mouse liver cytosolic GR stabilized at 4°C and treated without or with zinc at 100 μM. SEPH-BUGR2 and SEPH-MAR18.5 indicate immunoabsorption with BUGR2 or MAR18.5 respectively. AC88 is the monoclonal antibody against hsp90.

Figure 8-25. Diagram of experimental scheme for determining effect of zinc on transformed GR binding to isolated thymocyte nuclei.

Figure 8-26. Effect of zinc on transformed GR binding to isolated thymocyte nuclei. Mouse liver cytosol was transformed at 20°C without zinc and incubated with nuclei in the presence of zinc at indicated concentrations. Right-most value is the 4°C ("untransformed" control). Data is expressed as percentages of the transformed no zinc control.

Figure 8-27. Diagram of experimental scheme for determining effect of zinc on temperature-mediated transformation of GR based on binding to isolated nuclei.

Figure 8-28. Effect of zinc on temperature-mediated transformation of GR based on binding to isolated nuclei. Mouse liver cytosol was incubated at 20°C with zinc at the indicated concentrations prior to nuclei addition. Right-most value is a 4°C incubation control ("untransformed"). Data is expressed as percentages of the transformed no zinc control.

Figure 8-29. Diagram of experimental scheme for determining effect of zinc on cold stabilization of untransformed GR based on binding to isolated nuclei.

Figure 8-30. Effect of zinc on cold stabilization of untransformed GR based on binding to isolated nuclei. Mouse liver cytosol was maintained at 4°C with zinc at the indicated concentrations prior to nuclei addition. Right-most value is the 20°C ("transformed") control. Data is expressed as percentages of the transformed no zinc control.

Figure 8-31. Diagram of experimental scheme for determining effect of zinc on molybdate stabilization of untransformed GR based on binding to isolated nuclei.

Figure 8-32. Effect of zinc on molybdate stabilization of untransformed GR based on

binding to isolated nuclei. Mouse liver cytosol was incubated at 20°C with molybdate at 30 mM and zinc at the indicated concentrations prior to nuclei addition. Right-most values are the 20°C ("transformed") and 4°C ("untransformed") controls with no sodium molybdate present. Data is expressed as percentages of the transformed no molybdate/no zinc control.

Figure 8-33. Diagram of experimental scheme for determining effect of zinc on transformation of mouse liver cytosolic GR based on ability to bind radiolabeled GRE-GRE in gel mobility shift assay.

Figure 8-34. Gel mobility shift assay of mouse liver cytosolic GR binding to radiolabeled GRE-GRE.

Figure 8-35. Specific activities of DNA-protein complexes formed in the absence or presence of zinc at 100 μM expressed as the percentage of total radiolabeled GRE-GRE the lane in the gel mobility shift assay in Figure 8-34.

ABBREVIATIONS

AC88	monoclonal mouse-anti-*Achlya ambisexualis* hsp88 antibody
BUGR2	monoclonal mouse-anti-rat GR antibody
CS	corticosterone
DAPI	4'-6-diaminido-2-phenylindole
DCC	dextran coated charcoal
DEX	dexamethasone
DTT	dithiothreitol
ER	estrogen receptor
FACS	fluorescence activated cell sorting
FBS	fetal bovine serum
FBS-DCC	fetal bovine serum, DCC extracted
FITC	fluorescein isothiocyanate
GR	glucocorticoid receptor
GRE	glucocorticoid response element
HDG	HEPES/dithiothreitol/glycerol buffer
HDGM	HEPES/dithiothreitol/glycerol/molybdate buffer
HRP	horseradish peroxidase
hsp	heat shock protein
Ig	immunoglobulin
MAR18.5	monoclonal mouse-anti-rat kappa light chain antibody
2-ME	2-mercaptoethanol
PAGE	polyacrylamide gel electrophoresis
PBS	phosphate buffered saline
PE	phycoerythrin
PI	propidium iodide
PR	progesterone receptor
RPMI	Roswell Park Memorial Institute 1640 culture medium
RU486	mifepristone (GR/PR antagonist)
SDS	sodium lauryl sulfate
TBS	Tris-buffered saline
TTBS	Tris-buffered saline with 0.05% Tween-20

CHAPTER 1: INTRODUCTION

Apoptosis is a unique form of physiological cell death, induced by a variety of biochemical cues and acting to regulate the number and types of cells in many tissues (Kerr *et al*, 1972; Wyllie *et al*, 1980b). Although apoptosis has been studied extensively in a variety of cellular systems, most of the mechanistic work directed at the process of physiological death has been carried out in the cells of the immune system, particularly in the mouse and rat. By far the best studied form of immune cell apoptosis is glucocorticoid-induced apoptosis in mouse thymocytes. When mouse thymocytes are treated with physiological concentrations of glucocorticoids *in vitro*, the majority of cells from a normal thymus undergo apoptosis over a period of several hours (Wyllie, 1980a). Current evidence strongly suggests that this phenomenon may be related to the process of thymic selection *in vivo*, although the functional involvement of glucococorticoids in this important selection process remains poorly understood. Nevertheless, this apoptotic system is currently the best-understood model of apoptotic death, both in the immune system and in mammalian cells in general.

An interesting observation made relatively soon after the initial observation that steroid hormones induced apoptosis in mouse thymocytes was that high concentrations of zinc salts (on the order of 500 to 5000 μM) inhibited cell death when added concurrently with hormone (Cohen and Duke, 1984). This initial observation was soon extended to many cell types both within and outside the immune system, and zinc was found to exert a protective effect in response to a wide variety of additional apoptotic stimuli, including radiation and cytotoxic drugs (reviewed by Zalewski and Forbes, 1993). Although subsequent experiments with crude nuclear lysates and isolated nuclei suggested that zinc might be acting via inhibition of the Ca^{2+}/Mg^{2+}-dependent endonuclease responsible for internucleosomal DNA fragmentation frequently observed to occur during apoptotic death,

this has never been adequately demonstrated in intact cells (Cohen and Duke, 1984; Giannakis *et al*, 1991). Although a number of other potential mechanisms have been proposed, no definitive mechanism has been demonstrated for the inhibitory effects of zinc on apoptotic death.

Identifying the operative mechanism behind this phenomenon is important for several reasons. While the requirements of apoptotic induction (including initial signal transduction events, transcriptional activation and subsequent downstream apoptotic effector mechanisms such as the endonuclease) have become better defined in recent years, much remains obscure. This is largely due to the rapid structural degradation that occurs during apoptotic death, making mechanistic studies difficult. Zinc is very likely blocking one or more critical mechanisms responsible for the initial induction and/or downstream resolution of cell death. Identifying the target or targets of zinc would almost certainly identify importants aspects of the death process.

Secondly, it is gradually becoming clear that zinc plays an important role in the regulation of the mammalian immune system. Zinc is a critical structural and/or catalytic component of over 200 metalloenzymes (Jackson, 1989). Zinc deficiency in rodents and humans results in a considerable loss of both cell-mediated and humoral immune function (DePasquale-Jardieu and Fraker, 1979). This loss of function is thought to be induced through clonal deletion in both the B and T cell compartments, possibly through the induction of physiological death via systemic increases in glucocorticoid levels. Intracellular zinc has been increasingly implicated in the regulation of cellular signal transduction. An example of this is the modulation of protein kinase C, which can be induced by low concentrations of zinc and which has been found to be involved in regulation of both cell proliferation and apoptosis (Csmerely *et al*, 1991) . Zinc is also an important structural component of the so-called "zinc finger" binding domain, necessary for high-affinity DNA binding activity in numerous transcriptional activator

proteins (Freeman, 1992). While the ability of high concentrations of zinc to inhibit apoptotic death may be an *in vitro* artifactual phenomenon, there is a strong possibility that it might also be simulating an actual *in vivo* regulatory event. Identifying the target(s) for zinc inhibition of cell death might therefore shed some light on the *in vivo* role of zinc in immune cell regulation. The importance of identifying the mechanism by which zinc prevents cell death has led to this study, which investigates one possible target for the observed inhibitory effects of zinc on hormone-induced apoptosis, namely the early steps of the glucocorticoid receptor (GR) signal transduction pathway.

The first part of this study (Chapter 5) was aimed at providing more definitive experimental support for a novel flow cytometric method of detecting glucocorticoid-induced apoptosis in mouse thymocytes (Telford *et al*, 1991). This methodology was then applied to confirm earlier observations that high concentrations of zinc inhibited glucocorticoid-induced apoptosis in mouse thymocytes, and to more clearly define the conditions and requirements of this inhibition, including effective concentration, metal specificity and intracellular zinc concentration (Chapter 6). The results of this and other studies suggested that zinc provided more or less "complete" protection from hormone-induced death, indirectly implicating an early signal transduction or transcriptional activation event as a likely target (reviewed in Chapter 3). The glucucorticoid receptor signalling pathway was chosen as a potential mechanism in hormone-induced cell death, and subsequent *in vivo* experiments with mouse thymocytes were carried out to determine whether zinc inhibited cytosolic glucocorticoid receptor-ligand binding, localization of the receptor to the nucleus, or both (Chapter 7). The observation that both these events were inhibited by zinc led to *in vitro* studies in a cell-free receptor system into the effects of zinc on receptor-ligand binding and subsequent events leading to nuclear translocation (Chapter 8). These experiments suggested that zinc prevented *in vivo* receptor signal transduction at the level of initial receptor-ligand binding. Taken together, these studies

strongly supported inhibition of early GR signalling events as a viable mechanism for the inhibitory effects of zinc on hormone-induced apoptotic death in mouse thymocytes.

CHAPTER 2: LITERATURE REVIEW

GLUCOCORTICOID-INDUCED APOPTOSIS IN THE IMMUNE SYSTEM.

Definition of apoptosis. Apoptosis is a unique form of physiological cell death, induced by a variety of biochemical cues and acting to regulate the number and nature of cells in a cellular system (Kerr *et al*, 1972; Wyllie *et al*, 1980b). It is distinct from necrotic death, which is usually accidental and the result of toxic injury. Apoptosis has been generally characterized by the specific stimuli required to induce it (often receptor mediated) followed by rapid chromatin degradation, cytoplasmic condensation, membrane blebbing and eventual removal by phagocytic cells. These events promote the rapid and clean removal of apoptotic cells from a particular tissue, without the bystander death and inflammation associated with necrosis.

Morphological and biochemical characteristics of apoptotic death. The morphological changes associated with thymocyte apoptosis are quite typical of apoptotic death in general and are illustrated in Figure 2-1. The nuclear space in the apoptotic thymocytes has contracted, and the nuclear chromatin has become highly condensed, marginated and associated with the inner nuclear membrane (Wyllie *et al*, 1984). This extensive chromatin degradation is associated with apoptotic death in many cellular systems. One aspect of this degradation is the cleavage of nuclear chromatin at the internucleosomal linker regions, resulting in 200 bp multimer fragments detectable by gel electrophoresis (Figure 2-2).

The cytoplasm also shows considerable condensation, the result of cytoskeletal breakdown mediated by an as-yet unknown mechanism. The plasma membrane also shows a distinctive loss of integrity, and membrane "blebs" are in evidence (Wyllie and

Morris, 1982). Despite the extensive degree of cytoplasmic condensation, intact mitochondria showing no obvious shrinkage or swelling are still visible. Apoptosis is an active, energy-dependent process, with mitochondrial function being one of the last aspects of cell physiology to be affected (Wyllie, 1980b).

Biochemically, apoptosis possesses a number of characteristics that distinguish it from necrosis. Apoptosis has been largely found to be dependent on *de novo* gene expression. In glucocorticoid-induced apoptosis, this has been demonstrated using transcriptional and translational inhibitors such as actinomycin D and cycloheximide, which effectively block apoptotic death (Cohen and Duke, 1984). This reinforces the notion of apoptosis as a physiological process, mediated by inducers of gene expression such as hormones, receptor activation or sublethal doses of radiation. There are examples of gene expression-independent apoptosis, however. (Martin and Cotter, 1993). Low concentrations of toxins that would normally induce necrosis have also been found to induce apoptosis, possibly through the activation of a stress or damage pathway intended to remove injured cells by apoptotic death (Cohen *et al*, 1992).

Induction of apoptosis in the immune system. Much of the work directed at the mechanism of apoptosis has been carried out in the cells of the immune system, particularly in the mouse and rat. Numerous cell types in the immune system are sensitive to many apoptotic stimuli, including hormones (such as glucocorticoids), ionizing radiation, engagement of clonal-specific receptors (such as the T cell receptor [TCR] on T lymphocytes and the immunoglobulin receptor on B lymphocytes) and other immune cell receptors in a more non-specific manner (such as Fas antigen and CD4). The vast number of cells in the immune system and the massive demand for both rapid production of new cells and equally rapid deletion of dysfunctional ones logically suggests that the ability of apoptosis to quickly and cleanly remove cells would be a highly advantageous

mechanism. The need for a stringent selection process during lymphocyte differentiation to eliminate potentially autoreactive T or B cells prior to lymphocyte maturation also suggests the need for apoptosis in immune cell development (reviewed by Golstein *et al*, 1991 and Cohen *et al*, 1992).

As expected, apoptosis has been found to play numerous roles in the development and regulation of the immune system. Deletion of autoreactive thymocytes in the thymus by TCR-mediated positive and negative selection is thought to occur by apoptotic death, and similar mechanisms have been proposed for B cell selection in the bone marrow. It is believed that damaged or senescent lymphocytes in the periphery are removed by apoptotic death, giving a mechanism for rapid turnover of circulating immune cells. Inappropriate activation of apoptotic death or loss of apoptotic control is thought to play a role in many immune-related pathologies. HIV-1 induces apoptosis in $CD4^+$ T lymphocytes through gp120 binding to the CD4 receptor coupled with activation via the TCR, and is believed to be the major cause of $CD4^+$ T cell depletion in this disease. Loss of the ability to undergo normal apoptotic death can result in autoimmune disease as evidenced by lymphoproliferative disorder, the result of a non-functional Fas antigen receptor in T cells through which apoptotic signalling normally occurs. Leukemia, lymphoma and myeloma development are also though to occur when normal cell death mechanisms cannot be triggered (Golstein *et al*, 1991; Cohen *et al*, 1992).

Glucocorticoid-induced apoptosis in the immune system. This remainder of this review will describe a very specific form of apoptotic death in the immune system, namely glucocorticoid-induced apoptosis in mouse immune cells. This system has been a popular model for study of the biochemical mechanisms of apoptotic death, and many of the observations made with it apply to other apoptotic systems as well, both within and outside the immune system. Many aspects of glucocorticoid-associated apoptotic

signalling (such as transcriptional activation, secondary signal transduction and endonuclease activity) may be potential targets for the inhibitory effects of zinc on thymocyte apoptosis. The effects of zinc on these aspects of apoptotic death will be discussed in Chapter 3.

General characteristics. Glucocorticoids are adrenal steroids that mediate their biological effects through binding to the cytoplasmic glucocorticoid receptor, a member of the steroid receptor superfamily (Pratt, 1987). Early observations in adrenalectomized animals, *in vitro* using cultured cell lines and *in vivo* using intravenous or intraperitoneal administration on glucocorticoids demonstrated that glucocorticoids have a deleterious effect on immune tissues (Hofert and White, 1968; Makman *et al*, 1968; Munck and Brinck-Johnson, 1968). Glucocorticoids also showed growth arrest and actual cytolysis in many T-lineage leukemias and cell lines (Yamamoto et al, 1974; Norman and Thompson, 1977; Harmon *et al*, 1979). *In vivo*, administration of pharmacological doses of steroids caused rapid involution of the thymus and the spleen in rodents. In addition, zinc deficiency and other forms of malnutrition in mice, conditions associated with elevations in plasma glucocorticoid levels also cause thymic involution, a condition that can be blocked by adrenalectomy (DePasquale-Jardieu and Fraker, 1979). The deleterious effects of glucocorticoids are also observed in the B lymphocyte repertoire both *in vivo* and *in vitro*, based on the reduced ability of B cells to produce immunoglobulin following stimulation with antigen and the disappearance of certain B cell lineages from the bone marrow in mice injected with steroids (Sabbele *et al*, 1987; Garvy and Fraker, 1991). Although this phenomenon was observed in many experimental systems, the mechanism was unknown.

In a significant paper by Andrew Wyllie (1980a), mouse thymocytes incubated with physiological levels of glucocorticoids underwent a unique form of cell death,

characterized by the cleavage of nuclear chromatin into internucleosomal fragments. Wyllie identified this form of cell death to be a form of apoptosis, which had been previously described in other cell types by Kerr and colleagues (1974). It was then proposed that glucocorticoids might stimulate apoptosis *in vivo*, explaining the immune tissue involution observed in rodents. It was also proposed that glucocorticoids might play a significant role in the regulation of immune tissues.

Distribution and sensitivity of lymphoid cells to glucocorticoids. Mouse thymocytes are the classical model for glucocorticoid-induced apoptosis, and approximately 80% of all thymocytes in a typical mouse thymus will undergo cell death following *in vitro* treatment with glucocorticoids (Wyllie, 1980a). This is shown in Figure 2-3, where mouse thymocytes were incubated with dexamethasone for eight hours and analyzed for apoptotic death by flow cytometry. While the entry of individual thymocytes into apoptosis was very rapid, the entire population died gradually, with all steroid-sensitive cells undergoing apoptosis by approximately ten hours. This has also been demonstrated *in vivo* by administration of glucocorticoids into rats or mice either by injection or pellet implantation, with the kinetics and gradual entry into apoptotic death similar to that observed *in vitro* (Compton and Cidlowski, 1986; Sun *et al*, 1992). Despite the overall high level of sensitivity of mouse thymocytes for steroid treatment, however, a small proportion of steroid-resistant thymocytes were detected in early studies in both rodents and humans, although their nature and phenotype were unknown (Weissman, 1973; Homo *et al*, 1980; Ranelletti *et al*, 1981).

Phenotype-specific analysis of apoptotic death for the CD4/CD8 surface receptors have demonstrated that the $CD4^+CD8^+$ subset is primarily sensitive to glucocorticoids *in vitro*, with lesser degrees of sensitivity in the $CD4^+$ and $CD8^+$ single positive subsets (Lyons *et al*, 1992; Telford *et al*, 1994). This sensitivity has also been demonstrated *in*

vivo using glucocorticoid pellet implantation (K. Dilley, W. Telford and P. Fraker, unpublished observations). *In vitro* studies of steroid-induced apoptosis in $\alpha\beta$TCR/CD3ϵ subsets also suggest that thymocytes bearing low levels of TCR are particularly sensitive to glucocorticoids (Telford *et al*, 1994). Glucocorticoids therefore appear to induce death in the immature, uncommitted $CD4^+CD8^+TCR^{lo}$ thymocyte subset, while the mature, committed single positive lineages are less sensitive.

The lineage specificity of glucocorticoid-induced cell death is similar to that observed for *in vitro* and *in vivo* models of antigen-induced thymic selection in mice. Autoreactive Vβ6-bearing $CD4^+CD8^+$ and $CD4^+CD8^-$ thymocytes from Mls^a mice undergo spontaneous apoptosis *in vitro*, manifested by their absence from the periphery *in vivo* (Robinson and Lees, 1990). Transgenic mouse studies investigating the process of self antigen-induced selection in the thymus suggest that negative and positive selection in the thymus primarily occurs prior to CD4/CD8 single positive expression and increased TCR expression, in immature thymocytes that are predominantly $CD4^+CD8^+\alpha\beta TCR^{lo}$ (Murphy *et al*, 1990; Vasquez *et al*, 1992). This lineage-specificity is similar to that observed for glucocorticoid treatment. Glucocorticoid-induced thymocyte death may therefore bear functional relevance to antigen-induced thymocyte deletion associated with positive and negative selection of T lymphocytes in the thymus (Rothenberg, 1990).

Current data therefore suggests that less mature T-lineage lymphocytes are glucocorticoid-sensitive, while lymphocytes maturing to a certain level of differentiation become glucocorticoid-resistant. Mature resting T-lymphocytes in the peripheral blood and spleen are generally resistant to glucocorticoid-induced apoptosis, although activation through the TCR can induce cell death (so-called activation-induced cell death), indicating that these cells are still capable of undergoing apoptosis (Iwata *et al*, 1993). Studies with transformed mouse T-lineage cell lines also tend to correlate with the lineage-specificity of glucocorticoid-induced cell death. The BW5147.3 and WEHI-7 thymoma lines are both

considered to be immature T lymphocytes, based on their low level of $\alpha\beta$TCR expression. Both of these lines have been found to undergo glucocorticoid-induced cell death, although the occurrence of resistant subclones is frequent, generally the result of receptor mutations. T cell hybridomas formed by fusions of thymomas such as BW5147.3 with mature T cells, including the lines D0-11.10 and BOG8 are also sensitive to glucocorticoids. More mature T cell tumor lines such as S49.1 mouse lymphoma and P1798 mouse lymphosarcoma are now uniformly glucocorticoid-resistant although both were once characterized as sensitive (Thompson, 1991; Vedeckis and Bradshaw, 1983). The human lymphoblastoid cell line CEM-C7 has been shown to be glucocorticoid-sensitive, although numerous steroid-resistant mutants have also been isolated (Harmon *et al*, 1979; Distelhorst, 1988; Alnemeri and Litwack, 1990; Yuh and Harmon, 1989; Bansal *et al*, 1991). Nevertheless, the mechanisms associated with sensitivity and resistance in T cell lines is unexplained, and may be unrelated to relevant factors in normal cells.

These results therefore indirectly suggest that T lymphocyte differentiation is critical to glucocorticoid sensitivity, and that activation of T cells to the mature resting state may be antagonistic to steroid-induced cell death. To test this more directly, thymocytes and T cell hybridomas have been treated simultaneously *in vitro* with glucocorticoids and T cell activating agents, including immobilized anti-CD3 antibodies or ionomycin and PMA. Restricted concentrations of anti-CD3 can prevent glucocorticoid-induced apoptosis in thymocytes (Cairns *et al*, 1993; Iwata *et al*, 1993). These results suggest an *in vivo* model where successful engagement of the thymocyte TCR at a very specific affinity during thymic selection might "rescue" a thymocyte from steroid-induced death, allowing it to mature. Studies with T cell hybridomas also show glucocorticoid resistance upon activation with either anti-CD3 antibody, ionomycin and PMA or cyclosporin A, further suggesting that T lymphocyte differentiation and activation

are antagonistic to glucocorticoid-induced cell death (Zacharchuk *et al*, 1990; Iwata *et al*, 1993). Mature T helper cells and T cell hybridomas can also be "rescued" from glucocorticoid-induced apoptosis by IL-4 and IL-2 treatment, further suggesting that steroid sensitivity is related to level of lymphoid differentiation (Fernandez-Ruiz *et al*, 1989; Nieto and Lopez-Rivas, 1989; Zubiaga *et al*, 1992). These results may therefore suggest a reasonable model for the role of glucocorticoids in thymic selection, where thymocytes not positively selected by receptor engagement are deleted through the GR pathway. Positive selection also presumably primes the cell for the process of activation-induced cell death frequently observed in mature lymphocytes but not occurring in immature cells, making for two mutually exclusive death pathways (Russell *et al*, 1991; Iseki *et al*, 1991).

Glucocorticoid sensitivity in the B lymphocyte lineage bears striking teleological resemblance to that observed for T cells, suggesting that steroids may play a similar role in B cell selection. Garvy and colleagues have found that glucocorticoids induce apoptosis in $B220^+$ bone marrow lymphocytes consistently across the IgM^-IgD^-, IgM^+IgD^- and IgM^+IgD^+ compartments both *in vitro* and *in vivo* using glucocorticoid pellet implantation, indicating that both immature and resting mature B lymphocytes are glucocorticoid-sensitive (Garvy *et al*, 1993; Garvy *et al*, 1994). Splenic B cells bearing membrane IgM but not IgG are also glucocorticoid-sensitive. IgG-positive B lymphocytes are uniformly steroid-resistant, however, indicating that B cell activation coupled with an γ class switch is antagonistic to glucocorticoid-induced cell death (W.G. Telford and P.J. Fraker, unpublished observations). Mouse Peyers patch B cells expressing IgA are also glucocorticoid-resistant, although they are still capable of undergoing apoptosis when treated with protein synthesis inhibitors (Dr. Jim Pestka, personal communication). Immature and mature resting B lymphocytes therefore appear to be steroid-sensitive, while further differentiation/activation confers resistance.

As with T cells, some transformed B cell data supports these observations. B-chronic lymphocytic leukemia (B-CLL) cells taken from human patients, thought to represent B lymphocytes at an intermediate level of differentiation are sensitive to hydrocortisone and methylprednisolone (Galili *et al*, 1982; McConkey *et al*, 1991; Alnemri and Litwack, 1993). This sensitivity can be reversed both *in vivo* and *in vitro* with IL-4 treatment, also suggesting that glucocorticoid sensitivity is related to the level of cell differentiation and proliferation.

Although studies in glucocorticoid-induced apoptosis in myeloid cells are fewer in number, *in vitro* treatment of both mouse macrophages and human HL-60 promyelocytic leukemia cells with steroids do not result in apoptosis, although they can be induced to die by drug treatment (Waring *et al*, 1989; Martin and Cotter, 1993). Certain human myelomas are sensitive to glucocorticoid treatment, although this varies widely from patient to patient (Gomo *et al*, 1989). Some myeloid cells may therefore be intrinsically less sensitive to glucocorticoid-induced cell death.

Biochemistry. The biochemical aspects of glucocorticoid-induced apoptosis include the activation requirements of the glucocorticoid receptor (GR) activation pathway, any gene expression induced by the GR that is associated with apoptotic death, secondary signal transduction events necessary for apoptotic induction, and the actual mediators of cell death such as nucleases, proteases, etc. that are synthesized or induced. The mechanisms of glucocorticoid-induced apoptosis in the immune system have been largely elucidated in the mouse thymocyte system. Nevertheless, most of the mechanistic aspects of thymocyte apoptosis have been found to be representative of the mouse immune system as a whole, and frequently the human immune system as well. Many of the mechanisms described in this chapter may also be targets for the inhibitory effects of zinc, an issue dealt with in Chapter 3.

Glucocorticoid receptor signalling pathway. Successful GR signal transduction is clearly required for steroid-induced apoptotic death. As described in more detail in Chapter 4, the glucocorticoid receptor (GR) is characterized by its particularly extreme degree of hormone dependence. Receptor activation therefore requires hormone binding to the cytoplasmic holoreceptor. Once hormone is bound, the receptor translocates to the nucleus. Following translocation the hsp90 homodimer and associated proteins dissociate from the core receptor protein, derepressing both the nuclear localization and DNA binding domains. The receptor can now enter the nucleus and bind to glucocorticoid response elements (GREs) followed by transcription of steroid-inducible genes (reviewed by Pratt, 1987; Pratt, 1992).

All the steps of the classical GR signalling pathway are required for steroid-induced cell death. Glucocorticoid antagonists such as RU 38486 and high concentrations of progesterone inhibit glucocorticoid-induced apoptosis in mouse thymocytes *in vitro*, demonstrating a clear need for successful ligand binding (Compton and Cidlowski, 1986; Telford *et al*, 1991).

Generally speaking, glucocorticoid resistance has been found to be a function of defects in receptor structure and function, and not of receptor number (Yamamoto *et al*, 1977; Gomo *et al*, 1990). Resistance to glucocorticoids has also been found to be unrelated to hsp90 expression levels (Norton and Latchman, 1989). The relationship between GR structure-function and apoptosis was originally demonstrated in glucocorticoid-resistant variants that accumulate in cultures of mouse lymphoma cell lines, with more precise characterization by transfection studies as the functional map of the GR has become more detailed. Glucocorticoid-resistant clones of S49.1 and WEHI-7 lymphomas contain GRs that are unable to translocate to the nucleus (termed nt$^-$ mutants)(Gehring *et al*, 1987). These receptors contain a variety of defects ranging from

large truncations to deletions and substitutions altering only a single residue. N-terminal truncations (the region upstream of the DNA binding and steroid binding domains, to which no clear function has been assigned) results in complete inhibition of cytolysis. Some point mutations in the nuclear localization and steroid binding domains, including the signal transducing domain (the proposed site of hsp90 binding) also result in partial or complete inhibition of steroid-induced cell death. Deletions in the DNA binding domain completely abolish sensitivity to glucocorticoids.

The requirements for receptor DNA binding were further delineated by transfection of GR fragment genes into GR-negative CEM-C7 cells. These studies indicated that at least one and a half zinc fingers (with an absolute requirement for the N-terminal finger) are required for steroid-induced cytolysis (Nazareth *et al*, 1991; Thompson *et al*, 1992). Transfection of GRs containing mutations in the N-terminal modulating domain have no effect on induction of apoptosis. Truncation of the steroid binding domain causes apoptosis even in the absence of steroid, indicating that the receptor is no longer under ligand control and induces gene expression constitutively.

Inhibition of glucocorticoid-induced apoptosis by transcriptional and translational inhibitors such as actinomycin D and cycloheximide indicate that steroid-associated gene activation is also required for cell death (Cohen and Duke, 1984). Virtually all aspects of the classical GR signalling pathway are therefore required for hormone-induced apoptosis. While this may appear to be obvious, the recent finding that a membrane-associated GR may also be involved in cellular signalling makes defining the requirement for cytoplasm-to nuclear GR signalling important. Recent studies with S49.1 lymphomas suggest that these cells may possess membrane receptors, and that they may also be involved in steroid-mediated cytolysis (Gametchu *et al*, 1991).

Intracellular signal transduction. Although steroid-associated gene expression is clearly

required for cell death, secondary signalling events normally associated with lymphocyte activation have also been found to be needed for successful activation of steroid-induced apoptosis.

An increase in intracellular calcium levels is an event frequently associated with apoptotic death. The role of calcium in glucocorticoid-induced apoptosis is murky, however, and the subject of many conflicting reports. Early studies (made prior to the precise definition of apoptotic death) suggested that glucocorticoid-induced death in rat thymocytes did not require calcium uptake from extracellular sources, based on the absence of effect of chelators such as EDTA (Kaiser and Edelman, 1977). More recent studies by McConkey and colleagues, however, demonstrated that extracellular chelators such as EGTA and modulators of intracellular calcium such as calmidazolium (a calmodulin inhibitor) and quin-2 (an intracellular chelator) inhibited mouse thymocyte apoptosis induced by glucocorticoids. Glucocorticoids were also found to induce a small but sustained increase in intracellular calcium in mouse thymocytes by fura-2 fluorescent chelator analysis (McConkey *et al*, 1989b). Glucocorticoid-induced calcium flux was blocked by cycloheximide, suggesting that a *de novo* gene product was involved.

More recent studies, however, have failed to find a requirement for either intracellular or extracellular calcium flux in glucocorticoid-induced apoptosis in mouse and rat thymocytes and human leukemia cell lines based on the same inhibitor criterion as the earlier studies (Alnemri and Litwack, 1990; Bansal *et al*, 1990; Iwata et al, 1993). The requirement of calcium flux, while undisputed in other apoptotic systems, therefore remains uncertain for glucocorticoids.

Protein kinase C activity has been repeatedly found to be involved in the regulation of glucocorticoid-induced apoptosis, although also with conflicting results. Protein kinase C is activated through binding to 1,2-diacylglycerol (DAG), a breakdown product of phosphatidylinositol diphosphate (PIP_2). Phorbol esters such as PMA also bind to and

induce a sustained activation of PKC. PMA can inhibit calcium ionophore-induced apoptosis, and has also been found to inhibit glucocorticoid-induced cell death in mouse thymocytes (McConkey *et al*, 1989; Tadakuma *et al*, 1990. Treatment of thymocytes with Con A or IL-1, both of which induce PKC activation, also inhibits calcium ionophore and glucocorticoid-induced apoptosis (McConkey *et al*, 1989b; McConkey *et al*, 1990a). Activation of PKC may therefore be associated with the inhibition of apoptosis. However, other laboratories have reported that PKC may actually induce apoptosis under some circumstances, since PKC inhibitors such as H-7 can block cell death (Ojeda *et al*, 1990). PKC has been found to phosphorylate GR in lymphoid cells, and also regulates the activity of other transcriptional activators such as AP-1 that have also been implicated in the modulation of apoptotic death (Walker *et al*, 1993).

Elevation of cAMP and subsequent activation of protein kinase A (PKA) is also associated with glucocorticoid-induced apoptosis in mouse and rat thymocytes and in T cell leukemias such as CEM-C7 and WEHI-7. Inducers of cAMP such as E-prostaglandins and the adenosine analog NECA can induce thymocyte apoptosis (McConkey *et al*, 1990c). Agents that stimulate cAMP production also act synergistically with glucocorticoids to induce apoptosis in mouse thymocytes, and lower the threshold dose of steroid required to induce cell death, suggesting that a steroid-dependent increase in cAMP levels may be a necessary signal in glucocorticoid-induced cell death (Durant, 1986; McConkey *et al*, 1993). GR receptor levels in thymocytes do not increase substantially with cAMP activation as has been observed for other cell types, however, suggesting that receptor upregulation is not a likely mechanism (Gruol *et al*, 1986; McConkey *et al*, 1993). Interestingly, cell death induced by the cAMP upregulating agent NECA can be blocked by the glucocorticoid antagonist RU486, suggesting that cAMP may be regulating GR posttranslationally and promoting GR-mediated cell death. Several S49.1 mutants which show increased resistance to low concentrations of glucocorticoids

but contains a normal GR have been found to possess defects in cAMP upregulation resulting in low levels of PKA activity. Stimulation of PKA activity in these cells with cAMP analogs restores glucocorticoid sensitivity, possibly by increasing receptor affinity for ligand (Gruol and Bourgeois, 1987; Gruol *et al*, 1989a). Forskolin, a cAMP stimulator, also increases receptor affinity for ligand and increases steroid sensitivity in S49.1 and W7 leukemia cell lines (Gruol *et al*, 1989b). GR and cAMP are therefore probably acting together to induce receptor-associated transcription and subsequent cell death.

Gene expression. The activated, nuclear GR is a transcriptional activator, and the requirement for *de novo* transcription and translation in steroid-induced apoptosis indicates a requirement for gene expression. Glucocorticoid treatment has been found to induce a spectrum of both new mRNAs and new proteins in thymocytes and leukemia lines relatively early in the death process (Voris and Young, 1981; Colbert and Young, 1986; Van den Bogert *et al*, 1989; Domashenko *et al*, 1990). Several groups have undertaken the search for apoptosis-specific genes and gene products, induced both by glucocorticoids and other stimuli. Most of these studies have been carried out using subtractive hybridization or subtractive screening techniques, using libraries constructed from both unstimulated and stimulated cells (Goldstone and Lavin, 1993; Tenniswood *et al*, 1994). While the rapid RNA degradation associated with apoptotic death has complicated the isolation of intact message from treated cells (Owens *et al*, 1991), several alterations in gene expression are consistently associated with apoptotic death, and more specifically glucocorticoid-induced death.

Early studies in rat thymocytes indicated that between five and nine early proteins appear following glucocorticoid treatment (Voris and Young, 1981; Colbert and Young, 1986). Genes found to increase expression levels in lymphoid cells following

glucocorticoid treatment include c-*jun* (Goldstone and Lavin, 1993), calmodulin (Dowd *et al*, 1991), and sulfonated glycoprotein-2 (Bettuzzi *et al*, 1991). Lavin and colleagues have isolated message encoding a β-galactoside binding protein (HL-14) and mitochondrial cytochrome oxidase subunit 1 from CEM-C7 leukemia cells treated with dexamethasone (Goldstone and Lavin, 1991) as well as mRNAS encoding two unique proteins. Osborne and colleagues have isolated a gene designated *apt-4* by subtractive screening that is associated with steroid-induced death and also induced during irradiation and TCR-activated apoptosis. It bears no homology to any known proteins (Dr. B. Osborne, personal communication). Cohen and colleagues have isolated nine apoptosis-associated mRNAs from glucocorticoid-treated rat thymocytes by subtractive hybridization including a transmembrane protein and a zinc finger protein (Owens *et al*, 1991). Harrigan and colleagues have isolated eleven upregulated mRNAs from T lymphocytes treated with cAMP stimulating agents and dexamethasone, including Tcl-30, a protein that may associate with G-proteins (Harrigan et al, 1989). Tissue transglutaminases are also expressed in thymocytes treated with dexamethasone (Fesus *et al*, 1987). These proteins crosslink plasma membranes and may be involved in the "blebbing" process.

Studies by Eastman-Reks and Vedeckis (1987) examined the levels of c-*myb*, c-*myc* and c-Ki-*ras* in WEHI-7 lymphoma cells and mouse thymocytes. Levels of all three oncogenes were found to decrease in both cell types during glucocorticoid-induced apoptotic death. Oncogene levels in a glucocorticoid-resistant WEHI-7 subclone were not found to drop, indicating a dependence on steroid-mediated gene expression. C-*myc* levels were also depressed in CEM-C7 leukemia cells by dexamethasone treatment (Yuh and Thompson, 1989; Thompson *et al*, 1992). Interestingly, c-*myc* downregulation appears to be entirely dependent on the presence of a completely functional GR; cell lines with transfected GR mutants do not downregulate c-*myc*. Transfection of c-*myc* into

CEM-C7 cells under control of a non-GR-inducible promoter confers glucocorticoid resistance, while subsequent treatment with c-*myc* antisense RNA restores sensitivity (Thompson *et al*, 1992). Glucocorticoid-associated gene expression in lymphocytes may therefore differ from other apoptotic systems such as the prostate, liver and epithelium which generally show increases in c-*myc* and other protooncogenes (Buttyan *et al*, 1988). AP-1, a transcription factor composed of c-*fos*/c-*jun* or c-*jun*/c-*jun* dimers, is also downregulated in T lymphocytes upon dexamethasone treatment (Walker *et al*, 1993). Upregulation of Ap-1 by treatment with IL-2 is thought to be one mechanism of conferred resistance to glucocorticoid-induced apoptotic death.

Recent studies of apoptosis have demonstrated the presence of *bcl-2*, a protooncogene associated with the inner mitochrondrial membrane (Hockenbery *et al*, 1990). Expression or overexpression of *bcl-2* inhibits apoptosis in a variety of cell types from a variety of stimuli. Although not specifically upregulated by glucocorticoids, expression of *bcl-2* can inhibit glucocorticoid-induced apoptosis both in thymocytes and in pre-B lymphocytes (Sentman *et al*, 1991; Alnemeri *et al*, 1992). Overexpression of *bcl-2* in transgenic mice exerts an even greater inhibitory effect on glucocorticoid-induced apoptosis. *Bcl-2* is though to act as an mitochrondrial antioxidant, preventing free radical formation and subsequent cell death (Hockenbery *et al*, 1993).

Downstream mediators of apoptosis. Glucocorticoid-associated gene expression and secondary signal transduction both serve to synthesize or posttranslationally activate enzymes that actually cause the biochemical and morphological changes of apoptosis. Early studies characterized a number of events induced by glucocorticoids in an attempt to isolate the downstream mediators of apoptotic death. DNA, RNA and protein degradation were all observed to occur in steroid-treated rat thymocytes, suggesting the

activation of nucleases and proteases early in the death process (Wyllie, 1980; MacDonald *et al*, 1980; Cidlowski, 1982; MacDonald and Cidlowski, 1982). Glucose uptake and metabolism and hexose transport were also found to be depressed during thymocyte apoptosis, implicating changes in energy utilization as another potential mediator of apoptosis (Zyskowski and Munck, 1979; Munck and Crabtree, 1981).

Probably the most visible of these downstream mediators is the Ca^{2+}/Mg^{2+}-dependent endogenous endonuclease, which cleaves nuclear chromatin at internucleosomal linker regions into the characteristic DNA "ladder" pattern. Early studies with crude endonuclease preparations and with isolated nuclei demonstrated the presence of an endogenous endonuclease dependent on calcium and magnesium or manganese (Ishida *et al*, 1974; Cohen and Duke, 1984). Zinc was found to inhibit endonuclease activity both in crude preparations and in nuclei (Cohen and Duke, 1984). Later attempts to purify the endonuclease to homogeneity were largely unsuccessful, possibly the result of multiple endonucleases or the presence of many pre- and pro-pre forms (Nakamuru *et al*, 1981; Stratling *et al*, 1984). More recently, Cidlowski and colleagues have purified the glucocorticoid-induced thymocyte endonuclease to homogeneity by 2-D gel electrophoresis (Compton and Cidlowski, 1987; Schwartzman and Cidlowski, 1991; Gaido and Cidlowski, 1991). The endonuclease (designated NUC18) is 18 kd and bears striking homology to the cyclophilin family, a group of cellular signalling molecules that possess nuclease activity. Further studies by Cidlowski and colleagues and others suggest that the endonuclease is constitutively present in the thymocyte nucleus in an inactive form, activated only following glucocorticoid treatment (Alnemri and Litwack, 1989). These results argue that the endonuclease is therefore not synthesized *de novo* following steroid treatment, but is activated posttranslationally. The endonuclease activated during glucocorticoid-induced cell death is the same protein as that observed during calcium ionophore-induced death (Caron-Leslie and Cidlowski, 1991). The ability of zinc to

inhibit endonuclease activity may be one mechanism for zinc-associated inhibition of apoptotic death (Cohen and Duke, 1984).

A factor that may control endonuclease activity is the presence of topoisomerases, which may maintain chromatin in a conformational state that renders linker regions inaccessible to cleavage. Induction of apoptosis would result in the inhibition of topoisomerase activity and the induction of DNA degradation. Topoisomerase II inhibitors can themselves induce apoptosis in lymphoid cell lines (Walker *et al*, 1991). Spermine, a polyamine that can bind to double stranded DNA prevents endonuclease-associated DNA fragmentation during steroid-induced cell death, also suggesting that modification or stabilization of the double helix can affect the activity of the endonuclease (Brune *et al*, 1991). Interestingly, mitochondrial DNA is not cleaved during glucocorticoid-induced apoptosis, consistent with the requirement for energy production until very late in the process (Murgia *et al*, 1992).

Other biochemical mediators of apoptotic death have also been characterized. Transglutaminases are believed to crosslink plasma membranes and permit the process of "blebbing" (Fesus *et al*, 1987). These proteins are thought to be newly synthesized following glucocorticoid induction of cell death and during other forms of apoptosis as well. Although protease activity would appear necessary to mediate apoptosis-associated cytoskeletal breakdown, broad-spectrum protease inhibitors do not inhibit glucocorticoid-induced cell death, making the possible role of proteases uncertain. The protease calpain is induced very early in steroid-induced thymocyte apoptosis, however, and is thought to play a role in the "flipping" of phosphatidylserine residues to the outside of the plasma membrane, a possible mechanism of phagocytic cell recognition (Fadok *et al*, 1992).

Another interesting potential mediator of glucocorticoid-induced apoptotic death is the poly(ADP-ribosyl)ation pathway of DNA excision-repair. This process involves the repair of double-stranded DNA nicks by the formation of ADP-ribose polymeric

structures, utilizing ADP-ribose groups from NAD and catalyzed by the enzymes mono(ADP-ribose) and poly(ADP-ribose) synthetase. When this pathway is activated, intracellular pools of NAD and eventually ATP are rapidly depleted, resulting in energy starvation. It has been proposed that DNA repair process represents a last-ditch attempt to counter glucocorticoid-induced apoptosis, and may be the actual reason for cell death as a result of energy depletion (Schwartzman and Cidlowski, 1993). This notion is supported by results obtained with mono and poly(ADP-ribose) synthetase inhibitors, which increase glucocorticoid sensitivity in treated cells (Wielckens and Delfs, 1986; Smets *et al*, 1988; Smets *et al*, 1990). In addition, preincubation of rat thymocytes with NAD increases their resistance to glucocorticoids (Nelipovich *et al*, 1988). Nevertheless, multiple observations that NAD and ATP pools fail to deplete during glucocorticoid-induced apoptosis make the role of poly(ADP-ribosyl)ation uncertain.

Conclusion. Although glucocorticoid-induced apoptosis in lymphoid cells is one of the best-characterized of all apoptotic systems, most of the experimental work involving the moloecular mechanisms of apoptotis (such as gene expression and secondary signal transduction) are still in the preliminary stages. Nevertheless, biochemical characteristics of physiological death that are currently defined provide a number of potential targets for the inhibitory effects of zinc. The possible effects of zinc on many of these biochemical characteristics will be discussed in Chapter 3.

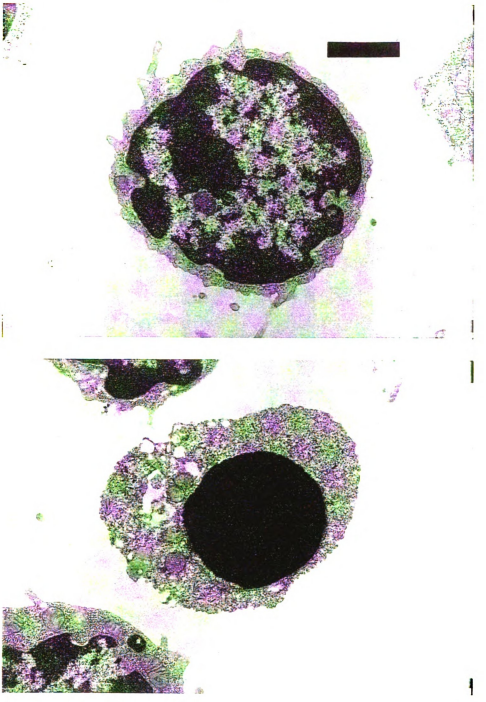

Figure 2-1. Normal (top) and apoptotic (bottom) mouse thymocytes. Apoptotic thymocytes were treated with dexamethasone at 0.1 μM for eight hours as described in Chapter 5 Materials and Methods. Cells were gluteraldehyde-fixed, embedded, sectioned and imaged on a Phillips 300 transmission electron microscopy at 50,000 X magnification. Bar equals 2 μm.

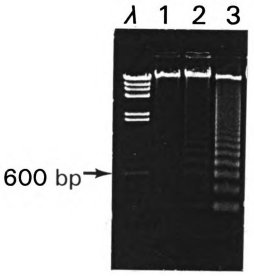

Figure 2-2. Agarose gel electrophoresis of internucleosomal DNA fragments from apoptotic mouse thymocytes. Cells were analyzed fresh (1) or after eight hours incubation without (2) or with corticosterone at 1 μM (3) as described in Chapter 5 Materials and Methods. Lambda phage HindIII digest molecular weight markers were included (λ) with 600 bp band indicated.

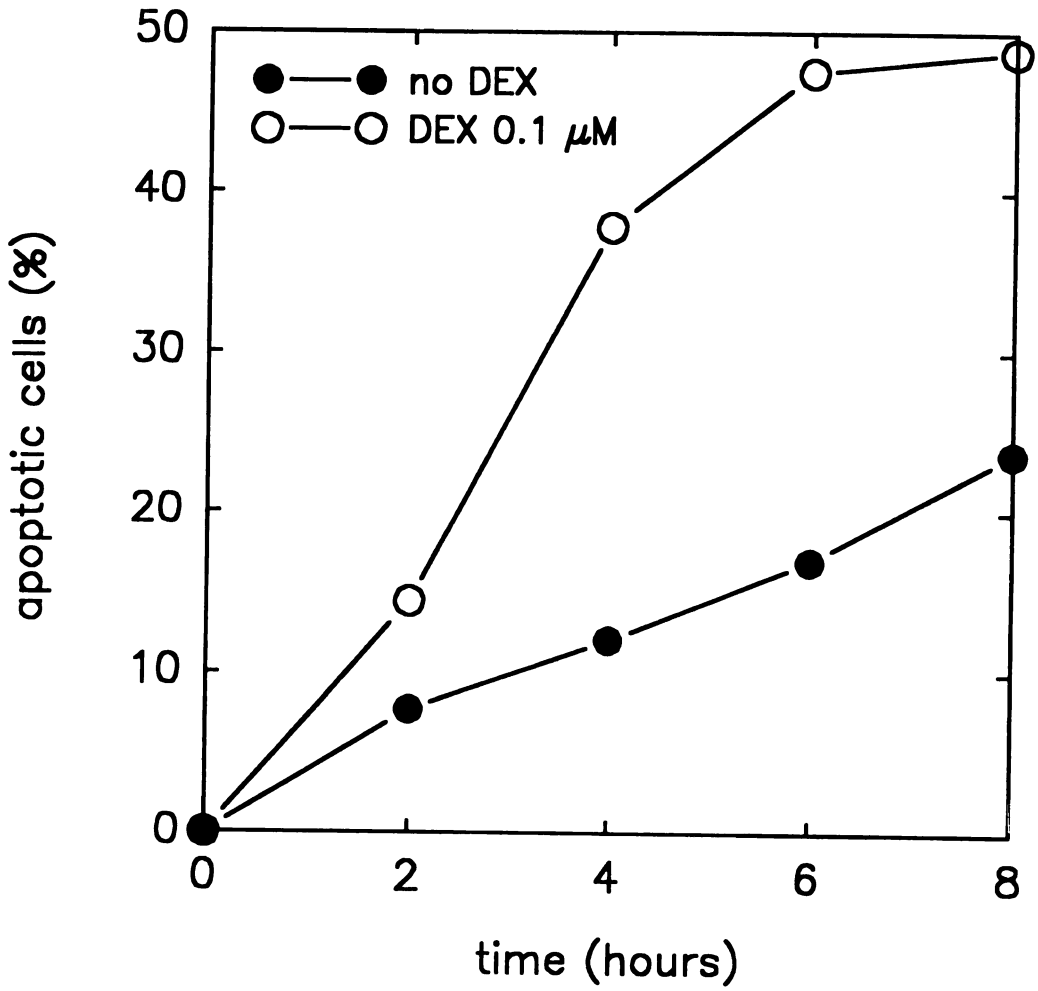

Figure 2-3. Sequential induction of apoptosis in mouse thymocytes by glucocorticoids. Thymocytes were incubated without or with dexamethasone at 1 μM for the indicated timepoints, fixed with ethanol, stained with propidium iodide and flow cytometrically analyzed for apoptotic cells as described in Chapter 5 Materials and Methods. All values are single samples.

CHAPTER 3: LITERATURE REVIEW

INHIBITORY EFFECT OF ZINC ON MAMMALIAN CELL APOPTOSIS: CHARACTERISTICS AND POSSIBLE MECHANISMS

Introduction. High concentrations of zinc salts (on the order of 500 μM and greater) have been shown to be an almost universal inhibitor of the process of *in vitro* apoptotic death in mammalian cells (reviewed by Zalewski and Forbes, 1993). Despite the fact that the ability of zinc to inhibit physiological death has been recognized almost as long as the process of apoptotis itself, a mechanism for this inhibitory ability has not been clearly defined. This review will therefore examine the studies of zinc-associated inhibition of apoptosis (particularly in the immune system) and the work dealing with possible mechanisms to explain these inhibitory effects. Potential targets for zinc in the biochemical activation and progression of apoptotic death will then be explored with subsequent recommendations for further study into the mechanism behind this phenomenon.

Zinc-associated inhibition of apoptosis. High concentrations of zinc have been found to inhibit apoptotic death induced by a wide variety of stimuli in a wide variety of cell types. Zinc concentrations of 500 μM and greater have been found to inhibit mouse thymocyte apoptosis induced by stimuli as diverse as glucocorticoids, gamma radiation, adenosine and ATP (Cohen and Duke, 1984; Sellins and Cohen, 1987; Kizaki *et al*, 1988; Zheng *et al*, 1991). Zinc at 500 μM has also been found to inhibit glucocorticoid- and gamma-radiation-induced apoptosis in mouse bone marrow B-lineage lymphocytes (Garvy *et al*, 1991). Zinc at 1 mM inhibited TNF-induced death in WEHI 164S fibrosarcoma cell line (Flieger *et al*, 1989). Zinc at 500 μM to 1 mM has also inhibited sporodesmin

and gliotoxin-induced cell death in T lymphoblasts and macrophages respectively, as well as etoposide- and UV radiation-induced cell death in HL-60 promyelocytic leukemia cells and cycloheximide- and actinomycin D-induced death in mouse thymocytes (Waring *et al*, 1990; Shimuzu *et al*, 1990; Martin *et al*, 1991; Telford and Fraker, unpublished data). Hypothermia- and hyperthermia-induced cell death in fibroblasts and human lymphoma cell lines can also be prevented with zinc at 200 to 500 μM (Nagle *et al*, 1990; Takano *et al*, 1991. Mature T lymphocyte and T cell hybridoma cell death induced by IL-2 withdrawal can also be inhibited by zinc (Nieto and Lopez-Rivas, 1989), as is LPS-induced DNA fragmentation in mouse thymocytes (Thomas and Caffrey, 1991). Collectively, all of these stimuli, including hormones, radiation, cytokines, chemotherapeutic cytotoxins and environmental stresses, represent a tremendous variety of apoptotic inducers that can be antagonized by zinc. The cells represented in these studies, although primarily of immune and epithelial origin, also represent a broad spectrum with regard to level of differentiation and physiological state.

Zinc can also prevent the induction of more specialized forms of apoptotic death. Apoptosis-associated DNA fragmentation is thought to be a component of cytolytic T cell killing and is induced in the target cell prior to lysis (Duke *et al*, 1983; Chayen *et al*, 1990). Zinc at concentrations ranging from 500 μM to 5 mM have been repeatedly found to inhibit this aspect of CTL killing. This has been demonstrated in mouse CTL killing of the P815 mastocytoma YAC-1 lymphoma, BW5147.3 thymoma and TA-3 B cell hybridoma cell lines in several systems (Duke *et al*, 1983; Albritton *et al*, 1988; Zychlinsky *et al* 1991; Ju, 1991). In some cases, zinc can also prevent the target cell lysis that also occurs during cytolytic killing, although this varies from study to study.

When attempting to define potential mechanisms for the ability of zinc to inhibit apoptotic death, it is important to define precisely what aspects of apoptotic death (all or only some) are being inhibited. In almost all of the above cases, zinc inhibition of

apoptotic death was measured both by analysis of DNA fragmentation (usually by gel electrophoresis) and morphological examination by electron microscopy. In all but a few of the above cases, zinc was found to arrest both DNA fragmentation and the morphological changes associated with apoptotic death, including collapse of the cytoplasm and nuclear condensation and margination. An ultrastructural study carried out on dexamethasone-induced apoptosis in mouse thymocytes showed that zinc-treated thymocytes were almost identical in appearance to normal thymocytes, with only minimal nuclear chromatin margination and nuclear envelope breakdown (Cohen *et al*, 1993). The authors interpret these results as indicating that zinc probably inhibited apoptosis at a very early stage, prior to the induction of endogenous endonuclease. A study with etoposide-induced apoptosis in a mouse lymphoma cell line gave similar results (Cohen *et al*, 1993). Flow cytometric studies on zinc inhibition of glucocorticoid-induced apoptosis in mouse thymocytes indicate that zinc inhibits both the chromatin degradation and cytoplasmic collapse associated with apoptotic death, further arguing that zinc is not simply inhibiting isolated characteristics of apoptosis (W.G. Telford and P.J. Fraker, unpublished observations).

Nevertheless, zinc does show more limited protection against some apoptotic stimuli. Examples of these include zinc protection of mouse thymocytes from adenosine-induced apoptosis and some cases of CTL-induced target cell DNA fragmentation (Kizaki *et al*, 1988; Zheng *et al*, 1991). In these systems, only DNA fragmentation is inhibited by the presence of zinc, with other characteristics of apoptotic death such as cytoplasmic collapse and blebbing of the plasma membrane still occurring. Barbieri *et al* (1992) have also found that zinc prevented DNA fragmentation during spontaneous apoptosis in rat thymocytes, but failed to prevent cytoplasmic collapse and loss of membrane integrity, particularly over prolonged incubation. The limited ability of zinc to protect cells from apoptotic death in these systems therefore questions whether zinc can prevent all the

manifestations of apoptotic death, and may provide valuable information as to the mode of action for zinc in the inhibition of apoptosis in other apoptotic models where protection is more complete. At this point, however, the reasons for these observations is not known.

Effects of zinc on the apoptosis-associated Ca^{2+}/Mg^{2+}-dependent endogenous endonuclease activity. Although a mechanism to explain the effects of zinc on apoptotic death has not yet been defined, the best-explored mode of action (and the most frequently cited) to date has been the endogenous endonuclease associated with apoptosis-associated DNA fragmentation. Internucleosomal DNA fragmentation is believed to occur by posttranslational activation of at least one Ca^{2+}/Mg^{2+}-dependent endogenous endonuclease, which cleaves DNA at the linker regions between nucleosomes (Wyllie, 1980a). Endonuclease inhibitors such as aurintricarboxylic acid can inhibit glucocorticoid-induced apoptosis in mouse thymocytes, suggesting that an inhibitory effect exerted by zinc might produce similar effects (McConkey *et al*, 1989a).

Early studies that generated crude nuclear lysates containing endogenous endonuclease demonstrated that calcium and magnesium or manganese induced endonuclease activity in these preparations, and zinc at relatively low concentrations (5 to 50 μM) completely inhibited it (Ishida *et al*, 1974). Later studies demonstrated that the chromatin in isolated thymocyte nuclei could be induced to undergo DNA fragmentation with the addition of calcium and magnesium; zinc at 5 to 50 μM was also able to inhibit the DNA damage induced under these conditions (Cohen and Duke, 1984). In 1991, Cidlowski and colleagues were able to purify the endogenous endonuclease to heterogeneity (NUC18), and confirmed that zinc acted as an inhibitor (Compton and Cidlowski, 1987; Schwartzman and Cidlowski, 1991; Gaido and Cidlowski, 1991). No putative zinc binding domain was found to exist in the protein, however, suggesting that

zinc may act by competing with calcium. Recent observations in isolated nuclei suggest that careful regulation of zinc and calcium concentrations may be able to tightly regulate endonuclease activity, suggesting a possible *in vivo* mechanism (Giannakis *et al*, 1991; Lohmann and Beyersmann, 1993).

This evidence therefore suggests that zinc might be inhibiting apoptotic death by inhibiting endonuclease activity. The fact that higher concentrations of zinc (500 to 5000 μM) are required to inhibit DNA fragmentation in intact cells than in purified preparations or isolated nuclei (5 to 50 μM) may be explained by the fact that 500 to 5 mM extracellular zinc concentration will likely not result in an intracellular zinc concentration of the same magnitude. Concentrations of 5 to 50 μM in cell-free systems or isolated nuclei may therefore be relevant to the higher concentrations required to inhibit apoptosis *in vivo*.

In a particularly interesting study, zinc at 2 mM was found to inhibit both the internucleosomal DNA fragmentation and associated breakdown of the nuclear lamins and the nuclear envelope in isolated HeLa cell nuclei induced to undergo apoptosis-associated chromatin degradation (Lazebnick *et al*, 1993). However, lower concentrations of zinc (500 μM to 1 mM) only prevented changes in nuclear morphology (chromatin condensation, margination and breakdown of the nuclear lamins and envelope) while not inhibiting actual internucleosomal DNA fragmentation as determined by gel electrophoresis. These observations reinforce the idea that endonuclease activity is not the only cause of chromatin degradation during apoptosis, and suggest that zinc may be inhibiting these other factors in addition to endonuclease. Topoisomerases are believed to play a role in maintaining nuclear chromatin in a conformational state that is resistant to endonuclease cleavage with this control being released during apoptotic death (Walker *et al*, 1991). Zinc may be playing an inhibitory role in mechanisms such as this as well.

Other potential mechanisms. Although inhibition of endonuclease activity is the most popularly cited potential mechanism for the inhibitory effects of zinc on mammalian cell apoptosis, no direct evidence exists that zinc is in fact inhibiting endonuclease activity in intact cells and that any subsequent inhibition is preventing apoptotic death. It is also unclear whether sole inhibition of endonuclease activity would go on to inhibit all aspects of apoptotic death (such as cytoplasmic collapse) or simply chromatin degradation. The apparent ability of zinc to completely protect cells from apoptosis in many systems and the lack of clear evidence for endonuclease inhibition therefore suggests that zinc may be inhibiting cell death through one or more other mechanisms. The question of why zinc inhibits apoptotic death is therefore still very much open to speculation and study. In the following section, a number of potential targets for zinc (based on current knowledge of apoptotic induction and mediation as described in Chapter 1) will be reviewed, with the ultimate goal to identify potential mechanisms for further study. For the sake of clarity, these mechanisms will be reviewed in the approximate order in which physiological death proceeds.

Effects of zinc on transcriptional activation. A consistent (although not entirely universal) characteristic of apoptotic death is the requirement for *de novo* transcription and translation of genes and gene products required to complete the death process (Cohen and Duke, 1984). Transcriptional and translational inhibitors effectively block many types of apoptotic death. A necessary component of apoptotic activation is therefore the activation of transcriptional activators that mediate apoptosis-associated gene expression. In the case of glucocorticoid-induced apoptosis, the transcriptional activator is the glucocorticoid receptor (GR) which becomes active upon addition of ligand (Pratt, 1993). Other transcription factors, including the AP-1 complex have also been shown to be necessary in the induction and modulation of a wide variety of apoptotic stimuli, including

glucocorticoids (Walker *et al*, 1993). Zinc might exert an inhibitory effect on transcriptional activation at several levels, effectively blocking cell death. Although the classical GR system will be used to outline the possible mechanisms below, many of these concepts can be applied to other transcriptional activators as well.

In the case of GR, the initial event in the pathway is the binding of ligand to cytoplasmic receptor. Following ligand binding, the receptor is altered such that it can translocate to the nucleus, bind to the nuclear envelope and enter the nuclear space, presumably through nuclear pores. In the case of GR, this involves the release of an hsp90 homodimer and associated proteins from the receptor core protein, exposing a nuclear recognition signal and a zinc finger DNA binding domain. The receptor must then interact with specific response element DNA sequences to induce GR-associated transcription (reviewed by Pratt, 1992).

Zinc might act to inhibit any one of these steps. Receptor-ligand binding and hsp90 association/dissociation have both been found to require closely spaced sulfhydryl-bearing amino acid residues in the steroid binding domain of the receptor (Pratt, 1987). Both processes have been found to require these thiol residues in a reduced form. Heavy metal ions and oxyanions such as arsenite, cadmium and selenite have all been found to prevent receptor-ligand binding in GR through crosslinking of vicinal dithiol residues. Zinc has been found to prevent thyroid receptor-ligand binding by a similar mechanism. Zinc has also been postulated to play a role in GR-hsp90 association (Schwartz *et al*, 1993). These results suggest that zinc might inhibit transcriptional activation at these early levels of GR signal transduction. Current evidence also suggests that reduced thiols are necessary for interaction of the receptor with the nuclear matrix, suggesting another possible target for zinc (Kaufmann *et al*, 1986).

Zinc might also modulate transcriptional activation at the level of transcription factor binding to DNA. GR is a zinc finger DNA binding protein, containing two zinc

fingers of the Cys_2-Cys_2 variety (unlike DNA binding proteins such as TFIIIA, which are Cys_2-His_2)(see Figure 4-6)(Archer *et al*, 1990; Freeman, 1992). The N-terminal finger (see Chapter 4 for details) has a relatively high affinity for zinc (approximately 10^{-9} M) due to the small number of residues separating the second and third coordinate cysteine residue. The C-terminal finger, on the other hand, has a larger number of residues separating the second and third cysteine, resulting in greater conformational strain at the coordinate binding site and a concomitant reduction in binding affinity (about 10^{-6} M)(Pan *et al*, 1990). While the N-terminal finger zinc is probably almost non-exchangeable, the C-terminal finger may be more likely to lose or gain zinc dependent on the surrounding intracellular zinc concentration. High concentrations of zinc might therefore enhance the DNA binding affinity of many transcription factors. Removal of zinc from the C-terminal finger by dialysis and chromatography over Chelex-100 (a metal binding anionic exchange resin) reduces DNA binding activity in both GR and PR receptor (Freeman *et al*, 1988; Westin *et al*, 1988). A recent study demonstrated that the metal binding protein metallothionein introduced into a cell-free system could reduce Sp1 transcription factor binding to DNA by limiting free zinc (Zeng *et al*, 1991). Alterations in dietary zinc in rats also results in increased metallothionein expression via specific transcription factor interaction with metal responsive elements (Cousins and Lee-Ambrose, 1992). These results and other studies indicate that modifying the level of zinc in the environment can potentially modulate zinc finger binding affinity for DNA (Chesters, 1992). Increasing the extracellular zinc concentration could therefore modulate gene-directed apoptotic death, in either a positive or negative manner. Although this has been postulated primarily for GR, it could apply to any apoptosis-associated transcription factor with a zinc finger binding moiety.

Zinc-induced gene expression. Although high concentrations of zinc have the potential

to alter zinc finger transcription factor binding DNA and subsequently alter transcription, zinc and other metals have also been found to induce transcription themselves. Heavy metals such as zinc and cadmium induce expression of a variety of genes in mammalian cells, including metallothionein-I and -II, heat shock protein 70 (hsp70) and the protooncogenes c-*jun*, c-*fos* and, c-*myc* (Bremner and Beatie, 1990; Karin *et al*, 1984; Richards *et al*, 1984; Mitani *et al*, 1990; Andrews *et al*, 1987; Jin and Ringhertz, 1990; Epner and Herschman, 1991). The ability of zinc to upregulate expression of the metal binding proteins metallothionein-I and -II expression in hepatocytes and lymphocytes has been particularly well-characterized. Metallothionein may regulate intracellular influxes of zinc induced by hormones and other stimuli and may also represent a stress response aimed at controlling high concentrations of potentially toxic heavy metals in cells (Etzel *et al*, 1979; Cousins *et al*, 1986). It is believed that zinc and other metals induce gene expression by enhancing zinc finger transcription factor binding to metal responsive elements (MREs), which may share transcriptional control with glucocorticoid, phorbol ester and other enhancer regions (Karin *et al*, 1984; Anderson *et al*, 1987). Although metal-inducible transcription factors (MITF) have not been unambiguously isolated, several low molecular weight proteins have been isolated that may constitute transcription factors or cofactors.

Zinc may therefore induce expression of metal-inducible gene products concomitant with glucocorticoids. One possible inhibitory mechanism here might be the zinc-induced expression of gene products that could antagonize glucocorticoid-induced apoptosis. Zinc and cadmium have been found to induce c-*myc* expression in Swiss 3T3 cells (Jin and Ringhertz, 1990). Glucocorticoids downregulate c-*myc* expression in lymphocytes and lymphoid cell lines (Eastman-Reks and Vedeckis, 1987; Yuh and Thompson, 1989). Elevation of c-*myc* is antagonistic to glucocorticoid-induced apoptosis (although not to activation-induced apoptosis), as demonstrated with T cell hybridomas

transfected with the c-*myc* gene under control of a non-GR-inducible promoter; these cells became glucocorticoid-resistant despite the presence of a normal GR (Thompson *et al*, 1992). Zinc-induced gene expression may therefore be antagonizing GR-associated apoptosis by a mechanism of this type.

Effects of zinc on apoptosis-associated signal transduction. Although most apoptotic mechanisms require *de novo* gene expression, a number of cellular signal transduction events described in Chapter 1 have also been found necessary for the successful resolution of apoptotic death. Signalling normally associated with cell growth and proliferation have been found to occur during apoptotic death, including calcium flux, cAMP upregulation, protein kinase C modulation, protooncogene upregulation and others (reviewed by Cohen *et al*, 1992). In some cases induction of the signalling event (such as calcium flux by calcium ionophores or cAMP upregulation with prostaglandins) can induce apoptosis in the absence of any other stimuli. Zinc has been found to block or modulate many of these signalling events and might prevent apoptotic death via this route. Some potential examples are given below.

Effects of zinc on calcium binding proteins. Zinc and other trace metals at high concentrations can compete with calcium for binding sites on certain calcium binding proteins. The ability of heavy metals to compete for calcium binding sites on calcium binding proteins is believed to form the basis for the toxicity of many heavy metals, such as cadmium, lead and mercury (Habermann and Richardt. 1986). The best-characterized example of this phenomenon for zinc is the calcium sequestration/transport protein calmodulin, which normally binds four calcium ions per molecule (Brewer, 1980). High concentrations of zinc (on the order of 200 μM) can inhibit *in vitro* calmodulin calcium binding activity as measured by calmodulin-dependent Ca^{2+}-ATPase activity. High concentrations of zinc can also inhibit erythrocyte shrinkage and sickling associated with

high intracellular calcium concentrations. This effect is also presumably due to inhibition of calmodulin activity, since calmodulin inhibitors produce effects similar to those observed for zinc. The example of inhibition of calmodulin activity by zinc is particularly relevant to apoptotic death, since calmodulin is upregulated in thymocytes during glucocorticoid-induced apoptosis (Dowd *et al*, 1991). Calmodulin may also play a role in the control of intracellular calcium flux during apoptotic signalling, since calmodulin inhibitors such as trifluoroperazine and calmidazolium can inhibit glucocorticoid-induced apoptosis in mouse thymocytes (McConkey *et al*, 1989b). The possibility that increased calcium flux is an important component of apoptotic signal transduction also indicates that calmodulin and other calcium binding proteins may be necessary for apoptotic death (McConkey *et al*, 1993b). Zinc might competitively inhibit the activity of calmodulin and other calcium binding proteins, resulting in the inhibition of cell death.

Effects of zinc on protein kinase C. Zinc has been found to modulate the activity of protein kinase C (PKC) both *in vitro* and *in vivo* in mouse and human lymphocytes, both by increasing the affinity of PKC for phorbol esters and diacylglycerol and by increasing the translocation rate of the PKC-ligand complex to the plasma membrane (Murakami *et al*, 1987; Csermely *et al*, 1988a). PKC possesses a putative regulatory zinc binding domain (Parker *et al*, 1986) and recent work suggests that zinc and calcium are both required for interaction of PKC with diacylglycerol or phorbol ester and subsequent translocation to and interaction with the plasma membrane and the cytoskeleton in mouse lymphocytes (Csermely *et al*, 1988b; Zalewski *et al*, 1990a; Zalewski *et al*, 1991). Incubation of cells with high concentrations of zinc salts (10 to 100 μM) increase the activity of PKC in *vivo* (Forbes *et al*, 1989), and a regulatory mechanism for PKC implicating high concentrations of sequestered zinc has been proposed (Forbes *et al*, 1990; Zalewski *et al*, 1990b; Forbes *et al*, 1991). Zinc may also translocate within the cell

upon PKC activation with phorbol esters (Csermely *et al*, 1987; Csermely and Somogyi, 1989). As discussed in Chapter 1, activation of PKC by phorbol esters has been found to both inhibit and activate calcium ionophore- glucocorticoid- and radiation-induced apoptotic death in mouse and human lymphocytes, implicating it in the apoptotic signal transduction cascade. Zinc may therefore be inhibiting apoptosis through modulation of PKC activity. This mechanism is probably distinct from that postulated for calmodulin, since zinc is probably not competing with calcium for kinase binding but likely has its own regulatory binding site.

Although no inhibitory effects of zinc on cAMP upregulation and subsequent activation of cAMP-dependent protein kinase (PKA) have been observed, this would be another potentially important target for zinc. The importance of cAMP elevation in glucocorticoid- and other apoptosis-associated gene expression make this another point at which inhibitory effects would almost certainly affect downstream apoptotic death (McConkey et al, 1990b).

Effects of zinc on inositol phosphate metabolism. High concentrations of zinc (500 μM) have been found to induce changes in the distribution and phosphorylation state of inositol mono-, di-, tri- and tetraphosphates isolated from T lymphoblasts and macrophages induced to undergo apoptosis with sporodesmin and gliotoxin respectively (Waring *et al*, 1990). Inositol phosphates are phosphatidylinositiol diphosphate breakdown products (along with diacylglycerol) and are involved in regulation of intracellular calcium flux. Zinc may therefore be inhibiting apoptotic death at the level of inositol phosphate metabolism.

Zinc-induced mitogenesis in lymphocytes: antagonism to apoptotic death. A unique mechanism that may be involved in the inhibitory effects of zinc on glucocorticoid-induced lymphocyte death is the induction of mitogenesis. Although a number of studies have

demonstrated zinc to be an inhibitor of cell growth and proliferation (Borovansky and Riley, 1985; Borovansky *et al*, 1985; Borovansky and Riley, 1989), supplementation of cells with zinc salts in culture has frequently resulted in the opposite effect. Zinc chloride at 40 μM has been found to enhance EGF-stimulated DNA synthesis in primary mouse hepatocytes based on thymidine incorporation, although zinc alone resulted in no increase (Kobusch and Bock, 1990). Perhaps some of the most intriguing work with zinc as a growth stimulator is the observation that zinc can act as a weak mitogen for lymphocyte proliferation. Concentrations of zinc salts in the 10 to 200 μM range have been repeatedly shown to have a weak mitogenic effect on mouse and human lymphocytes, both alone and in synergy with mitogenic lectins (Chesters *et al*, 1972; Berger and Skinner, 1974). Zinc chloride at 50 μM stimulates proliferation in human peripheral blood lymphocytes, although to a significantly lower degree than mitogens such as concanavalin A or pokeweed mitogen (approximately 10%)(Ruhl and Kirschner, 1978). Similar results have been obtained for mouse splenocytes and hamster lymph node cells (Warner *et al*, 1986; Pocino *et al*, 1992; Hart, 1978). Zinc salts at 50 μM also act in synergy with the T lymphocyte mitogen phytohemagglutinin in stimulating mouse splenocyte proliferation (Kirschner and Ruhl, 1971). These effects have been attributed to mitogenesis in the T lymphocyte subpopulations of peripheral blood and the spleen. Zinc and mercury have also been found to stimulate interferon-gamma production in mouse T lymphocytes (Reardon and Lucas, 1971). Zinc stimulates mouse thymocytes with lipopolysaccharide as a cofactor, a characteristic shared with other mitogens and alloantigens in thymocyte mitogenesis. The addition of 2-mercaptoethanol was also required for thymocyte stimulation by zinc and LPS, suggesting that reduced sulfhydryl residues may be modified by zinc as part of the mitogenic mechanism (Reardon and Lucas, 1987). In addition, zinc has been found to increase *in vitro* antibody production in mouse splenic B lymphocytes when stimulated with T-dependent and T-independent antigens (including

lipopolysaccharide)(Cunningham-Rundles *et al*, 1980). All of these effects have been shown to occur only within a relatively small dose range of zinc (10 to 100 μM). No mechanism has yet been defined for zinc-induced lymphocyte mitogenesis, although direct induction of gene expression via activation of metal responsive transcription factors or enhancement of secondary signalling events have both been suggested to play a role (Grummt *et al*, 1986).

As discussed in Chapter 1, induction of proliferation and/or differentiation in immature lymphocytes is antagonistic to glucocorticoid-induced cell death. Lymphocyte activation by calcium ionophores and tumor promoters or by lectins is said to "rescue" lymphocytes from hormone-induced death, and may bear considerable functional relevance to the positive selection of functional, non-autoreactive immune cells during *in vivo* lymphocyte differentiation (Iwata *et al*, 1993). High concentrations of zinc may therefore be able to "rescue" lymphocytes from glucocorticoid-induced apoptosis by induction of mitogenesis. Although there are no studies suggesting that this is in fact the case, this mechanism warrants further consideration.

Effects of zinc on chromatin structure. Zinc exerts strong stabilizing effects on chromatin in *in vitro* systems. The ability of zinc to stabilize or alter chromatin has many implications for the control and inhibition of apoptosis, including transcriptional activation and control based on the conformation of active chromatin, and the ability of endogenous endonuclease to cleave DNA at exposed linker regions during apoptotic death. Added zinc could presumably affect one or both of these activities in cultured cells by altering or maintaining the structure of nuclear chromatin.

In vitro, low concentrations of zinc (10 μM) have been found to promote reversible denaturation and renaturation of DNA upon heating and subsequent cooling, possibly by stabilizing the DNA helix (Borochov *et al*, 1984). Zinc can also convert B-

form DNA to Z-form at higher concentrations (1 mM)(Fazakerley, 1984). Melting profile studies of DNA in the presence of zinc suggest that zinc may facilitate the initial transition of highly condensed chromatin to the "beads on a string" conformation resulting from the removal of H1 histones (McGhee and Felsenfeld, 1980). This is also supported by the observation that the presence of zinc stimulates histone phosphorylation, a posttranslational modification closely coupled to the interactions of histones with DNA in the nucleosome (Sen and Crothers, 1986). Zinc might therefore be responsible for "relaxing" chromatin, altering the accessibility of the internucleosomal linker regions. This might be closely coupled to gene unmasking, allowing transcription to proceed. It might also be a component of the endonucleolytic cleavage process of apoptotic death, which would presumably require access to the linker regions.

Zinc effects on membrane structure and membrane-associated proteins. Zinc supplementation has been found to exert profound effects both on the structure of plasma membranes and on a variety of transmembrane proteins, although most of the relevant studies have been carried out *in vitro*. Zinc has been used as a stabilizing agent to prevent the hemolysis of erythrocytes and isolated lysosomes, making them more resistant to changes in osmolarity (Chvapil *et al*, 1972; Chvapil, 1973). Although the mechanism behind this is not clearly defined, it may be due to the ability of zinc to inhibit membrane lipid peroxidation (Girotti et al, 1985; Coppen *et al*, 1985; Coppen *et al*, 1986). Lipid peroxidation contributes to membrane breakdown during necrotic death, and possibly apoptotic death as well (Kerr, 1993). Zinc also alters potassium permeability and subsequent transmembrane potential in muscle cells and across neuronal membranes (Bettger and O'Dell, 1982). Zinc may therefore be able to stabilize or alter the structure and permeability of plasma membranes, with implications for membrane transport and membrane-associated signalling events and membrane stability as well.

Physiological events at the level of plasma membrane organization are likely to be critical for the progression of apoptotic death. Changes in transmembrane potential via alterations in ion flux have been implicated in cell proliferation-associated signalling; while they have not yet been implicated in apoptotic signalling, they have not yet been excluded. Zinc associated alterations in ion flux may exert an inhibitory effect on apoptosis-associated changes in transmembrane potential, altering apoptotic signalling and preventing cell death. While recent inhibitor studies have played down the role of lipid peroxidation in the blebbing process of membrane breakdown during apoptosis, zinc may be playing an inhibitory role at this level as well (Golstein *et al*, 1991).

Zinc has also been found to modify the *in vitro* activity of several membrane-associated proteins, including guanylate cyclase, adenylate cyclase, Na^+/K^+-ATPase, Ca^{2+}-ATPase and microsomal NADH oxidase (Bettger and O'Dell, 1982). Although many of the signalling events in mammalian cell apoptosis remain obscure, the importance of cAMP elevation in lymphocyte apoptosis and the possible importance of G-proteins in lymphocyte signalling suggest that adenylate and/or guanylate cyclases may be important for apoptosis-associated signal transduction. Na^+/K^+- and Ca^{2+}-ATPases are also likely to be necessary for energy-dependent apoptotic death. Ca^{2+}-ATPase activity could be indirectly inhibited by zinc-associated inhibition of calmodulin activity (Brewer, 1980).

Effects of zinc on microtubule structure and assembly. Zinc at concentrations ranging from 100 μM to 1 mM has been repeatedly observed to stabilize microtubules both *in vitro* and *in vivo* in neurons, hepatocytes and a variety of other cell types, and prevent tubulin depolymerization even in the presence of destabilizing agents such as colchicine (Gaskin and Kress, 1977; Hensketh, 1982; Hensketh, 1984). *In vitro*, zinc spontaneously induces tubulin polymerization into sheets (Gaskin and Kress, 1977). Agents able to induce microtubule depolymerization such as colchicine and cold shock can induce

apoptosis in HL-60 cells, with chemical inhibitors of depolymerization such as vinblastine inhibiting cell death (Nagle *et al*, 1990; Martin *et al*, 1991; Lennon *et al*, 1991). Zinc can also prevent cell death in these systems. Zinc may therefore be inhibiting apoptotic death by stabilizing microtubule structure and promoting polymerization.

Effect of zinc on poly(ADP-ribosyl)ation. As discussed in Chapter 1, poly(ADP-ribosyl)ation is a DNA excision-repair mechanism that may be triggered by glucocorticoid-induced apoptosis and may actually be responsible for cell death by depleting cells of their intracellular NAD and ATP stores. Shimuzu *et al* have demonstrated that 1 mM zinc inhibition of etoposide-induced apoptosis in HL-60 cells was accompanied by inhibition of poly(ADP-ribosyl(ation), as determined by inhibition of both mono(ADP-ribose) and poly(ADP-ribose) synthetase. Poly(ADP-ribose) synthetase possesses a zinc finger domain, suggesting that it might be regulated by zinc (Gradwohl et al, 1989). This study did not however demonstrate that inhibition of poly(ADP-ribosyl(ation) was the actual cause of cell death inhibition.

Conclusion. All of the potential mechanisms for the inhibitory effects of zinc on physiological death presented in this section represent viable targets of investigation into the phenomenon of zinc inhibition. Nevertheless, zinc inhibition of apoptosis has received very little experimental attention. While all of these mechanisms fit the required conditions of zinc inhibition with regard to zinc concentration, much of this work represents cell-free, *in vitro* experimentation that needs to be applied to *in vivo* zinc inhibition models. The problem of zinc prevention of apoptosis therefore remains quite open for further study.

CHAPTER 4: LITERATURE REVIEW

GLUCOCORTICOID RECEPTOR STRUCTURE, FUNCTION AND SIGNAL TRANSDUCTION

Introduction. The glucocorticoid receptor (GR) is a member of the extensive steroid receptor superfamily of transcription factors (Carson-Jurica *et al*, 1990). It is virtually ubiquitous in all mammalian tissues. Although it shares many characteristics with other members of the steroid receptor family (including estrogen, progesterone, thyroid and aryl hydrocarbon) it is characterized by its unique degree of hormone dependence, with nuclear translocation and transcriptional activation only occurring following binding of ligand (Beato, 1989; Burnstein and Cidlowski, 1989). The structure/function relationship that maintains GR-associated transcription under rigid hormonal control may represent a common theme among transcription factors that must be precisely regulated (Pratt, 1993). This literature review will attempt to provide a historical background of work involving GR, as well as a survey of the most recent findings.

Isolation and characterization of steroid receptors. Early studies of phosphoproteins capable of binding natural adrenal steroids (such as corticosterone or hydrocortisone) or synthetic steroids (such as dexamethasone or prednisolone) as well as progesterone binding proteins resulted in the isolation of two steroid binding forms: a large 8-9S form (based on separation by sucrose gradient centrifugation) and a smaller 4S form (reviewed by Pratt, 1987). The 8-9S form was predominant in cells that had been maintained in hormone-free conditions (either in culture of from adrenalectomized animals), and was generally isolated from cytosolic fractions. The 4S form was present at higher levels following treatment with steroids and was isolated from nuclear fractions. DNA binding

studies using herring sperm DNA coupled to cellulose demonstrated that the 4S form had a high affinity for DNA, while the 8-9S form did not (Kalimi *et al*, 1975). Following cell lysis the 8-9S form was found to degrade to the 4S form while maintaining its association with steroid. This process was found to be accelerated by increases in temperature, salt concentration and pH, conditions that were often present during receptor isolation (Schmidt *et al*, 1982). These results were obtained from a variety of tissues, including rat thymus and liver, mouse fibroblast and thymoma cell lines for glucocorticoids and chick oviduct and rabbit uterine wall for progesterone (Holbrook *et al*, 1983). The extreme lability of the 9S form made its characterization difficult and its physiological significance unclear.

The use of molybdate and other transition metal oxyanions as phosphatase inhibitors in early studies of receptor phosphorylation resulted in the accidental discovery that these compounds could stabilize the glucocorticoid receptor in the 8-9S form, even under conditions that normally resulted in 4S formation (Leach *et al*, 1979). Stabilization of receptor by molybdate was found to be independent of its activity as a phosphatase inhibitor (Housely *et al*, 1982). Molecular sieve chromatography of stabilized and unstabilized receptors gave an approximate M_r of 300,000 for the 8-9S form and 95,000 for the 4S form (Holbrook *et al*, 1982). It was therefore proposed that the 8-9S form represented a heteromeric complex containing at least one steroid binding species, while the 4S form represented the steroid binding protein (Schmid *et al*, 1985).

Receptor structure was also related to subcellular distribution within the cell. The 8-9S receptor form was found predominantly in the cytoplasm, while the 4S form was localized to the nucleus. Stimulation of hormone would decrease the amount of 8-9S form in the cytoplasm and increase 4S levels in the nucleus, suggesting that hormone was inducing receptor conversion from the 8-9S to 4S form that was accompanied by nuclear translocation. Subsequent immunocytochemical studies confirmed that hormone induced

translocation of GR to the nucleus (Govindan, 1980; LaFond *et al*, 1988).

The cellular localization and DNA binding data resulted in a model where the 8-9S form represented a cytosolic, non-DNA binding form of the receptor. Upon *activation* by hormone binding, the heteromeric 8-9S form would *transform* to the single 4S steroid binding species, which could subsequently enter the nucleus and bind DNA (Figure 4-1). While this model was very attractive due to its simplicity, it was not clear at the time what relevance it had to *in vivo* GR signal transduction, as it could only be demonstrated in *vitro* conditions. The precise identity and role of the steroid and non-steroid binding proteins in the 8-9S untransformed receptor were unknown.

Components of the untransformed steroid receptor. In the early 1980s, GR and other steroid receptors (including estrogen [ER] and progesterone [PR]) were purified by affinity resin chromatography from a variety of tissues, including L cell and rat liver cytosol for GR (Housely *et al*, 1983; Grandics *et al*, 1984). A 90,000 M_r protein was the predominant species isolated from purified molybdate-stabilized cytosolic receptors. The subsequent availability of site-specific, radiolabeled affinity ligands for GR and PR (^{3}H] dexamethasone 21-mesylate and [^{3}H]R5020, respectively) and denaturing polyacrylamide gel electrophoresis allowed covalent labeling and precise identification of steroid binding proteins in the 8-9S heterometic complexes. These experiments determined that the 90kd proteins isolated by affinity chromatography did not bind to either glucocorticoid or progesterone (Idziorek *et al*, 1985; Renoir *et al*, 1984). L cell and rat thymoma glucocorticoid binding protein was found to migrate at approximately 100 kd, while rat liver receptor migrated at 95 kd (Housely *et al*, 1985). In all cases, the 90 kd component did not bind steroid but was present in the 8-9S heteromeric form.

Preparation of monoclonal antibodies against GR and PR has resulted in antibodies that react either with the steroid binding proteins in the molybdate-stabilized heteromer

or with the 90 kd non-steroid binding protein, but not with both (Radanyi *et al*, 1983; Gametchu and Harrison, 1984; Housely *et al*, 1985; Sullivan *et al*, 1985). Antibodies against the 90kd protein can both immunoprecipitate and shift the sedimentation velocity of the 8-9S forms of GR and PR but not the 4S forms (Radanyi *et al*, 1983). Antibodies against GR (particularly BUGR1 and BUGR2 [Gametchu and Harrison, 1984]) used to immunopurify receptors from molybdate-stabilized cytosol resulted in the coabsorption of the 90kd protein (Housely *et al*, 1985). Antibodies against the 90kd protein (such as AC88) could be similarly used to coabsorbed the 95kd steroid binding protein from rat liver cysotol (Sanchez *et al*, 1987). These results all suggested that the 90kd protein was associated with the molybdate-stabilized, 8-9S form, while the 4S form was not.

Shortly after its discovery the 90kd protein component of the 8-9S GR form was strongly suspected to be heat shock protein 90 (hsp90). This was initially due to the ability of the 90kd protein to be recognized by the monoclonal antibody AC88 by Western blotting, which was originally raised against an 88kd protein associated with the sex pheromone antheridiol in the water mold *Achlya ambisexualis* (Sanchez *et al*, 1986). This antibody recognized 90kd proteins in a variety of avian and mammalian tissues, and was eventually recognized to identify a highly conserved heat shock protein. Similarly, antibodies against receptor-associated 90kd protein also recognized hsp90 (Radanyi *et al*, 1983; Riehl *et al*, 1985). Hsp90 has also been found to be associated with a wide variety of proteins, including actin, several tyrosine kinases and eukaryotic initiation factor 2 (Craig, 1985). Peptide mapping ultimately determined that the 90kd protein and hsp90 were the same protein for both GR and PR (Sanchez *et al*, 1986; Catelli *et al*, 1985). Stoichiometric studies with rat liver and L cell cytosolic GR and chick oviduct PR using metabolic labeling followed by anion exchange chromatography or SDS-PAGE suggested that the 8-9S form contains one molecule of the steroid binding protein and two molecules

of hsp90 (Renoir *et al*, 1984; Wrange *et al*, 1986; Mendel and Orti, 1988; Denis *et al*, 1987; Gustafsson *et al*, 1989; Bresnick *et al*, 1990). The combined molecular weights of these combinations range from 265 to 290 kd for PR and 270 to 290 kd for GR, approaching the experimental M_r of 300,000 obtained by gel filtration for both receptors (Holbrook *et al*, 1982; Dougherty and Toft, 1982; Bresnick *et al*, 1990). Nevertheless, other associated protein subunits may contribute to this total molecular weight as well.

Role of hsp90 in receptor transformation. The above results suggested that the dissociation of hsp90 from the core GR protein correlated with receptor transformation as defined by the 8-9S to 4S transition. Hsp90 dissociation could be induced *in vitro* by incubation at 20°C in the absence of molybdate (identical conditions to those found to induce receptor transformation), providing an experimental system to determine whether this was the case (Sanchez *et al*, 1986). Most of these studies were carried out *in vitro* in cell lysates and in immunoimmobilized receptor preparations, although a body of evidence suggested that these events also occur *in vivo*. Numerous studies have demonstrated that dissociation of hsp90 was associated with increased affinity for DNA, observations consistent with the DNA binding properties of the 8-9S and 4S receptor forms. Hsp90 dissociation also correlated with the ability to bind isolated nuclei. Molybdate and related oxyanions prevent temperature-mediated hsp90 release and subsequent binding to both DNA and isolated nuclei (Leach *et al*, 1979). Studies with mutant cell lines expressing truncated GR incapable of binding hsp90 show constitutive expression of GR-associated reporter genes, suggesting that hsp90 prevents DNA binding and subsequent transactivation (Cadepond *et al*, 1991). Current evidence therefore suggests that hsp90 dissociation from GR is at least one component of the receptor transformation process. Hsp90 appears to maintain GR in a nonfunctional state with respect to nuclear localization and DNA binding (Figure 4-1).

The functional association of hsp90 with GR has also been shown using both *in vivo* and genetic *in vitro* approaches. Metabolic labeling and crosslinking studies have shown that GR and hsp90 are associated *in vivo* in mouse L cell cytosols, but not in nuclear extracts, suggesting that hsp90 dissociation must occur prior to nuclear localization (Howard and Distelhorst, 1988; Rexin *et al*, 1991). Molybdate can prevent nuclear localization of GR *in vivo*, suggesting that it is stabilizing 8-9S receptor forms (Raaka *et al*, 1985). Several metabolic labeling studies have shown that mouse GR and hsp90 are translated simultaneously and become associated almost immediately following post-translational modification (Dalman *et al*, 1989; Ohara-Nemoto *et al*, 1990). Cell-free translation of GR and hsp90 in a rabbit reticulocyte system resulted in the formation of 8-9S heteromers, indicating that receptor heteromers can form spontaneously even in cell-free systems (Denis and Gustaffson, 1989b; Dalman *et al*, 1989; Scherrer *et al*, 1990). Strains of *S. cerevisiae* modified to produce only 5% normals levels of hsp90 show reduced levels of GR activation when compared to strains expressing normal levels of hsp90 (Picard *et al*, 1990b). Heat shock in mouse L929 cells with subsequent hsp90 upregulation has also been found to stimulate translocation of the unliganded GR (Sanchez *et al*, 1992). All of these results support the functional association of hsp90 with steroid receptors, with these last studies suggesting a strong dependence of steroid receptor function on hsp90 expression.

Relationship between ligand binding, hsp90 dissociation and subsequent events. Upon discovery that hsp90 dissociation was associated with receptor transformation to the 4S form, numerous studies were done to characterize the conditions required for hsp90 dissociation from the receptor. Cytosolic receptors transformed *in vitro* by incubation at 20°C required the presence of hormone (Sanchez *et al*, 1986). Hsp90 dissociation can be

induced in ligand-free GR *in vitro* only by high salt treatment. Hsp90 dissociation has therefore been considered to be induced by productive hormone binding to receptor, maintaining receptor transformation and subsequent downstream effects under negative control of steroid. Receptor maintained in a steroid-free environment were originally believed to not undergo transformation at all; it has been recently determined by immunoabsorption studies that transformation occurs at a much lower rate when ligand was absent (Sanchez *et al*, 1987b). GR and PR treated with steroid antagonists such as RU486 also showed minimal transformation to the DNA binding state, indicating that a productive ligand binding event was required for hsp90 dissociation (Pratt, 1987). These observations suggested that the role of ligand binding in GR signal transduction may be to initiate dissociation of hsp90 from the receptor, possibly through modification of a stabilizing factor that is as yet uncharacterized.

Although steroid binding appears necessary for hsp90 dissociation, it does not appear necessary for DNA binding *in vitro*. Steroid-free untransformed glucocorticoid receptors stripped of their hsp90 proteins have almost equal affinity for DNA-cellulose to hormone-bound receptors, suggesting that the presence of ligand is not required for DNA binding (Sanchez *et al*, 1987b). A similar result has been found for hormone-free receptor binding to glucocorticoid response elements (GREs) by gel mobility shift (Willman and Beato, 1986). Similarly, RU486-bound receptors also have equal affinity for GREs as dexamethasone-bound receptors (Bailly *et al*, 1986; Burnstein *et al*, 1991). These results suggest that ligand may only be necessary for conversion of steroid receptor to the DNA binding form, and not for subsequent interaction with DNA. Nevertheless, GRE binding *in vivo* as gauged by reporter gene expression is strongly dependent on ligand binding (Becker *et al*, 1986; Hock *et al*, 1989). Interaction of ligand with the steroid binding domain can be said to remove this repressor effect and initiate hsp90 dissociation (Figure 4-1).

While ligand binding appears to be necessary for hsp90 dissociation and subsequent derepression of nuclear localization and DNA binding activity, it has also been proposed that hsp90 association is required for ligand binding to GR. The activated L cell and rat liver cytosolic GR have been shown to have an extremely low affinity for steroid compared to intact hsp90-bound receptors (Bresnick *et al*, 1988; Bresnick *et al*, 1989). Normal affinity can be restored, however, by reconstitution of the 4S form with hsp90 and rabbit reticulocyte lysates to the 8-9S form (Burnstein *et al*, 1991). It is therefore likely that normal ligand binding is itself dependent on hsp90 association, possibly through maintenance of a folded conformation optimal for high affinity ligand binding.

Genetic mapping of steroid binding/hsp90 binding domains and transfection studies. Limited proteolysis analysis (Wrange *et al*, 1978; Gustaffson *et al*, 1986; Carlstedt-Duke and Gustaffson, 1988; Gustaffson *et al*, 1990) and cloning of the human (Hollenberg *et al*, 1985) mouse (Danielson *et al*, 1986) and rat receptor (Miesfield *et al*, 1986; Govindan, 1987) with subsequent analysis of insertional/deletional mutants have allowed an in-depth analysis of the protein domains involved in steroid binding and hsp90 association and the possible functional connections between these two events through transfection studies (Figure 4-2)(Giguere *et al*, 1986). The hormone binding domain of the mammalian GR and virtually all other steroid receptors has been mapped to the C-terminal region, encompassing residues 550 to 720 for mouse GR (Giguere *et al*, 1986; Pratt *et al*, 1987)(Figure 4-2). Nuclear localization domains have been mapped between the DNA and ligand binding domains and within the ligand binding domain itself. The N-terminal end of the receptor has not been found necessary for ligand or DNA binding, but may play a role in maintaining the folded conformation of the receptor and might interact with transcriptional cofactors during GRE binding.

Transfection studies in L cells with cDNAs encoding for GR containing an intact

steroid binding domain (steroid-inducible) results in the production of receptors that are in the 8-9S form in molybdate-stabilized cytosols. Transfection with receptor cDNAS that contain a non-functional steroid binding domain (non-inducible) resulted in the expression of the 4S form with normal DNA binding affinity. The ability of cells to produce 8-9S receptors and their ability to bind hsp90 therefore map to the steroid binding domain. While much of this domain is relatively non-homologous for different steroid receptors (probably reflecting specificities for different steroids), a 20 amino acid region at the N-terminal region of the steroid binding domain with high degree of homology for a variety of steroid receptors has been found (residues 583-602 for mouse receptor)(Pratt *et al*, 1988). Deletion mutants in this region cause constitutive expression of transfected GR-induced reporter genes, suggesting that these sequences are necessary for hsp90 binding and maintenance of the receptor in an inactive form (Cadepond *et al*, 1991). Receptor translation and hsp90 association have been mapped to this region, strongly suggesting that it is here that the highly conserved hsp90 interacts with the receptor (Pratt *et al*, 1988; Housely *et al*, 1990). This "transducing domain" may therefore be the location at which steroid binding results in dissociation of hsp90 from the steroid receptor (Figure 4-2). The proximity of the transducing domain to the DNA binding and nuclear localization domains has also suggested a mechanism by which hsp90 may repress DNA binding activity, namely by "masking" the domains required for nuclear localization and DNA binding.

Role of MoO_4^{2-} in steroid receptor-hsp90 stabilization. Intact 8-9S steroid receptors could only be isolated and characterized after the fortuitous observation that molybdate (MoO_4^{2-}) and other transition metal oxyanions (including tungstate and vanadate) stabilized these structures and prevented dissociation to the 4S forms (Leach *et al*, 1979). The mechanism through which molybdate stabilizes steroid receptors is not clearly understood,

although crosslinking studies have demonstrated that molybdate may be in physical contact with both receptor and hsp90. It has been postulated that molybdate may crosslink phosphorylated amino acids, or possibly crosslink sulfhydryl residues. It is also unclear whether molybdate stabilizes receptors *in vivo*. Although molybdenum is an important enzyme cofactor in nature, current evidence suggests that it may not serve to stabilize GR *in vivo* (Sanchez *et al*, 1986). Trace metals with higher *in vivo* concentrations (i.e. Zn, Cu, Fe) fail to stabilize receptors *in vitro* (Dahmer *et al*, 1984). These results have stimulated a search for endogenous factor that may stabilize the 8-9S form *in vivo*. Several groups have found increased receptor transformation in cytosols in which all low molecular weight components have been removed by filtration of dialysis (Bodine and Litwack, 1988; Meshinchini *et al*, 1988). Readdition of the low molecular weight fraction restores stabilizing activity. Pratt and colleagues have purified an extremely low molecular weight factor (M_r < 400) from rat liver cytosols that can stabilize glucocorticoid receptor *in vitro* in a manner similar to molybdate (Meshinchi *et al*, 1988). This factor is an anion, is heat stable, protease resistant and can be removed by treatment with Chelex-100, suggesting that it is a metal (Meshinchi and Pratt, 1989; Hutchinson *et al*, 1992a). It is also bound by a sulfhydryl matrix, suggesting it may act by crosslinking sulfhydryl residues. Molybdate may therefore be acting at the same site as this endogenous stabilizing factor. Other studies, however, suggest that stabilizing factor may be an aminophosphoglyceride that stabilizes GR in a manner similar to molybdate (Bodine and Litwack, 1988a; Bodine and Litwack, 1988b).

Effects of receptor phosphorylation on ligand binding and transformation. The ability of steroid receptor to bind ligand and subsequently undergo transformation may be dependent on posttranslational modifications to the steroid receptor or associated proteins such as phosphorylation. The GR and hsp90 were both originally isolated as

phosphoproteins based on their ability to bind ^{32}P in the presence of ATP (Housely and Pratt, 1983; Grandics *et al*, 1984; Housely *et al*, 1985). Both GR and associated hsp90 have been found to be phosphorylated almost entirely on serine residues (Housely and Pratt, 1983). Six phosphorylated serines and one threonine are predominantly found in the N-terminal end of the receptor as determined by limited proteolysis and phosphopeptide mapping of rat liver, WEHI-7 lymphoma and rat L-cell receptor, and to a lesser degree in the DNA binding and steroid binding domains (Tienrungroj et al, 1987a; Hoeck and Groner, 1990; Dalman *et al*, 1988; Smith *et al*, 1989). Anti-phosphotyrosine antibodies can also precipitate GR, indirectly suggesting tyrosine phosphorylation (Auricchio *et al*, 1989). Almost all serine and threonine phosphorylation sites are in known kinase consensus sequences, including casein kinase II and $p34^{cdc2}$-$p58^{cyclinA}$ (Bodwell *et al*, 1991). Rat L-cell GR may even autophosphorylate at threonine residues, although results are conflicting (Miller-Diener *et al*, 1985). Mouse L cells show a stoichiometric relationship of approximately 2-3 phosphates per molecule of [3H] dexamethasone 21-mesylate in the untransformed receptor, containing hsp90 (Mendel *et al*, 1987). GR and other steroid receptors therefore have the structural requirements to be phosphorylated and dephosphorylated in a regulatory manner.

Early experiments with rat thymocytes and other cell types demonstrated that GR hormone binding capacity increases and decreases simultaneously with cellular ATP levels, even when protein synthesis is inhibited (Sloman and Bell, 1976). These results suggested that steroid receptor was regulated by a phosphorylation/dephosphorylation cycle dependent on cellular levels of ATP. Treatment with alkaline phosphatase has been found to inactivate hormone binding in GR, suggesting that receptor phosphorylation is necessary for successful ligand binding (Barnett *et al*, 1980). More recently, phosphatase inhibitors such as okadaic acid have been found to both promote ligand binding and

activate transcription at a GRE-containing reporter gene (DeFranco *et al*, 1991). Protein kinase C, among other serine/threonine kinases, has also been found to influence hormone binding to GR. Phorbol esters have been found to increase hormone-induced gene expression of liver enzymes, while PKC inhibitors such as staurosporin inhibited glucocorticoid-associated nuclear translocation and transcription (Kido *et al*, 1987). Nevertheless the role of PKC in GR modulation shows much conflicting data as to its effects. The need for phosphorylation for ligand binding and subsequent gene expression has also been demonstrated for virtually all known steroid receptors (reviewed by Orti *et al*, 1992).

Despite the apparent need for phosphorylation/dephosphorylation activity in initial GR activation, the precise sequence of events and effects on receptor transformation have been difficult to ascertain and are frequently conflicting. Inhibitor studies have indirectly concluded that activation of glucocorticoid receptors is generally preceded by dephosphorylation of the receptor (Housely *et al*, 1985). This is supported by the effects of phosphatases in deactivating ligand binding and phosphatase inhibitors in stimulating activation. Nevertheless, more recent metabolic labeling studies have shown no such phosphorylation during activation (Mendel *et al*, 1987; Mendel *et al*, 1990). Kinetic studies have also indicated that hyperphosphorylation of the receptor may occur immediately after ligand binding (Orti *et al*, 1992). Phosphorylation may therefore not be directly responsible for ligand binding, but may facilitate alterations in the receptor leading to transformation. A dephosphorylation/phosphorylation cycling model has been proposed to maintain cellular receptors in a state that promotes affinity of receptor for ligand (Orti *et al*, 1989; Orti *et al*, 1993). Interestingly, phosphorylation occurs following agonist binding but not antagonist binding, suggesting that it is dependent on a productive ligand binding event.

Following activation and hyperphosphorylation, no *in vivo* changes in receptor phosphorylation have been observed during the transformation process or DNA binding. This is also true for hsp90, which possesses several serines that can be phosphorylated. *In vitro* dephosphorylation has also been found to have no effect on salt-induced transformation or DNA binding of activated GR. Dephosphorylation may however be a necessary step in the association of the transformed receptor with the nuclear matrix (Miller-Diener *et al*, 1987; Auricchio, 1989; Mendel *et al*, 1990). The effects of phosphorylation on post-activation receptor events is therefore only now being elucidated.

Effects of receptor oxidation/reduction state on ligand binding and transformation. The oxidation or reduction state of sulfhydryl residues have been shown to exert profound effects on the ability of GR to bind steroid and the subsequent transformation to the DNA binding form (Grippo *et al*, 1983; reviewed by Pratt, 1987). The role of sulfhydryl residues in receptor function has been studied extensively using affinity ligands and reagents that alter the redox state of these residues through crosslinking or low molecular weight modification.

Cloning of the GR has revealed multiple cysteine residues, both single and clustered. They are located in all receptor domains including the DNA binding and steroid binding regions. The best characterized functionally relevant sulfhydryl residues are a series of cysteines present in the steroid binding domain (Chakraborti *et al*, 1990). Three cysteines in the rat glucocorticoid receptor, residues 640, 656 and 661 are believed to play an important role in high affinity binding of ligand to receptor (Figure 4-3)(Chakraborti *et al*, 1990). Radiosequenation following affinity labeling with [^{3}H]-dexamethasone 21-mesylate has demonstrated that Cys656 is the target of this affinity ligand, strongly arguing important role for this region of the steroid binding domain in ligand recognition and binding (Simons *et al* 1987; Smith *et al*, 1988). Early

experiments demonstrated that maintenance of these residues in a reduced state using dithiothreitol (DTT) or 2-mercaptoethanol (2-ME) was necessary for high affinity *in vitro* ligand binding (Simons *et al*, 1981). Ligand binding was also inhibited by agents that crosslinked vicinal thiols (Cullen *et al*, 1984), including arsenite (AsO_2^-), cadmium and selenite (SeO_2^-), effects that could be reversed by DTT or 2-ME (Simons *et al*, 1990). Interestingly, zinc has been observed not to inhibit ligand binding in rat fibroblast cytosols, despite its similarity to cadmium. Low molecular weight modification of vicinal thiols in such a way as to inhibit crosslinking (such as methylation of cysteines with agents such as MMTS) do not inhibit ligand binding but do prevent affinity labeling with dexamethasone 21-mesylate (Simons *et al*, 1990; Chakraboti *et al*, 1990). Site-directed mutagenesis of cysteine residues in the steroid binding domain of transfected rat GR in rat HTC cells also suggest that Cys656 and Cys660 are necessary for normal steroid binding (Chakraboti *et al*, 1992). These results suggest that vicinal thiols in the steroid binding domain play an important role in steroid binding, and that the redox state of these residues affect binding affinity.

Sulfhydryl-reactive agents have also been used to determine whether thiol residues are involved in receptor transformation. Iodoacetamide and N-ethylmaleimide have both been used to modify receptor sulfhydryls and have been shown to inhibit receptor transformation (Kalimi and Love, 1980). Hydrogen peroxide has been used to oxidize sulfhydryl residues in rat liver and L cell cysotolic receptor, the result being the inhibition of transformation to the 4S form even following incubation at 20°C (Tienrungroj *et al*, 1987b). Reduction of the sulfhydryls with DTT reverses this inhibition, resulting in conversion to the 4S form. Hydrogen peroxide also prevents transformation of L cell receptor immunoabsorbed to protein A-Sepharose with BUGR2 antibody (Tienrungroj *et al*, 1987b). This behavior is similar to that observed for transition metal oxyanions such

as molybdate. Although no specific studies have looked at the effects of metal ions and oxyanions on receptor transformation, an early study suggests that zinc at high concentrations might prevent GR transformation (Kalimi and Love, 1980). All of these experiments suggest that the GR possesses thiol residues that must be in a reduced form for successful transformation to the 4S form to proceed. In addition, the oxidation/reduction state of sulfhydryl residues may also play a role in the binding of activated GR to the nuclear matrix (Kaufmann *et al*, 1986).

The fact that molybdate and other transition metal oxyanions can inhibit receptor transformation and preserve the structure of the 8-9S form begs the question of whether molybdate may be forming stable bridges between cysteines located in close proximity on the GR and hsp90 in the docked position. Computer analysis of the protein folding patterns produced by the receptor and hsp90 resulted in three instances where weak leucine zippers and proximal cysteines might permit the formation of stable bridges that would facilitate protein-protein binding (Figure 4-4)(Schwartz *et al*, 1993). Although one or more of these structures may be the site of molybdate interaction, the actual endogenous stabilizing factor may be another metal that can crosslink adjacent thiols.

Other proteins associated with untransformed steroid receptors. Although hsp90 was the earliest non-steroid binding protein found to be associated with GR, several other proteins are associated with the 8-9S form, detected either by coabsorption with GR followed by SDS-PAGE or by HPLC (Idziorek *et al*, 1985; Denis *et al*, 1988; Perdew and Whitelaw, 1991; Rexin *et al*, 1991a; Smith and Toft, 1993). The number and identity of these proteins often varies between cell types and preparative methods, and may carry some functional significance with regard to the roles of these accessory components. **Hsp70** is an abundant heat shock protein that is strongly associated with overexpressed GR isolated from Chinese hamster ovary cells, but not with rat liver or

mouse L cell cytosol (Sanchez *et al*, 1990a) as well as with avian PR (Kost *et al*, 1989). This may be functionally significant as CHO receptor is almost entirely sequestered in the nucleus of the cell as opposed to the cytoplasm. Hsp70 has also been found in stable complexes with hsp90 in cytosol. In PR, hsp70 is found to associate transiently with untransformed receptor in the cytosol (Smith *et al*, 1992b) and can bind ATP both in GR (Hutchinson *et al*, 1992a) and in PR (Kost *et al*, 1989). These results suggest that hsp70 may serve in combination with other proteins to facilitate receptor-hsp90 assembly through regulation of receptor unfolding, therefore acting as a *molecular chaperon* (Pratt *et al*, 1992). Recent in vitro evidence suggests that hsp70 is in fact required for this (Hutchinson *et al*, 1994). The failure of hsp70 to dissociate from GR in CHO cells may explain their abnormal receptor sequestration in the nucleus in the absence of hormone (Sanchez *et al*, 1990).

Two other proteins have been found to coprecipitate with GR in multiple systems. **P56** (hsp56)(isolated as a 59 to 60 kd protein in some systems) is thought to interact with receptor through interaction with hsp90, and is thus lost during transformation (Renoir *et al*, 1990; Perdew and Whitelaw, 1991). It can also be crosslinked both to receptor and to hsp90. p56 is also found in complexes with hsp90 and hsp70 in cytosol, and also is expressed in a manner consistent with heat shock proteins (Sanchez *et al*, 1990b). Hsp56 may therefore also act as a molecular chaperone in a manner similar to hsp70, although it appears to associate in a manner comparable to hsp90. Perhaps of greater significance is the finding that hsp90 binds the immunophilin ligand and immunosuppressant FK506, which in combination with protein homology data makes it a member of the immunophilins (Ku Tai *et al*, 1992; Lebeau *et al*, 1993). This implies that hsp56 may play an important signalling role via activation of calcineurin. The implications for GR are as yet unknown, although FK506 and another immunophilin ligand rapamycin have

been found to stimulate dexamethasone-induced MMTV-CAT gene expression in L929 cells (Ning and Sanchez, 1993). This stimulation is believed to be the result of increased translocation of the transformed receptor to the nucleus.

P23 is an acidic phosphoprotein associated with both GR and PR (Sanchez *et al*, 1990b). P23 may be a low molecular weight heat shock protein, and may possess some unique features as well. It has been suggested that p23 belong to a group of recently isolated low molecular weight FK506-binding immunophilins.

The currently postulated GR holoreceptor is depicted in Figure 5. It consists of the core receptor protein (97 kd), two molecules of hsp90, hsp56 and one or more units of p50, p23 or p14. Hsp70 is not associated with GR in the same manner as hsp90 and its interaction is assumed to be transient. Assuming single units of these smaller subunits, the total molecular weight of the GR holoreceptor would be approximately 290 kd, comparable to the value arrived at by molecular sieve chromatography (Bresnick *et al*, 1990). While most of these studies have been carried out in molybdate-stabilized cytosolic extracts, recent cell crosslinking studies suggest that a similar holoreceptor exists *in vivo* as well (Rexin *et al*, 1992).

Current concepts in steroid receptor transformation and translocation. The complexity of the cytosolic GR and the precise regulation of its association with hsp90 and other associated proteins have suggested that its role is not limited to the masking the nuclear localization and DNA binding domains to prevent ligand-independent nuclear localization. Hsp90 has been found in cytosols in complex with hsp70, hsp56 and p23 independent of GR association. These complexes have been termed "docking complexes" (Pratt, 1990a; reviewed by Pratt, 1992). In association with the receptor as an untransformed heteromer, these docking complexes are believed to regulate ATP-dependent receptor and hsp90 unfolding such that hsp90 can productively associate and

dissociate from the receptor (Csermely *et al*, 1993). They may also maintain the receptor in such a conformation that it can successfully interact with ligand. Following transient association with hsp70, the receptor-hsp90-hsp56-p23 complex has also been found to interact with tubulin *in vitro*, thus providing a potential mechanism for transport of the receptor to the outer nuclear envelope (Pratt *et al*, 1989; Scherrer and Pratt, 1992). This complex has been thus termed a *transportosome*, and requires the unfolding activity of hsp70 to form an active structure of this type (Pratt *et al*, 1992). A proportion of receptors in the cell have in fact been postulated to contain "misfolded" receptors and as a result are inactive (Hutchinson *et al*, 1992). The association of GR with hsp90 occurs soon after translation, suggesting that hsp70 would interact almost immediately to facilitate the receptor-hsp90 complex followed by attachment to a cytoskeletal element for transport to the nucleus. Following ligand binding, nuclear localization and DNA binding are derepressed by hsp90 dissociation, and response element binding can proceed. Receptors can then be cycled in and out of the nucleus, allowing tight control over transcriptional activation. This model for transcriptional control of GR has been observed for other transcriptional activators as well (including $pp60^{v\text{-}src}$) and makes it a precisely regulated system of transcriptional control (Pratt, 1992).

Nuclear localization and translocation. Following steroid binding, receptor transformation and cytoskeleton-mediated transport the receptor must interact with the outer nuclear envelope and translocate across the nuclear membrane to gain access to the nuclear chromatin, presumably through nuclear pores. Early work has shown that 4S transformed receptors preferentially bind to isolated nuclei *in vitro* over 9S untransformed receptors (Hubbard and Kalimi, 1983). Cloning of the GR and subsequent deletional mapping have isolated two nuclear localization signals, termed NL1 and NL2 (Figure 4-2)(Picard and Yamamoto, 1987). NL1 is approximately 28 residues long and is located

between the steroid binding and DNA binding domains. The 7 residue core (TKKKIKG) has roughly 50% homology to the nuclear localization signal of SV40 large T antigen (PPKKKRKV) and bears considerable homology to other steroid receptor nuclear localization signals. Homology between mouse, rat and human NL1 in GR is highly conserved. Mutations in this region prevent nuclear localization but do not block *in vitro* DNA binding, suggesting that these two events are distinct (Picard *et al*, 1987). Synthetic NLS peptide can inhibit binding to isolated nuclei (LaCasse and Lefebvre, 1991). NL2 covers the entire steroid binding domain, and may be made up of several separate sequences that are brought together during protein folding. NL2 has been termed an inactivation signal, since its presence in the steroid binding/hsp90 interaction domain resultings in the masking of NL1 in the untransformed receptor, blocking nuclear localization. Neither NL1 nor NL2 can bind DNA *in vitro*, also suggesting the separate nature of nuclear localization and DNA binding. Fusion proteins constructed with NL1 and/or NL2 with *E. coli* β-galatosidase (normally non-nuclear) without inclusion of the steroid binding domain constitutively localize to the nucleus, while constructs containing the steroid binding domain do so only in the presence of dexamethasone (Picard *et al*, 1988). GR contrasts with ER in the structure of NL2 and its subsequent ability to inactivate NL1; this may be functionally reflected in the fact that ER sequesters to the nucleus even in the absence of ligand (Picard *et al*, 1990a). Posttranslational modification of GR with O-linked N-acetylglucosamine residues may also be necessary for successful nuclear localization. To date, it is unclear whether changes in phosphorylation are necessary for nuclear translocation, although some reports suggest that GR receptor is dephosphorylated to some extent once in the nucleus (Mendel *et al*, 1990).

It has now been shown definitively that hsp90 must dissociate from the GR prior to nuclear translocation *in vivo*. It is now known from immunocytochemical localization studies that hsp90 likely masks both the DNA binding and nuclear localization domains,

making dissociation a necessity for both processes (LaFond *et al*, 1988; Antakly *et al*, 1989; Cidlowski *et al*, 1990; McGimsey *et al*, 1991). The GR has also been shown to be in precisely the same structural form for DNA binding and isolated nuclei binding by anion exchange chromatography (Groul *et al*, 1989). The receptor cycling model also suggests that transformed receptor should be able to be exported out of the nucleus, an ability that has been demonstrated for a fairly small number of proteins. Recent studies with heterokaryons have shown that glucocorticoids can be bidirectionally transported in and out of the nucleus, consistent with the receptor cycling model (Madan and DeFranco, 1993).

DNA binding. The ability of GR to bind DNA was one of its earliest known characteristics. Receptor binding to herring sperm DNA chemically coupled to cellulose or other solid supports has until recently been the most frequently used methods to assay for the transformed 4S, DNA binding form of the receptor versus the untransformed, 9S receptor form. The ability to bind DNA led to speculation that GR could affect gene regulation.

A specific DNA sequence recognized by the GR was first demonstrated using sequences derived from the mammary tumor virus (MTV), a retrovirus whose expression is induced by glucocorticoids (Scheiderit *et al*, 1983). Receptor-specific DNA sequences were then isolated from mammalian cells. Analysis of these sequences by deletion analysis and methylation protection studies has resulted in the identification of a consensus binding sequence, 5'-AG(A/G)ACATCCTGTACA-3', an imperfect palindrome. Glucocorticoid response elements (GREs) have been found associated with a number of glucocorticoid-responsive genes including human metallothionein IIA and rat tyrosine aminotransferase, almost always within the 5'-flanking regions of the promoter but infrequently on the 3' side of the promoter as well (Gustaffson *et al*, 1990). GREs

derived from MTV can confer inducibility by glucocorticoids on heterologous promoters. GREs are usually found in multiple numbers, and both *in vivo* transfection studies and *in vitro* gel mobility shift assays suggest that GR interacts and enhances transcription more effectively when multiple GREs are present (Wrange *et al*, 1986; Schmid *et al*, 1989; Wright and Gustaffson, 1991). The length of the intervening sequences between GREs and the subsequent physical positioning of the GREs indicates that receptor binding occurs most efficiently when the sequences are oriented identically (Schmid *et al*, 1989). These results suggest that the receptor may bind DNA in multiple units. Current evidence suggests that receptors bind DNA in a homodimeric fashion (Vedeckis, 1992). Regions required for dimerization are located in both the steroid binding and DNA binding domain (Dahlman-Wright *et al*, 1992; Dahlman-Wright *et al*, 1993). Overexpressed DNA binding domains alone cannot dimerize, also suggesting that regions outside the DNA binding domain are necessary for high affinity DNA binding (Vedeckis, 1992).

Very recent evidence also suggests that two forms of the transformed receptor, non-DNA binding and DNA binding may also exist, lending another level of control to GR-mediated gene expression. Tryptic fragments from both forms containing the DNA binding domain both bind DNA, suggesting that structural differences accounting for non-DNA binding behavior must occur outside this domain (Hutchinson *et al*, 1992b). Alterations in disulfide crosslinking in the N-terminal domain (modulating) may account for these differences.

DNA binding domain and zinc fingers. The DNA binding domain of glucocorticoid receptor is located on the C-terminal side of the protein immediately N-terminal to the steroid binding domain and NL1 (Figure 4-2), in the 17 kd C-terminal core fragment isolated by limited proteolysis and approximately 90 residues long (Wrange *et al*, 1978). Cloning and sequencing of the receptor revealed a cysteine-rich region in the DNA

binding domain. This region was found to contain two so-called zinc fingers, zinc-stabilized peptide loops that have been found in other DNA binding proteins such as transcription factor IIIA (Vallee *et al*, 1991). While many zinc fingers (including TFIIIA) utilize two cysteines and two histidines to bind zinc in a tetrahedral structure, steroid receptor zinc fingers appear to utilize four cysteines to coordinate zinc in a similar fashion (Figure 4-6)(Archer *et al*, 1990; Freedman, 1992; Dahlman-Wright *et al*, 1992). The presence of zinc fingers in the DNA binding domain has been further supported by the recent elucidation of the solution structure of rat GR by NMR (Hard *et al*, 1990). The requirement of zinc occupancy in the zinc fingers for DNA binding is absolute; stripping GR and PR of bound zinc by dialysis or Chelex-100 treatment reduced receptor affinity for DNA by over 20-fold (Freeman *et al*, 1988; Westin and Schaffner, 1988).

The amino acid sequence for rat GR is Cys-X_2-Cys-X_{13}-Cys-X_2-Cys-X_{15}-Cys-X_5-Cys-X_9-Cys-X_2-Cys-X_4, giving two zinc fingers of different loop sizes in close proximity (Freedman, 1992). The C-terminal finger contains five highly conserved cysteines, although only four are required for zinc binding. Two-dimensional NMR and crystal structures indicate that Cys500 (at the C-terminal end of the finger) is not involved in zinc coordination, but is probably necessary for α-helix formation and is thus conserved (Hard *et al*, 1990. This has also been found true for human GR (Cys481)(Zilliacus *et al*, 1992a). The C-terminal finger also contains five cysteines, but only the four coordinating residues are conserved. The intervening residues in the loops are dissimilar and unique to each finger. Genetic analysis has demonstrated that each zinc finger is encoded for by a separate exon (Freeman, 1992).

Traditional site-directed mutagenesis in mammalian cells and random mutational selection studies in yeast with degree of function based both on ability to bind GREs and to transactivate CAT expression have revealed that all cysteines predicted to bind zinc are necessary for both DNA binding and transactivation, but do not alter hormone binding

(Schena and Yamamoto, 1988; Segard-Maurel *et al*, 1992). In addition, all residues immediately C-terminal to the loops are also essential for function. Mutations of residues on the "tips" of the zinc fingers do not abolish DNA binding but do reduce transcriptional activation, indicating that they may be required for the interaction of additional transcription factors following DNA binding (Schena *et al*, 1989).

Specificity of GR binding to GREs is conferred by the zinc fingers and surrounding sequences. Chimeric ER/GRs have been constructed that incorporate a GR DNA binding domain into a truncated ER (Green and Chambon, 1987). These chimeric receptors activate a GRE-dependent CAT reporter gene in response to estradiol, but not an ERE-dependent reporter. Functional analysis carried out in this way reveals that the N-terminal finger is primarily responsible for receptor specificity, but the C-terminal finger is necessary for increased binding affinity. Basic residues at the C-terminal side of the zinc fingers appear to be required as well. Gly458, Ser459 and Val462 in the N-terminal finger of rat GR appear particularly important in receptor specificity, results that have also been confirmed for human receptor (Glu439, Ser440 and Val443)(Danielson *et al*, 1989; Zilliacus *et al*, 1992b). The α-helical structure of the fingers and C-terminal domain appear to be very important in maintaining the DNA binding affinity of the DNA binding domain.

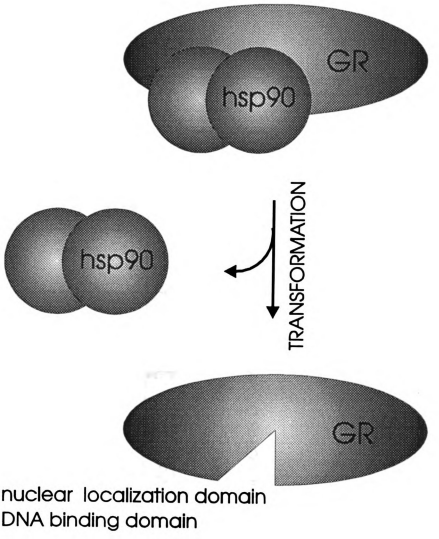

Figure 4-1. Simplified model for glucocorticoid receptor (GR) transformation. Dissociation of the hsp90 homodimer and other associated protein subunits (not shown) results in "unmasking" of the nuclear localization and DNA binding domains.

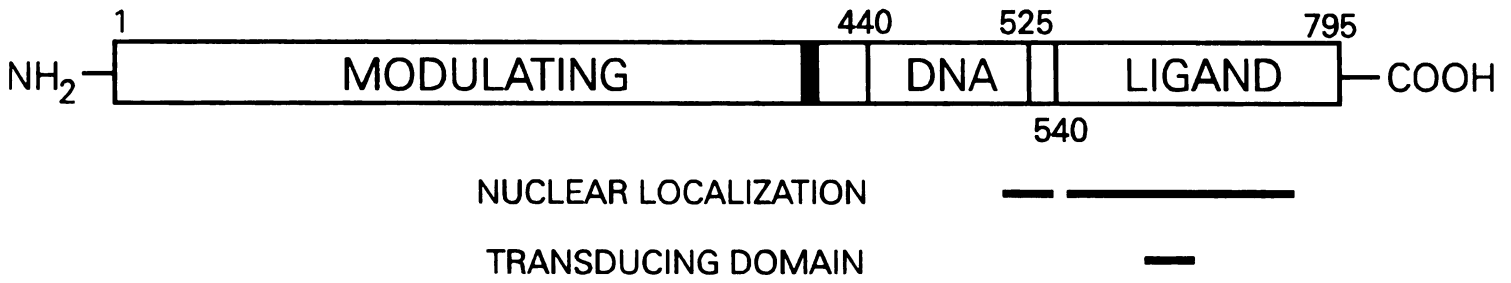

Figure 4-2. Linear map of the rat GR functional domains (ligand binding, DNA binding, modulating, signal transducing and nuclear localization). The shaded bar in the modulating domain represents the binding epitope of the monoclonal anti-GR antibody BUGR2 (Gametchu and Harrison, 1984).

Figure 4-3. Residues 630 through 670 of the rat GR steroid binding domain, showing the location of the vicinal thiol residues (arrows).

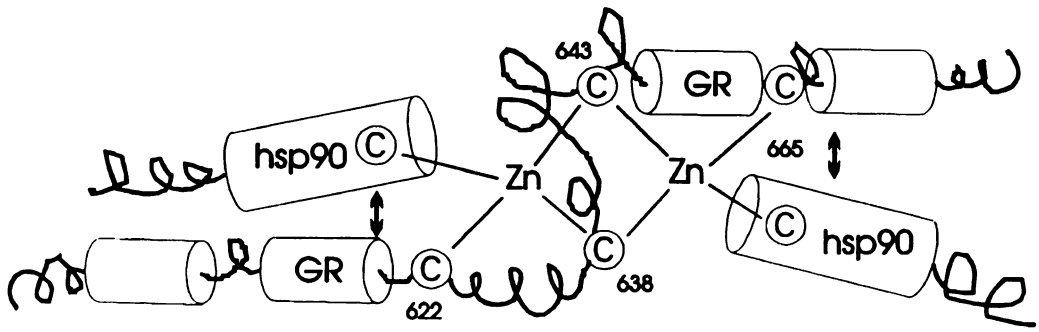

Figure 4-4. A possible model for rat GR-hsp90 interaction through zinc-cysteine crosslinking and weak leucine zippers based on predicted polypeptide folding patterns from amino acid sequence data. Cylinders represent weak leucine zipper moieties (LLLR) in GR and hsp90. Arrows indicate potential leucine zipper interactions. Adapted from Schwartz *et al*, 1993.

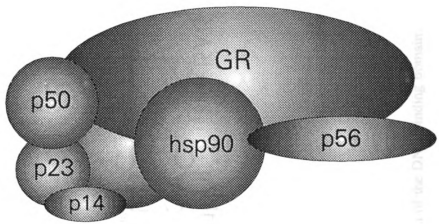

Figure 4-5. Current model for GR holoreceptor. Association in this diagram indicates actual association in holoreceptor based on crosslinking and coprecipitation data. Adapted from Smith and Toft, 1992a.

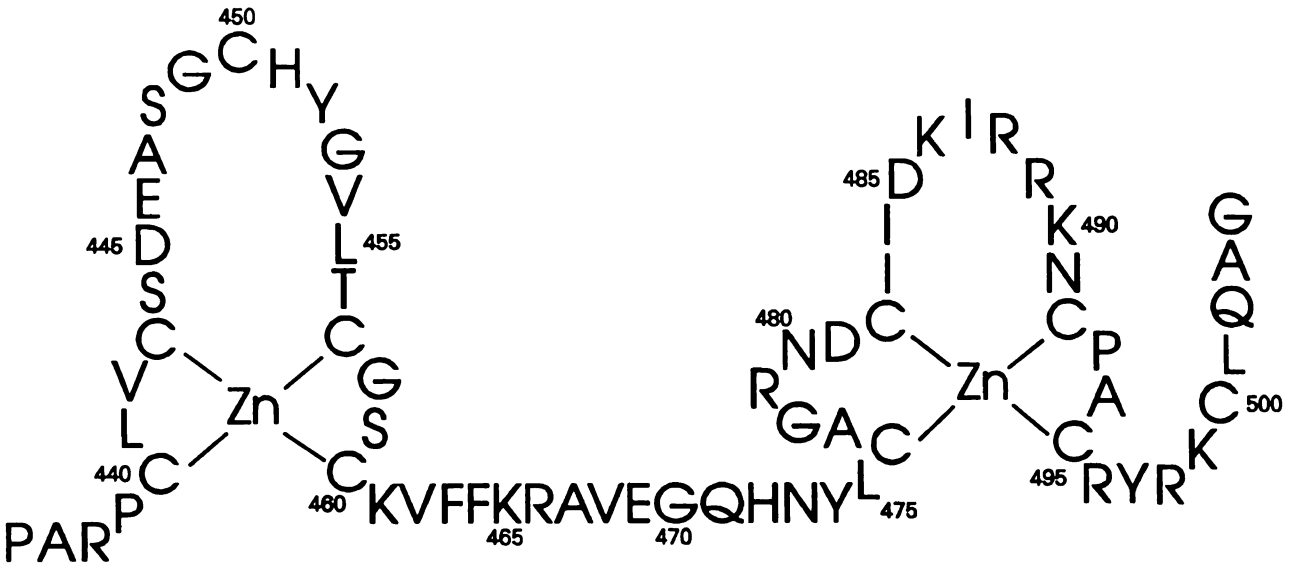

Figure 4-6. Amino acid sequence of rat GR zinc finger binding region of the DNA binding domain.

CHAPTER 5

GLUCOCORTICOID-INDUCED APOPTOSIS IN MOUSE THYMOCYTES

CHAPTER 5: ABSTRACT

Previous work has demonstrated that flow cytometric DNA content analysis can be a useful tool in the detection of apoptotic death in rodent thymocytes and lymphocytes. Apoptotic cells have been found to accumulate in a hypodiploid ($< G_0/G_1$) region of the flow cytometric DNA cell cycle, making the percentage apoptotic cells in a typical sample easy to quantitate and allowing apoptotic analysis on an individual cell basis. In this chapter, these observations have been further supported by correlation of cells in the hypodiploid region with apoptotis-associated cytoplasmic collapse (as analyzed by flow cytometric forward scatter analysis), visible apoptosis-associated morphological changes (as analyzed by electron microscopy) and DNA fragmentation by fluorescence-activated sorting of apoptotic cells. In addition, the sequential kinetics and glucocorticoid-dependency of steroid-induced death have been further defined. Fluorescent immunophenotyping has also been combined with flow cytometric apoptotic analysis to determine that glucocorticoids induce lineage-specific apoptosis in the $CD4^+CD8^+\alpha\beta TCR^{lo}CD3\epsilon^{lo}$ thymocyte subset, supporting the notion that glucocorticoids may play a role in the positive and negative selection of maturing T lymphocytes.

CHAPTER 5: INTRODUCTION

As reviewed in Chapter 1, apoptosis (or physiological cell death) is believed to play a critical role in the regulation of the immune system. Perhaps the most-studied model for the mechanism and role of apoptotic death in immune regulation is the induction of cell death in the murine thymus by glucocorticoids (Cohen *et al*, 1992). Physiologically relevant concentrations of natural glucocorticoids and lower concentrations of synthetic glucocorticoids (10^{-8} to 10^{-6} M) can induce dose- and time-dependent *in vitro* apoptotic death in cell cultures of mouse thymocytes within hours following addition (Cohen and Duke, 1984). Elevation of *in vivo* glucocorticoid levels with implanted glucocorticoid tablets can also induce rapid thymic atrophy in mice, a process directly linked to the induction of thymocyte apoptosis (Garvy *et al*, 1994). The importance of apoptosis in the clonal deletion of potentially autoreactive or dysfunctional immature thymocytes through the mechanisms of positive and negative thymic selection has made the induction of thymocyte apoptosis by glucocorticoid treatment an important model of elucidating the mechanism of apoptotic death in thymocytes. Although the role that *in vivo* glucocorticoid levels play in the normal thymocyte apoptosis is only now being elucidated (a process that is probably in part mediated through through appropriate engagement of the T cell receptor complex at the appropriate point during thymic selection), studies in glucocorticoid-induced thymocyte apoptosis almost certainly have mechanistic relevance to the process of thymic clonal deletion (Iwata *et al*, 1993).

The study of apoptosis in mouse thymocytes and all other cell types is dependent on the identification of biochemical and morphological changes that occur in cells during physiological death. Mouse thymocyte apoptosis has most frequently been detected and quantified by the presence of endonuclease-induced internucleosomal DNA fragmentation that occurs during the course of apoptotic death (Wyllie *et al*, 1980a). DNA

fragmentation in apoptotic thymocytes is traditionally measured either by separation and quantitation of fragmented DNA as a percentage of total chromatin, or by gel electrophoresis of thymocyte lysates, with the fragmented DNA appearing as a 200 bp multimer "ladder" of internucleosomal fragments. Both of these assays are considered qualitative indicators of apoptotic death, since they measure the relative amount of fragmented DNA and not the actual percentage of cells undergoing apoptosis.

Recently, our laboratory presented a novel method for the detection of apoptotic cells in single cell suspensions by flow cytometric analysis. Apoptotic thymocytes were found to bind stoichiometrically lower amounts of DNA binding dyes such as propidium iodide than normal G_0/G_1 cells. When thymocyte populations containing apoptotic cells (following treatment with glucocorticoids, for example) were analyzed for DNA dye fluorescence, a hypodiploid ($< G_0/G_1$) region appeared in the context of the normal DNA cell cycle. In Telford *et al* (1991), cells in this region were shown to have undergone apoptosis-associated chromatin degradation. Flow cytometry could therefore be used to accurately quantitate apoptotic cells in a single cell suspension on an individual cell basis. In addition to providing a more experimentally relevant analysis of immune cell apoptosis, flow cytometric analysis has allowed a more comprehensive analysis of the kinetics, glucocorticoid dependency and lineage specificity of hormone-induced thymocyte apoptosis. In addition, the incorporation of fluorescent immunophenotyping for T-lineage surface markers with flow cytometric analysis of apoptotic death has permitted a detailed analysis of the lineage-specificity of glucocorticoid-induced cell death. These studies have more clearly defined the mechanism and regulation of *in vitro* steroid-induced cell death, with possible relevance to *in vivo* thymocyte death as well. In the first part of this chapter, new data are presented that further bolsters the conclusion that thymocytes in the hypodiploid region of the cell cycle represent cells that have undergone the biochemical and morphological changes characteristic of physiological cell death. In the second part

of this chapter, this methodology is used to more clearly define the kinetics, requirements and specificity of steroid-induced thymocyte apoptosis.

CHAPTER 5: MATERIALS AND METHODS

The flow cytometric methodology used herein is as described in Telford *et al* (1991). Exceptions and modifications are noted.

Preparation of mouse thymocytes. Whole thymuses from young (6 to 12 weeks old) male A/J mice were surgically removed and extruded through 100 micron stainless steel screens into Hanks balanced salt solution (HBSS) or phosphate buffered saline (PBS) containing 2% FBS. Cells were erythrocyte-depleted over Histopaque 1083 gradients (Sigma), washed twice by centrifugation at 800 x g followed by resuspension in HBSS/FBS or PBS/FBS.

***In vitro* treatment of thymocytes with glucocorticoids.** Thymocytes were resuspended in RPMI-1640 supplemented with 10% heat-inactivated FBS and incubated in 24 well plates at 2 x 10^6 cells/ml/well at 37°C under atmospheric conditions of 5% CO_2 for periods up to ten hours. Dexamethasone and corticosterone were added at the beginning of the culture period at 0.1 μM and 1 μM respectively.

In the glucocorticoid treatment experiment described in Figure 5-6, mouse thymocytes were plated with corticosterone at 1 μM as described above. Following incubation periods with steroid ranging from 30 minutes to 4 hours, the cells were removed, washed twice with RPMI/FBS and replated without corticosterone. Cells were then allowed to incubate for a total of eight hours from the beginning of culture and were analyzed for apoptotic death. Cells incubated either with corticosterone for the incubation period and replated with corticosterone, or without corticosterone and replated without corticosterone were run simultaneously as controls for the effects of the washing process. All data points shown are for eight hours incubation. All experiments were repeated at

least twice.

Detection of thymocyte apoptosis by flow cytometry. Following incubation, thymocytes were removed from culture and washed once with cold PBS. Samples were then decanted and and ethanol-fixed by one of two methods. In the first method, 2 mls of cold 80% ethanol was added directly to cells, the technique described in Telford *et al* (1991). In the second method, cells were resuspended in 0.4 mls 50% FBS in PBS followed by dropwise addition of 1.2 mls cold 70% ethanol with gentle vortexing (Garvy *et al*, 1993). Samples were then incubated for at least one hour at 4°C with both methods. The fixed cells were then washed twice with cold PBS and finally resuspended in 1 ml of 50 μg/ml propidium iodide in PBS supplemented with DNase-free RNase at 0.05 mg/ml and EDTA at 0.5 mM. Samples fixed by the first method required the inclusion of 0.1% Triton-X-100 in the staining reagent, while the second method required no detergent. Samples were then stored overnight at 4°C prior to flow cytometric analysis.

Detection of phenotype-specific apoptosis in mouse thymocytes. Following incubation, thymocytes were resuspended in PBS supplemented with 10% FBS and 0.1% sodium azide at 2 x 10^6 cells per ml per sample and immunophenotyped for T-lineage markers. $\alpha\beta$TCR and CD3ϵ were labeled with FITC-conjugated monoclonal antibodies to these markers (from H57-597 and 145-2C11 murine hybridomas) for two-color analysis with PI. CD4 α-chain was labeled with a FITC-conjugated monoclonal (GK1.5) and CD8 with a biotin-conjugated monoclonal (53.2) followed by secondary labeling with PE-conjugated avidin for three-color analysis with DAPI. All labeling was carried out at 4°C for 30 minutes.

Following immunophenotypic labeling all samples were washed twice with PBS/FBS/sodium azide, fixed by the gentle fixation used by Garvy *et al* (1993) as

described above and resuspended in the PI staining reagent described above at 50 μg/ml (for two-color analysis of $\alpha\beta$TCR/CD3ϵ subsets) or the DNA dye 4'-6-diaminido-2-phenylindole (DAPI) at 1 μg/ml with EDTA at 0.1 mM (for three-color analysis of CD4/CD8 subsets). RNase treatment was not required with DAPI staining (Telford *et al*, 1992a). Samples were stored at 4°C until analysis.

Flow cytometry. Thymocyte samples with no fluorescent immunophenotyping or samples immunophenotypically labeled with a FITC-conjugated antibody and subsequently stained with PI (two-color) were flow cytometrically analyzed on an Ortho Cytofluorograph 50-H fluorescence-activated cell sorter (Becton-Dickinson, San Jose, CA) with an Intel 80386 processor-based microcomputer using Acqcyte™ data acquisition and MultiPlus™ data analysis software (Pheonix Flow Systems, Palo Alto, CA). Samples stained with DAPI, FITC and PE (three-color) were analyzed on a Vantage™ fluorescence activated cell sorter (Becton-Dickinson, San Jose, CA) using LYSYS-2™ data acquisition and analysis software. Fluorochrome excitation for two-color analysis required single argon laser excitation at 488 nm. Three-color analysis required simultaneous argon laser excitation at 488 nm for FITC and PE and krypton laser excitation at 350 nm for DAPI. PI or PE fluorescence was detected with a 620 - 700 nm long pass filter. FITC was detected using a 430 $\pm$ 15 nm wide bandpass filter. DAPI was detected using a 530 $\pm$ 20 nm wide bandpass filter.

Quantitation of apoptosis was carried out by determining the percentage of cells in the apoptotic or hypodiploid region of the PI or DAPI DNA cell cycle as previously described, either directly or following gating for phenotype (Telford *et al*, 1991; Garvy *et al*, 1993). Initial gating through PI or DAPI DNA width versus area fluorescence with inclusion of cells in the apoptotic region excluded debris and doublets prior to cell cycle and immunophenotypic analysis.

Flow cytometric sorting of apoptotic thymocytes and subsequent DNA labeling and gel electrophoresis. Thymocytes (50 x 10^6) were incubated with corticosterone at 1 μM using the culture conditions described above for five hours (calculated to give approximately 50% apoptotic thymocytes). The cells were then washed, fixed and stained with PI according to Garvy *et al* (1993) as described above. The resulting fixed cell suspensions were then sorted into apoptotic and G_0/G_1 fractions using an Ortho 50-H fluorescence activated cell sorter (the gating strategy is depicted in the top panel of Figure 5-3). Cells were sorted directly into guanidine HCl lysis buffer (1.52 M guanidine HCl, 20 mM Tris-HCl, 20 mM EDTA, 20 mM NaCl, pH 8.5) at a 1:1 volume:volume ratio. The resulting cell lysates were then adjusted to pH 8.5 and passed over anionic exchange genomic DNA purification columns (Qiagen) and the DNA fractions eluted, precipitated and resuspended in TE buffer (10 mM Tris-base, 0.1 mM EDTA, pH 8.0) according to the manufacturers instructions. The DNA concentration and purity was determined by 260/280 nm spectrophotometry and 0.2 μg DNA per sample was labeled with ^{32}P-α-CTP by nick translation (Boerhinger-Mannheim). The resulting radiolabeled genomic DNA was purified of unreacted deoxynucleosides using G-50 Sephadex minicolumns and the specific activity determined by precipitation with 10% trichloroacetic acid and spotting on glass fibre filters. The DNA samples were then loaded on 1.8% horizontal agarose gels in TAE buffer at 1 to 2 nCi specific activity per sample and electrophoresed at 60V for 4 hours. The resulting gels were dried under vacuum and autoradiographed for 24 to 72 hours. pBR322 plasmid and lambda phage HindIII digested DNA were labeled and electrophoresed concurrently to calculate the efficiency of the labeling reaction and as molecular weight markers respectively.

Electron microscopy of apoptotic thymocytes. 50 x 10^6 thymocytes were incubated with or without corticosterone at 1 μM using the culture conditions described above for eight

hours. The cells were then washed twice with cold PBS with centrifugation at 800 g for 5 minutes, transferred to 1.5 ml Eppendorf microcentrifuge tubes and washed one more time. The supernatant was decanted and the cells resuspended in 0.1% EM grade gluteraldehyde in PBS at 4°C. The cells were centrifuged, the supernatant decanted and 4% EM grade gluteraldehyde at 4°C in PBS was layered over the cell pellet. The cell pellets were incubated at 4°C overnight, the superantant removed, and PBS at 4°C was carefully layered over the cell pellets. The pellets were incubated another 24 hours at 4°C and subsequently embedded, sectioned and viewed by electron microscopy (Philips 300 transmission) at 5000 X magnification. Sufficient numbers of photomicrographs per sample were taken to allow at least 200 thymocytes to be scored for normal versus apoptotic morphology. A percentage of apoptotic cells per sample was then calculated.

CHAPTER 5: RESULTS

DETECTION OF GLUCOCORTICOID-INDUCED APOPTOSIS IN MOUSE THYMOCYTES BY FLOW CYTOMETRY.

Apoptotic thymocytes accumulate in a hypodiploid region of the DNA cell cycle referred to as the apoptotic region. *In vitro* treatment with physiological levels of glucocorticoids causes apoptosis in mouse thymocytes. When glucocorticoid-treated thymocytes were fixed with ethanol, stained with propidium iodide (PI) and flow cytometrically analyzed for PI fluorescence, the apoptotic cells appear in the hypodiploid region ($<G_0/G_1$) of the thymocyte DNA cell cycle (Figure 5-1). This region is well-separated from the G_0/G_1 cell cycle region and occurs at an approximate fluorescence of 0.46 (with G_0/G_1 being equal to 1.0). The presence of cells in this region has been found to correlate with the presence of apoptotic thymocytes as analyzed by classical methods such as detection of internucleosomal DNA fragmentation by gel electrophoresis (Telford *et al*, 1991).

In Telford *et al* (1991), classical inhibitors of glucocorticoid-induced apoptosis in mouse thymocytes, including the glucocorticoid antagonist RU486, transcriptional and translational inhibitors actinomycin D and cycloheximide and the endonuclease inhibitor aurintricarboxylic acid were found to inhibit accumulation of cells in the apoptotic region. Induction of apoptotic death in mouse thymocytes by gamma radiation also resulted in cell accumulation in the apoptotic region. These results strongly suggested that cells in the apoptotic region had in fact undergone physiological death and that this methodology represented a valid means of detecting apoptotic cells.

Cells in the apoptotic region of the DNA cell cycle show a loss in forward light scatter

indicative of cytoplasmic collapse. Although chromatin degradation is a frequently observed characteristic of physiological death, other morphological changes are also associated with this process, including degradation of nuclear lamins and the nuclear envelope, depolymerization of the cytoskeleton and subsequent cell shrinkage, and a gradual loss of membrane integrity. To determine whether the previously described cytoplasmic collapse could also be detected by flow cytometry, thymocytes were analyzed for forward light scatter (an indicator of cell size) versus 90° side scatter (an indicator of cell optical density). The results are shown in Figure 5-2. Fixed apoptotic thymocytes show a considerable decrease in forward light scatter compared to normal cells. This decrease in forward scatter correlated precisely with loss of DNA fluorescence (data not shown). Interestingly, apoptotic cells show no detectable loss in 90° side scatter.

The presence of cells in the apoptotic region correlates with the presence of cells with apoptotic morphology as detected by electron microscopy. To determine whether the presence of cells in the apoptotic region correlated with other morphological characteristics of apoptotic death (including chromatin condensation and margination and cytoplasmic collapse), thymocytes treated with glucocorticoids were simultaneously analyzed for apoptosis by flow cytometry and by transmission electron micrography (TEM). A typical photomicrograph of thymocytes is shown in Figure 5-3. Apoptotic thymocytes are clearly visible as evidenced by their extreme chromatin condensation and margination and loss of cytoplasmic volume.

The number of cells in TEM photomicrographs displaying apoptotic morphologies were then counted, expressed as a percentage of the total number of cells, and compared to percentages obtained for apoptotic cells by flow cytometry. The results are shown in Table 5-1. The percentage apoptotic cells determined by flow cytometry correlates fairly well with the percentage of apoptotic cells in the TEM photomicrographs, indicating that

the presence of cells in the apoptotic region of the cell cycle correlates well with the presence of thymocytes with apoptotic morphologies.

Cells in the apoptotic region of the DNA cell cycle contain fragmented DNA and almost no high molecular weight chromatin. Although the biochemical inhibitor data in Telford *et al* (1991) strongly suggested that cells in the hypodiploid region represented apoptotic cells, they did not directly show that cells in this region actually contained the degraded chromatin characteristic of apoptotic death. To directly demonstrate that reduced PI fluorescence correlated with internucleosomal DNA fragmentation, fixed and PI-stained thymocyte samples containing apoptotic cells were sorted by fluorescence activated cell sorting into apoptotic and G_0/G_1 fractions. The fractions were lysed and the resulting DNA purified, radiolabeled and electrophoresed on agarose gels. Autoradiography and scanning densitometry revealed the distribution of high and low molecular weight chromatin in these cell fractions. The results are shown in Figure 5-4. The densitometric histograms show that the DNA from the sorted apoptotic fraction (bottom trace) was almost entirely fragmented in roughly 200 bp multimers, containing little of the high molecular weight DNA visible in the unsorted DNA fraction (top trace). The G_0/G_1 fraction (middle trace) contained little fragmented DNA and the normal amount of high molecular weight chromatin observed in unsorted cells. Interestingly, the apparent size of visible DNA fragments in the apoptotic fraction does not exceed 2300 bp. These results directly demonstrate that cells in the apoptotic region contain internucleosomal DNA fragmentation characteristic of apoptotic death, and indicate that the chromatin degradation in apoptotic cells is remarkably extensive.

Taken together, the above data further reinforce the conclusion of Telford *et al* (1991) that cells in the hypodiploid region of the DNA cell cycle represent thymocytes undergoing apoptotic death.

Functional characterization of glucocorticoid-induced apoptosis in mouse thymocytes. The ability to detect apoptosis in individual cells has allowed a more detailed and functionally relevant analysis of both the kinetics and hormone requirements of thymocyte entry into apoptotic death, and into the lineage specificity of glucocorticoid-induced apoptosis.

Sequential activation of apoptosis in mouse thymocytes by glucocorticoids. Although glucocorticoid-induced thymocyte apoptosis has for some time been referred to as "time-dependent" phenomenon, the functional significance of this description is unclear as a result of the methodology used to detect apoptotic death, namely the presence of fragmented DNA in cell lysates. Incubation of thymocytes with glucocorticoids causes a gradual increase in the amount of fragmented DNA in thymocyte lysates over time (Wyllie, 1980a; Compton and Cidlowski, 1986). It has not been clear, however, whether this increase represents an increase in the amount of DNA damage in the same number of cells all induced to enter cell death immediately upon hormone treatment, or whether the amount of DNA damage per cell is fixed upon cell death and the number of cells entering apoptosis increases with time. The detailed time-response curve shown in Figure 5-5, with corticosterone at 1 μM added to thymocytes at time zero followed by incubation for 10 hours, shows that thymocytes sequentially enter apoptosis over an extended period. This gradual entry into cell death occurs despite the constant presence of saturating concentrations of steroids in culture. Thymocyte apoptosis does not occur simultaneously for all cells, and there can be a considerable delay between addition of hormone and activation of apoptotic death for a typical cell.

Continuous glucocorticoid treatment is required for sequential activation of mouse thymocyte apoptosis. The sequential nature of thymocyte entry into apoptosis has led

to the question of whether an initial receptor-saturating incubation with hormone would ultimately stimulate all sensitive thymocytes to enter apoptotic death, or whether continuous hormone presence over the entire incubation period was required. In Figure 5-6, mouse thymocytes were exposed to corticosterone at 1 μM for periods ranging from 30 minutes to 4 hours, followed by removal of exogenous steroid and continued incubation for a total of eight hours. The level of apoptotic death was then measured by flow cytometry (all data points represent the level of apoptotic death for the given treatment interval at the end of eight hours). From these results, it is clear that incubation with saturating levels of corticosterone for a period of time sufficient to allow cytoplasmic binding and nuclear translocation (one to two hours) caused minimal apoptosis if the steroid was then removed. The continuous presence of steroid is therefore required for the continuous entry of thymocytes into apoptosis.

Glucocorticoids induce lineage-specific apoptosis in mouse thymocytes. Although most thymocytes are eventually sensitive to glucocorticoid-induced apoptosis (approximately 70 to 90%), a small percentage of cells are glucocorticoid-resistant, even after prolonged glucocorticoid treatment. Mouse thymocytes therefore are likely to have lineage-specific sensitivity to glucocorticoids. Previous *in vitro* and *in vivo* experiments with mice transgenic for a self-antigen-specific T cell receptor specificity have indirectly demonstrated that clonal deletion associated with positive and negative selection during thymocyte differentiation occurs primarily in double positive $CD4^+CD8^+$ thymocytes expressing low levels of the T cell receptor complex. Deletion of potentially nonfunctional or autoreactive T lymphocytes is therefore believed to occur prior to thymocyte committment to the $CD4^+$ (helper/inducer) or $CD8^+$ (cytotoxic/suppressor) T lymphocyte lineage. Glucocorticoids are believed to induce thymic deletion in thymocytes that have not been positively selected by productive engagement of their T cell receptor

complex via class I MHC on thymic epithelial cells. Any lineage-specific death induced by glucocorticoids will almost certainly have functional relevance to the level of differentiation at which positive selection occurs.

To determine whether glucocorticoids induced lineage-specific apoptosis in mouse thymocytes, flow cytometric analysis of apoptosis was combined with fluorescence immunophenotyping for CD4, CD8 and the T cell receptor complex to determine which developmental subsets of thymocytes demonstrated resistance or sensitivity to glucocorticoids.

Figure 5-7 and Table 5-2 shows the results for thymocyte CD4/CD8 subsets. Mouse thymocytes were incubated in the presence or absence of corticosterone at 1 μM for eight hours and immunophenotyped with FITC-conjugated antibodies against mouse CD4 and PE-conjugated antibodies against CD8. The cells were subsequently fixed with ethanol, stained with the DNA dye DAPI and flow cytometrically analyzed for all three fluorochromes. DAPI demonstrates the same phenomenon of reduced staining in apoptotic thymocytes observed for PI, making it useful for three-color phenotype-specific analysis of apoptotic death (Telford *et al*, 1992). The top panels show cytograms for CD8 (PE) versus CD4 (FITC) expression. In a typical mouse thymus the percentage of the immature, uncommitted $CD4^+CD8^+$ double positive thymocyte subset was approximately 75% to 80%, with the more mature $CD4^+CD8^-$ and $CD4^-CD8^+$ single positive subsets at roughly 15% and 5% respectively. All $CD8^+$ and $CD4^+$ thymocytes were then gated into $CD4^+$ or $CD8^+$ versus DAPI fluorescence (DNA content) cytograms, and the percentage apoptotic cells determined for each subset directly from the cytograms. The data are summarized in Table 5-2. Corticosterone induced the highest level of apoptotic death in the $CD4^+CD8^+$ double positive thymocyte subset (77.8%), with lower levels of cell death in the $CD4^+CD8^-$ and $CD4^-CD8^+$ single positive subsets (42.7% and 27.6% respectively). The amount of cell death in the single positive subsets varied from experiment to

experiment and no clear trends of specificity for the lesser degrees of single positive thymocyte apoptosis were observed. Glucocorticoids were therefore found to induce preferential apoptosis in the uncommitted $CD4^+CD8^+$ thymocyte subset.

Degree of T cell receptor (TCR) expression is a functional indicator of thymocyte differentiation. $\alpha\beta$TCR and the associated CD3 complex are expressed in low levels on immature $CD4^+CD8^+$ thymocytes, but increase following positive and negative thymic selection and CD4/CD8 single positive expression. Phenotype-specific apoptotic analysis was therefore applied to $\alpha\beta$TCR and CD3ϵ subsets of mouse thymocytes as was done for CD4/CD8 to determine whether glucocorticoid sensitivity was lineage-specific for T cell receptor expression as well. Thymocytes treated as described above were labeled with FITC-conjugated antibodies against $\alpha\beta$TCR or CD3ϵ, fixed, stained with PI and flow cytometrically analyzed for both fluorochromes. The results are shown in Figure 5-8 and Table 5-3. The top panels show cytograms for $\alpha\beta$TCR expression (FITC) versus DNA content (PI), with corresponding histograms for $\alpha\beta$TCR expression and DNA content shown below and to the right of the cytograms respectively. $\alpha\beta$TCR expression was divided into low (lo), intermediate (int) and high (hi) levels of expression. The distribution of apoptotic cells in the cytograms shows that cell death occurred primarily in the $\alpha\beta TCR^{lo}$ and $\alpha\beta TCR^{int}$ subsets following treatment with corticosterone. Table 5-3 shows that the greatest levels of apoptoic death occurred in the $\alpha\beta TCR^{lo}$ and $\alpha\beta TCR^{int}$ subsets (55.1% and 44.1% respectively) with less death in the $\alpha\beta TCR^{hi}$ subpopulation (28.1%). The lower panels show cytograms for CD3ϵ expression (FITC) versus DNA content (PI), with CD3ϵ expression subdivided into low (lo) and high (hi) subsets. The greatest level of apoptotic death occurred in the $CD3\epsilon^{lo}$ subset (55.6%), with less cell death in the $CD3\epsilon^{hi}$ subset (29.6%). Collectively, these results suggest that glucocorticoid preferentially induced apoptosis in the $CD4^+CD8^+\alpha\beta TCR^{lo}CD3\epsilon^{lo}$ subset of mouse thymocytes.

CHAPTER 5: DISCUSSION

Detection of thymocyte apoptosis by flow cytometry. The study described in Telford *et al* (1991) demonstrated that apoptotic thymocytes induced by glucocorticoids or other stimuli accumulate in a hypodiploid region of the normal DNA cells cycle referred to as the apoptotic region. The original observations made in this paper have been extended by additional work confirming that the cells in this region are indeed apoptotic. Additional flow cytometric analysis for forward versus side scatter indicated that this subpopulation of cells also demonstrated cytoplasmic collapse characteristic of apoptotic death, while a simultaneous TEM study indicated that the presence of an flow cytometric apoptotic region correlated strongly with the visible morphological changes associated with apoptosis. In addition, sorting the apoptotic region by fluorescence activated cell sorting followed by cell lysis and gel electrophoresis of the resulting cell lysates indicated that the cells in the apoptotic region are highly enriched for fragmented DNA, suggesting that internucleosomal DNA fragmentation and loss of PI fluorescence are strongly linked. All of these results provide further confirmation that flow cytometric DNA cell cycle analysis represents a valid means of detecting apoptosis in rodent immune cells.

Sequential activation of apoptosis in mouse thymocytes by glucocorticoids. Individual cell analysis of apoptotic death has yielded several new insights to be gained into the process of glucocorticoid-induced apoptosis in mouse thymocytes. The data in Figure 5-5 demonstrated that thymocytes underwent gradual entry into apoptotic death over a period of many hours, rather than entering apoptosis simultaneously. Gradual entry into apoptotic death occurred despite the constant presence of saturating levels of glucocorticoids in the culture system. Although earlier work using DNA fragmentation

as detected by gel electrophoresis has determined that the amount of fragmented DNA in a fixed number of thymocytes increased with time, it was not certain whether this represented increased DNA fragmentation in all cells over time, or whether the amount of DNA fragmentation in individual apoptotic cells was fixed and the number of cells undergoing apoptosis was increasing (Cohen and Duke, 1984; Compton and Cidlowski, 1986). Analysis by flow cytometry clarified the nature of this phenomenon, indicating that apoptosis-associated chromatin degradation proceeded rapidly to a fixed point, and that the number of cells entering apoptosis increased with time. Exposure to steroid therefore does not induce apoptosis immediately in all thymocytes, despite the fact that virtually all thymocytes (>85%) are destined to undergo hormone-induced death if steroid is present for a long enough period. A regulatory mechanism at the level of hormone-induced gene expression may therefore exist that regulates thymocyte entry into apoptotic death (a process dependent on *de novo* gene expression). Alternately, regulation of entry into apoptosis may occur at the level of hormone-dependent transcriptional activation.

Continuous glucocorticoid treatment is required for sequential activation of mouse thymocyte apoptosis. The steroid requirements of hormone-induced death were further elucidated by the experiment in Figure 5-3. The incubation of thymocytes with dexamethasone for periods ranging from 30 minutes to 4 hours indicated that steroid had to be continuously present for thymocytes to continue to enter apoptotic death. Incubation of cells with saturating levels of steroid for periods of time sufficient for complete saturation of cytoplasmic receptor and subsequent translocation to the nucleus induced only minimal thymocyte apoptosis if steroid was then removed. These results suggest that hormone must be present at the moment a thymocyte is "ready" to undergo steroid-induced apoptosis. Presumably many receptor-hormone interactions therefore do not

result in apoptosis if they occur at an inappropriate time. Although the sequential nature of hormone-induced thymocyte apoptosis and its requirement for continual hormone presence have not yet been explained, they may in large part be due to the mechanism of glucocorticoid receptor cycling in mammalian cells and its role in regulation hormone-mediated gene regulation. This issue will be discussed in the context of the *in vivo* and *in vitro* glucocorticoid receptor-ligand binding studies described in Chapters 7 and 8.

Glucocorticoids induce lineage-specific apoptosis in mouse thymocytes. Flow cytometric apoptotic analysis combined with fluorescent immunophenotyping for the T-lineage markers allowed the detection of lineage specificity in glucocorticoid-induced thymocyte apoptosis. The $CD4^+CD8^+\alpha\beta TCR^{lo}CD3\epsilon^{lo}$ thymocyte subset was found to be primarily sensitive to glucocorticoid treatment, although other thymocyte subsets were also hormone-sensitive to lesser degrees. These results are consistent with previous indirect data suggesting that double-positive thymocytes are particularly sensitive to both *in vitro* and *in vivo* glucocorticoid treatment based on their gradual deletion either from the culture system or from the thymus. In addition, transgenic mouse studies investigating the process of self antigen-induced selection in the thymus suggest that negative and positive selection in the thymus primarily occurs prior to CD4/CD8 single positive expression and increased TCR expression, in immature thymocytes that are predominantly $CD4^+CD8^+\alpha\beta TCR^{lo}$ (MacDonald and Lees, 1990; Murphy *et al*, 1990; Vasquez *et al*, 1992). Flow cytometric analysis has permitted the direct detection of *in vitro* lineage-specific apoptosis in glucocorticoid-treated mouse thymocytes, determining that it occurs preferentially at the level of thymocyte differentiation associated with thymic selection. The recent *in vitro* studies suggesting that glucocorticoids may be responsible for deleting thymocytes that have not been positively selected by productive TCR engagement means

that this preferential induction coincides with the thymocyte subsets susceptible to deletion during *in vivo* thymic selection.

Table 5-1. Comparison of percentage apoptotic cells detected by flow cytometric analysis of DNA cell cycle (FACS) and visual analysis of apoptotic morphology by electron microscopy (TEM). Cells were analyzed fresh (No Incubation) or following incubation without (No Treatment) or with corticosterone at 1 μM (CS 1 μM). Flow cytometric data is expressed as the mean plus or minus standard deviation of duplicate samples. Electron microscopy data is expressed as the percentage of apoptotic cells in a total cell sample size of at least 200.

Treatment	FACS	TEM
No Incubation	0.2 $\pm$ 0.1%	0.1%
No Treatment	9.4 $\pm$ 0.3%	11.7%
CS 1 μM	67.4 $\pm$ 1.8%	70.1%

Table 5-2. Corticosterone-induced apoptosis in CD4/CD8 subsets of mouse thymocytes. The percentage of cells undergoing apoptosis in the total thymocyte population (TOTAL) and in the $CD4^+CD8^+$, $CD4^+CD8^-$ and $CD4^-CD8^+$ subpopulations was calculated from the CD4 versus CD8 and subsequently derived CD4- and CD8-gated cytograms illustrated in Figure 5-7. Values are expressed as the mean plus or minus standard deviation of duplicate samples. In a typical thymus the percentages of cells were 75%, 12% and 3% in the $CD4^+CD8^+$, $CD4^+CD8^-$ and $CD4^-CD8^+$ subpopulations respectively.

Treatment	Percentage apoptosis			
	TOTAL	$CD4^+CD8^+$	$CD4^+CD8^-$	$CD4^-CD8^+$
No treatment	16.0 ± 0.2%	15.4 ± 0.6%	15.2 ± 0.5%	8.0 ± 1.2%
CS 1 μM	71.6 ± 0.3%	78.0 ± 0.2%	42.0 ± 1.0%	28.3 ± 1.0%

Table 5-3. Corticosterone- and zinc-induced apoptosis in $\alpha\beta$TCR and CD3ϵ subsets of mouse thymocytes. The percentage of cells undergoing apoptosis in the total population (TOTAL), the $\alpha\beta TCR^{lo}$ (low), $\alpha\beta TCR^{int}$ (intermediate), $\alpha\beta TCR^{hi}$ (high) or in the $CD3\epsilon^{lo}$ (low) or $CD3\epsilon^{hi}$ (high) subsets was calculated from the $\alpha\beta$TCR or CD3ϵ versus DNA content cytograms illustrated in Figure 5-8. Values are expressed as the mean plus or minus standard deviation of duplicate samples. In a typical thymus the percentages of cells were 23%, 19% and 8% in the $\alpha\beta TCR^{lo}$, $\alpha\beta TCR^{int}$ and $\alpha\beta TCR^{hi}$ subpopulations and 32% and 21% for the $CD3\epsilon^{lo}$ and $CD3\epsilon^{hi}$ subpopulations respectively.

Treatment	**Percentage apoptosis**			
	TOTAL	$\alpha\beta TCR^{lo}$	$\alpha\beta TCR^{int}$	$\alpha\beta TCR^{hi}$
No treatment	10.1 ± 0.3%	10.3 ± 0.2%	12.4 ± 0.4%	17.1 ± 0.4%
CS 1 μM	46.7 ± 0.1%	56.1 ± 1.3%	43.8 ± 0.4%	27.9 ± 0.3%

Treatment	**Percentage apoptosis**		
	TOTAL	$CD3\epsilon^{lo}$	$CD3\epsilon^{hi}$
No treatment	10.3 ± 0.5%	12.4 ± 1.1%	9.4 ± 2.0%
CS 1 μM	44.8 ± 0.8%	54.8 ± 1.1%	30.4 ± 1.1%

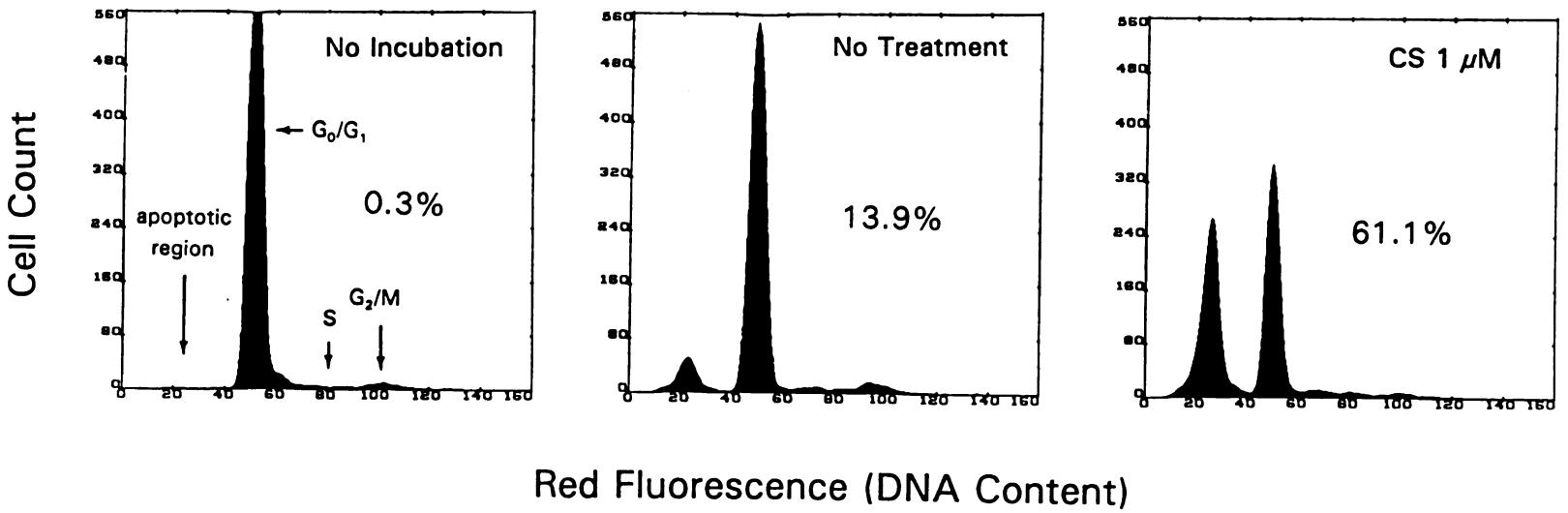

Figure 5-1. Presence of thymocytes in the apoptotic region of the PI DNA cell cycle following incubation without (no treatment) or with corticosterone at 1 μM (CS 1 μM) for eight hours. Apoptotic regions are indicated with arrows.

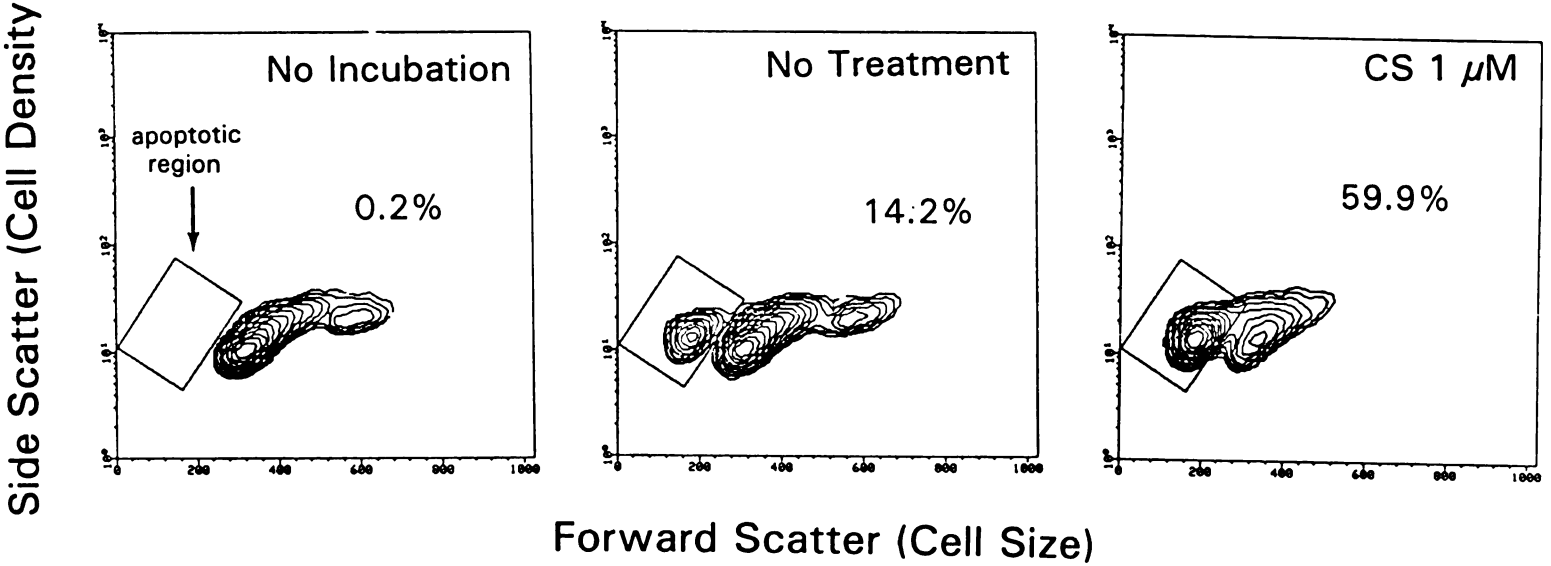

Figure 5-2. Presence of apoptotic thymocytes with reduced forward light scatter following incubation without (no treatment) or with corticosterone at 1 μM (CS 1 μM) for eight hours. Apoptotic cells are indicated by the outlined regions.

Figure 5-3. Electron micrograph of unfixed mouse thymocytes treated with corticosterone at 1 μM for eight hours. Representative apoptotic cells are indicated with arrows.

Figure 5-4. Densitometric tracings from agarose electrophoresis of purified DNA lysates from corticosterone-treated mouse thymocytes, either unsorted (top densitometric trace) or sorted by fluorescence activated cell sorting for G_0/G_1 cells (middle trace) or apoptotic cells (bottom trace) from the subpopulations indicated in the DNA histogram (top illustration) as described in Materials and Methods. Lambda HindIII molecular weight markers of 200, 400, 600, 800, 2000, 2300 and 4400 bp markers and fragments are shown.

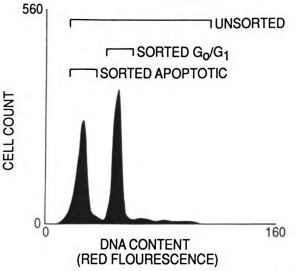
560
UNSORTED
SORTED G_0/G_1
SORTED APOPTOTIC
CELL COUNT
0
0
160
DNA CONTENT
(RED FLOURESCENCE)

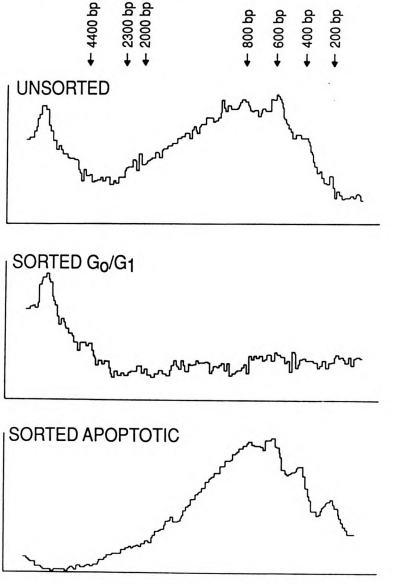
4400 bp
2300 bp
2000 bp
800 bp
600 bp
400 bp
200 bp
UNSORTED
SORTED G_0/G_1
SORTED APOPTOTIC

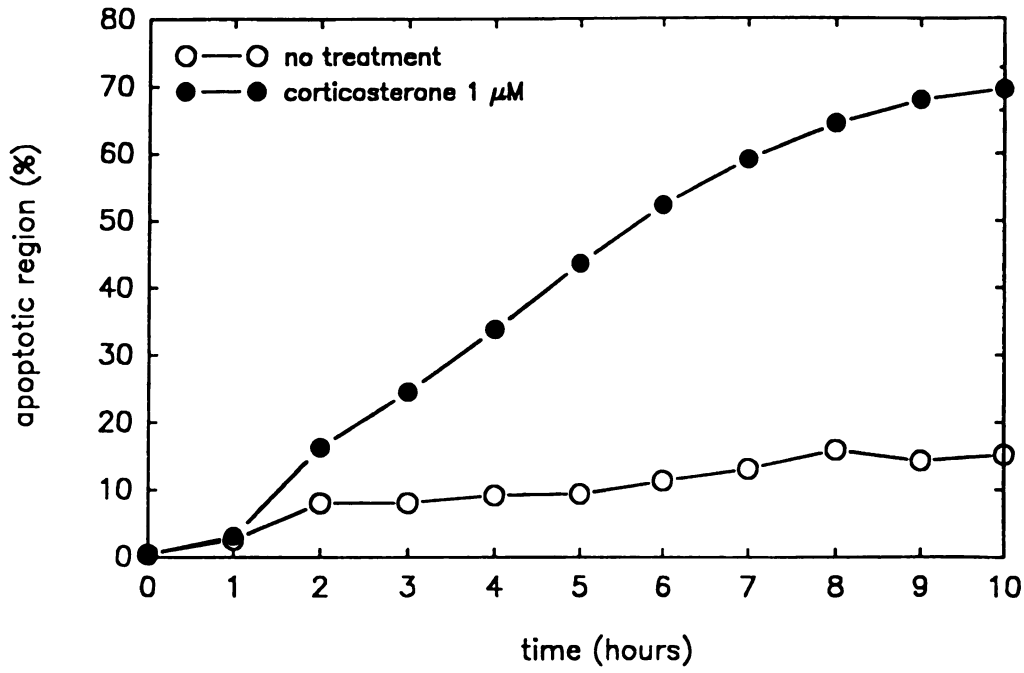

Figure 5-5. Time-response curves for mouse thymocytes incubated without (open circles) or with corticosterone at 1 μM (closed circles). Percentage apoptotic cells was calculated as the percentage of cells in the apoptotic region of the PI DNA cell cycle. Data are the mean plus or minus standard deviation of duplicate samples (error bars are not visible).

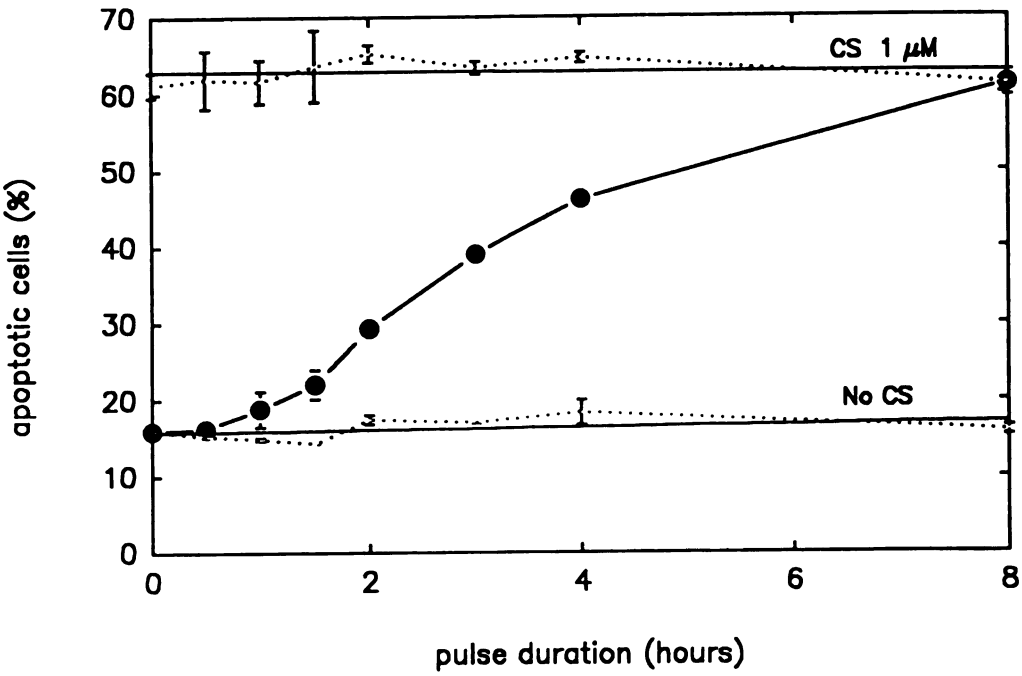

Figure 5-6. Induction of apoptosis in mouse thymocytes by brief treatment with corticosterone at 1 μM. Cells were incubated with corticosterone for indicated periods (30 minutes to 4 hours) followed by removal of steroid and continued incubation to eight hours. Cells were then analyzed for the presence of apoptotic cells by flow cytometry (filled circles). Cell samples incubated with steroid, washed and reincubated with steroid (top dotted line, CS 1 μM) or incubated without steroid, washed and reincubated without steroid (bottom dotted line, No CS) were carried out simultaneously as controls for effects of the washing process on resulting cell death. Data are the mean plus or minus standard deviation of duplicate samples.

Figure 5-7. Corticosterone-induced apoptosis in CD4/CD8 subsets of mouse thymocytes. Fresh thymocytes (no incubation) or thymocytes incubated without (no treatment) or with corticosterone (CS 1 μM), for eight hours were immunophenotypically labeled for CD4 and CD8 expression (FITC and PE respectively), ethanol fixed, stained for cell cycle with DAPI, and flow cytometrically analyzed for all three fluorochromes as described in the text. Top panels show cytograms for FITC-CD4 versus PE-CD8. Arrows mark the division between negative and positive staining for both CD4 and CD8. Negative control fluorescence in fresh thymocytes is illustrated in the upper right corner of the no incubation cytogram. $CD4^+$ and $CD8^+$ subpopulations were then gated into CD8 or CD4 versus DNA content (DAPI) cytograms (middle and bottom rows respectively). Percentage apoptotic cells was then calculated for the total population and $CD4^+CD8^+$, $CD4^+CD8^-$ and $CD4^-CD8^+$ subsets directly from the cytograms based on the percentage of cells in the apoptotic region of the phenotype-specific cell cycles (marked with arrows as in the top panels). Apoptotic percentages for the total population and three subpopulations are given in Table 5-2. Data are representative of two separate experiments.

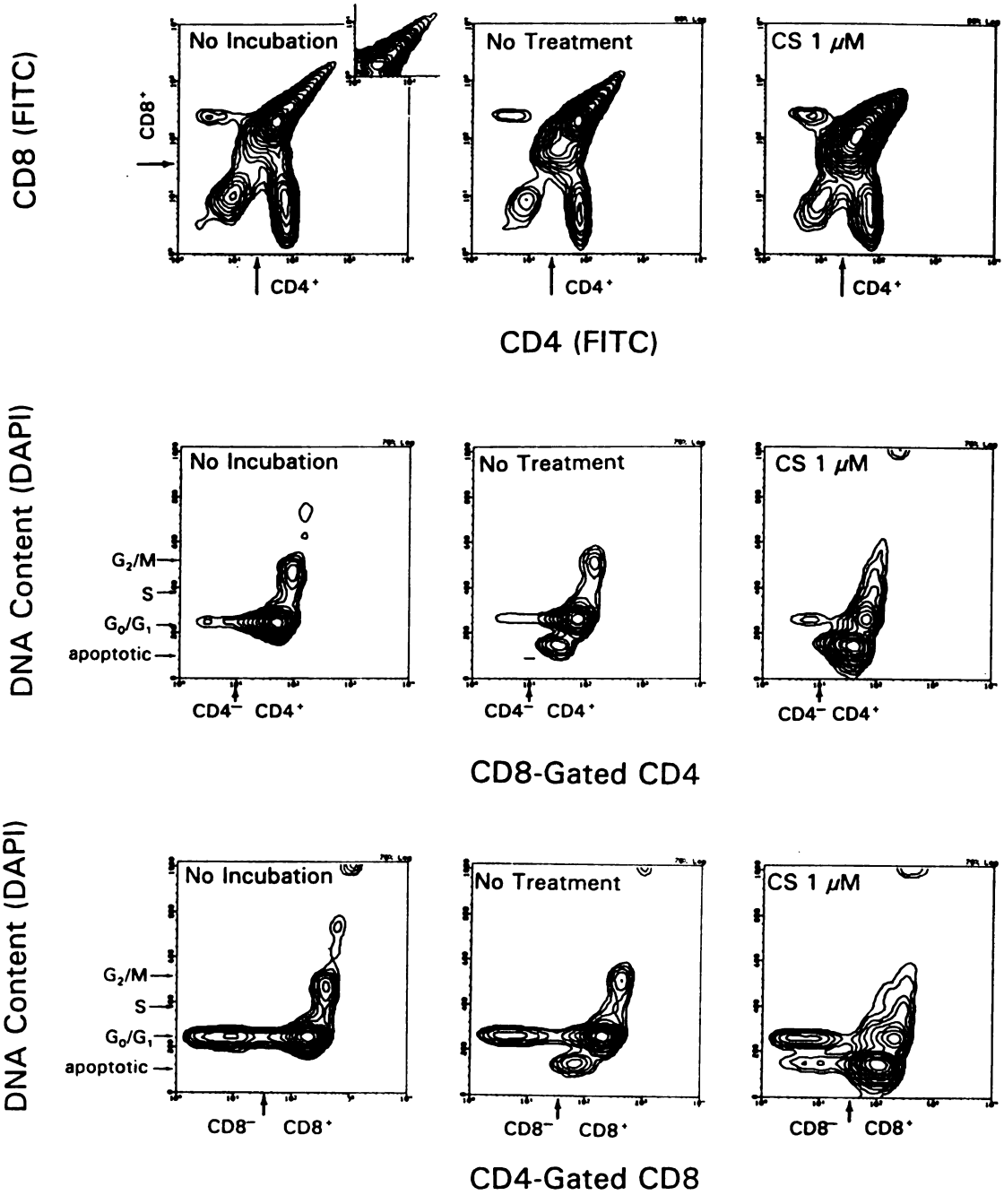
CD8 (FITC)
No Incubation
No Treatment
CS 1 μM
CD8+
CD4+
CD4 (FITC)
DNA Content (DAPI)
G2/M
S
G0/G1
apoptotic
CD4− CD4+
CD8-Gated CD4
CD8−
CD8+
CD4-Gated CD8

Figure 5-8. Corticosterone-induced apoptosis in $\alpha\beta$TCR or CD3ϵ subsets of mouse thymocytes. Thymocytes were incubated without (no treatment) or with corticosterone (CS 1 μM) for eight hours. Cells were then immunophenotypically labeled for either $\alpha\beta$TCR or CD3ϵ (FITC), ethanol-fixed, stained for DNA content with PI as described in the text and flow cytometrically analyzed for both fluorochromes as described in the text. Top and bottom panels show $\alpha\beta$TCR or CD3ϵ expression versus DNA content (PI) cytograms respectively, with corresponding histograms showing distribution of $\alpha\beta$TCR or CD3ϵ expression subsets and DNA content (including the apoptotic region as indicated). Negative control fluorescence in untreated samples is shown in the no treatment phenotypic histograms. Percentage apoptotic cells in the $\alpha\beta$TCR^{lo} (low), $\alpha\beta$TCR^{int} (intermediate), $\alpha\beta$TCR^{hi} (high) and the CD3ϵ^{lo} and CD3ϵ^{hi} subsets were calculated directly from marker expression versus DNA content cytograms based on the percentage of cells in the apoptotic region of each phenotype-specific cell cycle (marked with arrows). Apoptotic percentages for the total population and three subpopulations are given in Table 5-3. Data are representative of two experiments.

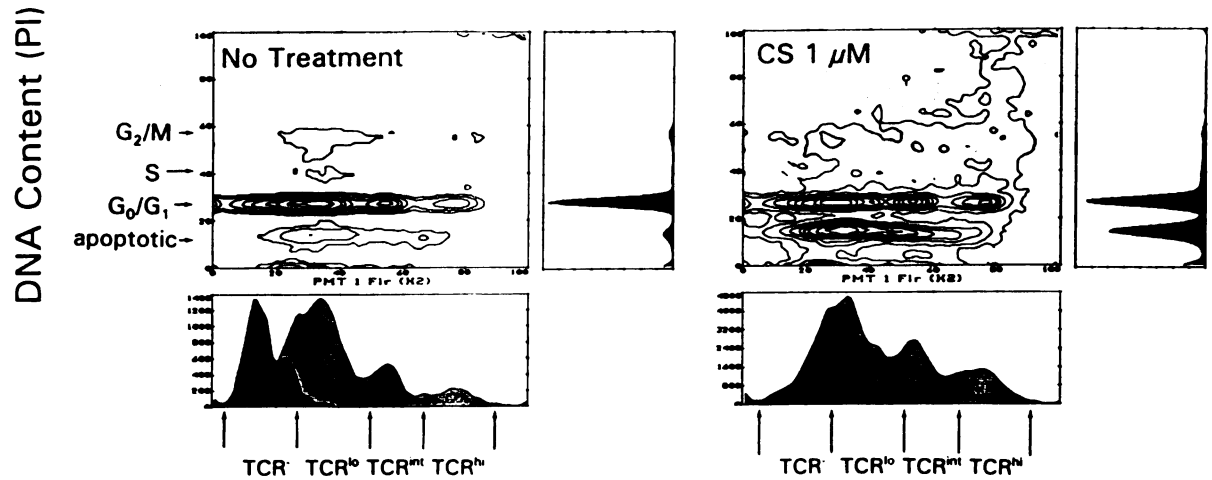
DNA Content (PI)
No Treatment
CS 1 μM
G2/M
S
G0/G1
apoptotic
TCR- TCRlo TCRint TCRhi
αβTCR (FITC)

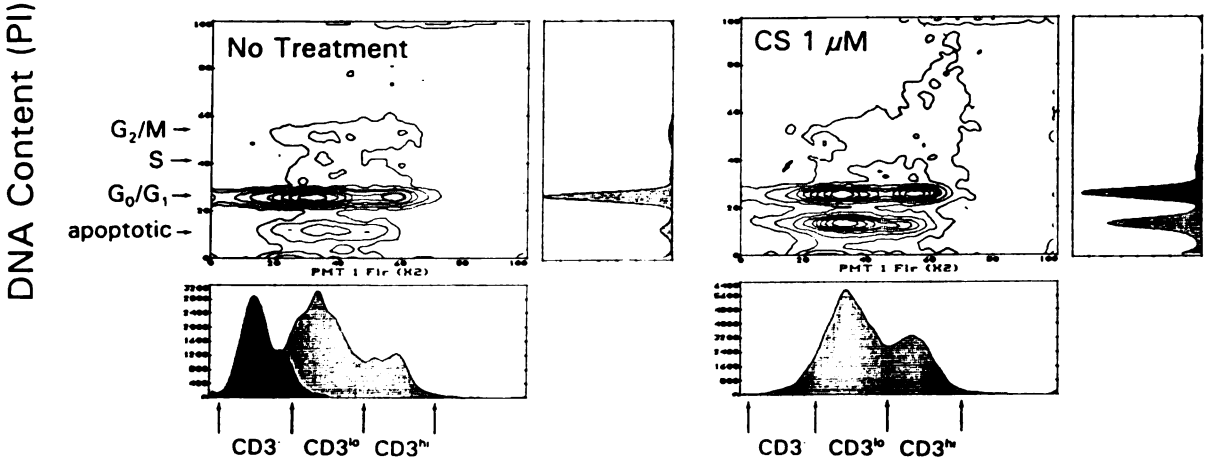
DNA Content (PI)
No Treatment
CS 1 μM
G2/M
S
G0/G1
apoptotic
CD3- CD3lo CD3hi
CD3ε (FITC)

CHAPTER 6

ZINC-ASSOCIATED INHIBITION OF GLUCOCORTICOID-INDUCED APOPTOSIS IN MOUSE THYMOCYTES

CHAPTER 6: ABSTRACT

High concentrations of zinc have been previously found to be an almost universal inhibitor of mammalian cell apoptosis. Glucocorticoid-induced apoptosis in mouse thymocytes is a well-defined experimental model for studying the inhibitory effects of zinc on physiological cell death, as determined by inhibition of DNA fragmentation and apoptotic morphology. This study determined whether zinc also inhibited the characteristics of apoptotic death detected by flow cytometry as described in Chapter 5, including reduced DNA dye fluorescence (indicative of chromatin degradation) and reduced forward scatter (indicative of cell shrinkage). Zinc at 500 μM was found to inhibit steroid-induced apoptosis by both these criteria, indicating that flow cytometry represents a useful technique for analyzing and quantifying this phenomenon. Using flow cytometry, the requirements for zinc inhibition were also more precisely defined, including the effective dose range and metal specificity. The conditions of zinc inhibition were later compared to the effects of zinc on glucocorticoid receptor (GR) binding and nuclear localization (Chapter 7) to determine whether effects of GR signalling represented a potential mechanism for the inhibitory effects of zinc on steroid-induced cell death. In addition, the zinc content of thymocytes incubated with high concentrations of zinc salts was measured to determine the intracellular zinc concentration necessary to prevent cell death, and its relationship with extracellular zinc levels.

CHAPTER 6: INTRODUCTION

Zinc salts at high concentrations (usually 500 μM and greater) have been repeatedly found to be potent **in vitro** inhibitors of apoptotic death in mammalian cells. As reviewed in Chapter 3, this phenomenon has been particular well-demonstrated in the immune system, where zinc can block apoptosis in a variety of immune cell types induced by a variety of stimuli. Nevertheless, a clearly defined mechanism for this phenomenon has not been defined.

Glucocorticoid-induced apoptosis in mouse thymocytes has been previously used as an experimental model for zinc inhibition of cell death, with zinc inhibiting both internucleosomal DNA fragmentation and morphological changes such as cytoplasmic collapse and membrane blebbing in these cells (Cohen *et al*, 1993). The transcriptional activation and intracellular signalling requirements of steroid-induced cell death are also relatively well understood, making this a good potential model for studies into the role of zinc in inhibiting apoptosis (Cohen *et al*, 1992). With the intent of using mouse thymocytes as a model for subsequent investigations into the inhibitory effects of zinc, we confirmed that zinc inhibited steroid-induced DNA fragmentation in these cells. We also determined that zinc inhibited the manifestations of steroid-induced apoptosis detectable by flow cytometry, specifically chromatin degradation (detected by loss of DNA dye staining) and cell shrinkage (detected by reduced forward light scatter). Once flow cytometry was established as a useful tool for detecting zinc inhibition of thymocyte apoptosis, several previously uninvestigated characteristics of zinc-associated inhibition of apoptosis were examined, including the dose response, salt specificity and metal specificity. These results confirmed the validity of steroid-induced apoptosis in mouse thymocytes as a model for subsequent studies into the effects of zinc, and provided some initial clues as to possible mechanisms for its observed inhibitory effects. In addition, the approximate concentration

of zinc in thymocytes following incubation at inhibitory concentrations of zinc (500 μM) was also analyzed to determine the approximate intracellular concentration of zinc necessary to inhibit apoptosis. These results provided the basis for subsequent investigations into the effects of zinc on GR signal transduction in thymocytes and subsequent effects on apoptotic death.

CHAPTER 6: MATERIALS AND METHODS

Preparation of mouse thymocytes. Thymuses from young (6 to 12 weeks old) male A/J mice were surgically removed and extruded through 100 micron stainless steel screens into phosphate buffered saline (PBS) containing 2% FBS. Cells were erythrocyte-depleted over Histopaque 1083 gradients (Sigma), washed twice by centrifugation at 800 x g followed by resuspension in PBS/FBS.

Cell culture. Mouse thymocytes were resuspended in RPMI-1640 supplemented with 10% heat-inactivated FBS and incubated in 24 well plates at 2 x 10^6 cells/ml/well at 37°C under atmospheric conditions of 5% CO_2 for periods up to eight hours. Dexamethasone and corticosterone were dissolved in 95% ethanol at 1 mg/ml and added at the beginning of the culture period at 0.1 μM and 1 μM respectively. For radiation-induced apoptosis, thymocytes were irradiated to 0.5 Gy in a ^{60}Co variable flux irradiator (0.13 Gy/minute) prior to incubation.

Zinc sulfate heptahydrate (Aldrich, ultrapure grade) was diluted from a 1 M stock solution in sterile H_20 into culture medium at 1:1000 (10 μl into 10 mls in a typical preparation) giving a culture medium stock solution of 1 mM (1000 μM). This stock was added to thymocytes at 1:1 volumes at the beginning of culture to give a final concentration of 500 μM. Lower concentrations were prepared by diluting the culture medium stock solution. For specificity experiments zinc chloride, copper sulfate pentahydrate and nickle sulfate were prepared and added into cell culture in an identical fashion. Cell viabilities were measured by trypan blue exclusion and found to be greater than 90% for all treatments at all timepoints.

Detection of thymocyte apoptosis by flow cytometry. Following treatment mouse

thymocytes were removed from culture and washed once with cold PBS. Samples were then decanted and and ethanol-fixed by one of two methods. In the first method, 2 mls cold 80% ethanol was added directly to cells (Telford *et al*, 1991). In the second method, cells were resuspended in 0.4 mls 50% FBS in PBS followed by dropwise addition of 1.2 mls cold 70% ethanol with gentle vortexing (Garvy *et al*, 1993). Samples were then incubated for at least one hour at 4°C in each case, washed twice with cold PBS and finally resuspended in 1 ml of 50 μg/ml propidium iodide in PBS supplemented with DNase-free RNase at 0.05 mg/ml and EDTA at 0.5 mM. Samples were then stored overnight at 4°C prior to flow cytometric analysis.

Flow cytometry. Mouse thymocytes were flow cytometrically analyzed for forward scatter (cell size), 90° side scatter (cell density) and red fluorescence (propidium iodide DNA content). Thymocytes were initially gated by red fluorescence peak versus area or width versus area to exclude debris and doublets. This was followed by DNA content and/or forward versus side scatter analysis. Apoptotic cells showed reductions in propidium iodide fluorescence and in forward scatter as previously described (Telford *et al*, 1991; Telford *et al*, 1992). Cells were analyzed on an Ortho Cytofluorograph 50-H FACS with a dedicated Data General 2150 computer system. Some thymocyte samples were analyzed on a Becton-Dickinson Vantage FACS.

Detection of DNA fragmentation by gel electrophoresis. Mouse thymocytes were incubated for eight hours without or with corticosterone and without or with zinc sulfate heptahydrate at 500 μM. Genomic DNA from treated thymocytes (usually 5 to 10 x 10^6 cells/sample) was then extracted using an anionic exchange column DNA purification kit (Qiagen, Germany). The resulting purified DNA was electrophoresed on 1.8% agarose minigels at 60 V for 1 hour in TAE electrophoresis buffer as previously described (Telford

et al, 1991). The resulting gels were stained with ethidium bromide and photographed under ultraviolet light. Lambda phage HindIII restriction fragments were used as molecular weight markers.

Determination of intracellular zinc concentration by flame atomic absorption spectroscopy. This was carried out using the techniques described by Falchuk *et al* (1988) with some modifications. Mouse thymocytes at 10^7 cells/sample were incubated in the presence or absence of zinc sulfate as described above for periods up to eight hours. At two, four and eight hour intervals cells were removed from culture and washed four times with trace metal-free PBS at 4°C (prepared by elution over a Chelex-100 column). After the final wash the supernatant was carefully decanted and the cell pellet solublized in 200 μl metal-free concentrated nitric acid. The lysates were then incubated at 60°C for two hours. The lysates were then diluted with 1.8 mls ultrapure trace metal-free water (final acid concentration at 10%) and analyzed immediately by acetylene/air flame atomic absorption spectroscopy at 213.9 nm absorption wavelength with deuterium background correction. Zinc standard curve concentrations ranged from 0.02 to 0.2 ppm (μg/ml) and are shown in Figure 6-9. All culture tubes, pipets and containers were acid washed with 4N HCl and thoroughly rinsed with distilled, deionized water prior to use. Mock control samples (with no cells present but otherwise handled identically to normal samples) ensured that tubes, pipets, culture medium and handling were not sources of zinc contamination. Cell lysates "spiked" with known concentrations of zinc standards (standard addition) gave within 2% of predicted zinc concentration upon analysis, indicating that matrix effects were not affecting results.

CHAPTER 6: RESULTS

Effects of zinc salts on glucocorticoid-induced thymocyte apoptosis. Zinc salts at concentrations of 0.5 mM and higher have been previously found to inhibit glucocorticoid-induced apoptosis in mouse thymocytes, and in a host of other apoptotic systems (Zalewski and Forbes, 1993). To confirm that zinc exerted this inhibitory effect in our culture system, mouse thymocytes were incubated without or with corticosterone at 1 μM in the absence or presence of simultaneously added zinc sulfate heptahydrate at 500 μM. The effects of zinc on thymocyte apoptosis were then confirmed by traditional electrophoretic detection of apoptosis associated internucleosomal DNA fragmentation (Figure 6-1). Corticosterone treatment (lane 3) induced considerable DNA fragmentation as expected. Zinc at 500 μM completely inhibited corticosterone-induced DNA fragmentation (lane 5) to levels associated with other biochemical inhibitors of thymocyte apoptosis such as cycloheximide (See Chapter 5). Mouse thymocytes treated with zinc therefore behaved in a manner consistent with previous observations (Zalewski and Forbes, 1993).

Thymocytes treated with corticosterone and/or zinc were then examined flow cytometrically to determine whether or not zinc could prevent the apoptosis-associated reduction in propidium iodide binding to nuclear chromatin and loss of cellular volume manifested as a reduction in forward light scatter. The results are shown in Figures 6-2 and 6-3. In Figure 6-2, thymocytes were flow cytometrically analyzed for propidium iodide DNA content. Thymocytes treated with corticosterone show the characteristic apoptotic region (60.5%) containing cells with reduced propidium iodide fluorescence. Simultaneous treatment with zinc at 500 μM was found to inhibit corticosterone-induced apoptosis (14%) to below background levels (18.6%).

Similar results were obtained in the flow cytometric forward versus side scatter analysis shown in Figure 6-3. Treatment with corticosterone induced considerable apoptotic

death in thymocytes as illustrated by the characteristic decrease in forward scatter indicative of apoptosis-associated loss of cellular volume (Telford *et al*, 1992). Simultaneous treatment with zinc at 500 μM also inhibited the development of this apoptotic morphology (17.0%) to background levels (18.5%). It is significant that zinc did not appear to induce abnormal alterations in cell volume or density, which might be indicative of necrotic toxicity. This suggests that zinc is not inhibiting apoptosis by the prior induction of necrosis.

In summary, zinc was shown to inhibit both apoptosis-associated changes in chromatin structure and cellular volume as confirmed flow cytometrically by DNA content and forward scatter analysis respectively.

Effect of zinc on irradiation-induced thymocyte apoptosis. Other stimuli in addition to glucocorticoids can induce physiological death in mouse thymocytes. To determine whether zinc could inhibit hormone-independent cell death, mouse thymocytes were irradiated to 0.5 Gy and incubated in the absence or presence of zinc sulfate heptahydrate at 500 μM for eight hours. The results of DNA content and forward scatter analysis are shown in Figures 6-4 and 6-5. As with corticosterone, radiation induced considerable apoptosis evidenced both by cells in the apoptotic region of the DNA cell cycle and with reduced forward scatter. Zinc at 500 μM inhibited radiation-induced apoptosis to background levels by both criterion. Zinc was therefore able to inhibit thymocyte apoptosis triggered through a stimuli other than glucocorticoid.

Dose-response and time-response of zinc-associated inhibition of glucocorticoid-induced thymocyte apoptosis. Although high concentrations of zinc have been previously found to inhibit thymocyte apoptosis, the precise dose and time kinetics had not been elucidated. Since this information is relevant to the mechanism of zinc-associated inhibition, dose-

response experiments were carried out.

Figure 6-6 shows a dose-reponse curve for thymocytes treated without or with corticosterone in the presence of zinc at concentrations ranging from 50 to 500 μM for eight hours (from DNA content analysis). Zinc routinely conferred some protection at 200 μM, although inhibition was incomplete. Little or no protective effect was observed below this concentration. Interestingly, zinc alone at 80 to 100 μM induced apoptosis in the absence of glucocorticoid. This unexpected phenomenon did not occur at concentrations greater than 200 μM, although addition and removal of zinc at 500 μM (as was done for reversibility experiments described later) often induced some glucocorticoid-independent apoptosis that made experimental interpretation difficult. The issue of zinc-induced apoptosis is dealt with more completely in Appendix 1.

Zinc inhibits glucocorticoid-induced apoptosis irrespective of its salt form. Other zinc salts in addition to zinc sulfate heptahydrate inhibit glucocorticoid-induced apoptosis in mouse thymocytes. Figure 6-7 shows the inhibitory effects of zinc chloride on corticosterone-induced apoptosis. Zinc chloride was found to inhibit apoptosis at 500 μM with a loss of inhibition at 200 μM and below, a similar dose-response to that observed for zinc sulfate. It is also significant that lower concentrations of zinc chloride (80 to 200 μM) also induced apoptosis as was observed for zinc sulfate. The effects of zinc are therefore not an artifact of the salt form in which the zinc is delivered.

Zinc is specific in its inhibitory effects on glucocorticoid-induced apoptosis in mouse thymocytes. To determine the specificity of zinc in its effects on glucocorticoid-induced apoptosis, the effects of other biologically significant trace metals on thymocyte apoptosis were also assessed. Figure 6-8 compares the effects of zinc sulfate heptahydrate, copper sulfate pentahydrate and nickle sulfate on glucocorticoid-induced apoptosis in thymocytes.

Copper and nickle were found not to inhibit thymocyte apoptosis at 500 μM. Iron and molybdenum salts also had no inhibitory effects on glucocorticoid-induced apoptosis at 500 μM (data not shown). In addition, metals that can be substituted for zinc in some enzyme systems such as cadmium and gold were also evaluated for their effects on thymocyte apoptosis. Both metals induced extensive necrotic death in thymocytes at 500 μM down to concentrations as low as 50 μM, indicating that their effects were also dissimilar to zinc (data not shown). The induction of apoptosis by zinc at lower concentrations is also visible in Figure 6-8, as is the ability of copper to induce apoptosis at high concentrations (500 μM). Nevertheless, zinc appears to be relatively specific in its effects of glucocorticoid-induced apoptotic death.

Inhibitory concentrations of zinc salts increase the intracellular concentration of zinc in mouse thymocytes. Although zinc salts at 500 μM inhibit apoptosis, no information was available as to what degree the intracellular concentration of zinc is elevated in thymocytes with this treatment. Although extracellular zinc at 500 μM is required to inhibit cell death, it is unlikely that this concentration is attained in the cell, and the actual intracellular inhibitory concentration is much lower. To determine if this was the case, thymocytes were incubated with zinc for up to eight hours, washed, lysed and analyzed by atomic absorption spectroscopy for total cellular zinc content. A typical standard curve is shown in Figure 6-9 and the thymocyte results in Figure 6-10. Endogenous zinc levels were found to be less than 1 μg zinc per 10^9 cells, a value that is virtually at baseline for this particular analytical method. Incubation of thymocytes with zinc at 500 μM resulted in a steady increase in intracellular zinc concentration until four hours, plateauing at approximately 6 μg Zn/10^9 cells. Calculation of approximate intracellular concentration (done by calculating cell volume based on a typical thymocyte diameter of 6 μm) gives a value of 0.9 nM. While this estimate of intracellular zinc concentration is only approximate, it is still far below the

extracellular zinc concentration. The minimum sensitivity threshold of flame atomic absorption did not allow detection of endogenous zinc levels in untreated thymocytes.

CHAPTER 6: DISCUSSION

The results described in this chapter indicate that zinc prevented glucocorticoid-induced apoptosis in mouse thymocytes based on inhibition of DNA fragmentation as previously observed. In addition, zinc was also found to prevent the alterations in chromatin structure reflected in a reduced ability to bind propidium iodide, as well as the apoptosis-associated losses of cellular volume associated with cytoskeletal breakdown as detected by reductions in forward light scatter. These results confirm the inhibitory effects of zinc and demonstrate the usefulness of flow cytometry in detecting this inhibition.

The experimental conditions of zinc-associated inhibition of apoptosis were also more clearly defined. Zinc only inhibited glucocorticoid-induced thymocyte apoptosis at concentrations ranging from 300 to 500 μM and higher. Zinc was found to inhibit glucocorticoid-induced apoptosis with simultaneous addition, preincubation not being necessary for inhibition. The phenomenon of apoptotic inhibition was found to be restricted to zinc, with other trace metals exerting no inhibitory effects. It was also found that zinc inhibited radiation-induced apoptosis, showing its effect on hormone-independent apoptosis. In addition, the degree to which added zinc elevated the intracellular zinc concentration was found to be far lower than 500 μM. These data suggest that the intracellular concentration of zinc necessary to inhibit apoptosis is actually much lower than the extracellular concentration required to block apoptosis. Previous results with mammalian lymphocytes give typical intracellular zinc concentrations ranging widely from 0.1 to 400 nM, suggesting that high extracellular zinc concentrations may not elevate intracellular zinc to levels far above the endogenous norm (Jackson, 1989; Zalewski and Forbes, 1993). Nevertheless, high extracellular zinc concentrations are apparently necessary to maintain the *in vitro* intracellular levels necessary to prevent cell death.

What does the above information provide in terms of narrowing down the potential

mechanisms by which zinc could be inhibiting apoptosis? The biochemical and genetic requirements of apoptotic death dictate that the mechanism of zinc-associated apoptotic inhibition could be occurring in essentially three broad (and frequently overlapping) areas (as discussed in Chapter 3). Most cases of apoptotic death require *de novo* gene expression. A critical aspect of apoptotic signalling is therefore the activation of transcription, presumably through the induction of one or more apoptosis-associated transcription factors. In the case of glucocorticoid-induced cell death, the glucocorticoid receptor is obviously one of these factors. In other forms of gene-directed death such as radiation-induced apoptosis in mouse thymocytes, factors such as AP-1 (a heterodimer of c-*fos* and c-*jun*, both upregulated after radiation treatment) serve to transactivate gene expression. Zinc could therefore be targeting transcriptional activation, anywhere from initial induction of the transcription factor to initiation of transcription following factor binding to the appropriate response element.

A second general target area for zinc could be at the level of secondary signalling events associated with apoptotic death. While glucocorticoid receptor activation by the addition of hormone is clearly required to induce apoptosis (as evidenced by the complete inhibition observed with antagonist treatment), signal transduction mechanisms including increased Ca^{2+} flux and cAMP upregulation are also required for the successful resolution of apoptotic death. In fact, induction of these events can frequently induce apoptosis even in the absence of receptor activation. If zinc can inhibit or inappropriately activate one or more of these signal transduction mechanisms, inhibition of apoptosis might result. This mechanism might also overlap with the induction of gene expression; inhibition of protooncogene activation (such as c-*myc* or c-*fos*) might in turn inhibit transactivation by preventing successful formation of an oncogene-associated transcription factor.

A third broad category of potential targets for zinc includes effects on the effectors of apoptotic death synthesized or activated by apoptosis-associated transactivation and

secondary signal transduction. Included in this group are such proteins as the endogenous endonuclease(s) which cleave chromatin into internucleosomal fragments; topoisomerases which induce conformational changes into DNA favoring internucleosomal cleavage; proteases which cause cytoskeletal breakdown; and transglutaminases, which crosslink the plasma membrane and allow it to form stable "blebs". These are apoptotic effectors that are presumably synthesized *de novo* or postranslationally modified from an inactive form that actually mediate the process of apoptosis. Zinc acting at this level might however only inhibit certain aspects of apoptotic death, such as DNA fragentation or membrane blebbing.

While these and other studies have not evaluated all known physical manifestations of glucocorticoid-induced apoptosis, the fact that more than one apoptotic parameter (as opposed to just, for example, DNA fragmentation) was inhibited suggests that, for our purposes, inhibition was more or less "complete". This "complete" inhibition of apoptotic death therefore suggests that zinc inhibition of apoptotic effectors (such as the endonuclease) was a less likely mechanism, such zinc inhibited multiple manifestations of apoptosis rather than single ones. These observations would therefore seem to indicate that zinc is acting at an early site or sites of apoptotic activation, either at the level of transcriptional activation or secondary signal transduction. These results therefore provide a preliminary rationale for examining the effects of zinc on the major mechanism of transcriptional activation in steroid-induced cell death, namely the activation of the GR.

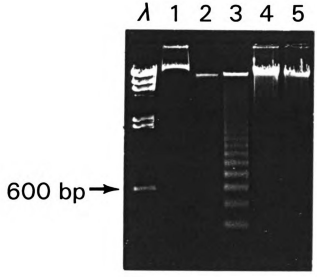

Figure 6-1. Inhibitory effects of zinc sulfate on corticosterone-induced apoptosis in mouse thymocytes based on internucleosomal DNA fragmentation. Thymocytes were incubated without or with corticosterone at 1 μM in the presence or absence of zinc sulfate heptahydrate at 500 μM for 8 hours. Cells were then lysed followed by DNA extraction. Resulting DNA samples were electrophoresed on 1.8% agarose gels, followed by ethidium bromide staining for detection of DNA fragmentation patterns. **Lane 1**, no incubation; **lane 2**, no treatment for 8 hours; **lane 3**, corticosterone alone at 1 μM for 8 hours; **lane 4**, zinc alone at 500 μM; **lane 5**, corticosterone at 1 μM and zinc at 500 μM for 8 hours; λ, lambda phage HindIII molecular weight markers. Arrow indicates 600 bp fragment.

Figure 6-2. Inhibitory effects of zinc sulfate on corticosterone-induced apoptosis in mouse thymocytes based on reduced flow cytometric PI fluorescence. Untreated thymocytes (no treatment) or thymocytes treated with corticosterone at 1 μM (CS 1 μM) and/or zinc sulfate (Zn 500 μM) were incubated for eight hours followed by fixation, PI staining and flow cytometric PI cell cycle analysis as described in the text. Data are expressed as DNA content histograms. The apoptotic subpopulation is indicated by the bracketed region, with the percentage of apoptotic cells given.

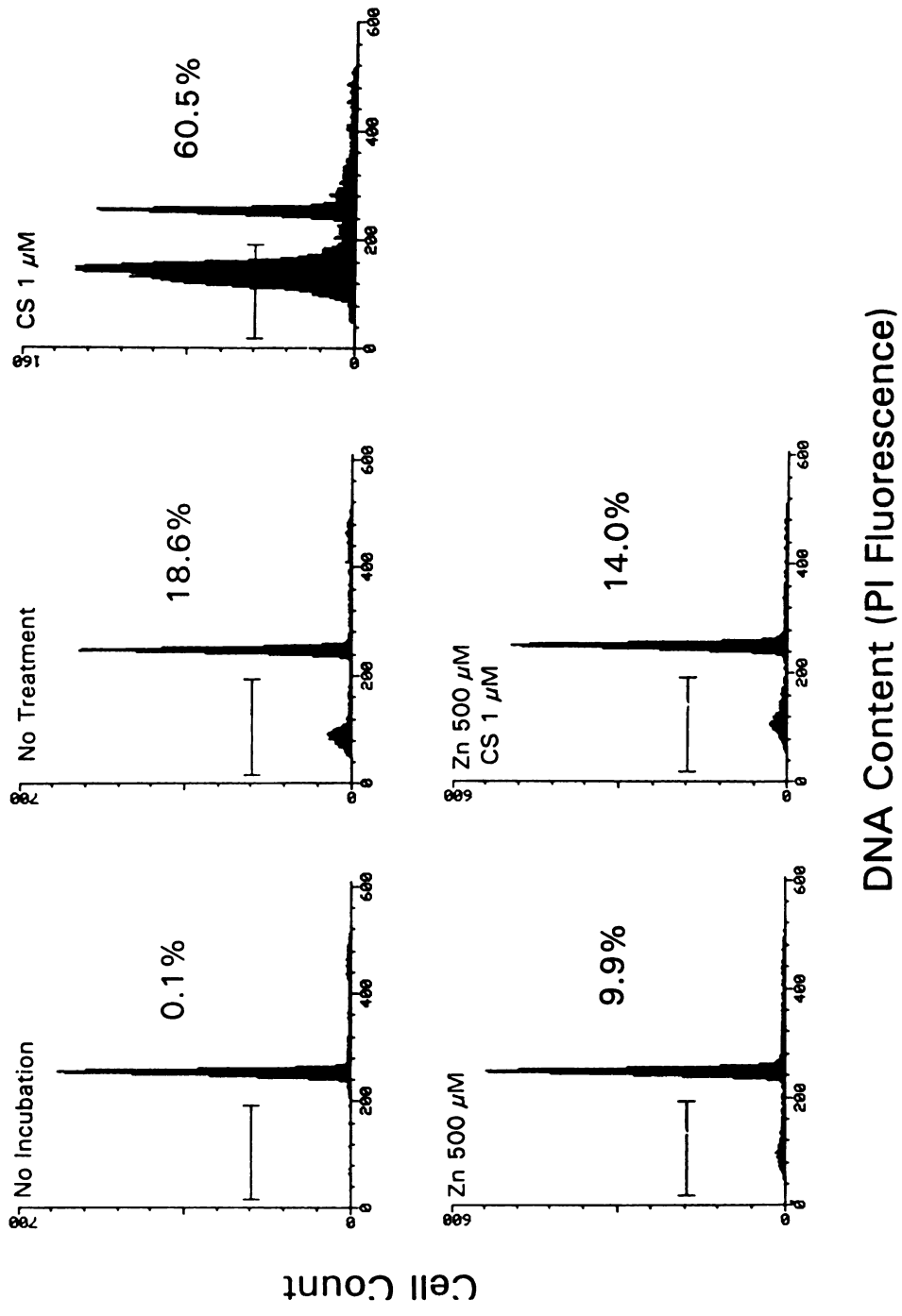
No Incubation
0.1%
No Treatment
18.6%
CS 1 μM
60.5%
Zn 500 μM
9.9%
Zn 500 μM
CS 1 μM
14.0%
Cell Count
DNA Content (PI Fluorescence)

Figure 6-3. Inhibitory effects of zinc sulfate on corticosterone-induced apoptosis in mouse thymocytes based on reduced flow cytometric forward light scatter. Untreated thymocytes (no treatment) or thymocytes treated with corticosterone at 1 μM (CS 1 μM) and/or zinc sulfate (Zn 500 μM) were incubated for eight hours followed by fixation and flow cytometric analysis for forward scatter (cell size) versus side scatter (cell density) as described in the text. Percentages of apoptotic cells are derived from the percentage cells in the apoptotic region of the PI DNA cell cycle. Data are expressed as forward versus side scatter cytograms. The apoptotic subpopulation is indicated by the outlined region, with the percentage of apoptotic cells given.

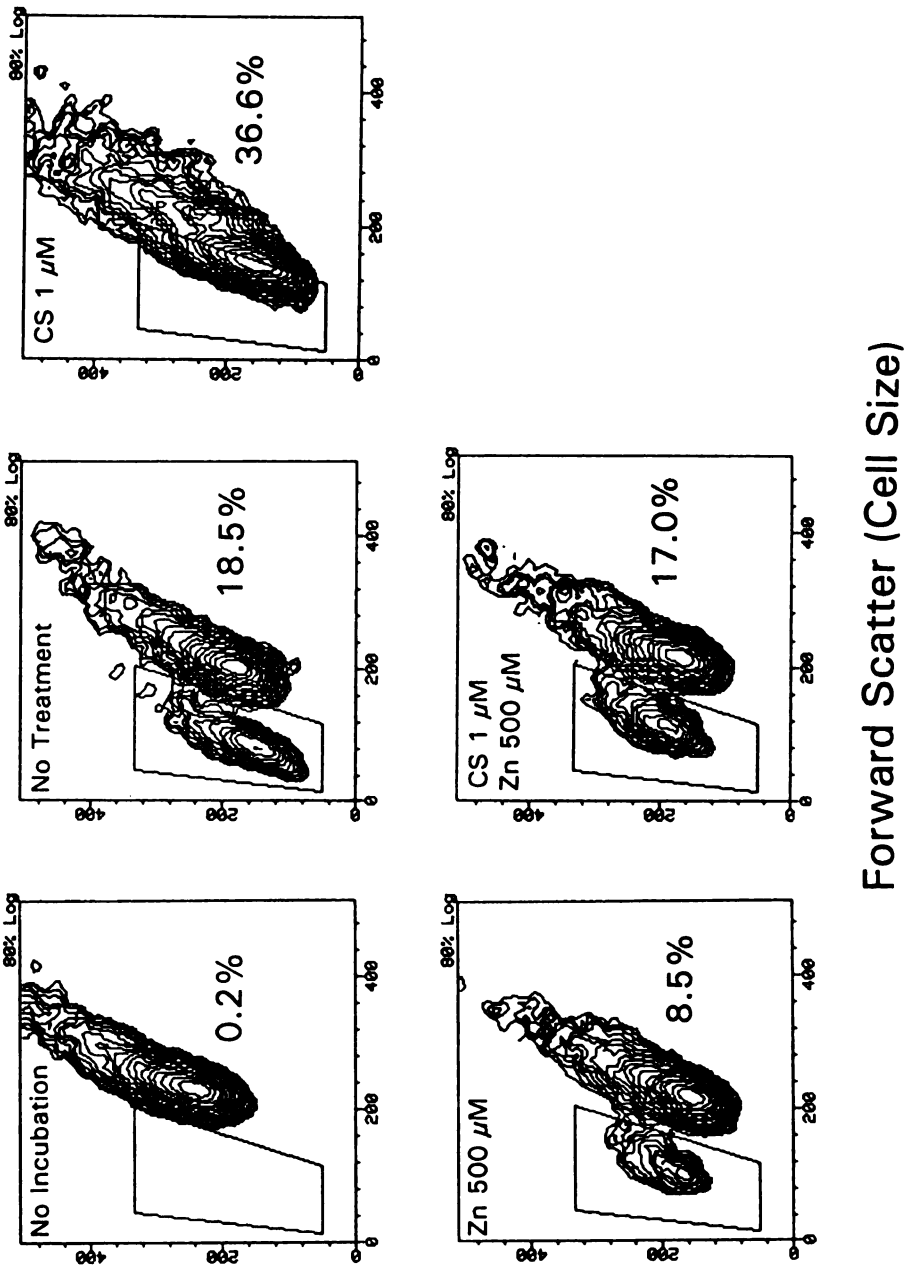
No Incubation
0.2%
No Treatment
18.5%
CS 1 μM
36.6%
Zn 500 μM
8.5%
CS 1 μM
Zn 500 μM
17.0%
Side Scatter (Cell Density)
Forward Scatter (Cell Size)

Figure 6-4. Inhibitory effects of zinc sulfate on radiation-induced apoptosis in mouse thymocytes based on reduced flow cytometric PI fluorescence. Untreated thymocytes (no treatment) or thymocytes irradiated at 0.5 gray (0.5 Gy) and/or treated with zinc sulfate (Zn 500 μM) were incubated for eight hours followed by fixation, PI staining and flow cytometric PI cell cycle analysis as described in the text. Data are expressed as DNA content histograms. The apoptotic subpopulation is indicated by the bracketed region, with the percentage of apoptotic cells given.

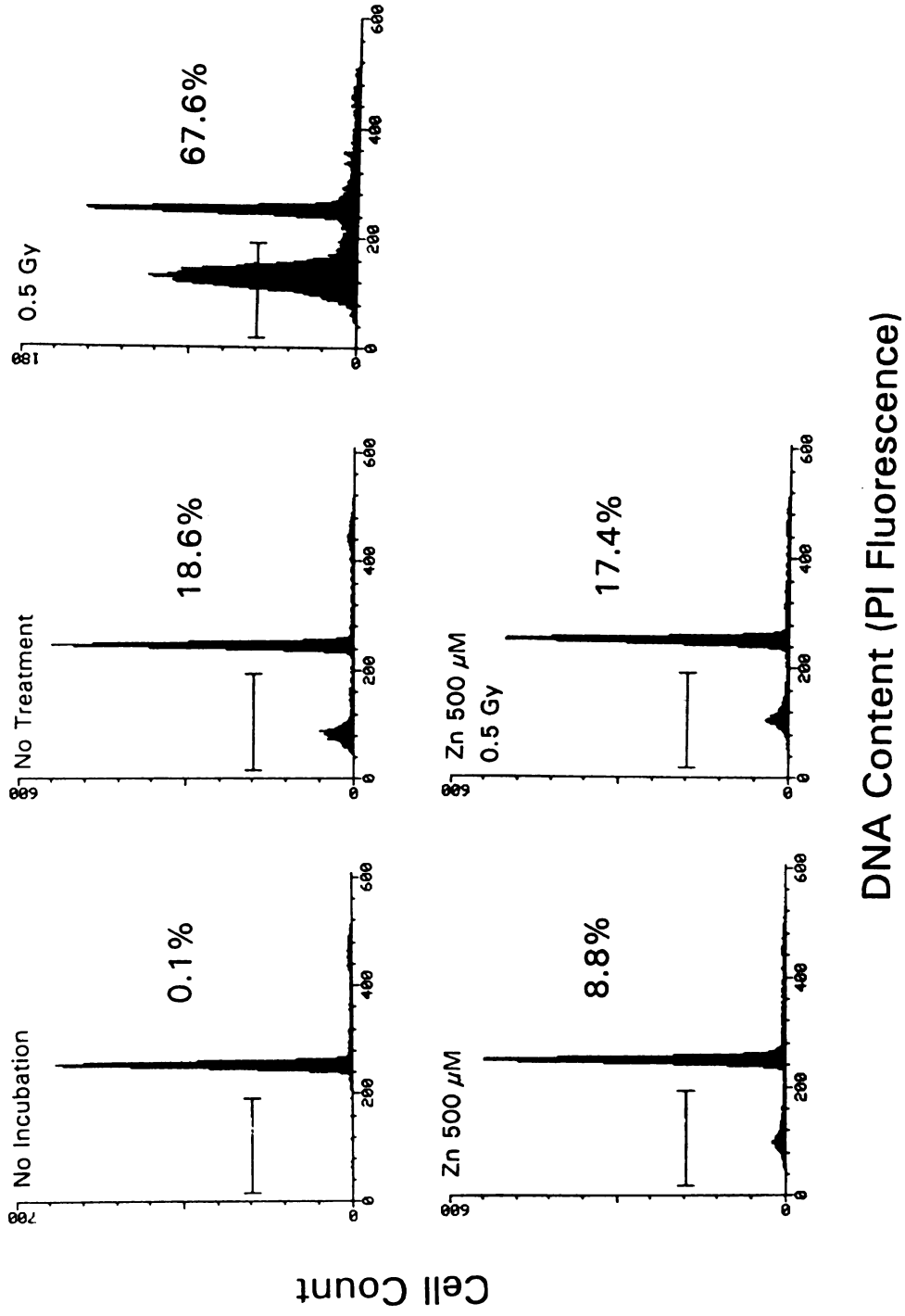
No Incubation
0.1%
No Treatment
18.6%
0.5 Gy
67.6%
Zn 500 μM
8.8%
Zn 500 μM
0.5 Gy
17.4%
Cell Count
DNA Content (PI Fluorescence)

Figure 6-5. Inhibitory effects of zinc sulfate on radiation-induced apoptosis in mouse thymocytes based on reduced flow cytometric forward light scatter. Untreated thymocytes (no treatment) or thymocytes irradiated at 0.5 gray (0.5 Gy) and/or zinc sulfate (Zn 500 μM) were incubated for eight hours followed by fixation and flow cytometric analysis for forward scatter (cell size) versus side scatter (cell density) as described in the text. Percentages of apoptotic cells are derived from the percentage cells in the apoptotic region of the PI DNA cell cycle. Data are expressed as forward versus side scatter cytograms. The apoptotic subpopulation is indicated by the outlined region, with the percentage of apoptotic cells given.

No Incubation
0.2%
No Treatment
18.5%
0.5 Gy
49.3%
Zn 500 μM
98% Log
9.9%
0.5 Gy
Zn 500 μM
98% Log
13.6%
SSC-H-SSC-Height ---->
Side Scatter (Cell Density)
Forward Scatter (Cell Size)

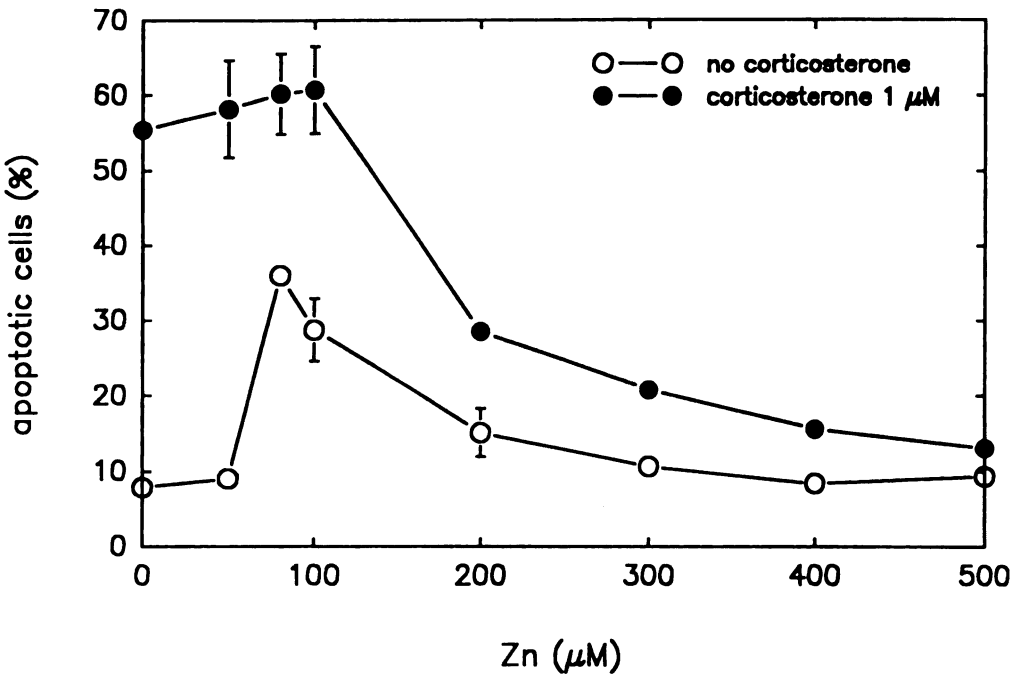

Figure 6-6. Dose-response curve for the inhibitory effects of zinc sulfate on corticosterone-induced apoptosis in mouse thymocytes. Cells were incubated without (open circles) or with corticosterone at 1 μM (closed circles) for eight hours with simultaneous addition of zinc sulfate at the indicated concentration. Percentages of apoptotic cells are derived from the percentage cells in the apoptotic region of the PI DNA cell cycle. Data are expressed as the mean plus or minus standard deviation of duplicate samples.

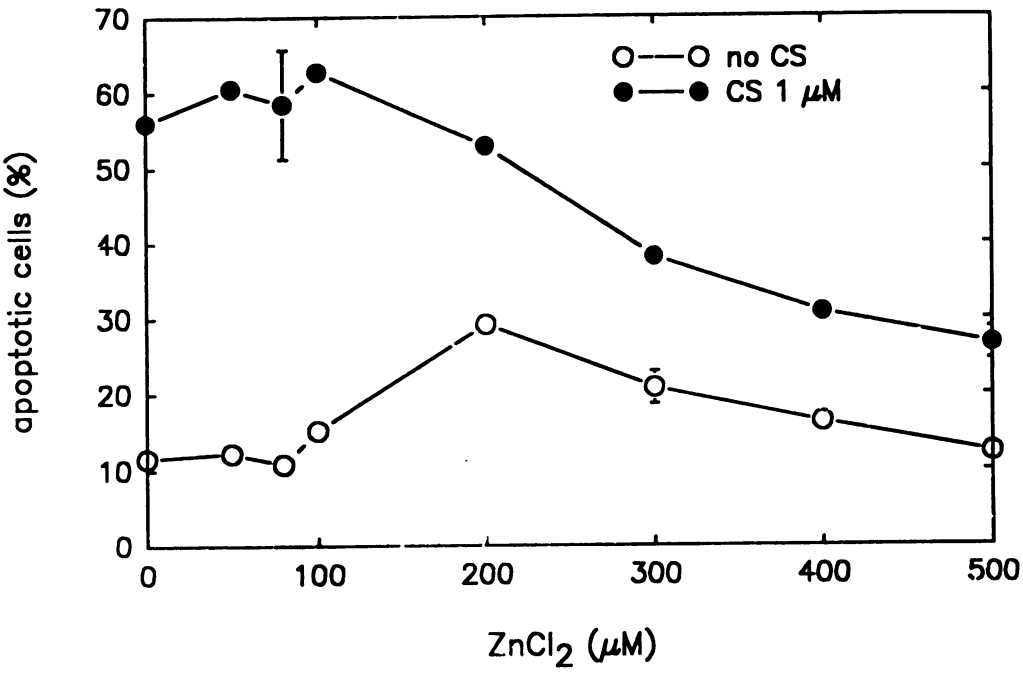

Figure 6-7. Dose-response curve for the inhibitory effects of zinc chloride on corticosterone-induced apoptosis in mouse thymocytes. Cells were incubated without (open circles) or with corticosterone at 1 μM (closed circles) for eight hours with simultaneous addition of zinc chloride at the indicated concentration. Percentages of apoptotic cells are derived from the percentage cells in the apoptotic region of the PI DNA cell cycle. Data are expressed as the mean plus or minus standard deviation of duplicate samples.

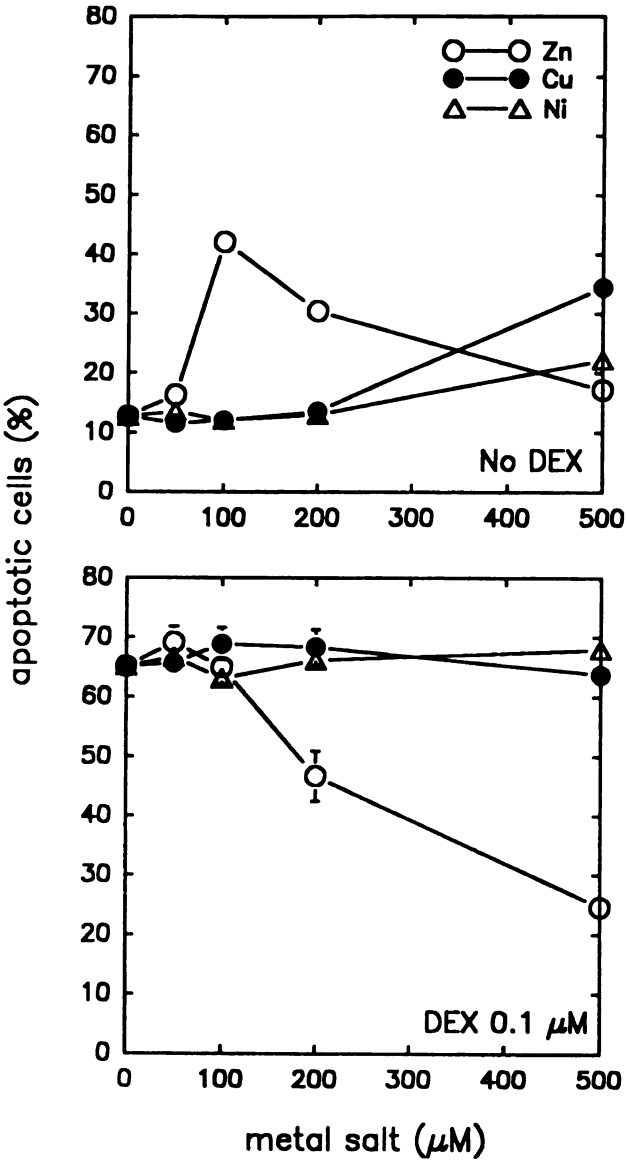

Figure 6-8. Dose-response curves for the effects of zinc sulfate, copper sulfate and nickle sulfate on DEX-induced apoptosis in mouse thymocytes. Cells were incubated without (top panel) or with dexamethasone at 0.1 μM (bottom panel) for eight hours with simultaneous addition of indicated metal salt at the indicated concentrations. Percentages of apoptotic cells are derived from the percentage cells in the apoptotic region of the PI DNA cell cycle. Data are expressed as the mean plus or minus standard deviation of duplicate samples.

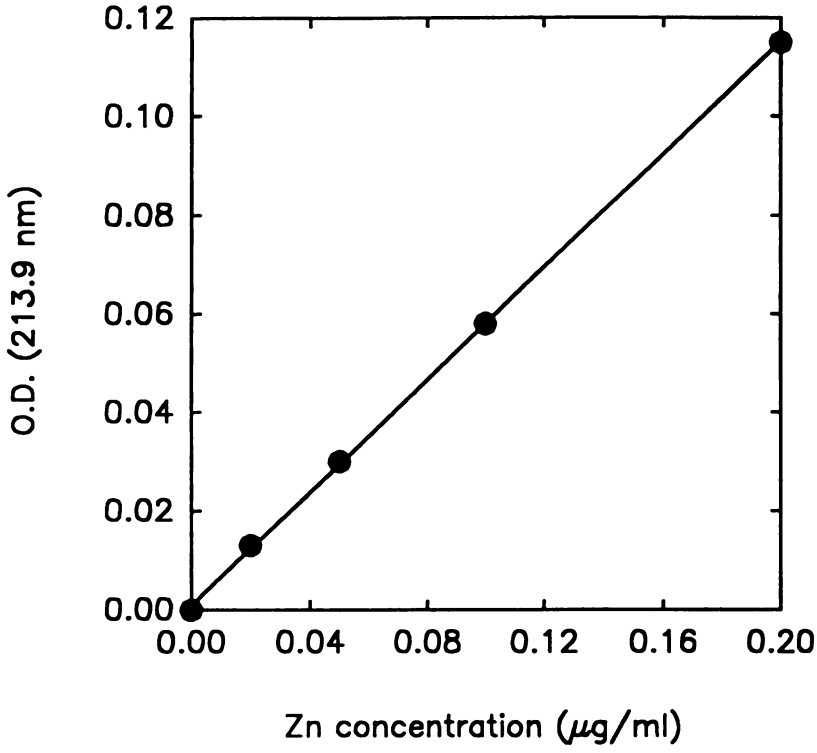

Figure 6-9. Standard curve for acetylene/air flame atomic absorption spectroscopy of zinc at 213.9 nm absorption wavelength with deuterium background correction. Concentrations range from 0.02 to 0.2 ppm (μg/ml). Values are expressed as the mean plus or minus standard deviation of triplicate samples.

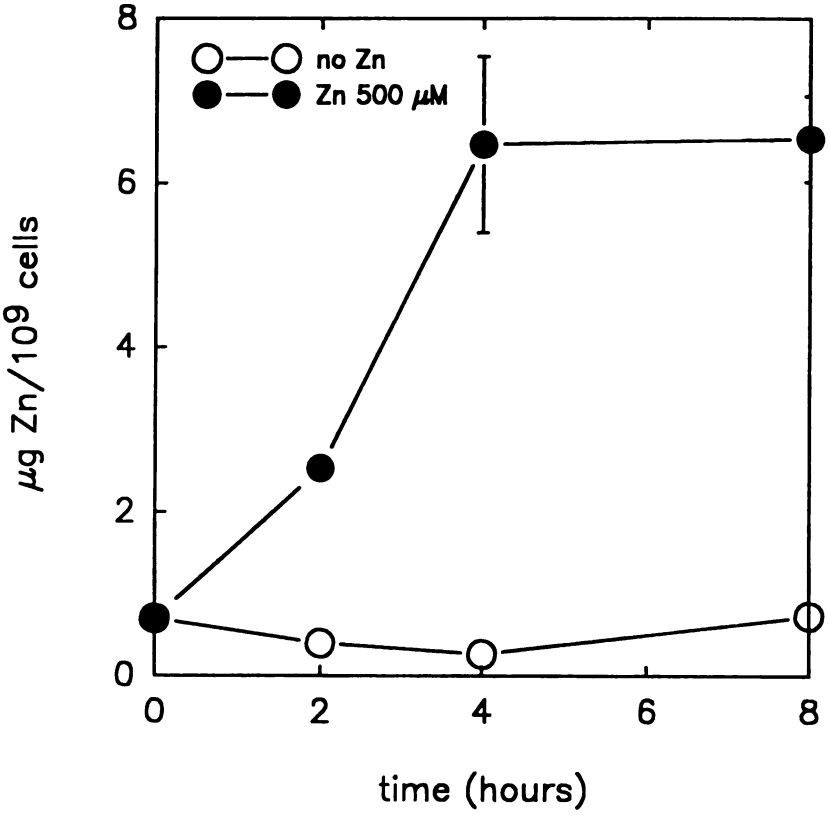

Figure 6-10. Zinc content of mouse thymocytes incubated without (open circles) or with zinc sulfate at 500 μM (filled circles) for 2, 4 or 8 hours as analyzed by atomic absorption spectroscopy. Data are expressed as the mean plus or minus standard error of μg Zn/10^9 cells.

CHAPTER 7

EFFECTS OF ZINC ON *IN VIVO* GLUCOCORTICOID RECEPTOR-LIGAND BINDING AND SUBSEQUENT NUCLEAR LOCALIZATION.

CHAPTER 7: ABSTRACT

Glucocorticoid receptor (GR) signal transduction was chosen as a potential mechanism for the inhibitory effects of zinc on glucocorticoid-induced apoptosis in mouse thymocytes. Radiolabeled dexamethasone was incubated with mouse thymocytes under equilibrium binding conditions in the presence of zinc salts. The degree of cytoplasmic receptor-ligand binding and localization of the receptor to the nucleus was then determined. Zinc at concentrations roughly equivalent to those previously found to inhibit apoptosis were also found to block cytoplasmic ligand binding and almost completely inhibit nuclear localization in mouse thymocytes. These results suggest that zinc can block GR signal transduction at least at the level of receptor-ligand binding and possibly at other pre-nuclear localization steps as well. They provide a rationale for further *in vitro* studies into the effects of zinc on the receptor-ligand binding and transformation process of GR to more precisely define an operative mechanism for these *in vivo* observations.

CHAPTER 7: INTRODUCTION

Previous work and the experimental data presented in Chapter 6 demonstrated that high concentrations of zinc salts almost completely inhibit glucocorticoid-induced apoptosis in mouse thymocytes, as analyzed both by traditional criterion (DNA fragmentation and cellular morphology) and by flow cytometric criterion (reduced DNA fluorescence and forward light scatter). As previously discussed, a defined mechanism for the action of zinc in preventing cell death has not been established despite considerable speculation in this area.

Although there has been considerable speculation regarding the role of zinc in inhibiting glucocorticoid-induced apoptosis, little attention has been paid to the possible effects of zinc on the primary events of the GR signalling pathway itself. The GR as described in Chapter 4 is a transcription factor maintained under unusually strict hormonal control with respect to nuclear translocation. The studies described in Chapter 4 suggest that classical GR cytoplasm-to-nuclear signalling is absolutely necessary for hormone-induced thymocyte death. Any agent that acted to disrupt this chain of events would ultimately block glucocorticoid-induced apoptotic death.

Considerable evidence exists that zinc might regulate GR signalling. Transition metals and their oxyanions have been previously found to inhibit receptor-ligand binding in several steroid superfamily receptors. Arsenite (AsO_2^-) and cadmium have been found to inhibit normal dexamethasone and affinity ligand binding to rat GR (Simons *et al*, 1987; Simons *et al*, 1990; Chakraboti *et al*, 1990). Selenite (SeO_2^-) has also been found to inhibit glucocorticoid binding to rat receptor, and zinc has been found to inhibit ligand binding to thyroid receptor (Tashima *et al*, 1989; Surks *et al*, 1989). Since glucocorticoid affinity labels such as dexamethasone 21-mesylate covalently bind to receptor primarily at particular cysteines in the steroid binding core domain, it has been postulated that arsenite, cadmium

and other compounds may be chemically modifying cysteine or crosslinking it to other adjacent thiol residues. It is therefore possible that zinc might inhibit glucocorticoid signalling by inhibition of ligand binding to receptor.

Next, the intervening events between initial ligand binding and DNA binding, including receptor transformation, translocation to and entry into the nucleus may also be affected by high concentrations of zinc. The oxidation/reduction state of cysteines in the steroid binding domain has been found to affect receptor transformation as well as steroid binding (Kalimi and Love, 1980; Tienrungroj *et al*, 1987b), implying that the inhibitory effects of metal ions and oxyanions observed for ligand binding may apply to transformation as well. Pratt and colleagues have purified an extremely low molecular weight stabilizing factor (Mr < 400) from rat liver cytosols that can stabilize GR *in vitro* in a manner similar to molybdate and other Group VI metal oxyanions, favoring association of GR with hsp90 (Meshinchi *et al*, 1988). This factor is an anion, and can be removed by treatment with Chelex-100, suggesting that it is a metal (Meshinchi and Pratt, 1989; Hutchinson *et al*, 1992a). While current evidence suggests that this factor is not zinc, zinc might compete with this factor, affecting GR-hsp90 association as a result. Computer modeling of predicted polypeptide folding patterns in GR and hsp90 when hsp90 is associated with GR at the steroid binding domain predict at least three sites where adjacent cysteines in combination with weak leucine zippers might allow the formation of Cys_2-metal-Cys_2 bridges that might facilitate GR-hsp90 binding. Introduction of certain metals such as zinc might also cause stabilization, alteration or disruption of GR-hsp90 binding (Schwartz *et al*, 1993). While the well-characterized nature of hsp90 interaction with GR permits the most speculation on the possible effects of zinc, other sites at which zinc could interfere with receptor transformation and nuclear translocation. Effects on receptor "transportosome" movement along cytoskeletal elements, transient association and "unfoldase" activity of hsp70 necessary for hsp90 association and dissociation, binding to

the nucleus and nuclear transport could all be affected by treatment with zinc.

Finally, the possibility that zinc might be blocking apoptosis via the glucocorticoid signalling pathway is also supported by recent observations regarding the binding affinities of zinc finger transcription factors. GR possesses two zinc fingers of the Cys_2-Cys_2 variety (distinguished from other transcription factors such as TFIIIA by the lack of histidine residues). The amino acid sequence of the zinc finger region for rat GR is Cys-X_2-Cys-X_{13}-Cys-X_2-Cys-X_{15}-Cys-X_5-Cys-X_9-Cys-X_2-Cys-X_4, giving two zinc fingers of different loop sizes in close proximity (Freedman, 1992; Dahlman-Wright *et al*, 1992). The N-terminal zinc finger has two and two amino acid residues separating its first and second and third and fourth cysteine respectively, providing a high-affinity coordinate binding site for zinc. The C-terminal zinc finger has five and two residues separating its first and second and third and fourth cysteine respectively. The greater degree of separation between the first and second cysteine in the C-terminal finger results in a lower affinity for zinc (estimated to be almost a thousand-fold less than the N-terminal finger)(Pan *et al*, 1990). The concentration of zinc present with the GR may therefore have a profound effect on the occupancy of the C-terminal zinc finger.

In an effort to determine whether zinc might be inhibiting glucocorticoid-induced apoptosis in mouse thymocytes by interfering with glucocorticoid signalling, studies were carried out to determine whether zinc altered the ability of ^{3}H-dexamethasone (^{3}H-DEX) to bind to cytoplasmic GR in mouse thymocytes. In addition, the effects of zinc on the ability of ligand-bound receptor to be localized to the nucleus was also examined. These preliminary experiments were therefore designed to determine whether zinc inhibited inital receptor-ligand binding, nuclear localization or both.

CHAPTER 7: MATERIALS AND METHODS

Culture reagents. Cell culture of mouse thymocytes for studies of *in vivo* GR-ligand binding required that all culture media was depleted of endogenous steroids, and that media did not contain components that might act as glucocorticoid agonists or antagonists. For this reason, all fetal bovine serum used in these experiments was depleted of steroids by dextran coated charcoal (DCC) absorption (FBS-DCC). This was done by incubating serum with 10% w/v activated charcoal (10 mg/ml) and 1% cell culture grade dextran (1 mg/ml) for 30 minutes at 50°C with constant mixing. Serum was then centrifuged at 5,000 x g at 4°C to remove charcoal, sterile filtered and stored at -20°C. In addition, phenol red was omitted from culture medium since it has been shown to be a weak glucocorticoid antagonist.

Preparation of mouse thymocytes. Thymuses from young male A/J mice (6 to 12 weeks old) were surgically removed and extruded through 100 micron stainless steel screens into phosphate buffered saline (PBS) containing 2% FBS-DCC. Cells were erythrocyte-depleted over Histopaque 1083 gradients (Sigma), washed twice by centrifugation at 800 x g followed by resuspension in PBS/FBS-DCC.

Cell culture. Cells were then resuspended in phenol red-free RPMI medium supplemented with 10% FBS-DCC. Cells were then plated in triplicate into 24-well plates at 2 x 10^6 cells/1.6 mls/well (1.25 x 10^6 cells/ml) and incubated for 15 minutes at 37°C to equilibrate medium temperature. [6,7-^{3}H(N)]-dexamethasone (^{3}H-DEX) obtained from NEN-Dupont, 40 - 50 Ci/mmol specific activity) was then added at 50 nM final concentration, as 200 μl of a 500 nM stock solution in prewarmed RPMI/FBS. Unlabeled DEX at 50 μM final concentration (1000-fold excess), as 200 μl of a 500 μM stock concentration in RPMI/FBS-

DCC, or RPMI/FBS-DCC alone was added to non-specific and total binding samples respectively. For some experiments the antagonist RU486 was used in place of DEX at 100-fold excess. Both unlabeled competitors gave comparable non-specific binding values. Plates were then incubated for 60 minutes at 37°C with periodic shaking.

For experiments determining the effects of zinc on cytosolic receptor-ligand interaction or nuclear localization, zinc sulfate heptahydrate diluted in RPMI/FBS was added to cells and allowed to preincubate for four hours prior to addition of radiolabeled ligand and unlabeled competitor. This preincubation was found to be necessary for zinc to exert the observed inhibitory effects on receptor-ligand binding and nuclear localization. Viability of cells was periodically evaluated by trypan blue exclusion.

Following incubation cells were removed from wells and transferred to 12 x 75 mm polypropylene tubes precooled on ice. Samples were then centrifuged at 800 x g at 4°C for 5 minutes, decanted and resuspended in 4 mls cold PBS. This washing step was repeated three times. This was followed by extraction of cytosolic or nuclear fractions.

Extraction of cytosolic fractions and determination of cytosolic GR-ligand binding. This was carried out as previously described (Leake and Habib, 1987). Following washing with PBS the samples were decanted and resuspended in 0.5 mls cold PBS. Two mls of nuclei extraction buffer with DCC (320 mM sucrose, 5 mM $MgCl_2$, 10 mM HEPES, 1% Triton X-100, 10 mg/ml activated charcoal and 1 mg/ml dextran at pH 7.2) was added with constant gentle vortexing. The samples were then incubated on ice for an additional 10 minutes with periodic vortexing, followed by centrifugation at 2000 x g for 5 minutes to pellet nuclei and DCC. The DCC was present to remove free cytosolic ligand, presumably leaving protein-bound ligand behind. One ml of the resulting supernatant was then added to vials of aqueous scintillation cocktail and counted on a scintillation counter for ^3H activity. Specific binding of ^3H-DEX to cytosolic proteins was calculated as the difference

between total binding (in samples with no excess of unlabeled competitor) and non-specific binding (samples with 1000-fold excess of unlabeled competitor).

Extraction of nuclear fractions and determination of GR nuclear localization. This was carried out as previously described (Leake and Habib, 1987). Following washing cells were resuspended in 0.5 mls cold PBS. Two mls of nuclei extraction buffer (320 mM sucrose, 5 mM $MgCl_2$, 10 mM HEPES and membrane-grade 1% Triton X-100 at pH 7.2) was added with constant gentle vortexing. The samples were incubated on ice for 10 minutes with periodic vortexing, followed by centrifugation at 2000 x g for 5 minutes to pellet isolated nuclei. The nuclei were then washed three times with cold nuclei wash buffer (320 mM sucrose, 5 mM $MgCl_2$ and 10 mM HEPES at pH 7.2) with centrifugation at 2000 x g. After decanting the final wash 0.5 ml of 0.4 M KSCN was added to each tube followed by vigorous vortexing to solublize nuclei. The lysates were incubated on ice for 30 minutes and centrifuged at 2500 x g for 5 minutes. Three hundred μl of the supernatant was added to vials of aqueous scintillation cocktail and counted for ^3H.

Immunoabsorption of mouse thymocyte cytosolic GR, SDS-PAGE and Western blotting. Following erythrocyte-depletion and washing, mouse thymocytes were washed twice with cold PBS, decanted and resuspended in the remaining supernatant (approximately 100 μl). Four hundred μl nuclei extraction buffer (described above) was then added with gentle vortexing. Samples were incubated on ice for 10 minutes followed by centrifugation at 2000 x g to pellet nuclei. The supernatants (300 μl) were transferred to a 1.5 ml Eppendorf tube to which 10 μl of the monoclonal mouse-anti-rat GR antibody BUGR2 at 50 μg/ml (500 ng) was added. An isotype-matched (IgG_{2a}) monoclonal antibody MAR18.5 (mouse anti-rat immunoglobulin kappa chain) was used as a negative control for non-specific binding at equivalent protein concentration. Samples were incubated for two hours

at 4°C with constant shaking. Two hundred microliters of Sepharose-protein A suspension at 25 mg/ml (5 mg/sample) in HGM buffer (10 mM HEPES, 10% glycerol and 30 mM Na_2MoO_4 at pH 7.2) was then added to each sample, and the tubes incubated another hour at 4°C. The tubes were then centrifuged at 2000 x g to pellet Sepharose beads, decanted and resuspended in HGM buffer. The pellets were washed three times with a final decanting to remove almost all of the supernatant. For subsequent SDS-PAGE and Western blotting, the pellet was resuspended in 30 μl Laemmli denaturation and running buffer and heated for 3 minutes in a boiling water bath. The samples were then cooled, and 10 μl aliquots were then loaded on an 8% SDS-PAGE stacking minigel (Hoeffer). Molecular weight markers constituting molecular weights of 200 kd, 117 kd, 98 kd, 66 kd and 45 kd were simultaneously loaded in empty slots. The gel was electrophoresed in SDS-glycine electrophoresis buffer at 20 mA for 2 hours at a constant current setting. The gel was then transferred to an electroblotting apparatus and blotted onto PVDF membranes in Towbin transfer buffer at 200 mA for 1 hour at 4°C. Transfer membranes were then equilibrated with Tris-buffered saline (TBS) with 50 mM Tris-HCl, 0.9% NaCl, pH 7.2 and blocked with 5% non-fat dried milk in TBS for at least 1 hour. Blots were then immunoblotted overnight with BUGR2 antibody at 1:1000 in 1% nonfat dry milk in TBS supplemented with 0.05% Tween 20 (TTBS). Blots were then washed 4 times with 1% milk in TTBS and incubated for 1 hour in horseradish peroxidase (HRP)-conjugated sheep-anti-mouse IgG (Amersham) at 1:3000 in 5% dried milk in TTBS. Blots were washed 3 times in 1% milk in TTBS and three times in TBS alone. Blots were then sealed in plastic bags and incubated for two minutes with a luminol chemiluminescent substrate reagent with enhancers (Amersham or NEN-Dupont). Reagent was then removed and the blots immediately exposed to autoradiography film (Kodak) for periods from 30 seconds to two minutes to detect protein bands.

For some experiments, immunoabsorption was used to determine the percentage of

total cytosolic radioisotope counts that represented ligand bound to GR. Cells were incubated with ^{3}H-DEX with or without unlabeled competitor prior to lysis. After immunoabsorption, the Sepharose pellet was discarded and the supernatants counted for ^{3}H. Some experiments were done with or without prior DCC absorption to determine the proportion of protein-free and bound counts in cytoplasm.

CHAPTER 7: RESULTS

CHARACTERIZATION OF MOUSE THYMOCYTE CYTOSOLIC AND NUCLEAR GLUCOCORTICOID RECEPTOR.

***In vivo* receptor-ligand binding.** Specific ligand binding activity can be detected in the cytosolic and nuclear fractions of mouse thymocytes incubated with 50 nM ^{3}H-DEX (Figure 7-1). Specific ^{3}H-DEX binding activity is defined as the difference between total binding (with no unlabeled competitor added) and non-specific binding (with 500-fold unlabeled competitor added). Specific ^{3}H-DEX binding in the cytosol was approximately 1000 dpm per 10^6 cells following 60 minutes incubation. Specific ^{3}H-DEX binding in the nucleus was approximately 100 dpm per 10^6 cells following 60 minutes incubation. Incubation periods greater than 60 minutes (up to 120 minutes) did not give higher levels of ligand binding in the cytosol or nucleus, indicating that equilibrium binding has been reached (data not shown). Both of these values were comparable with previous observations made for ^{3}H-DEX binding in mouse and rat thymocytes by other laboratories (Lippman and Barr, 1977).

It was then necessary to determine whether the specific ^{3}H-DEX binding observed above was due to GR. To determine how much ligand was specifically bound to GR, DCC-absorbed cytosols from thymocytes incubated with ^{3}H-DEX were immunoprecipitated with BUGR2 (anti-GR) or MAR18.5 (isotype-matched irrelevant control) antibodies and the resulting cytosols analyzed for residual ^{3}H-DEX (Figure 7-2). BUGR2 absorption reduced ^{3}H-DEX in DCC-absorbed cytosols by approximately 70% compared to MAR18.5 at 10%. These results suggest that specific ligand binding to GR accounts for at least 70% of the total protein-ligand interactions in the cytosol. A significant proportion of protein-bound ligand in the cytosol is therefore bound to GR. Nevertheless, the apparent presence of other DEX-binding components needed to be considered when evaluating potential

inhibitory effects of zinc on specific cytoplasmic ligand binding.

Western blotting. Ligand binding and immunoabsorption experiments demonstrated that GR was present in mouse thymocytes. To directly show the presence of receptor in thymocytes independent of ligand binding, cytosols were immunoabsorbed with BUGR2 and Western blotted for glucocorticoid receptor. A typical immunoblot is shown in Figure 7-3. Immunoblotting with BUGR2 followed by a enzyme-conjugated sheep-anti-mouse secondary antibody gave two bands, one a 50 kd band that represents immunoglobulin heavy chains and a second that correlated almost precisely with the 97 kd immunoabsorbed mouse liver GR (see Chapter 8 Results for more information). No 97 kd band appeared when the isotype-matched irrelevant control antibody MAR18.5 is substituted for BUGR2 during immunoabsorption, or when BUGR2 is omitted from the immunoblotting procedure, although the immunoglobulin band still appeared in both samples. The 97 kd band is therefore thought to represent mouse thymocyte cytosolic GR.

EFFECTS OF ZINC ON CYTOSOLIC GLUCOCORTICOID RECEPTOR-LIGAND BINDING AND SUBSEQUENT NUCLEAR LOCALIZATION

Effects of zinc on *in vivo* cytosolic glucocorticoid receptor-ligand binding. To determine the effects of zinc on *in vivo* cytosolic receptor-ligand binding, mouse thymocytes were incubated with concentrations of zinc sulfate heptahydrate ranging from 50 to 500 μM with preincubation times ranging from zero to four hours. Specific binding values were then determined after 60 minutes incubation, previously found to give equilibrium binding both in the cytosolic and nuclear compartments.

The results are shown in Figures 7-4 and 7-5. Figure 7-5 shows the effects of zero, two and four hour preincubations with zinc at 500 μM with data expressed as percentages

of specific binding in control samples. Zinc added simultaneously with ligand has no apparent effect on receptor-ligand binding in the cytosol. Preincubation with zinc, however, did result in a loss of binding, with maximal inhibition of receptor-ligand interaction occurring after four hour preincubation with zinc at 500 μM. Thymocytes viability during these experiments remained at levels over 90% as determined by trypan blue exclusion.

After the optimal zinc preincubation time of four hours was determined, dose-response curves were carried out to determine the minimal effective dose needed for inhibition. Figure 7-6 shows that zinc exerted an inhibitory effect down to approximately 100 to 200 μM, below which little or no effect was observed. Even at higher concentrations, however, zinc reduced receptor-ligand binding only by approximately 70 to 80%.

Effect of zinc on *in vivo* ligand-dependent nuclear localization of glucocorticoid receptor. Since zinc inhibited receptor-ligand interaction in the cytoplasm of mouse thymocytes to a considerable degree, it was of of further interest whether subsequent translocation of ligand-bound receptor to the nucleus would also be inhibited. Nuclei were isolated following preincubation with zinc and incubated with ligand using the conditions described above. Figure 7-6 shows that sequestration of ligand-bound receptor to the nucleus was indeed inhibited by zinc with similar effective dose concentrations. Unlike cytoplasmic binding, nuclear localization was almost completely inhibited, usually by over 90%.

CHAPTER 7: DISCUSSION

Summary. These results indicate that zinc at concentrations relevant to the inhibition of glucocorticoid-induced apoptosis in mouse thymocytes (100 to 500 uM) also inhibited both glucocorticoid receptor-ligand interaction in the cytoplasm and subsequent localization to the nucleus, although a preincubation with zinc of four hours was required to produce this phenomenon. While inhibition of nuclear localization was found to be almost complete (greater than 90%), inhibition of cytoplasmic receptor-ligand binding was reproducibly inhibited by approximately 70%. Nevertheless, the percentage of ^{3}H-DEX specifically bound to GR determined by immunoabsorption studies was also approximately 70%, indicating that inhibition of cytoplasmic receptor-ligand binding might also be nearly total.

Interpretation of *in vivo* data: receptor-ligand interaction. One mechanism by which zinc might be acting is by inhibition of receptor-ligand interaction. Translocation of the receptor to the nucleus is entirely hormone-dependent in GR (unlike progesterone and estrogen receptor, which are found in the nucleus in the absence of hormone)(Pratt, 1987). Successful ligand binding is therefore necessary for receptor transformation via release of the hsp90 homodimer, derepressing the nuclear localization domains. Zinc inhibition of receptor-ligand interaction in the cytoplasm could therefore cause downstream inhibition of nuclear localization, consistent with both the cytoplasmic binding and nuclear localization data. As discussed previously, zinc might be crosslinking vicinal dithiols in a manner similar to that observed for arsenite, cadmium and selenium in GR and other steroid receptors (Simons *et al*, 1990). Modification of vicinal dithiols would almost certainly inhibition ligand binding. This is a potential mechanism that could be easily examined *in vitro*.

Effects of zinc on receptor transformation. Although inhibition of receptor-ligand binding was only partial at about 70%, the percentage of GR-specific ^{3}H-DEX binding in thymocytes was also about 70%, suggesting that inhibition of receptor-ligand binding may actually have been almost total. Nevertheless, ligand binding as the sole target of zinc may not be entirely consistent with the observed cytoplasmic receptor-ligand binding, since it cannot be proven that these two observations correlate. If inhibition of nuclear localization is entirely dependent on receptor-ligand binding inhibition, then partial binding inhibition would be expected to only partly inhibit nuclear localization. The partial inhibition of ligand binding to receptor and the almost total inhibition of nuclear localization raises the possibility that other elements of receptor signalling in addition to receptor-ligand interaction may also be affected by zinc.

Several important post-ligand binding events might therefore also be potential targets for zinc inhibition. Chief among these is the association of GR with the hsp90 homodimer, which as part of a larger heteromeric complex is believed to repress the DNA binding and nuclear localization domains when steroid is absent, placing these functions under strict hormonal control (Pratt, 1992). Modification of hsp90 interaction with GR by zinc *in vivo* would therefore almost certainly affect receptor translocation to the nucleus. Previous work suggests a number of possible effects for zinc on GR-hsp90 interaction, including hsp90 binding to the signal transducing site on the steroid binding domain, a condition which can be stabilized by molybdate *in vitro* and by an unknown endogenous metal stabilizing factor *in vivo*. Zinc could be acting at these or other sites to either prevent hsp90 dissociation, or to induce it at an inappropriate time. Either effect would result in an inhibition of nuclear localization such as was observed with zinc treatment. The effects of zinc on receptor transformation could also be examined in an *in vitro* cell-free receptor system.

***In vitro* studies.** Initial receptor-ligand binding and receptor transformation therefore represented two possible targets for zinc that would be consistent with the observations made in the *in vivo* thymocyte studies. Although the *in vivo* studies strongly implicate inhibition of receptor-ligand binding as the mechanism behind loss of both ligand binding and nuclear localization activity, they do not definitively show that other mechanisms (such as effects of receptor transformation) might not also be playing a role. In addition, the mechanism behind the inhibition of receptor-ligand inhibition is not clear. Although previous data suggest that zinc might be acting directly at the ligand binding site, another mechanism such as zinc-induced loss of hsp90 might also be a factor.

To more precisely identify the point at which zinc is inhibiting GR signalling and the underling mechanism for this inhibition, *in vitro* studies using both crude and immunopurified GR were subsequently undertaken to more specifically analyze and characterize the effects of zinc on (1) ligand binding to unactivated, untransformed GR, and (2) receptor transformation, both functionally (characterized by binding to isolated thymocyte nuclei and to glucocorticoid response element oligonucleotides) and biochemically based on hsp90 association with receptor. These studies allowed a precise determination of whether zinc was actually inhibiting ligand binding and/or receptor transformation. In addition, potential mechanisms for observed inhibitory activities of zinc (such as the role of vicinal dithiol crosslinking in the inhibition of ligand binding) could also be addressed.

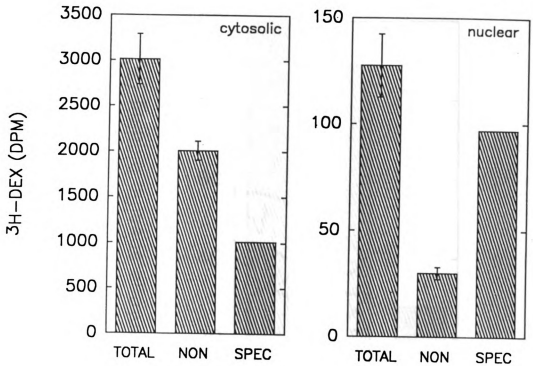

Figure 7-1. *In vivo* cytosolic ^{3}H-DEX binding assay **(left panel)** and nuclear localization assay **(right panel)** showing total (TOTAL, with no unlabeled competitor), non-specific (NON, with a 500-fold excess of unlabeled competitor) and specific (SPEC) ^{3}H-DEX binding for 10^6 cells incubated with ^{3}H-DEX at 50 nM for 60 minutes. Specific binding equals the difference between total and non-specific binding. Data are expressed as the mean plus or minus standard deviation of triplicate samples.

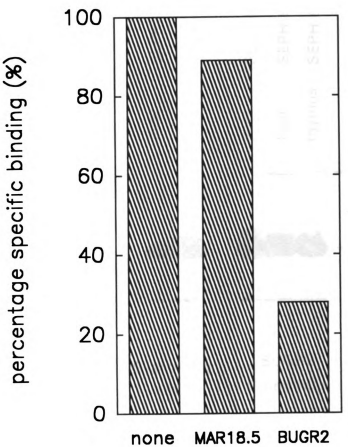

Figure 7-2. GR-specific ^{3}H-DEX binding activity in the mouse thymocyte cytoplasm. Mouse thymocytes were incubated with ^{3}H-DEX, lysed to obtain cytosol and immunoabsorbed with either BUGR2 (anti-GR) or MAR18.5 (negative control) followed by Sepharose-protein A. The Sepharose pellets were then removed and the cytosol counted for ^{3}H. Values are expressed as percentages of total cytoplasmic binding with no immunoabsorption.

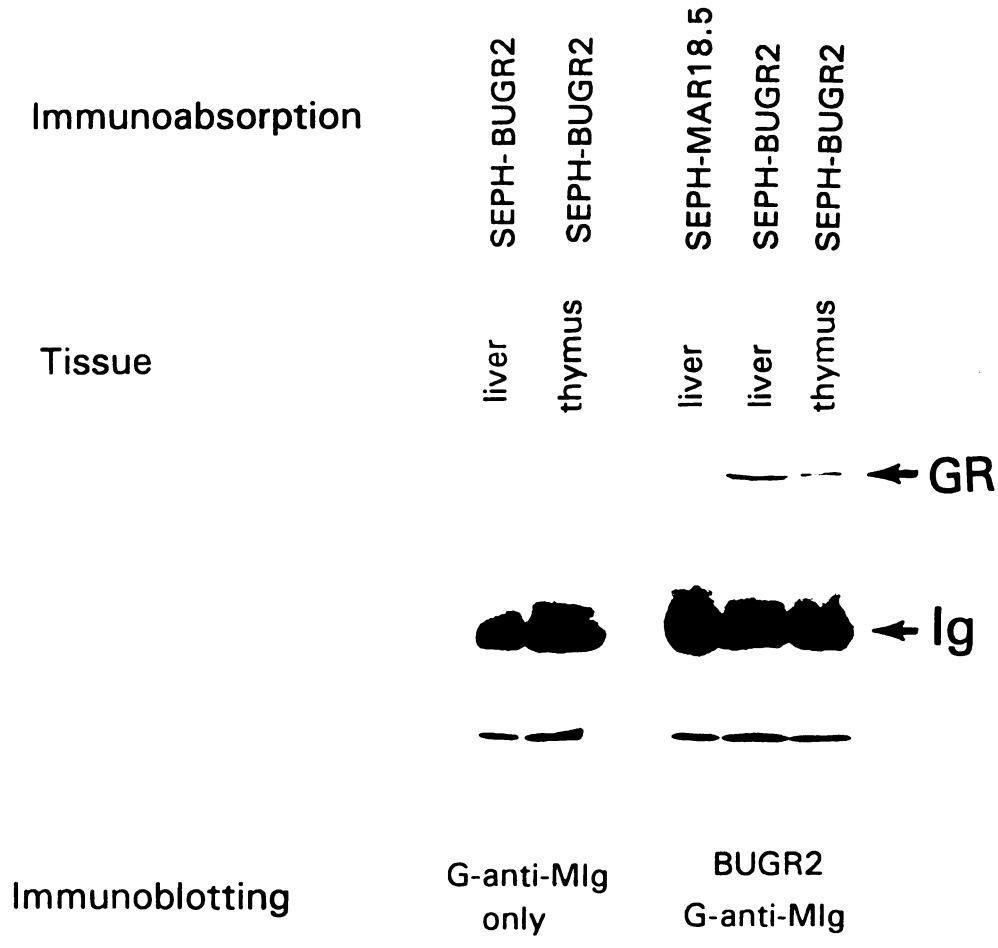

Figure 7-3. Western blotting of mouse thymocyte cytosolic GR in comparison with liver cytosolic GR. SEPH-BUGR2 and SEPH-MAR18.5 indicate immunoabsorption with anti-GR and negative control antibodies respectively. Immunoblotting was done with BUGR2 and/or HRP-conjugated sheep-anti-mouse IgG (G-anti-MIg).

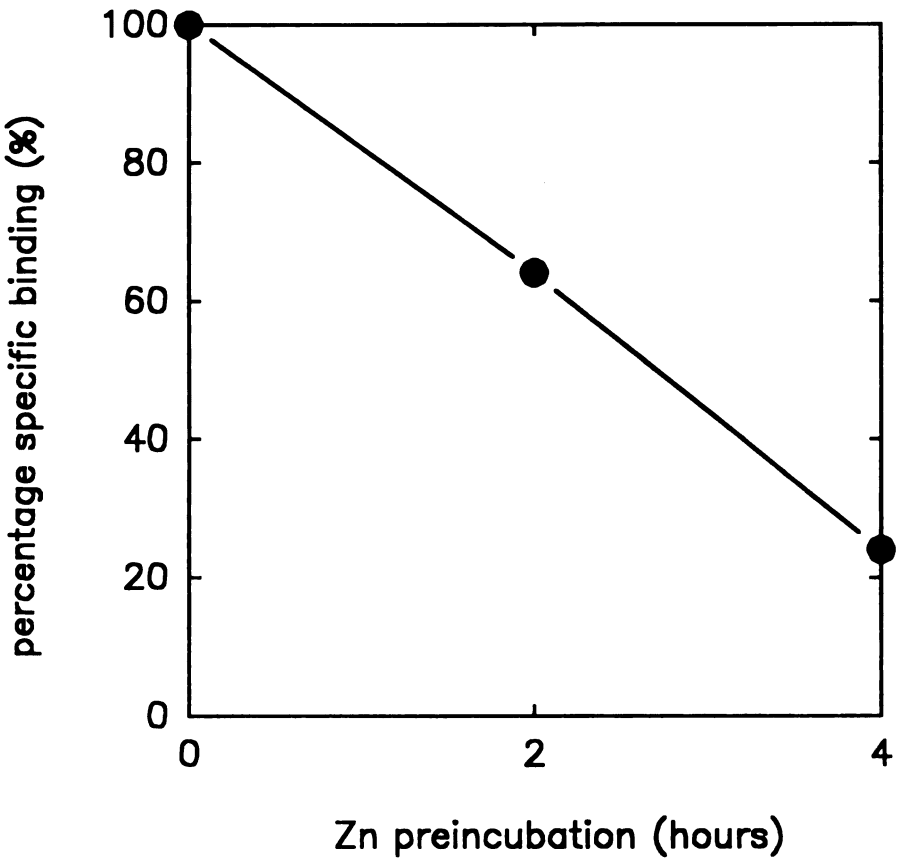

Figure 7-4. Effect of zinc preincubation (500 μM for 0, 2 and 4 hour preincubation) on cytosolic ^{3}H-DEX binding in mouse thymocytes. Data are expressed as percentages of specific binding in control samples.

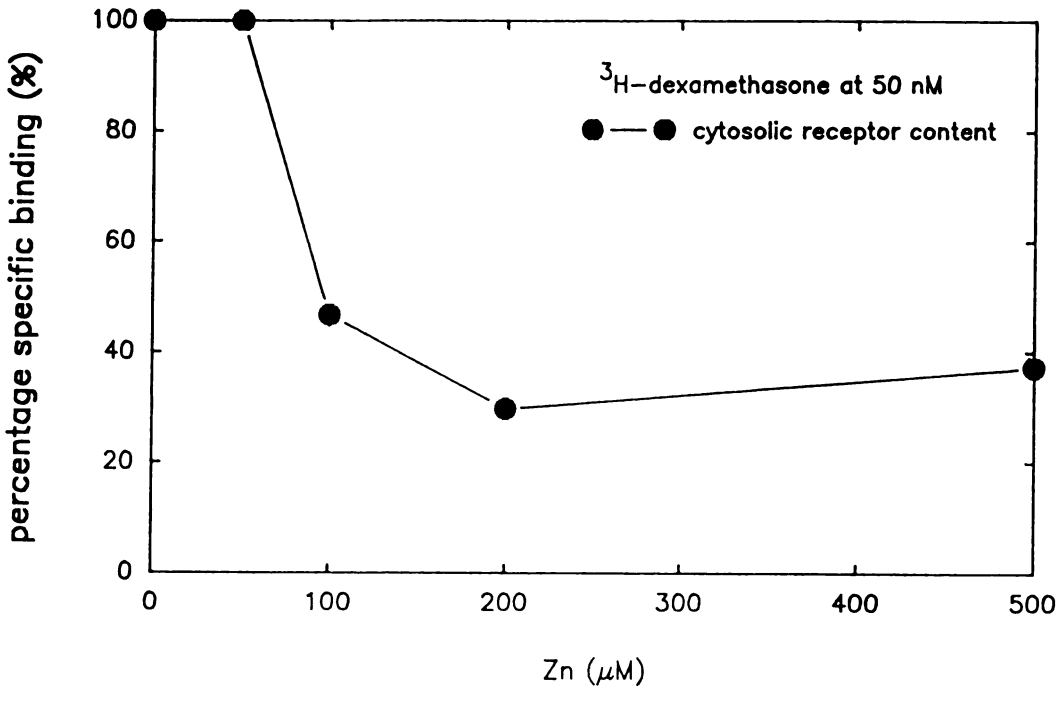

Figure 7-5. Effect of zinc preincubation (4 hours) on cytosolic ^{3}H-DEX binding in mouse thymocytes. Data are expressed as percentages of specific binding in control samples.

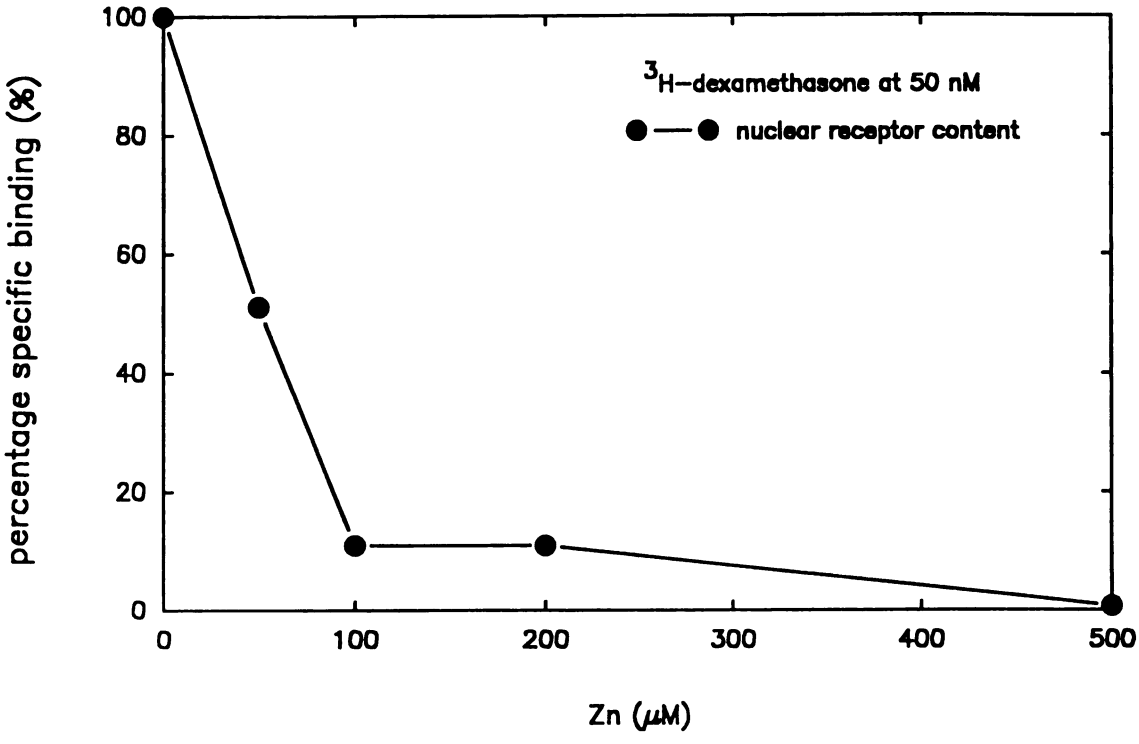

Figure 7-6. Effect of zinc preincubation (4 hours) on nuclear localization of ^{3}H-DEX in mouse thymocytes. Data are expressed as percentages of specific binding in control samples.

CHAPTER 8

EFFECTS OF ZINC ON *IN VITRO* GLUCOCORTICOID RECEPTOR-LIGAND BINDING AND SUBSEQUENT TRANSFORMATION

CHAPTER 8: ABSTRACT

The *in vivo* cytoplasmic GR-ligand binding and nuclear localization data clearly indicate that zinc at concentrations relevant to the inhibition of glucocorticoid-induced apoptosis also inhibit GR-ligand interaction and possibly receptor transformation as well. To more clearly define the mechanism by which zinc was exerting its effects, receptor-ligand interaction and receptor transformation were examined *in vitro* using mouse liver cytosolic GR. Zinc at concentrations ranging from 10 to 100 μM was found to exert an almost total yet reversible inhibitory effect on radiolabeled ligand binding to receptor. Zinc was found to exert no detectable effects of GR transformation, based both on physical association of GR with hsp90, and also by functional analysis of receptor binding to isolated nuclei and to glucocorticoid response oligomers by gel mobility shift assay.

CHAPTER 8: INTRODUCTION

The *in vivo* cytoplasmic GR-steroid binding and nuclear localization data presented in Chapter 7 suggested that zinc at concentrations consistent with inhibition of hormone-induced apoptosis in mouse thymocytes prevented receptor-ligand interaction and translocation of activated receptor to the nucleus. These results indicated that zinc might be affecting GR signalling at the level of receptor-ligand interaction and possibly at downstream steps as well.

Rationale for *in vitro* studies. Since the *in vivo* observations suggested that zinc may be exerting its effects at the level of cytoplasmic receptor-ligand interaction and possibly other areas as well, the effects of zinc on receptor structure and function were examined in an *in vitro* cell-free system. *In vitro* experiments allowed the steps of GR signalling to be dissected into more discrete steps (i.e. receptor-ligand binding, receptor transformation) to identify specific targets for zinc. Due to the relative low levels of cytosolic GR in mouse thymocytes (approximately 6000 receptors per cell), cytosolic receptor from the mouse liver was used, due to its greater per cell abundance and the greater amount of liver tissue available (Crabtree *et al*, 1980). This study had essentially two objectives:

1) The effects of zinc on cytoplasmic GR-ligand interaction. *In vivo* studies supported receptor-ligand interaction as at least one target for zinc. It was therefore determined whether zinc salts inhibited ^{3}H-DEX binding to mouse liver cytosolic GR *in vitro*, both by analysis of receptor-ligand binding in crude cytosolic preparations, and in immunopurified, immobilized receptor. Inhibitory effects of zinc were subsequently examined with regard to kinetics of inhibition, reversibility, and other chemical conditions

of inhibition (such as the presence of reducing agents). These experiments more clearly defined the mechanistic nature of zinc inhibition of receptor-ligand interaction.

2) The effects of zinc on post-ligand binding events in glucocorticoid receptor signal transduction. Association and dissociation of the hsp90 homodimer from GR is one of the best characterized post-hormone binding events in GR signalling. Previous work suggesting that zinc and other metals might affect GR-hsp90 interaction made this aspect of receptor function an obvious choice for study as a potential target for zinc (Pratt, 1987; Schwartz *et al*, 1993). Experiments were carried out to determine whether zinc induced or inhibited *in vitro* GR-hsp90 interaction, under hormone-dependent and hormone-independent conditions. Assays for receptor transformation, including the ability of transformed receptors to bind to isolated nuclei or glucocorticoid response element (GRE) oligonucleotides, and direct coabsorption of hsp90 with GR were utilized to assess the effects of zinc on *in vitro* GR-hsp90 association.

CHAPTER 8: MATERIALS AND METHODS

Preparation of crude liver cytosols. Livers from young (4 -12 week old) male A/J mice (The Jackson Laboratory), were removed, chilled on ice, washed and perfused through the hepatic portal vein with cold saline (0.15 M NaCl). They were then mechanically homogenized in a tight-fitting Potter-Elvehjem glass/Teflon tissue grinder at 4°C for 60 seconds in HDG buffer (10 mM HEPES, 10% glycerol, 1 mM dithiothreitol [DTT] at pH 7.2). DTT was added to the buffer immediately prior to use. In some cases, sodium molybdate (Na_2MoO_4) was added at 30 mM (HDGM buffer) prior to homogenization to stabilize receptor preparations. The resulting tissue suspension was filtered through cheesecloth and centrifuged at 5000 x g at 4°C to remove suspended particulates. The supernatant was then ultracentrifuged at 100,000 x g for 60 minutes at 4°C, and carefully removed by pipet to prevent contamination with lipid. The resulting cytosol was then frozen and stored at -70°C. Total protein concentration was determined by Bradford colorimetric protein assay (Biorad). For some experiments, ligand-free cytosols were prepared by absorption with 10% activated charcoal and 1% dextran using 2 mg charcoal per 1 mg protein (DCC).

Ligand binding assay: Dextran-coated charcoal absorption (DCC). This was carried out as previously described with some modifications (Leake and Habib, 1987). To 1.5 ml Eppendorf tubes the following were combined at 4°C: 1 mg crude liver cystosol (total protein), usually as 160 μl of a 6.25 mg/ml stock solution in HDG or HDGM buffer, [6,7-^{3}H(N)]-dexamethasone (^{3}H-DEX) (NEN-Dupont, 40 - 50 Ci/mmol specific activity) at 50 nM, usually as 20 μl of a 500 nM stock solution, and either unlabeled dexamethasone (DEX) at 25 μM (500-fold excess), usually as 20 μl of a 250 μM stock solution, of HDG or HDGM buffer with no cold competitor. In some experiments,

RU486 at 25 μM final concentration was used as a cold competitor in place of dexamethasone. Both gave roughly equivalent results with regard to blocking specific binding. The total reaction mixture volume was 200 μl. Tubes were mixed and allowed to incubate on ice for 2 hours. Following incubation, 200 μl of a 10 mg charcoal/1 mg dextran/ml suspension (2 mg charcoal/sample) was added per tube. The tubes were then incubated for an additional 15 minutes with vortexing every five minutes. Samples were then centrifuged at 2000 x g for 5 minutes to pellet charcoal/dextran. Aliquots of supernatants (100 μl) were added to vials of aqueous scintillation cocktail (Safety-Solve) and analyzed for ^{3}H on a scintillation counter. Specific binding was calculated as the difference between samples containing ^{3}H-DEX alone (total binding) and samples containing 500-fold excess of cold competitor (non-specific binding). In experiments with added zinc, 1 M $ZnSO_4 \cdot 7H_2O$ was diluted 1:1000 in HDG or HDGM buffer followed by adjustment to pH 7.2 to prepare a 1 mM stock solution. Lower zinc dilutions were prepared from this stock. Stock concentrations and volumes of cytosol were modified to accomodate addition of zinc. All samples were done in triplicate.

To determine whether the effects of zinc on ligand binding were reversible, 5 mg of Chelex-100 (100 μl of a 50 mg/ml suspension) were added to remove zinc following initial receptor-ligand binding. Tubes were then incubated at 4°C for 15 minutes with rapid shaking, followed by centrifugation and transfer of supernatants to new tubes. Na_2MoO_4 was added to the supernatants to a final concentration of 30 mM following Chelex extraction since Chelex-100 will also bind molybdenum.

Ligand binding assay: DEAE-cellulose filter. This was carried out as previously described with some modification (Baxter *et al*, 1975). Cytosols were incubated with ^{3}H-DEX and with or without cold competitor for two hours as described above. DEAE-cellulose filter circles (DE81, 25 mm diameter, Whatman) were mounted two-thick on a

filter manifold (Millipore), prewet with cold HDG or HDGM buffer and partially vacuum-dried. Fifty μl of incubated cytosols were then slowly added to the center of the filters and allowed to absorb for five minutes without vacuum. Vacuum was then applied and filters washed with three 20 ml volumes of cold HDG or HDGM buffer. Filters were dried, placed in vials with nonaqueous scintillation cocktail and counted for ^{3}H. Specific binding was calculated in the same manner as for the DCC absorption assay. All samples were done in triplicate.

Binding of transformed glucocorticoid receptor to isolated nuclei. Receptor binding to isolated nuclei was carried out as originally described by Hubbard and Kalimi (1983) with considerable modification. Crude liver cytosols (20 mg/ml) were labeled with 50 nM ^{3}H-DEX with or without cold competitor for two hours at 4°C in HDG or HDGM buffer supplemented with 5 mM $MgCl_2$ (to stabilize nuclei) followed by DCC extraction. Following ligand binding, some cytosol samples were "transformed" by warming to 20°C for 30 minutes, then kept on ice until use. Untransformed samples were kept on ice. Isolated nuclei were prepared from mouse thymocytes. Thymuses were harvested from young male A/J mice and extruded through 100 micron metal screens into phosphate buffered saline (PBS) supplemented with 4% fetal bovine serum (FBS). Thymocytes were then erythrocyte-depleted over a Histopaque 1083 gradient (Sigma Chemical Co., St. Louis, MO), washed twice by centrifugation at 800 x g followed by resuspension in PBS/FBS, then washed twice in cold PBS alone. Thymocytes were aliquoted into individual 12 x 75 mm polypropylene tubes at 5 x 10^6 cells/tube, washed again and resuspended in 0.5 mls cold PBS. Thymocytes were then treated with two mls cold nuclei extraction buffer (320 mM sucrose, 5 mM $MgCl_2$, 10 mM HEPES, 1% Triton X-100 at pH 7.4), gently vortexed and allowed to incubate on ice for 10 minutes. Nuclei were then pelleted by centrifugation at 2000 x g and washed twice with nuclei wash buffer (320 mM

sucrose, 5 mM $MgCl_2$, 10 mM HEPES at pH 7.4). Nuclei yield and integrity were confirmed by microscopic examination with trypan blue staining, giving greater than 98% successful lysis with little debris and minimal clumping. After decanting the last wash, 300 μl cytosol labeled with ^{3}H-DEX with or without cold competitor were added to each nuclei pellet, and the tubes allowed to incubated at 4°C with periodic shaking for two hours. Zinc sulfate heptahydrate was added at the beginning of incubation where indicated from a 1000 μM stock solution in nuclei wash buffer. Following incubation, pellets were washed twice with nuclei wash buffer and centrifugation at 2000 x g. Nuclei pellets were then solublized with 0.4 M KSCN, vortexed vigorously, incubated on ice for 30 minutes and centrifuged at 2500 x g for 5 minutes. Aliquots of 300 μl were added to aqueous scintillation cocktail and counted for ^{3}H. Typical specific binding values for "fully" transformed receptor binding (no Mo, 20°C) were 800 to 900 dpm, while Mo-stabilized receptors gave 200 to 250 dpm.

Immunoabsorption of glucocorticoid receptor, SDS-PAGE and Western blotting. Immunoabsorption of mouse cytosolic GR was carried out in a manner similar to that described by Sanchez *et al* (1987). Crude liver cytosols in HDGM buffer in 200 μl aliquots were incubated with or without 50 nM cold DEX for 2 hours for ligand-dependent and ligand-independent experiments respectively. Cytosols were then incubated with 0.5 μg (10 μl of 50 μg/ml stock) BUGR2 monoclonal mouse-anti-rat GR antibody (Affinity Bioreagents, Neshanic Station, NJ) for two hours at 4°C with constant gentle mixing. Five mg Sepharose-protein A (200 μl of 25 mg/ml stock suspension in HDGM) was then added to each sample followed by one hour incubation at 4°C with vigorous mixing. The Sepharose-protein A beads were then pelleted by centrifugation at 1500 x g for 30 seconds, the supernatant removed and the beads resuspended in 1 ml cold HDGM buffer. The beads were washed in this way four times, with the final supernatant

removed so as to leave a minimal amount of buffer above the bead pellet. For subsequent SDS-PAGE and Western blotting, the pellet was resuspended in 30 μl Laemmli denaturation and running buffer and heated for 3 minutes in a boiling water bath. The samples were then cooled, and 10 μl aliquots were then loaded on an 8% SDS-denaturing polyacrylamide stacking minigel (Hoeffer). Molecular weight markers consitituting molecular weights of 200 kd, 117 kd, 98 kd, 66 kd and 45 kd were simultaneously loaded in empty slots. The gel was electrophoresed in SDS-Tris-glycine electrophoresis buffer pH 8.3 at 20 mA for 2 hours at a constant current setting. The gel was then transferred to an electroblotting apparatus and blotted onto either PVDF membranes for GR immunodetection or supported nitrocellulose membranes for hsp90 immunodetection using 20% methanol Towbin transfer buffer at 4°C. For GR immunoblotting, electroblotting was carried out at 200 mA for 1 hour. For hsp90 immunoblotting, it was carried out at 50 mA for four hours. All transfer membranes were then equilibrated with Tris-buffered saline (TBS) with 50 mM Tris-HCl, 0.9% NaCl, pH 7.2. Membranes were blocked with 5% nonfat dried milk (Carnation) in TBS for at least 1 hour. Blots were then immunoblotted with BUGR2 antibody at 1:1000 or AC88 monoclonal mouse-anti-*Achlya ambisexualis* hsp88 antibody (crossreacts with rodent hsp90)(Stressgen, Victoria, BC, Canada) at 1:1000 in 1% dried milk in TBS supplemented with 0.05% Tween 20 (TTBS). Blots were then washed 4 times with 1% milk in TTBS and incubated for 1 hour in horseradish peroxidase (HRP) -conjugated sheep-anti-mouse IgG (Amersham) at 1:3000 in 5% dried milk in TTBS. Blots were washed 3 times in 1% dried milk in TTBS and three times in TBS alone, sealed in plastic bags and incubated for two minutes with luminol chemiluminescent substrate with oxidative enhancers (Amersham or NEN-Dupont). Reagent was removed and the blots exposed to autoradiography film for periods from 30 seconds to two minutes to detected protein bands.

To determine the effects of zinc on ligand binding to immunoabsorbed receptor,

cytosolic receptor was immunoabsorbed with BUGR2 and Sepharose-protein A as described above. Aliquots of beads were then incubated with 50 nM ^{3}H-DEX with or without cold competitor with or without zinc for 2 hours at 4°C with vigorous shaking. Pellets were then washed 4 times as above followed by solublization with 0.4 M KSCN. The beads were then pelleted, and a sample of supernatant counted for ^{3}H.

For detection of coabsorbed hsp90 to determine *in vitro* receptor transformation, ligand-bound or ligand-free cytosols were immunoabsorbed with BUGR2 and Sepharose-protein A in HDGM buffer. Following immunoabsorption the pellets were washed 3 times with HDG buffer to remove all molybdate. The pellets were then either maintained at 4°C or warmed to 20°C to induce transformation. The pellets were subsequently washed 4 times in HDGM buffer, followed by SDA-PAGE, electroblotting and immunoblotting for both GR and hsp90 as described above. PVDF membranes were found to bind GR well but hsp90 poorly, an observation that has been made previously. Supported nitrocellulose provided a better binding substrate for hsp90. In addition, the close molecular weights of GR and hsp90 (97 kd and 90 kd respectively) and the different electroblotting requirements for each protein made it necessary to blot for GR and hsp90 on separate membranes.

Liver cytosols cleared of GR were prepared for some experiments by immunoabsorption as described above. These cytosols contained no radiolabeled DEX binding activity compared to normal cytosols.

Gel mobility shift assay. These were done according to Henninghausen and Lubon (1987), Varshavsky (1987) and protocols provided by Dr. Michael Denison (UC-Davis). Crude liver cysotols in HDG or HDGM buffer prepared at 5 mg/ml stock concentration (100 μg/20 μl) were incubated with or without cold dexamethasone for ligand-dependent and -independent experiments respectively and then maintained at 4°C or "transformed"

at 20°C for 30 minutes. A glucocorticoid response element dimer identical to the cloned pBLCAT2 fragment used elsewhere (Schmid *et al*, 1989) was synthesized as two 42 bp single stranded oligomers (MSU Macromolecular Facility). The ssDNA oligomers were desalted on C_{18} Sep-Pak columns and both strands annealed. The sequence is (with GREs highlighted):

5'-TAGAACATCCTGTACAACTAGTAGAACATCCTGTACATCTAG-3'
3'-ATCTTGTAGGACATGTTGATCATCTTGTAGGACATGTAGATC-5'

This sequence contained a six base pair spacer between the GREs. For some experiments, a 26 bp oligomer containing a single GRE was also synthesized and used to illustrate reduced binding at monomeric sites. A 42 bp sequence containing a CTF/NF1 response element (Promega) was used both as a non-specific competitor sequence in unlabeled form and as an internal standard for comparing nuclear protein levels in different cytosols prepared with and without molybdate in radiolabeled form. The GRE dimer in 40 pmol amounts was radiolabeled by 5'-end labeling phosphate exchange with [γ-^{32}P]-ATP (NEN-Dupont) and terminal deoxytransferase (Boehringer-Mannheim). The radiolabeled oligomers were separated from unreacted radiolabel over Sephadex G-50 minicolumns. Specific activity was determined by 10% tricloroacetic acid precipitation followed by blotting onto glass fiber filters.

To assess receptor binding to oligomer, two μl radiolabeled GRE dimer (approximately 70,000 - 100,000 DPM) was then added to 20 μl cytosol (100 μg protein) and incubated on ice for two hours. Since background binding and total number of DNA-protein binding events observed was minimal, no poly[d(I-C)] appeared to be required for complex resolution and was therefore not included. Following incubation a bromphenol tracking dye was added and samples were loaded on a 4% nondenaturing low ionic

strength polyacrylamide gel (Tris-acetate-EDTA, prerun at 150 volts for 2 hours). Samples were electrophoresed at 120 volts for 4 hours or until the dye had migrated approximately 50% the length of the gel. The gel was then dried onto filter paper and autoradiographed for 24 hours or analyzed by autoradiographic densitometry (AMBIS).

CHAPTER 8: RESULTS

CHARACTERIZATION OF MOUSE LIVER CYTOSOLIC GLUCOCORTICOID RECEPTOR.

The following sections describe the initial optimization of the GR-ligand binding and transformation assays used later to assess the effects of zinc on these functions.

***In vitro* receptor-ligand binding.** Specific ^{3}H-DEX binding to cytosolic components was detected in crude mouse liver cytosols using a conventional dextran-coated charcoal (DCC) absorption assay, where specific binding was calculated as the difference between total binding (no cold DEX added) and non-specific binding (500-fold excess of cold DEX added) (Figure 8-1, left panel). Specific binding usually constituted approximately 60 to 80% of total counts, or approximately 2000 to 4000 DPM per mg total protein, values that are consistent with previous reports (Kalimi *et al*, 1975; Lippman and Barr, 1977). Since the removal of free ligand by DCC disrupts the binding equilibrium of the reaction mixture and hence may result in an underestimation of specific receptor binding, a DEAE-cellulose receptor binding was also employed (Figure 8-1, right panel). This assay immobilizes ligand-bound receptor while free ligand is washed away, resulting in little disruption of reaction equilibrium. The DEAE-cellulose filter binding assay gave results of similar magnitude to those found for DCC. Both assays exhibited equilibrium binding conditions by two hours as evidenced by no further increase in specific binding after this time (data not shown), indicating that this incubation interval was sufficient for both determination of relative binding values and receptor binding affinities by Eadie-Scatchard analysis.

Eadie-Scatchard analysis. Eadie-Scatchard analysis was used to determine the nature of ^{3}H-DEX binding to crude mouse liver cytosolic proteins (Scatchard, 1949; Segel, 1976). This was done for three reasons: 1) the number of binding affinities and hence the number of proteins binding DEX could be calculated (ideally this should be only one), 2) if only a single protein was binding DEX, the K_m can be calculated for comparison to literature values for glucocorticoid receptor (GR) and 3) the approximate concentration of GR in the cytosolic preparation could be calculated. Concentrations of ^{3}H-DEX ranging from 10 to 100 nM were used, with ligand treated as the substrate with known concentrations ($[S]_T$) and DEX binding proteins in the cytosol with unknown concentrations treated as enzyme ($[E_T]$). The derived Eadie-Scatchard plot is given in Figure 8-2. Linear regression of the plotted values resulted in a straight line, indicating a single binding affinity. The K_s derived from the slope of the curve is 2.41×10^{-8} M, a value which coincides within an order of magnitude to literature values for mouse liver GR (Beato and Feigelson, 1972). The total "enzyme" (^{3}H-DEX-bound protein) concentration $[E]_T$ equals the K_s times the y-intercept divided by the the number of ligand binding sites (assumed in this case to be one per receptor molecule) equaling 0.51 nM in a 5 mg/ml total protein concentration cytosol, a typical value for our cytosol samples. Classical equilibrium binding experiments therefore indicate that ^{3}H-DEX is likely binding to only one protein in the crude mouse liver cytosol, and the binding affinity of that protein is similar to literature values for mouse liver GR.

^{3}H-DEX is a high-affinity synthetic glucocorticoid commonly used in *in vitro* GR binding studies because of its specificity for GR. It does not bind low molecular weight steroid binding proteins such as corticosterone binding globulin that are found in liver and can bind corticosterone and other naturally occuring glucocorticoids (reviewed by Hammond, 1990 and Rosner, 1990). Since it was in the interest of this study to evaluate receptor-ligand interactions between natural as well as synthetic glucocorticoids,

radiolabeled corticosterone was also evaluated for its ability to bind proteins in crude mouse liver cytosol by Eadie-Scatchard as was done for ^{3}H-DEX. The derived Eadie-Scatchard binding curve is shown in Figure 8-3. A straight binding curve was also observed for corticosterone with a Ks of 5.41 x 10^{-8}M, a reduction consistent with the reduced affinity of naturally occuring glucocorticoids over synthetics (Beato and Feigleson, 1972). This binding curve suggests that no other proteins were present with significant affinity for steroid.

Glucocorticoid receptor immunoabsorption and Western blotting. To confirm that the ^{3}H-DEX binding protein in mouse liver cytosols detected by receptor-binding assays and Scatchard analysis was indeed GR, cytosols were immunoabsorbed using the monoclonal mouse-anti-rat GR antibody BUGR2 (isotype IgG_{2a}) (Gametchu and Harrison, 1984). BUGR2 recognizes rat GR within residues 395 - 410 as determined by epitope mapping, immediately N-terminal to the DNA binding domain. It recognizes both native and denatured receptor, and has been used for immunoprecipitation, Western blotting and immunocytochemistry by a number of laboratories. It is reported to react with all rodent GR including mouse (Harrison *et al*, 1987). In Figure 8-4, crude cytosols have been immunoabsorbed with BUGR2 and Sepharose-protein A followed by incubation with ^{3}H-DEX with or without cold competitor. The resulting Sepharose pellets have considerable ^{3}H-DEX binding capability with non-specific binding composing less than 10% of total binding. In contrast, immunoabsorption with MAR18.5, an isotype-matched irrelevant control antibody (IgG_{2a}, anti-rat kappa chain) resulted in virtually no DEX binding activity above background. In addition, cytosols absorbed with BUGR2 lost virtually all specific DEX binding activity (Figure 8-5). These results suggest that virtually all the DEX binding activity in crude cytosols is the result of GR, and that receptor can still bind ligand when immunoabsorbed with BUGR2 and Sepharose-protein A.

To confirm that BUGR2 was immunoabsorbing GR independent of its ability to bind radiolabeled ligand, immunoabsorbed proteins were run on 8% SDS-PAGE gels, electroblotted onto PVDF membranes and immunoblotted with BUGR2 antibody. Figure 8-6 shows a typical immunoblot. Two bands are identified by BUGR2 immunoblotting followed by secondary blotting with an HRP-conjugated anti-mouse secondary antibody. The 50 kd band is immunoglobulin heavy chains deduced from its appearance even when the membrane is blotted with secondary antibody alone. The single 97 kd band that does not appear when BUGR2 is omitted is believed to represent the mouse GR (with literature values of 97 to 98 kd). Immunoabsorption with MAR18.5 instead of BUGR2 does not result in the appearance of this band, indicating that it is probably not an artifact of the immunoabsorption system. These results indicate that BUGR2 selectively immunoabsorbs GR, and that receptor is present in crude mouse liver cytosols.

Glucocorticoid receptor transformation activity. Three assays were employed to detect and quantify GR transformation, that is the release of the hsp90 homodimer from the core receptor. The first assay, GR-hsp90 coabsorption, measured the physical association and dissociation hsp90 from GR. The second technique, the ability of transformed receptors to bind to isolated thymocyte nuclei is a functional measure of receptor transformation. The third method measured the ability of GR to bind to glucocorticoid response element (GRE) oligomer by gel mobility shift assay. In addition to optimizing these assays for later use in assessing the effects of zinc, they determined whether GR transformation occurred under conditions consistent with previous observations. In all cases, incubation at 20°C was used to induce *in vitro* receptor transformation. Maintenance at 4°C or incubation with sodium molybdate inhibited *in vitro* transformation (illustrated in Figure 8-7).

Temperature-mediated receptor transformation: coprecipitation of receptor-associated hsp90. To confirm whether hsp90 associated with mouse liver cytosolic GR and if transformation-associated dissociation could be induced *in vitro*, molybdate-stabilized cytosols were immunoabsorbed with BUGR2 antibody and Sepharose-protein A as diagrammed in Figure 8-8. The resulting pellets were then washed free of molybdate, and either maintained at 4°C or warmed to 20°C. The pellets were then washed, electrophoresed on SDS-PAGE and immunoblotted for hsp90 and GR. Typical blots for hsp90 and GR are shown in Figure 8-9. Hsp90 coprecipitates with GR and remains associated when kept at 4°C. At 20°C, however, hsp90 becomes dissociated from the receptor as expected. The amounts of GR are identical in both samples. These results suggest that hsp90 does indeed dissociate from GR during heat-induced transformation in our system.

Temperature-mediated receptor transformation: binding to isolated nuclei. One functional consequence of GR transformation is the ability of the receptor to localize to the nucleus. Previous work has demonstrated that transformed receptors can bind isolated nuclei *in vitro* (Hubbard and Kalimi, 1983). This binding does not occur with untransformed receptors. This has provided the basis for a transformation assay using ^{3}H-DEX-bound crude cytosolic receptors and isolated lymphocyte nuclei. To further evaluate the behavior of mouse liver cytosolic receptor and to determine whether receptor binding to isolated nuclei would make a useful transformation assay for subsequent assessment of zinc effects, cytosols were labeled with ^{3}H-DEX and incubated with isolated thymocyte nuclei. Prior to nuclei incubation cytosols were either maintained at 4°C or warmed to 20°C, in the presence or absence of 30 mM Na_2MoO_4. The results in Figure 8-10 are expressed as percentages of the binding value for "fully" transformed receptor (20°C without Mo). Cytosol incubated at 4°C without molybdate gave only 40% of the binding

observed for the transformed sample, indicating partial transformation. Molybdate stabilizes the receptor to only 20% binding even after warming to 20°C, indicating a minimal level of transformation. These results support previous findings that ligand-bound GR undergoes temperature-mediated transformation, and that molybdate stabilizes the receptor in the untransformed state even at transforming temperatures. It also identifies isolated nuclei binding as a valid experimental system for evaluating the effects of zinc on receptor transformation.

Temperature-mediated receptor transformation: ability to bind GRE sequences in gel mobility shift assay. The ability of GR to bind hormone response element oligomers is a very specific functional assay for the transformation state of the receptor and was carried out by gel mobility shift assay for specific DNA-protein complexes. DEX-labeled cytosols incubated at 4°C or 20°C with or without molybdate were incubated with a ^{32}P-radiolabeled GRE dimer and analyzed by the gel mobility shift assay. An example of a typical gel analyzed by autoradiographic densitometry is shown in Figure 8-11. One major (indicated by the arrow) and five minor DNA-protein complexes were routinely observed. When cytosols are incubated with increasing amounts of cold specific competitor (GRE-GRE), the one major complex was competed out but the other five complexes remained. This suggests that the major complex is the specific GR:GRE-GRE binding event, and the other complexes are low-affinity non-specific binding events. The CTF/NF1 response element, a nuclear transcription factor binding site with little homology to GRE-GRE, was a poorer competitor than cold GRE-GRE, showing a five- to ten-fold lower competitive binding activity than GRE-GRE (data not shown). This also suggests that the major DNA-protein complex is the high affinity of the binding event. Unfortunately, antibody supershift experiments using BUGR2 failed to supershift or ablate the complex (data not shown). The reason for this is not known. Nevertheless, cytosols

preabsorbed with BUGR2 antibody gave no major DNA-protein complex, strongly suggesting that this complex represents GR binding to the GRE-GRE oligomer (data not shown).

Cytosolic receptor in differing states of transformation were then evaluated for DNA binding activity. Cytosols that were initially prepared without molybdate showed considerable DNA binding activity with approximately 12% of all radiolabeled GRE-GRE in the major DNA-protein complex. Cytosols prepared with molybdate gave approximately 5% of all radiolabeled GRE-GRE in the major complex, consistent with the previous observation that molybdate prevents receptor transformation to the DNA binding form. Like the isolated nuclei binding assay, these results also indicate that receptor exists both in the untransformed and transformed state in cytosol, but that maintenance of cytosols under certain conditions can induce further ligand-dependent transformation.

EFFECTS OF ZINC ON RECEPTOR-LIGAND INTERACTION.

The ligand binding and receptor transformation assays optimized above were subsequently used to determine the effects of zinc salts on these processes.

Zinc inhibits crude cytosolic receptor-ligand interaction. The DCC absorption and DEAE-cellulose filter binding assays were employed to determine whether zinc salts have any effect on GR-ligand binding. Dilutions of $ZnSO_4 \cdot 7H_20$ were added simultaneously with ligand to receptor binding assays. The results of both experiments are shown in Figures 8-12 and 8-13. Zinc had a profound effect on ligand binding, with ED_{50}s between 10 to 50 μM. Zinc at 100 μM always showed complete inhibition. Zinc at 500 μM induced considerable protein precipitation in mouse liver cytosols, possibly exerting its effect through denaturing the receptor. Zinc at 100 μM did not cause visible protein

precipitation. To make certain that zinc at 100 μM was not precipitating receptor, zinc-treated cytosols were immunoabsorbed with BUGR2/Sepharose-protein A and Western blotted. As can be seen from Figure 8-14, soluble receptor was still present in that it can be immunoprecipitated from cytosol even after zinc treatment. This suggests that zinc concentrations at 100 μM and below exerted an effect on soluble receptor, and not simply precipitated it out of solution.

Interestingly, preincubation of cytosols with zinc exerted no greater inhibitory effect than zinc added simultaneously to ligand (Figure 8-15). This is in contrast to the effects of other metal inhibitors of GR ligand binding such as cadmium, arsenite and selenite, which reportedly require preincubation to exert their effects (Simons *et al*, 1990). In addition, the effects of zinc were independent of molybdate concentration in the cytosol. Zinc exerted an inhibitory effect in both the presence and absence of molybdate (Figure 8-16). This suggests that zinc and molybdate do not compete for the same sites on the GR. This conclusion was further supported by the observation that Mo at concentrations as high as 1 mM did not inhibit glucocorticoid-induced apoptosis in mouse thymocytes, also indirectly suggesting that zinc and molybdate do not act at the same site (data not shown).

Zinc cannot reverse crude cytosolic receptor-ligand binding. Zinc inhibited receptor-ligand binding when it is added prior to or simultaneously with ligand. When receptor-ligand complexes were formed and zinc was added two hours post-addition of ligand, it could not reverse the binding of preformed complexes (Figure 8-17). The inhibition at 500 μM was the result of protein precipitation and should be disregarded. Zinc could therefore only inhibit receptor-ligand binding prior to the binding event.

Inhibitory action of zinc on crude cytosolic receptor-ligand interaction is reversible

by removal of zinc. Experiments were then carried out to determine whether zinc inhibition of receptor-ligand binding could be reversed by removal of zinc. This was done by incubating crude cytosolic receptor and ^{3}H-DEX with varying concentrations of zinc as previously described. Zinc was then removed by brief incubation of the cytosolic complexes with pellets of Chelex-100 metal chelating resin. The Chelex-100 was removed by centrifugation and the cytosols resupplemented with sodium molybdate (also removed by Chelex-100). The resulting cytosols were then allowed to incubate an additional two hours and analyzed for specific binding to determine whether removal of zinc reversed its inhibitory effects. Figure 8-18 illustrates that the inhibition of receptor-ligand binding by zinc was almost completely reversed (filled circles) compared to controls (open circles) (the inhibition at 500 μM was the result of protein precipitation and should be disregarded). Zinc-associated inhibition of receptor-ligand binding was thus reversible for concentrations of 100 μM and less.

Zinc-associated inhibition of receptor-ligand interaction is completely reversed by high concentrations of DTT. It has been established that vicinal dithiols in the steroid binding domain need to be in a reduced state to facilitate ligand binding. Oxidation of these adjacent thiols can inhibit ligand binding. In addition, oxidation of thiols facilitates chemical modification of these residues by agents such as MMTS and crosslinking of adjacent thiols by transition metal ions and oxyanions (Simons *et al*, 1990; Chakraboti *et al*, 1990). This inhibitory effects are reportedly overcome by high concentrations of reducing agents such as DTT or 2-ME. To determine whether zinc inhibition could be overcome by reducing agents, high concentrations of DTT were added to liver cytosols simultaneously incubated with zinc at 100 μM. Figure 8-19 shows that high concentrations of DTT (10 mM) completely reversed the inhibitory effects of zinc at 100 μM on ligand binding. These results suggest that zinc may be crosslinking adjacent thiol

residues in the steroid binding domain. Maintaining the receptor under reducing conditions would presumably not favor zinc crosslinking. These results are consistent with literature reports of receptor-ligand binding inhibition by transition metals such as cadmium and selenium and oxyanions such as arsenite that can be reversed by treatment with reducing agents.

Zinc inhibits immunoabsorbed cytosolic receptor-ligand interaction. Thus far all binding studies were carried out using crude cytosol, where the interaction of other molecules may be responsible for the inhibitory effects of zinc on receptor-ligand binding. GR was immunoabsorbed to Sepharose beads with BUGR2 as previously described and then incubated with radiolabeled ligand with or without zinc to determine if "purified" receptor-ligand interaction was also inhibited by zinc. Figure 8-20 shows that ligand binding to immobilized receptor was also inhibited by zinc at 100 μM, though to a somewhat lesser degree (approximately 70 to 80% inhibition of specific binding) than that observed for crude cytosols. Western blotting of immunoabsorbed receptor (Figure 8-21) shows that zinc had no effect on the immunoabsorption of receptor to the beads, indicating that the effect was limited to ligand binding.

Zinc inhibits crude and immunoabsorbed mouse thymus cytosolic receptor-ligand interaction. To confirm that the inhibitory effects of zinc on crude and immunoabsorbed mouse liver cytosolic GR-ligand interaction also occurred in the thymus, thymocyte cytosols were either treated with zinc or immunoabsorbed and then treated with zinc as described above for liver. Zinc inhibited both crude and immunoabsorbed GR-ligand interaction to values comparable with liver (Figure 8-22). Zinc therefore has the same inhibitory effects on thymocyte as well as liver receptor, indicating that the results with liver GR are relevant to the *in vivo* observations made in Chapter 7.

EFFECTS OF ZINC ON LIGAND-DEPENDENT AND LIGAND-INDEPENDENT GLUCOCORTICOID RECEPTOR TRANSFORMATION

Effect of zinc on *in vitro* transformation state of glucocorticoid receptor: coabsorption of receptor-associated hsp90. The inhibitory effects of zinc on nuclear localization in mouse thymocytes and the potential role of zinc and other metals in receptor-hsp90 interaction suggested that another possible target of zinc may be the at the level of hsp90 dissociation following ligand binding. The effect of zinc on ligand-dependent receptor transformation was therefore initially examined by GR-hsp90 coprecipitation. Immunoabsorbed receptor was incubated without Mo at 4°C or 20°C with or without zinc at 100 μM. Figure 8-23 shows the results of Western blotting for receptor and hsp90. Hsp90 is retained at 4°C and released at 20°C with or without zinc present. These results also suggest that zinc has no effect on ligand-dependent transformation.

Hsp90 has been found necessary for high affinity GR binding to ligand. Premature release of hsp90 by ligand-free receptor would therefore inhibit subsequent ligand binding. This could therefore be a mechanism by which zinc could indirectly inhibit receptor-ligand interaction. To test this hypothesis, immunoabsorbed receptor from "ligand-free" crude cytosols (DCC-treated) were incubated at 4°C with or without zinc at 100 μM and hsp90 coprecipitation assessed by Western blotting. Figure 8-24 indicates that the presence of zinc did not induce ligand-independent dissociation of hsp90 (lanes 2 and 3). Zinc acting to facilitate hsp90 dissociation in the ligand-free receptor therefore also appears unlikely.

Effect of zinc on *in vitro* transformation state of glucocorticoid receptor: binding to isolated nuclei. To further investigate whether zinc affected ligand-dependent receptor transformation, the isolated nuclei binding assay was utilized with concentrations of zinc

ranging from 5 to 100 μM (higher concentrations of zinc precipitate proteins from cytosol and were therefore not used) to determine if zinc could either block or induce receptor transformation.

Before isolated nuclei binding could be used as an assay for receptor transformation, the effects of zinc on binding of previously transformed receptor to nuclei had to be assessed as illustrated in Figure 8-25. Figure 8-26 shows that zinc had little effect on heat-transformed receptor binding to nuclei when zinc was added after transformation. Since zinc had no apparent effect on transformed receptor binding to nuclei, this assay could be used strictly as an indicator of the effects of zinc on receptor transformation. Any changes to isolated nuclei binding induced by zinc could therefore be attributable to effects on transformation, not post-transformation nuclei binding

Zinc could potentially affect ligand-dependent transformation in two ways: 1) zinc could inhibit transformation under conditions where transformation would normally be favored (20°C without Mo), or 2) zinc could induce transformation under conditions where transformation would not normally occur (4°C, or 20°C with Mo). Both these scenarios would have a downstream effect on nuclear localization and subsequent gene expression. The first case is illustrated in Figure 8-27. Zinc was added to cytosols prior to transformation. Receptors were then transformed at 20°C and the effects of zinc on ligand binding observed. Figure 8-28 shows that zinc had little if any inhibitory effect on temperature-mediated transformation; in fact, it was reproducibly stimulated to a minor degree at higher concentrations. Zinc therefore does not appear to inhibit temperature mediated receptor transformation.

The second case is illustrated in Figures 8-29 and 8-31. Zinc was incubated with receptors maintained under stabilizing conditions (4°C or 20°C with Mo). Figures 8-30 and 8-32 show that zinc did not induce any significant degree of transformation in receptors stabilized under these conditions. Zinc therefore did not induce transformation

under nontransforming conditions. These experiments indicate that zinc does not act at the level of ligand-dependent transformation *in vitro*, either in a positive or negative manner.

Effect of zinc on *in vitro* transformation state of glucocorticoid receptor: ability to bind GRE sequences in gel mobility shift assay. High-affinity binding of glucocorticoid receptor to a GRE dimer measured by gel mobility shift was used as another indicator of the potential effects of zinc on ligand-dependent receptor transformation. Ligand-dependent transformation was evaluated as illustrated in Figure 8-33, with crude cytosolic receptor incubated at 4°C or 20°C with or without molybdate, with or without zinc. Figure 8-34 shows the resulting gel mobility shift assay, with the high-affinity protein:DNA complex indicated. The data in Figure 8-35 expressed as percentage GRE-GRE bound to receptor demonstrates that zinc had no apparent effect on the degree of transformation as assessed by protein:DNA binding. Zinc would therefore appear to have no effect, positive or negative, on GR transformation in this system, a conclusion also supported by isolated nuclei binding and hsp90 coprecipitation results.

CHAPTER 8: DISCUSSION

Summary of results. To summarize, zinc was found to exert an effect on initial receptor-ligand interaction *in vitro*, both in crude liver cytosolic receptor preparations and in immunoabsorbed receptor. Zinc was also found to inhibit GR-ligand binding in crude and immunoabsorbed mouse thymus cytosols as well. The dose range of this effect was between 10 to 100 μM. Treatment of crude cytosols and immunoabsorbed receptor with zinc in this dose range did not affect the solubility of the receptor, demonstrated by the fact that receptor could still be immunoabsorbed and detected by Western blotting following zinc treatment. Zinc was found to act prior to ligand binding in crude cytosols, and did not reverse receptor-ligand complexes once they were formed. This inhibitory effect was also reversible when zinc was removed by chelation.

All of these experiments suggest that zinc exerted a direct biochemical effect on the GR influencing its ability to bind ligand *in vitro*. In addition, the fact that zinc did not exert an inhibitory effect on preformed complexes strongly suggests that zinc may be acting directly within the steroid binding domain, since prior occupancy of the steroid binding site abolished the effect. The ability of DTT to reverse the inhibitory effect of zinc further suggests that its site of action may be amino acid residues capable of binding zinc such as cysteines, several of which are found in the steroid binding domain and are required for ligand binding.

In contrast to the receptor-ligand binding studies, zinc did not appear to affect the *in vitro* transformation state of GR. Isolated nuclei binding, GR-hsp90 coabsorption and gel mobility shift assays all suggested that zinc did not prevent ligand-dependent receptor transformation under transforming conditions, nor did it induce transformation under non-transforming conditions. GR-hsp90 coabsorption experiments demonstrated that zinc did not affect ligand-independent hsp90 dissociation.

Effect of zinc on receptor-ligand binding: interaction at the ligand binding domain. Previous studies have shown that transition metals and their anions can alter steroid binding to receptor. Arsenite (AsO_2^-) and cadmium have been found to inhibit both DEX and DEX-MES affinity ligand binding to rat glucocorticoid receptor (Simons et al, 1990; Chakraboti *et al*, 1990). Selenite (SeO_2^-) has also been found to inhibit DEX binding to rat GR, and zinc has been found to inhibit ligand binding to thyroid receptor (Tashimi *et al*, 1989; Surks *et al*, 1989). Since DEX-MES covalently binds to receptor primarily at Cys656 (for rat) in the steroid binding core domain (Simons *et al*, 1987), it has been postulated that arsenite, cadmium and other compounds may be crosslinking this residue to the adjacent thiol residues Cys640 and Cys661 (Simons *et al*, 1990; Chakraboti *et al*, 1992). All three of these residues has been found necessary for maintaining the conformation of the steroid binding cleft by site directed mutagenesis in rat HTC cells, and are therefore indirectly necessary for hormone binding. Low molecular weight chemical modification of vicinal dithiols without crosslinking has been found to inhibit affinity ligand but not normal DEX binding, while chemical crosslinking eliminates all steroid binding (Chakraboti *et al*, 1990). In addition, reducing agents such as DTT and 2-ME eliminate these inhibitory effects. These results suggest that zinc may also be crosslinking adjacent dithiols when they are in a reduced state and inhibiting ligand binding as a result. The ability of zinc and other metals to bind coordinately at two to four vicinal cysteines is well documented and forms the basis for zinc finger, zinc clusters and other putative zinc binding moieties.

However, one previous literature report found zinc ineffective at blocking DEX binding to rat receptor at concentrations up to 300 μM, although the authors expressed some surprise at this result, based on its similarity to cadmium and its predicted coordination chemistry with cysteine residues (Simons *et al*, 1990). Our results gave considerable binding inhibition by zinc down to 10 μM in crude mouse liver cytosolic

preparations. Predicted amino acid sequence data for the steroid binding domain from the cloned glucocorticoid receptor gene for *Mus musculus* and rat hepatoma cell line HTC indicates that there is almost perfect homology between the two domains and identical locations for the vicinal cysteines (Danielson *et al*, 1986; Miesfield *et al*, 1986).

```
630 SYRQSSGNLLCFAPDLIINEQRMSLPCMYDQCKHMLFVSSE 670   RAT
618 SYRQASGNLLCFAPDLIINEQRMTLPCMYDQCKHMLFISTE 658   MOUSE
```

It is therefore unlikely that differences in primary amino acid sequence account for different observations between mouse liver and rat HTC cytosolic receptor. Nevertheless, preliminary data and previous work suggests that zinc may well be acting at one or more of the cysteine residues in the steroid binding region and inhibiting *in vitro* steroid binding as a result. It is also possible that zinc might be altering ligand binding by acting at a more distal amino acid residue or residues and causing inhibition via another mechanism, although no model currently exists for such a phenomenon in the steroid receptor superfamily.

Effect of zinc on receptor-ligand binding: disruption of GR-hsp90 association.

As discussed previously, high-affinity ligand binding requires association of the hsp90 homodimer with the GR signal transducing domain. Premature dissociation of hsp90 induced by zinc might therefore result in a loss of ligand binding affinity. However, the hsp90-GR coabsorption experiments with "ligand-free" receptor demonstrated that zinc did not cause dissociation of hsp90 from GR *in vitro*. While experiments of this type cannot detect whether hsp90-GR interaction was affected in a more subtle way, it rules out the possibility of effects by complete dissociation. In addition, the presence or

absence of molybdate had no effect on the inhibitory effects of zinc. If zinc acted by destabilizing receptor in the absence of molybdate, a 60-fold excess (20 mM) of molybdate might act to overcome this destabilization. Zinc nevertheless inhibited receptor-ligand binding even in the presence of high concentrations of molybdate. This provides further circumstantial evidence that the effects of zinc are unrelated to its effect on GR-hsp90 association.

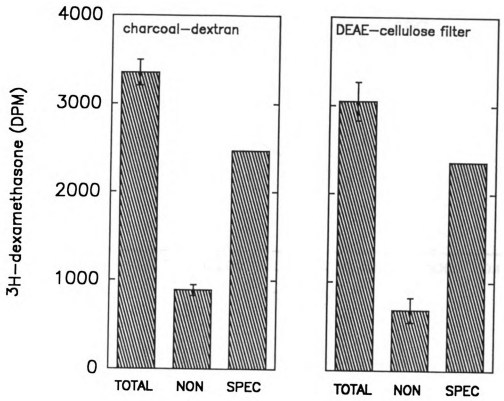

Figure 8-1. Comparison of total (TOTAL, with no cold competitor), non-specific (NON, with a 500-fold excess of unlabeled DEX as competitor) and specific (SPEC) ^{3}H-DEX binding activity in the DCC absorption (left panel) and DEAE-cellulose filter (right panel) assay in mouse liver cytosol. Specific binding equals the difference between total and non-specific binding. Total protein concentration were one mg per sample. The difference between total and non-specific binding equals specific binding. Data are expressed as the mean plus or minus standard deviation of triplicate samples.

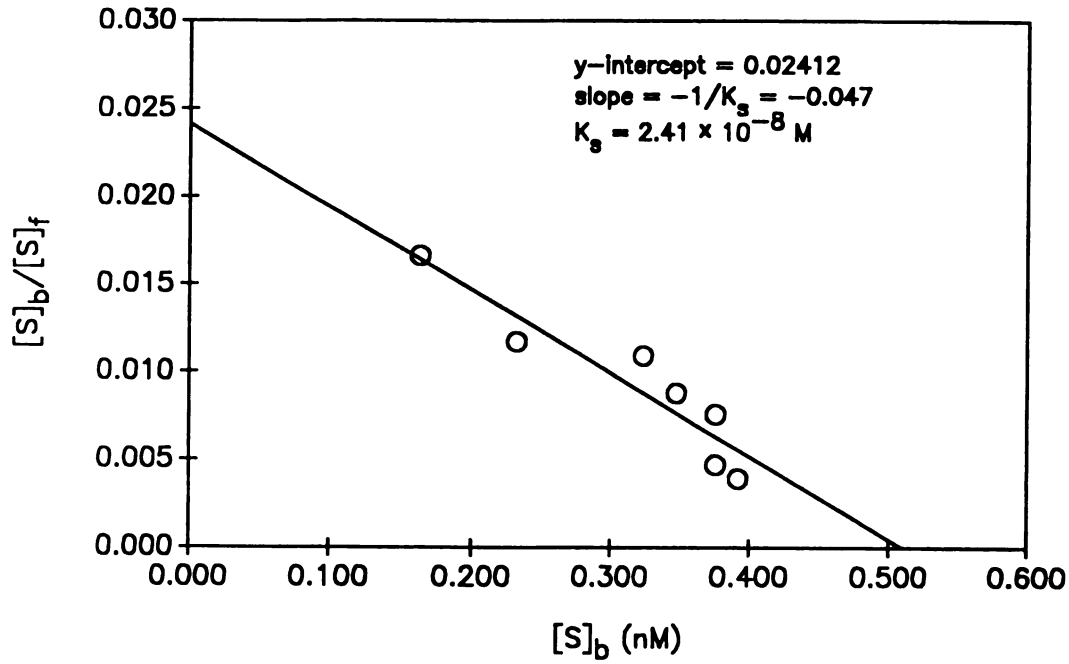

Figure 8-2. Eadie-Scatchard analysis of ^{3}H-DEX binding activity for mouse liver cytosol.

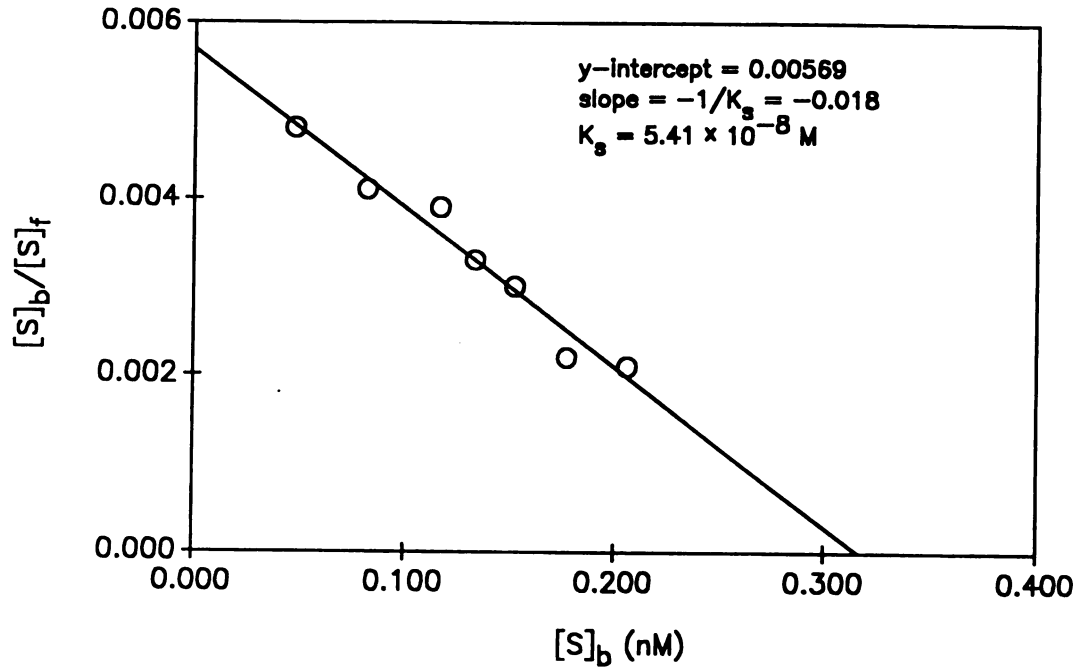

Figure 8-3. Eadie-Scatchard analysis of ^{3}H-corticosterone binding activity for mouse liver cytosol.

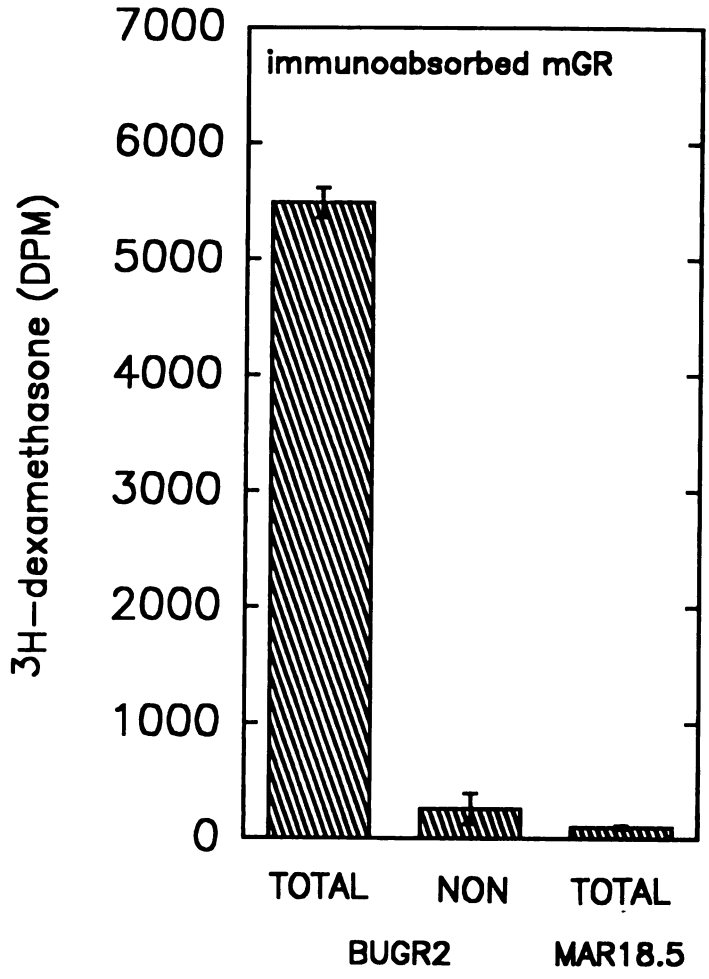

Figure 8-4. Total (TOTAL) and non-specific (NON) ^{3}H-DEX binding activity of mouse liver cytosol GR immunoabsorbed to Sepharose protein A. Cytosol was immunoabsorbed with BUGR2 (anti-GR) or MAR18.5 as a negative control followed by incubation with radiolabeled ligand. Total protein concentations were equalized to one mg/sample following absorption. Data are expressed as the mean plus or minus standard deviation of triplicate samples.

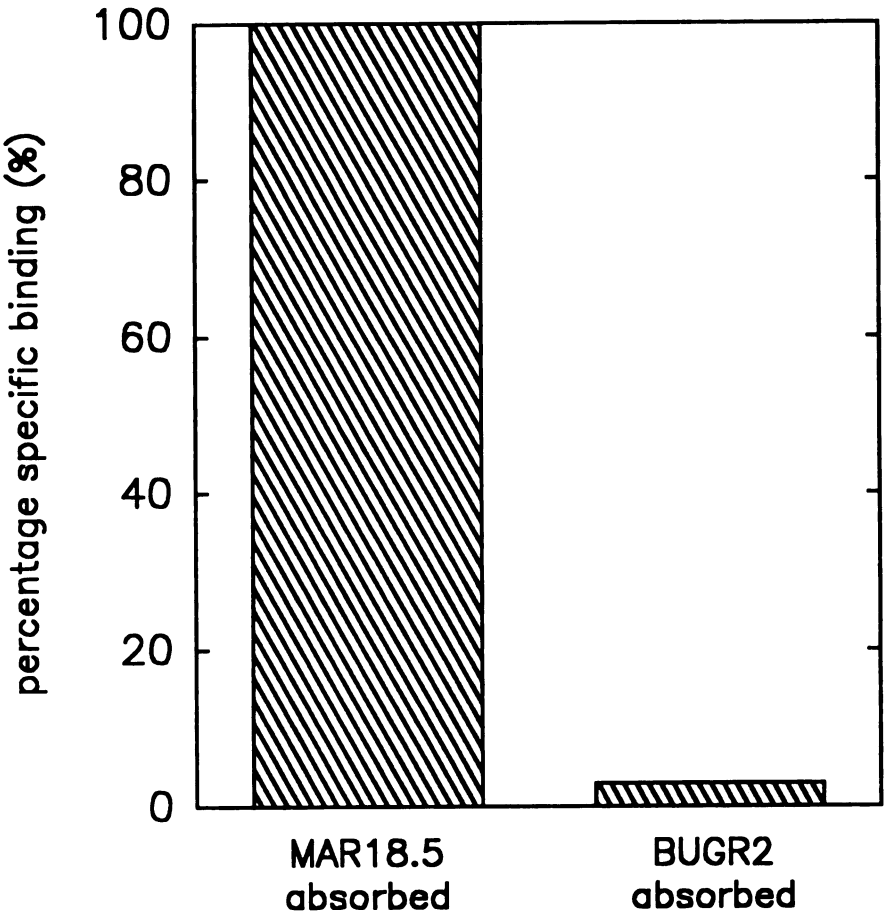

Figure 8-5. Specific ^{3}H-DEX binding activity of mouse liver cytosols preabsorbed with BUGR2 (anti-Ig) or MAR18.5 (negative control) antibody followed by Sepharose-protein A. Data are expressed as percentages of specific binding in MAR18.5-absorbed cytosol.

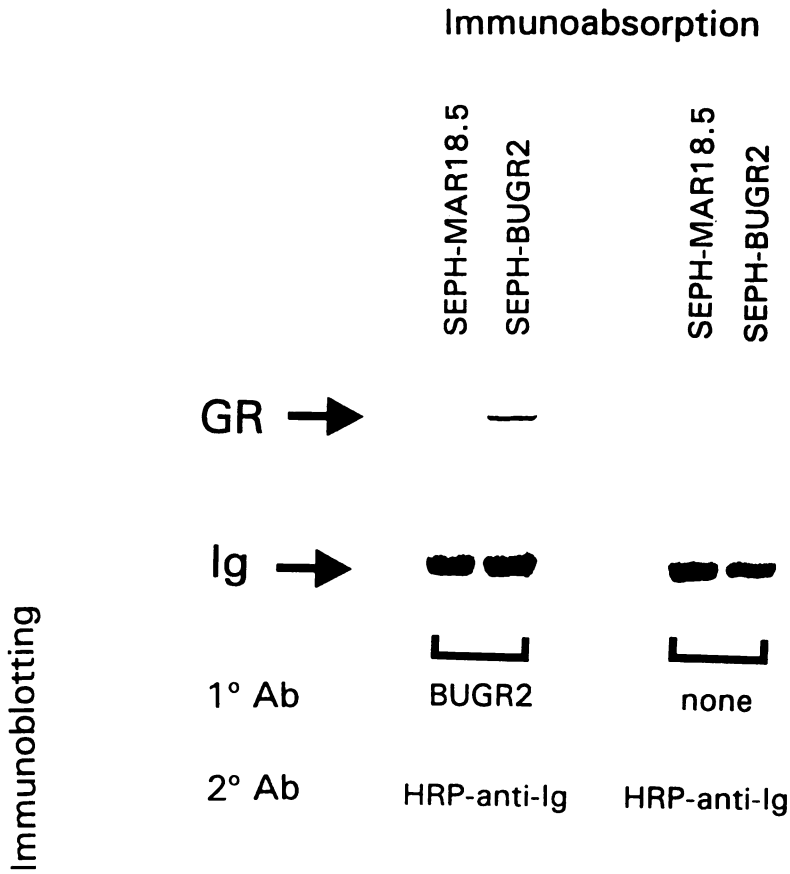

Figure 8-6. Western blot of immunoabsorbed GR from mouse liver cytosol. SEPH-BUGR2 and SEPH-MAR18.5 indicate immunoabsorption with BUGR2 (anti-Ig) or MAR18.5 (negative control) respectively. Ig indicates the immunoglobulin heavy chain band.

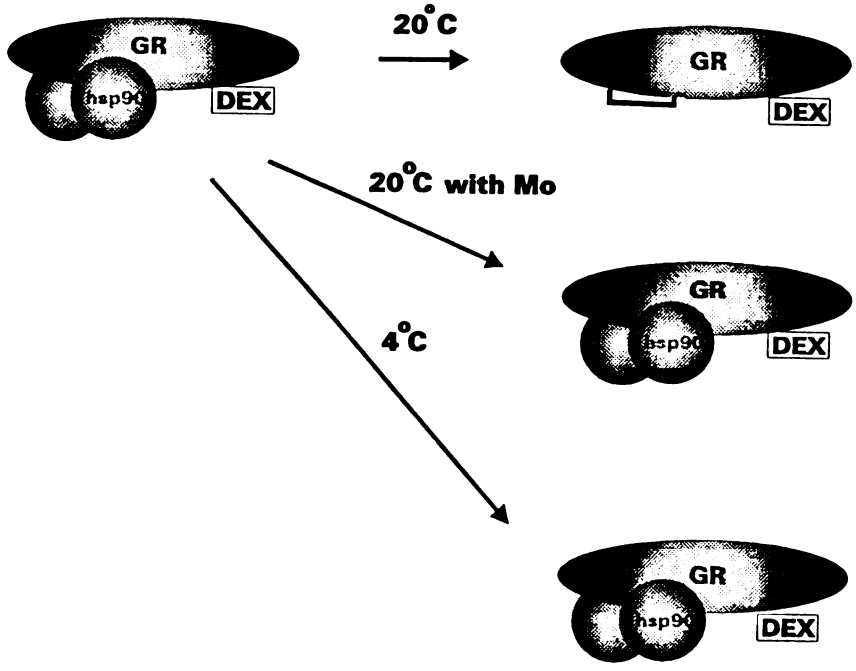

Figure 8-7. Current model of hsp90 homodimer association with GR and temperature-mediated dissociation. Diagram shows temperature-mediated dissociation of hsp90 homodimer following incubation at 20°C (top figure), while dissociation is inhibited with incubation at 4°C (middle panel) or 20°C with sodium molybdate (Na_2MoO_4)(bottom panel).

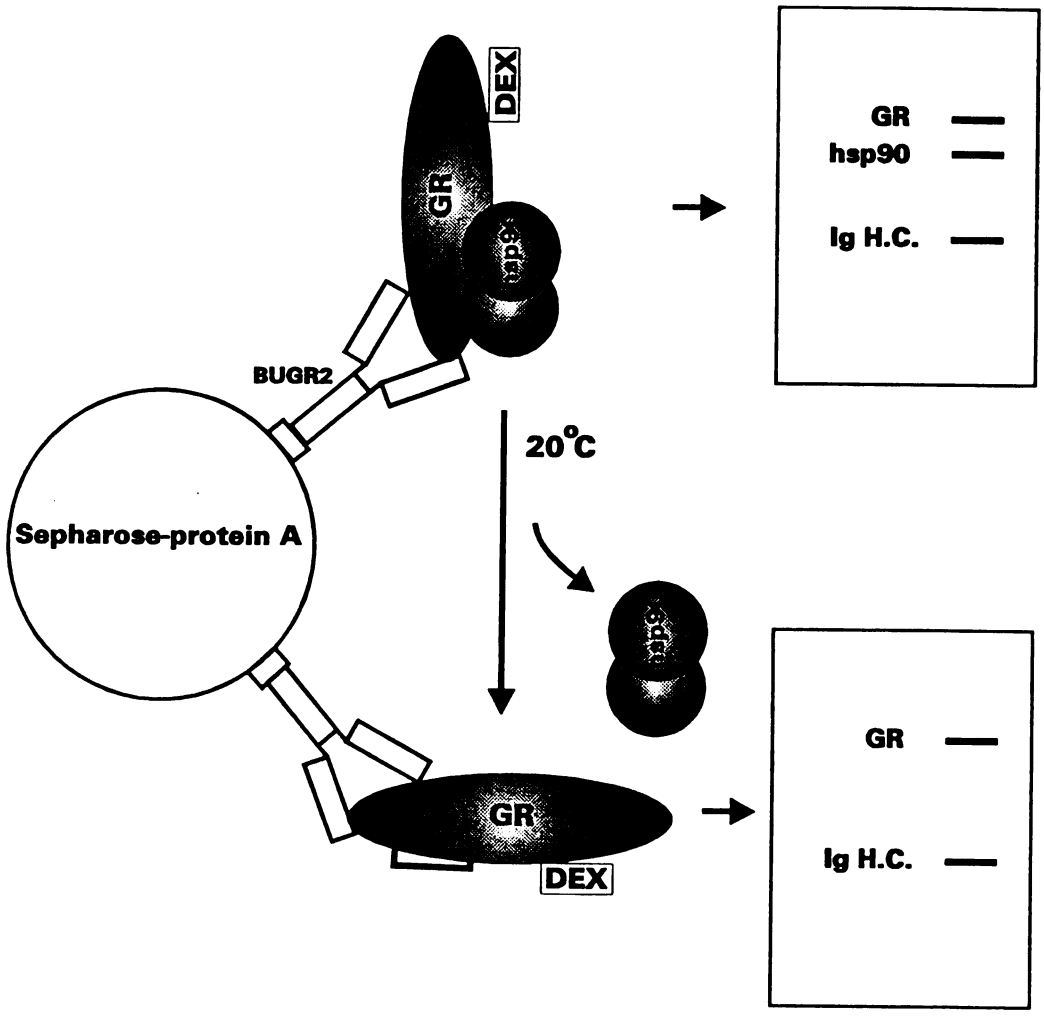

Figure 8-8. Diagram of method for detecting association and dissociation of hsp90 homodimer from immunoabsorbed mouse liver cytosolic GR.

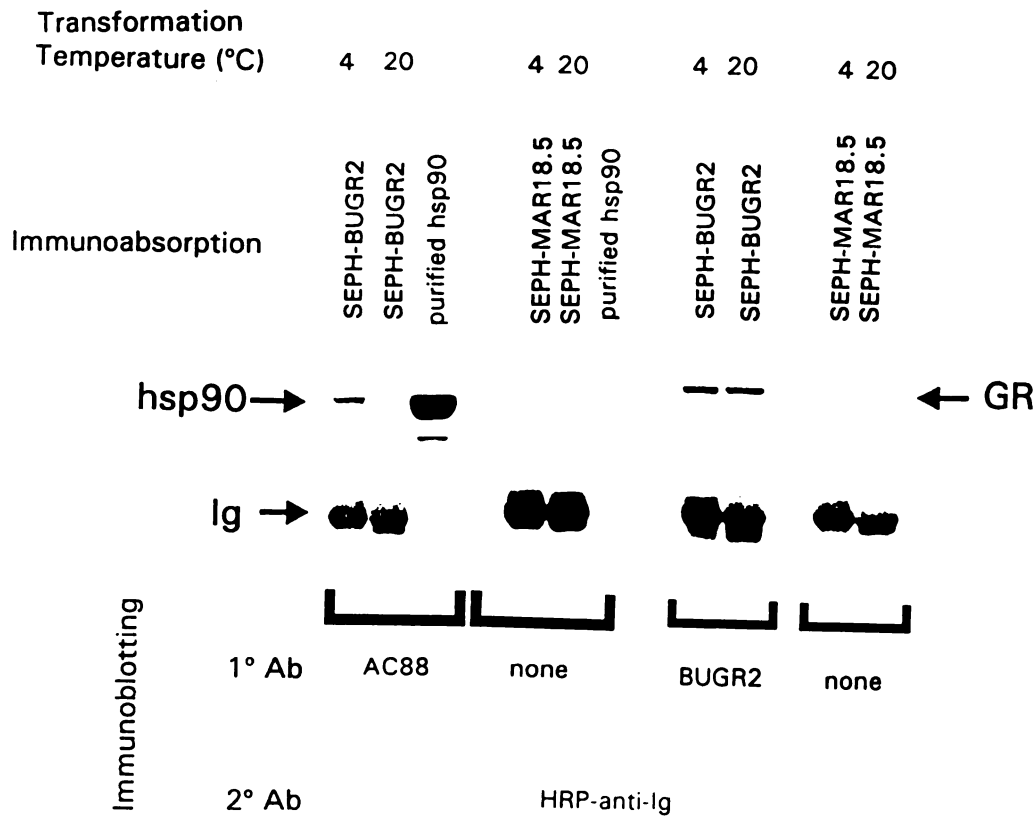

Figure 8-9. Western blots for GR and coabsorbed hsp90 of immunoabsorbed mouse liver cytosolic GR transformed at 20°C or stabilized in the untransformed state at 4°C. SEPH-BUGR2 and SEPH-MAR18.5 indicate immunoabsorption with BUGR2 or MAR18.5 respectively. AC88 is a monoclonal antibody against hsp90. Ig indicates immunoglobulin heavy chains.

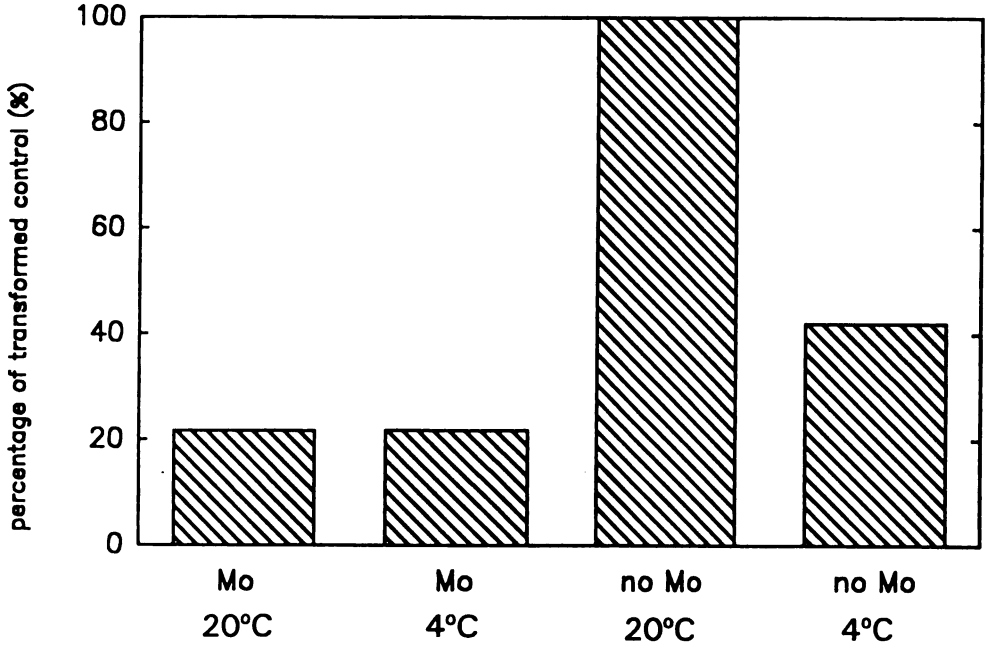

Figure 8-10. Binding of ^{3}H-DEX-bound GR to isolated thymocyte nuclei expressed as percentages of the transformed control (incubated at 20°C without sodium molybdate). Cytosols were incubated at 4°C (untransformed) or 20°C (transformed) in the presence of absence of 30 mM Na_2MoO_4.

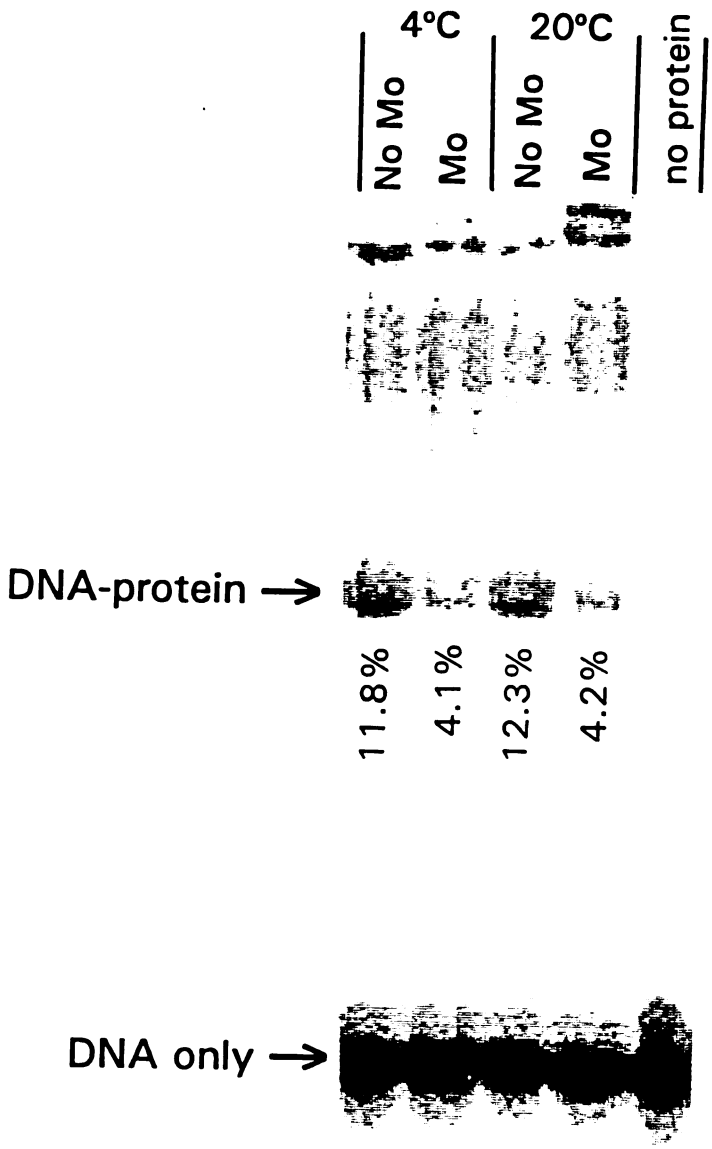

Figure 8-11. Gel mobility shift assay for crude mouse liver cytosolic GR preincubated at 4°C and 20°C in the absence of and 20°C with 30 mM Na_2MoO_4. The left-most lane contains no protein. The arrows indicated the primary specific protein-DNA complex and free DNA.

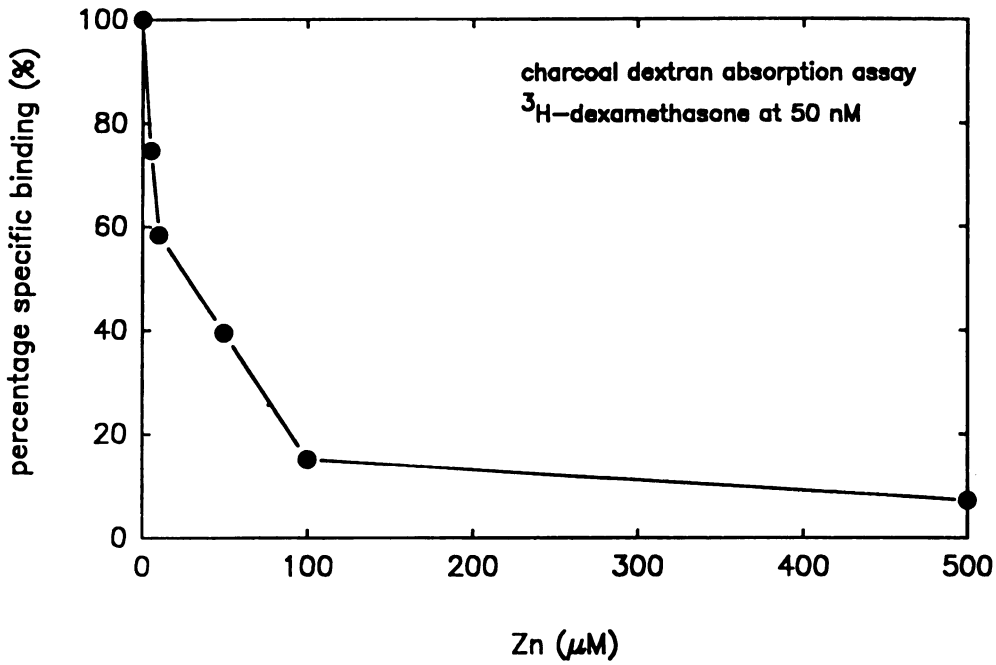

Figure 8-12. Effect of zinc on specific ^{3}H-DEX binding activity of crude mouse liver cytosolic GR using DCC absorption assay. Data are expressed as the percentage of specific binding in the no zinc control.

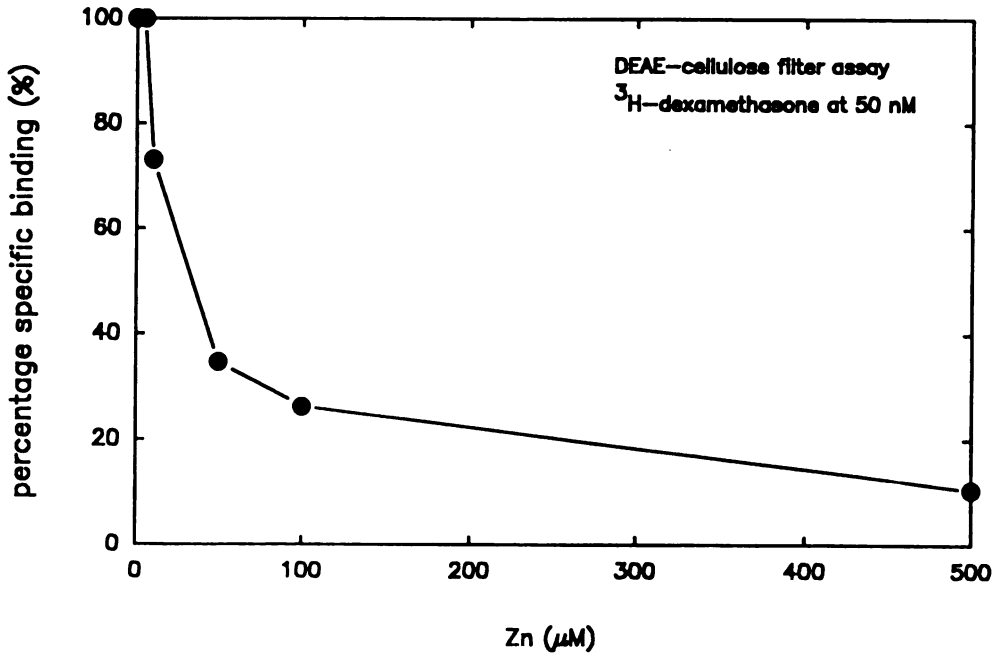

Figure 8-13. Effect of zinc on ^{3}H-DEX binding activity of crude mouse liver cytosolic GR using DEAE-cellulose filter binding assay. Data are expressed as the percentage of specific binding of the control.

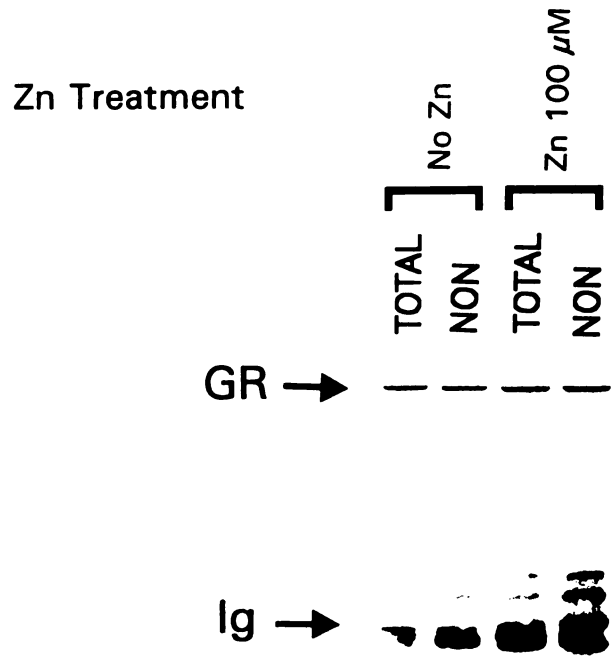

Figure 8-14. Western blot of mouse liver cytosolic GR immunoabsorbed from cytosols previously incubated without or with zinc at 100 μM. Samples without (TOTAL) and with 500-fold unlabeled DEX as competitor (NON) are included. Ig indicates immunoglobulin heavy chains.

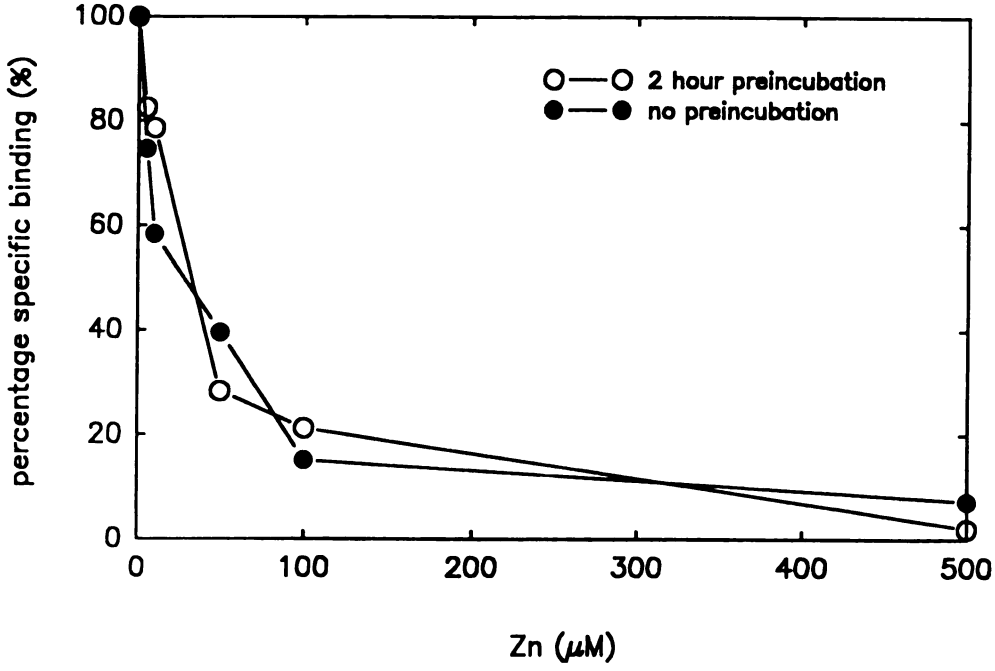

Figure 8-15. Effect of preincubation with zinc on specific ^{3}H-DEX binding activity of crude mouse liver cytosolic GR using DCC absorption binding assay. Open circles show binding activity with two hour preincubation, filled circles with simultaneous additions. Data are expressed as the percentage of specific binding for the control.

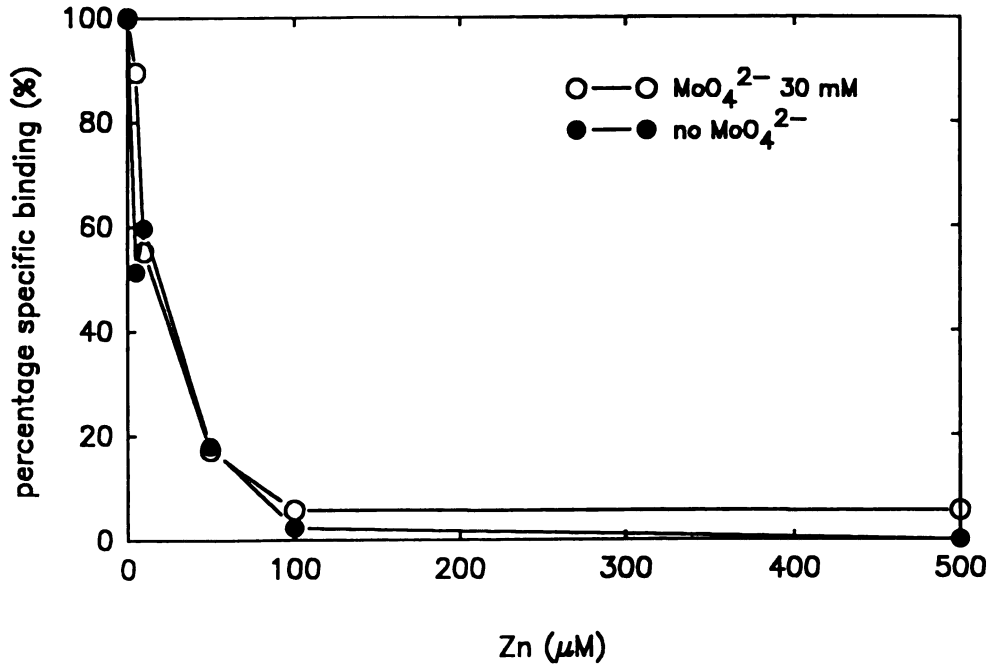

Figure 8-16. Effect of molybdate on zinc-associated ^{3}H-DEX-GR specific binding inhibition using DCC absorption assay. Open circles show binding activity with 30 mM sodium molybdate, filled circles with none. Data are expressed as the percentage of specific binding in the no zinc control.

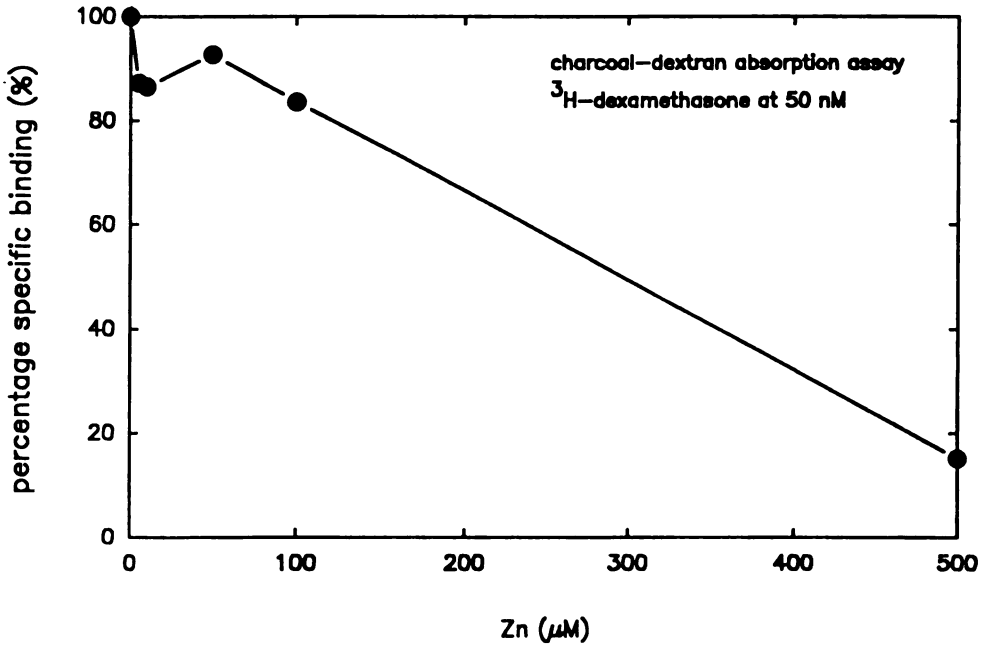

Figure 8-17. Effect of zinc on preformed ^{3}H-DEX-GR complexes using DCC absorption assay. Data are expressed as the percentage of specific binding for the control.

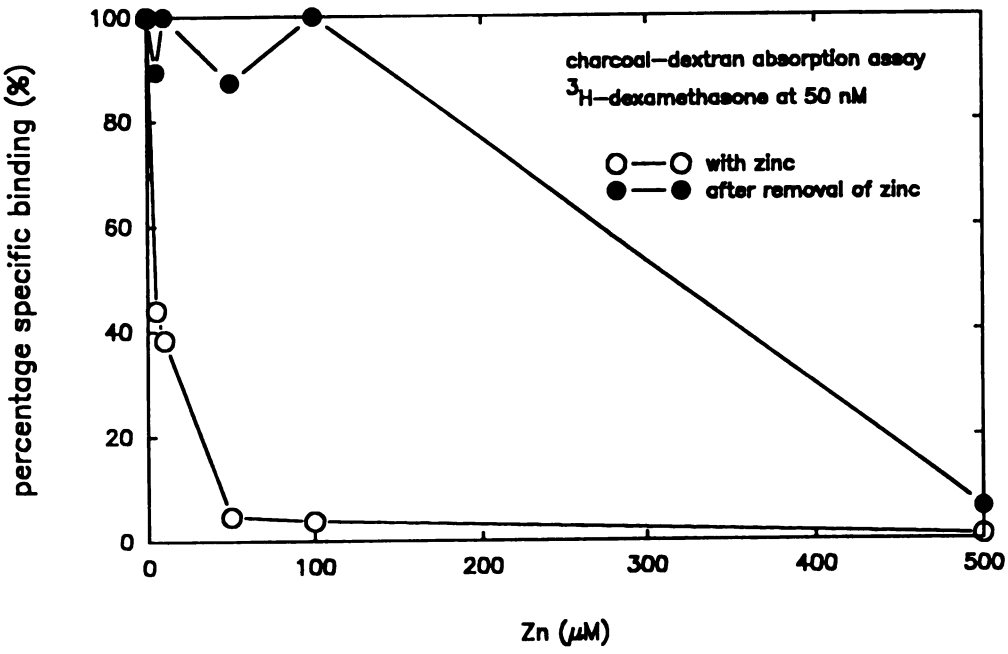

Figure 8-18. Reversibility of zinc-associated specific ^{3}H-DEX-GR binding inhibition using DCC absorption assay. Open circles show binding activity before removal of zinc, filled circles after removal of zinc by Chelex-100. Data are expressed as the percentage of specific binding in the no zinc control.

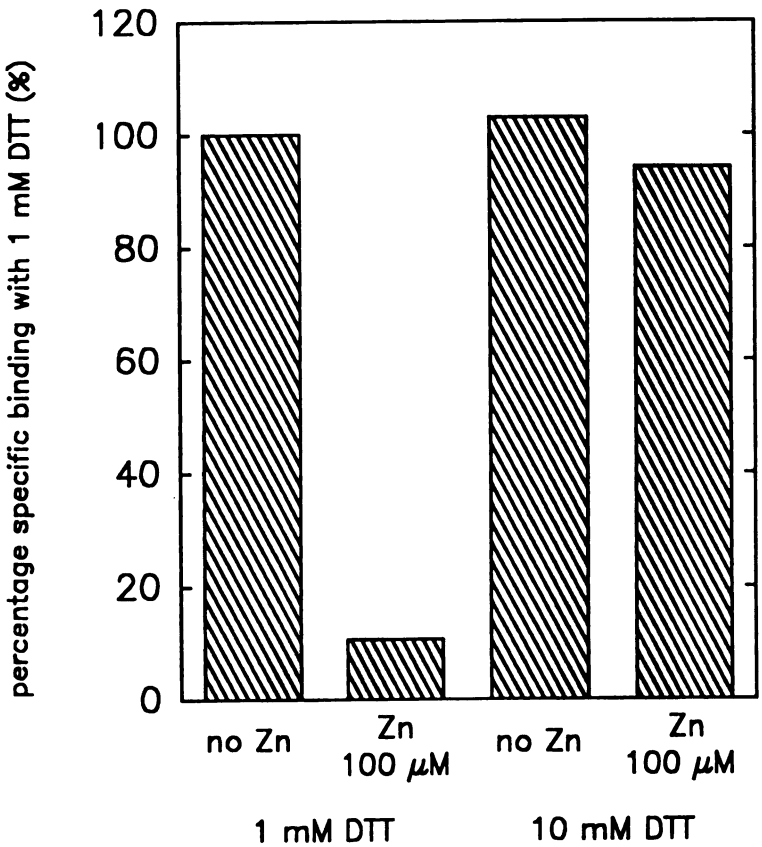

Figure 8-19. Reversibility of zinc-associated specific ^{3}H-DEX-GR binding inhibition with 10 mM DTT. Data are expressed as the percentage of specific binding in the no zinc control with 1 mM DTT.

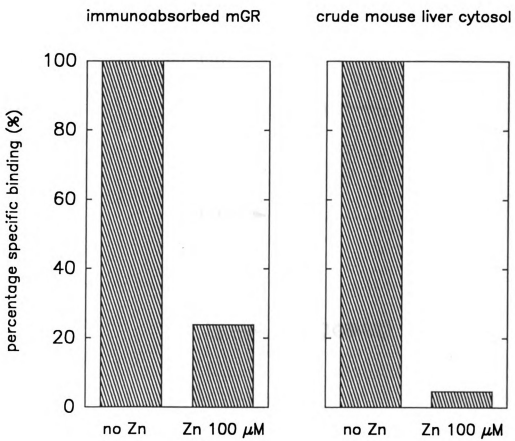

Figure 8-20. Effect of zinc on specific ^{3}H-DEX binding to immunoabsorbed mouse liver cytosolic GR (left panel) compared with crude cytosol (right panel). Data are expressed as the percentage specific binding in the no zinc control.

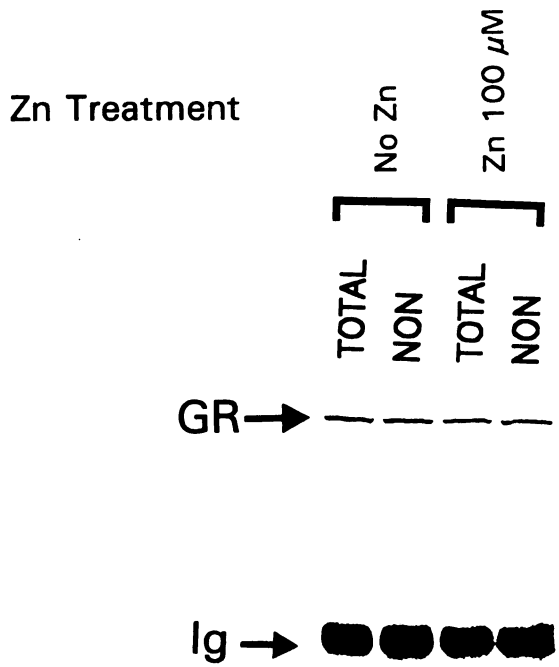

Figure 8-21. Western blot of immunoabsorbed mouse liver cytosolic GR following incubation without or with zinc at 100 μM. Samples without (TOTAL) and with 500-fold unlabeled competitor (NON) are included. Ig indicates immunoglobulin heavy chains.

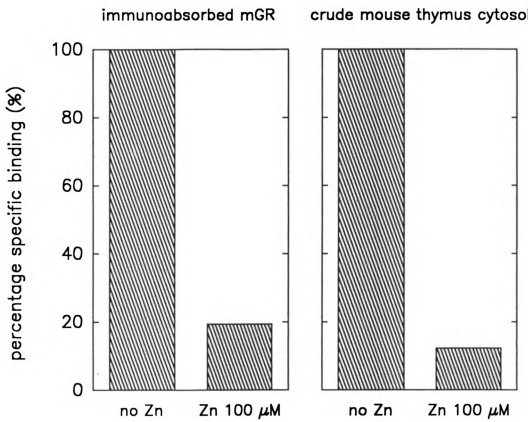

Figure 8-22. Effect of zinc on specific ^{3}H-DEX binding to immunoabsorbed mouse thymocyte cytosolic GR (left panel) compared with crude cytosol (right panel). Data is expressed as the percentage of specific binding in the no zinc control.

Figure 8-23. Top panel. Diagram of experimental scheme for determining effect of zinc on ligand-dependent temperature-mediated hsp90 dissociation from GR using hsp90-GR coabsorption and Western blotting. **Bottom panel.** Western blot of GR (upper blot) and coabsorbed hsp90 (lower blot) of BUGR2-immunoabsorbed ligand-bound mouse liver cytosolic GR stabilized at 4°C or transformed at 20°C, without or with zinc at 100 uM. SEPH-BUGR2 and SEPH-MAR18.5 indicate immunoabsorption with BUGR2 or MAR18.5 respectively. AC88 is the monoclonal antibody against hsp90.

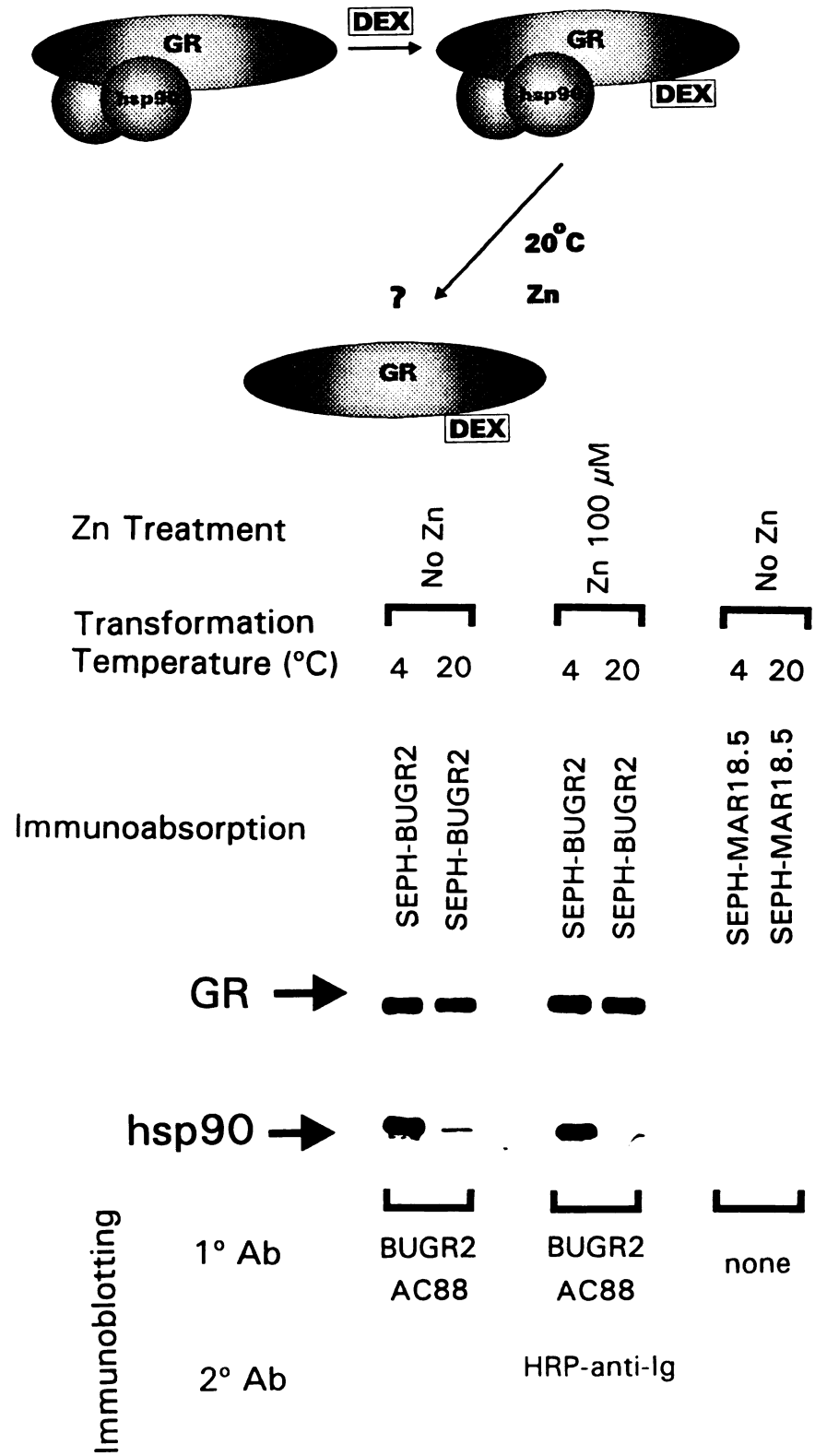
GR
DEX
GR
DEX
20°C
Zn
?
GR
DEX
Zn Treatment
No Zn
Zn 100 μM
No Zn
Transformation Temperature (°C)
4 20
4 20
4 20
Immunoabsorption
SEPH-BUGR2
SEPH-BUGR2
SEPH-BUGR2
SEPH-BUGR2
SEPH-MAR18.5
SEPH-MAR18.5
GR
hsp90
Immunoblotting
1° Ab
BUGR2
AC88
BUGR2
AC88
none
2° Ab
HRP-anti-Ig

Figure 8-24. Top panel. Diagram of experimental scheme for determining effect of zinc on ligand-independent hsp90 association with GR using hsp90-GR coabsorption and Western blotting. **Bottom panel.** Western blot of GR (upper blot) and coabsorbed hsp90 (lower blot) of BUGR2-immunoabsorbed "ligand-free" mouse liver cytosolic GR stabilized at 4°C and treated without or with zinc at 100 μM. SEPH-BUGR2 and SEPH-MAR18.5 indicate immunoabsorption with BUGR2 or MAR18.5 respectively. AC88 is the monoclonal antibody against hsp90.

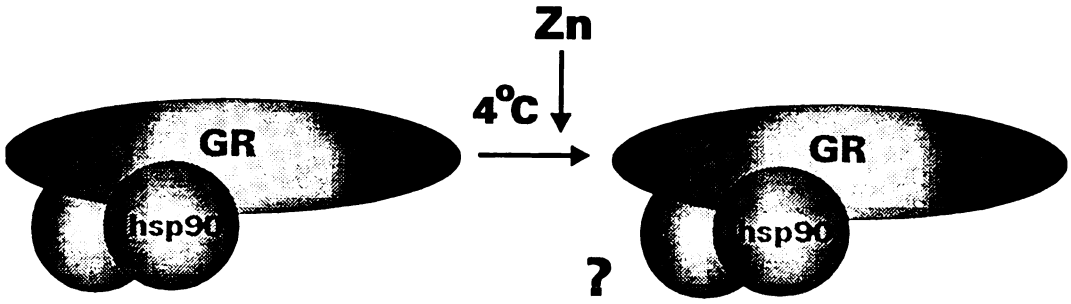
Zn
4°C
GR
hsp90
?
GR
hsp90

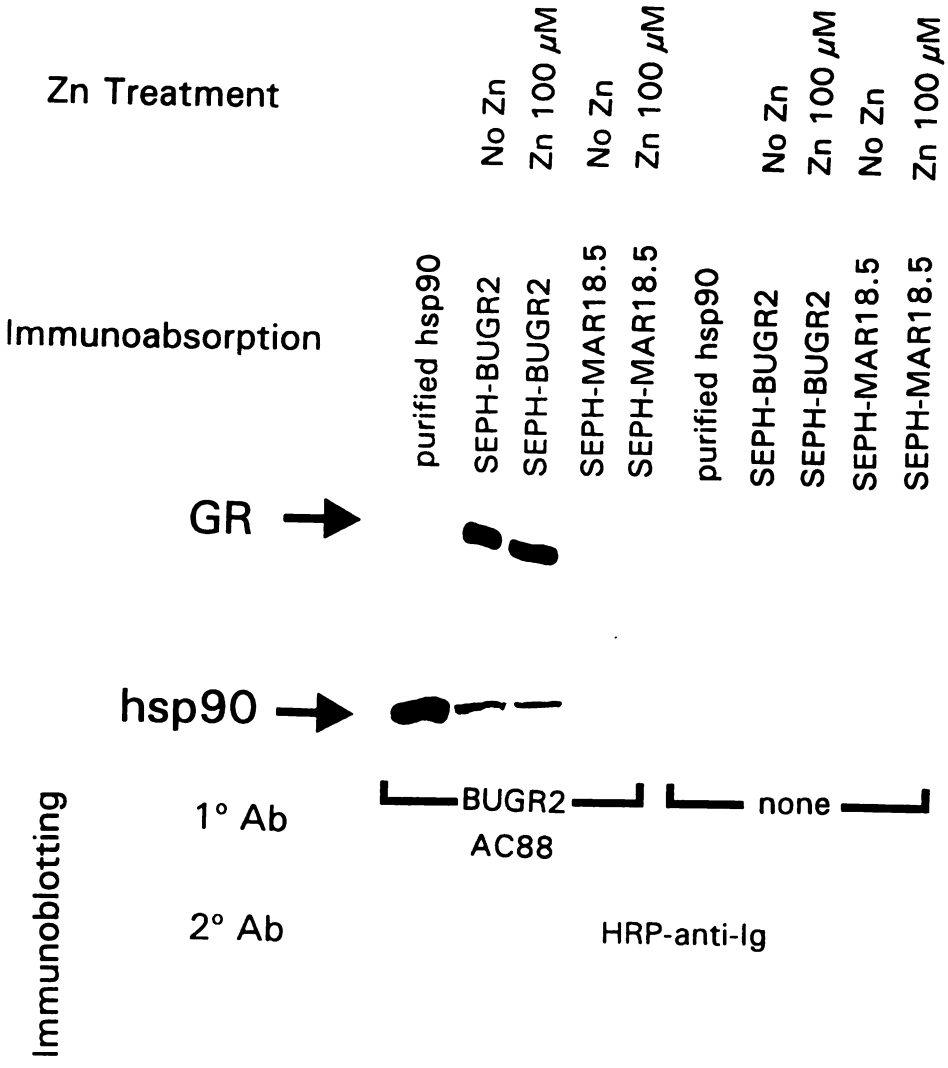
Zn Treatment
No Zn
Zn 100 μM
No Zn
Zn 100 μM
No Zn
Zn 100 μM
No Zn
Zn 100 μM
Immunoabsorption
purified hsp90
SEPH-BUGR2
SEPH-BUGR2
SEPH-MAR18.5
SEPH-MAR18.5
purified hsp90
SEPH-BUGR2
SEPH-BUGR2
SEPH-MAR18.5
SEPH-MAR18.5
GR
hsp90
Immunoblotting
1° Ab
BUGR2
AC88
none
2° Ab
HRP-anti-Ig

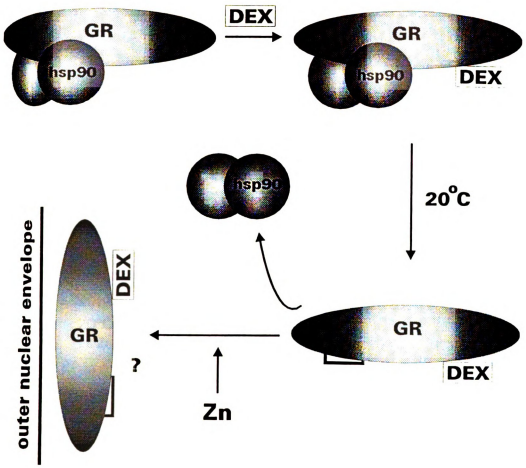

Figure 8-25. Diagram of experimental scheme for determining effect of zinc on *transformed* GR binding to isolated thymocyte nuclei.

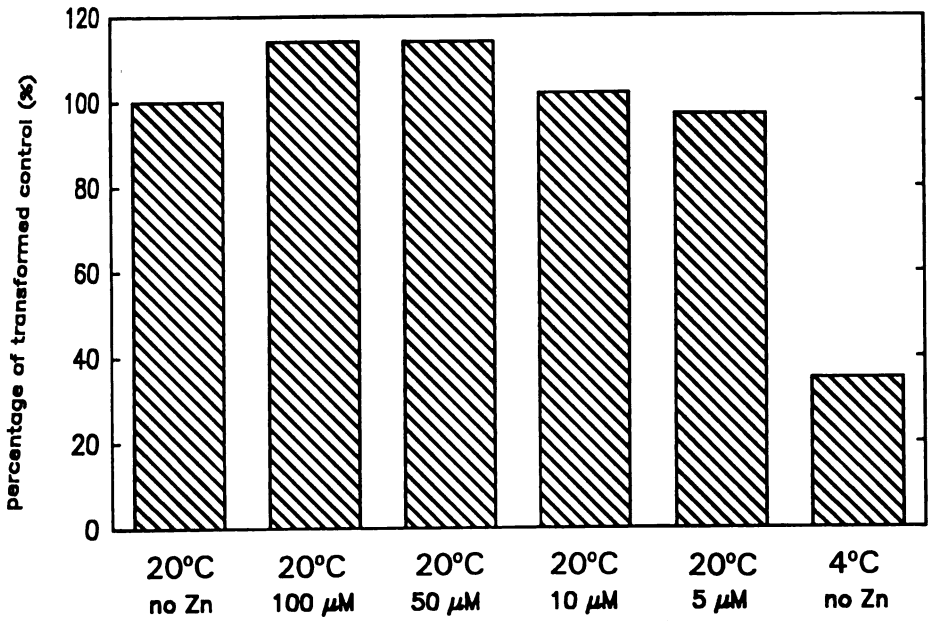

Figure 8-26. Effect of zinc on transformed GR binding to isolated thymocyte nuclei. *Mouse liver* cytosol was transformed at 20°C without zinc and incubated with nuclei in *the presence* of zinc at indicated concentrations. Right-most value is the 4°C *("untransformed"* control). Data are expressed as percentages of the transformed no zinc *control.*

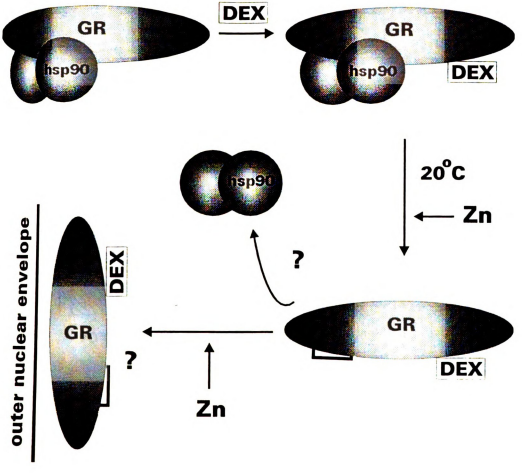

Figure 8-27. Diagram of experimental scheme for determining effect of zinc on *temperature*-mediated transformation of GR based on binding to isolated nuclei.

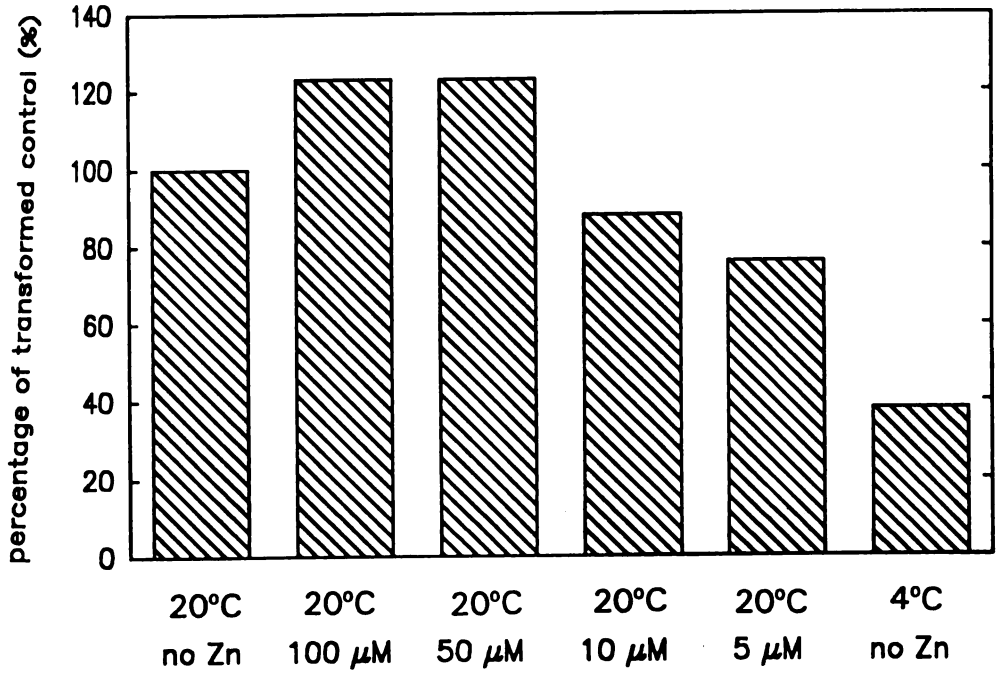

Figure 8-28. Effect of zinc on temperature-mediated transformation of GR based on *binding* to isolated nuclei. Mouse liver cytosol was incubated at 20°C with zinc at the *indicated* concentrations prior to nuclei addition. Right-most value is a 4°C incubation *control* ("untransformed"). Data are expressed as percentages of the transformed no zinc *control*.

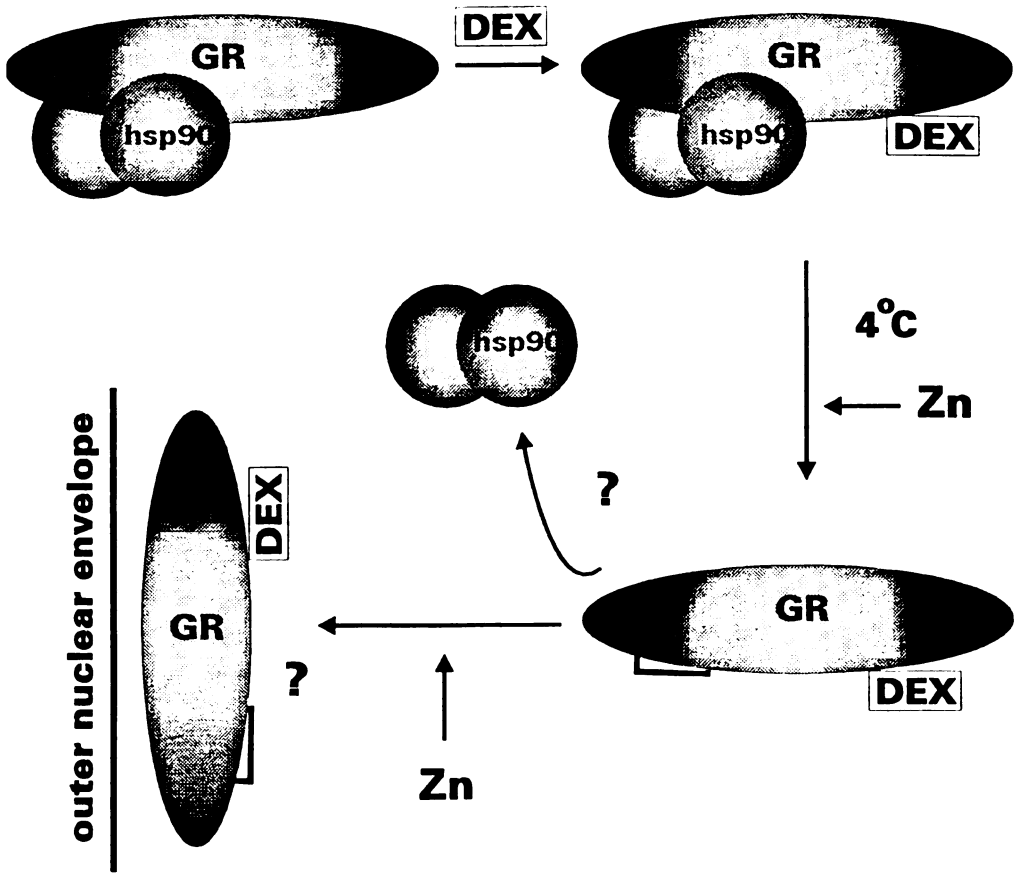

Figure 8-29. Diagram of experimental scheme for determining effect of zinc on cold stabilization of untransformed GR based on binding to isolated nuclei.

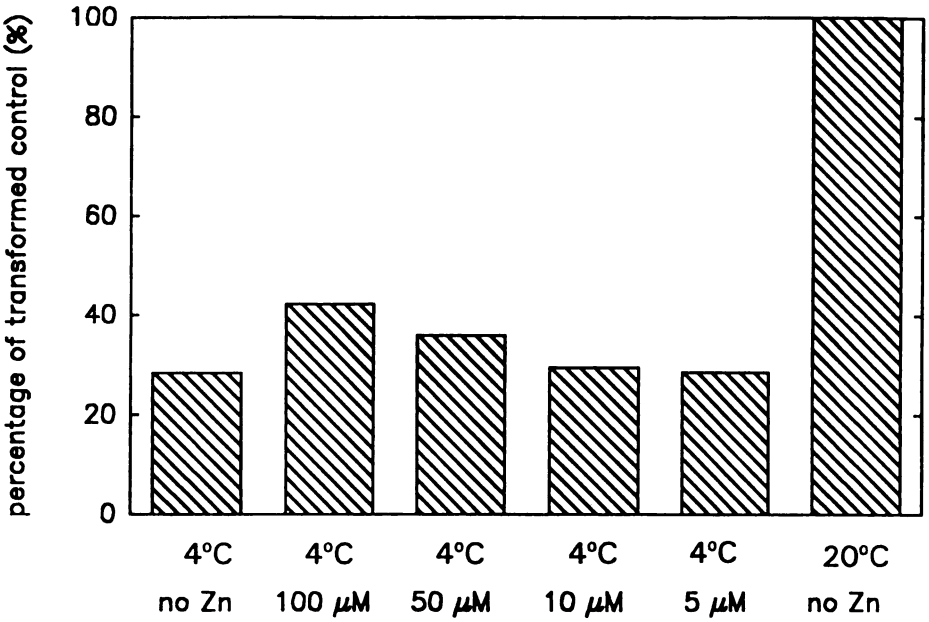

Figure 8-30. Effect of zinc on cold stabilization of untransformed GR based on binding to isolated nuclei. Mouse liver cytosol was maintained at 4°C with zinc at the indicated concentrations prior to nuclei addition. Right-most value is the 20°C ("transformed") control. Data are expressed as percentages of the transformed no zinc control.

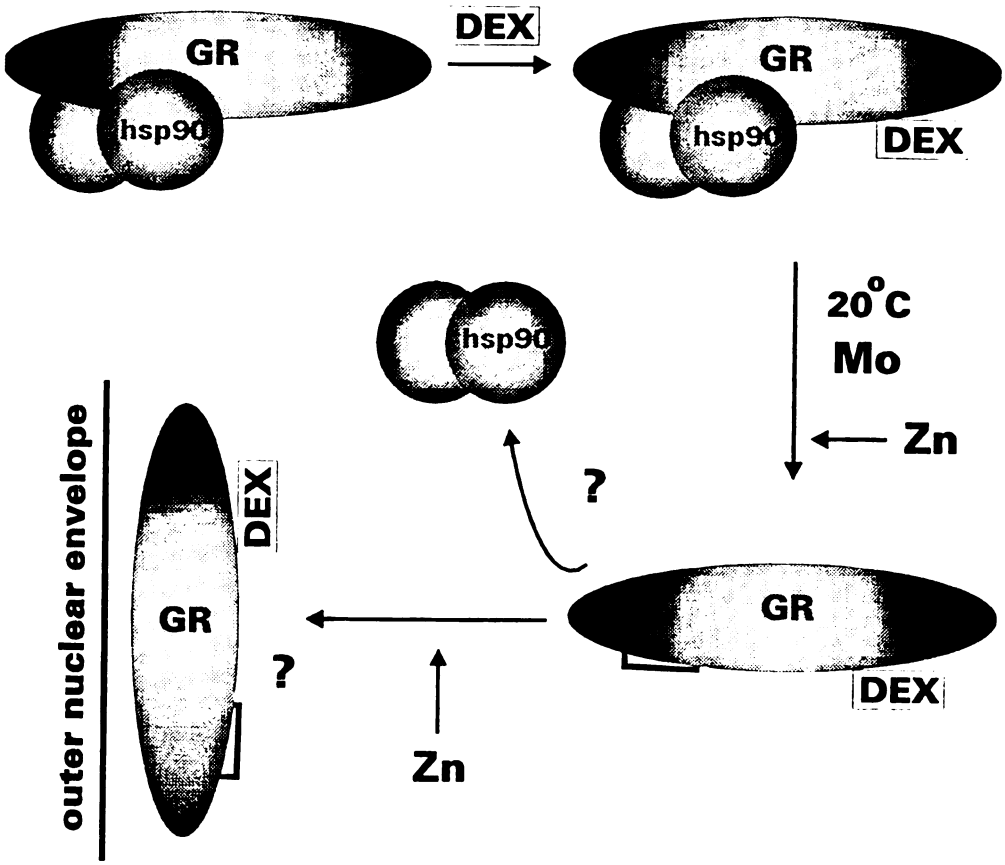

Figure 8-31. Diagram of experimental scheme for determining effect of zinc on molybdate stabilization of untransformed GR based on binding to isolated nuclei.

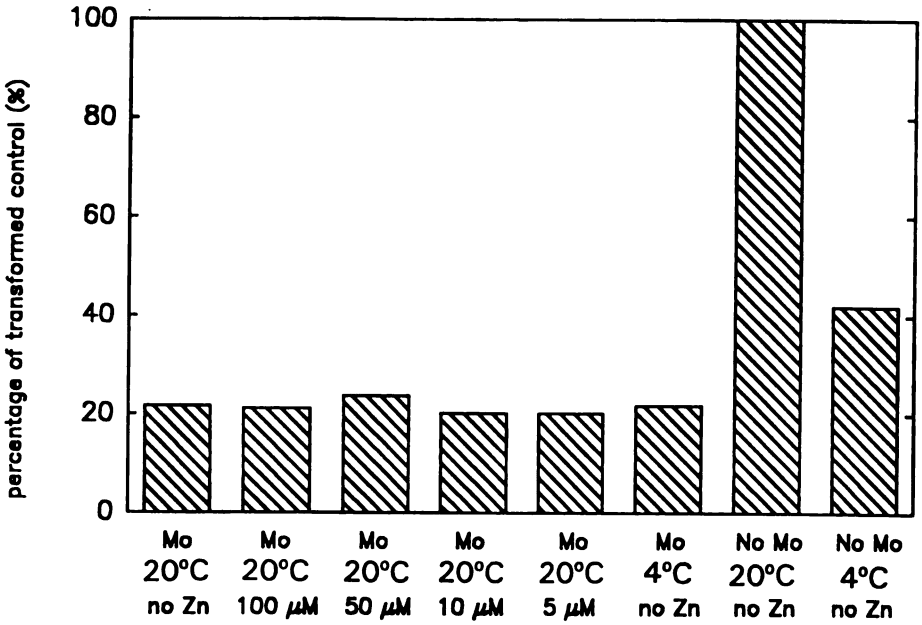

Figure 8-32. Effect of zinc on molybdate stabilization of untransformed GR based on binding to isolated nuclei. Mouse liver cytosol was incubated at 20°C with molybdate at 30 mM and zinc at the indicated concentrations prior to nuclei addition. Right-most values are the 20°C ("transformed") and 4°C ("untransformed") controls with no sodium molybdate present. Data are expressed as percentages of the transformed no molybdate/no zinc control.

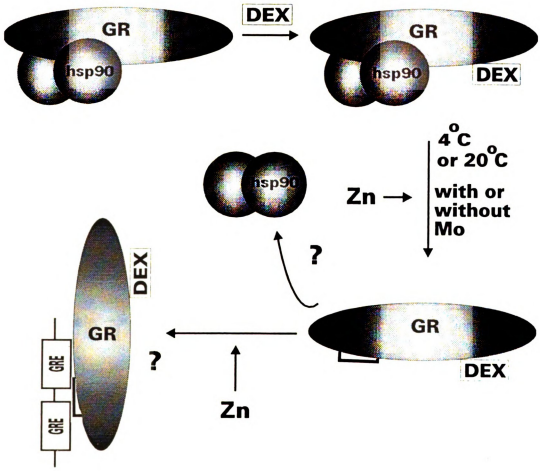

Figure 8-33. Diagram of experimental scheme for determining effect of zinc on transformation of mouse liver cytosolic GR based on ability to bind radiolabeled GRE-GRE in gel mobility shift assay.

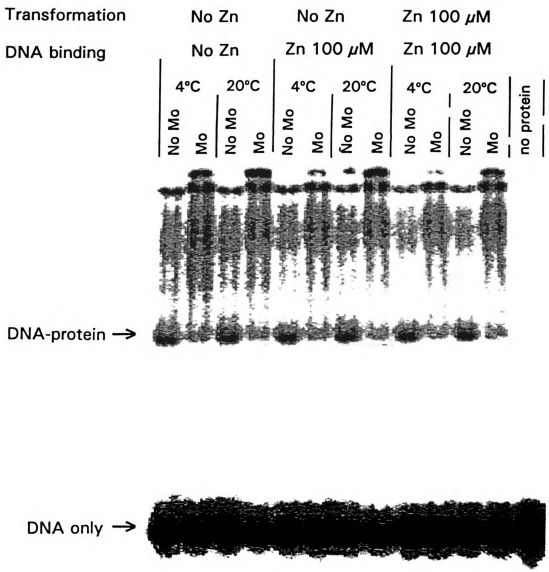

Figure 8-34. Gel mobility shift assay of mouse liver cytosolic GR binding to radiolabeled GRE-GRE.

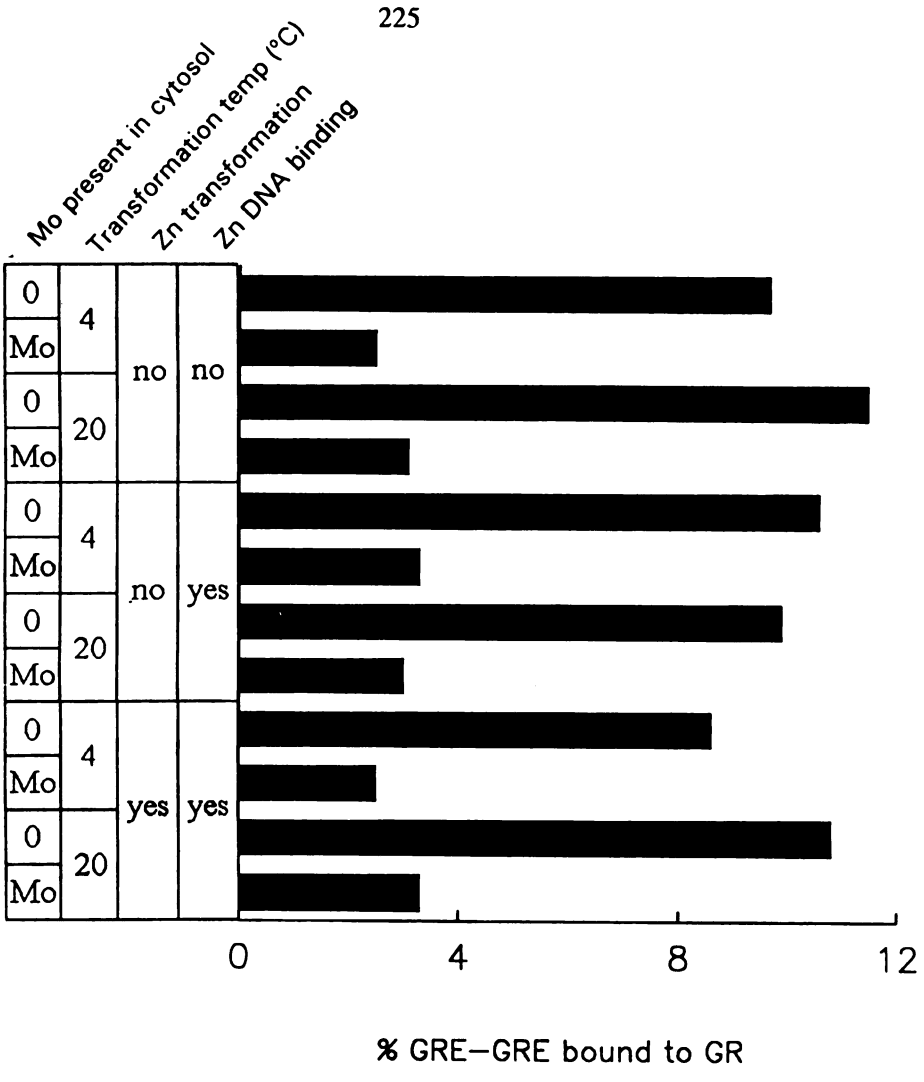

Figure 8-35. Specific activities of DNA-protein complexes formed in the absence or presence of zinc at 100 μM expressed as the percentage of total radiolabeled GRE-GRE the lane in the gel mobility shift assay in Figure 8-34.

SUMMARY AND CONCLUSIONS

Summary. The experiments described in the previous chapters tested the hypothesis that a potential target of zinc-associated inhibition of glucocorticoid-induced apoptosis in mouse thymocytes was interference with the GR signalling pathway. In Chapter 5, a novel flow cytometric method for detecting thymocyte apoptosis was further validated, and the conditions of glucocorticoid-induced cell death, including its sequential nature and the ligand requirements for form of cell death were further defined. This methodology was then used in Chapter 6 to confirm that zinc did inhibit steroid-induced cell death by flow cytometric criterion. The observation that zinc offered nearly "complete" protection from the effects of hormone then led to the hypothesis that an early event in thymocyte apoptosis such as transcriptional activation might be responsible for the inhibitory activities of zinc. The possibility that the GR signalling pathway itself might be the basis for this inhibition was tested in Chapter 7, which showed that both cytoplasmic receptor-ligand GR binding and ligand-dependent nuclear localization could be prevented by concentrations of zinc relevant to apoptotic inhibition. The *in vitro* GR experiments demonstrated that cytosolic GR-ligand binding was almost completely inhibited by zinc, suggesting that this was the mechanism likely for the observations in Chapter 7. Taken together, these results validate the hypothesis that zinc inhibition of GR signalling is a likely mechanism for the inhibitory activity of zinc on hormone-induced thymocyte apoptosis.

Reconciliation of *in vitro* and *in vivo* results of zinc effects on glucocorticoid receptor activity. The *in vitro* GR binding and transformation studies were carried out in response to *in vivo* data which suggested that zinc affected cytosolic ligand binding and nuclear

localization in mouse thymocytes. The *in vitro* experiments were therefore designed not only to look at effects on receptor-ligand binding but also at events crucial to transformation and translocation once ligand had already been bound. These studies determined that zinc acted at the level of initial receptor-ligand interaction with no apparent effect on *in vitro* receptor transformation.

Although the effective zinc concentrations required to inhibit receptor-ligand binding *in vitro* and *in vivo* differed considerably, these results can be explained by the differences between the effects of zinc on GR in whole cells versus a cell-free system. The dose-response curves for *in vitro* and *in vivo* inhibition differed, with ED_{50}s on the order of 10 to 50 μM for *in vitro* and 200 to 300 μM for *in vivo* inhibition. This discrepancy can be explained by the fact that the concentration of zinc added to thymocytes probably did not reflect the ultimate intracellular concentrations. Zinc at 500 μM in culture did not result in 500 μM intracellular zinc concentration, as indicated by the intracellular zinc measurements in Chapter 6. Intracellular zinc concentrations of thymocytes incubated with 500 μM zinc (based on calculations of predicted cellular volume) plateaued by four hours at considerably less than 1 μM and remained at this concentration even after prolonged incubation. The low concentrations of zinc required to inhibit receptor-ligand binding *in vitro* may therefore be quite relevant to the higher concentrations required to block the same binding events *in vivo*.

The *in vivo* data also raised the possibility that zinc may have had more than one site of action in its inhibitory effects. The ability of activated GR to transform depends on successful dissociation of the hsp90 homodimer. Our *in vitro* studies of ligand-dependent transformation suggested, however, that zinc had no effect on receptor transformation and that the inhibition of nuclear localization observed in Chapter 7 was probably limited to inhibition of receptor-ligand binding. Nevertheless, the importance

of hsp90 dissociation both as requirement for nuclear localization and for its possible effects on receptor-ligand binding made it a necessary mechanism to investigate, particularly in light of considerable indirect evidence for the role of zinc in its regulation. The *in vitro* transformation studies therefore excluded a critical potential mechanism for the effects of zinc on receptor transformation/translocation.

Although receptor-ligand binding and receptor transformation were obvious initial mechanisms as possible targets for zinc, the situation is naturally more complex than covered by the scope of these experiments. Dissociation with hsp90 is only one part of the receptor transformation/translocation process. Other proteins, such as hsp56 and p23, are also associated with hsp90 both in the receptor-bound and free cytoplasmic form. Although their functions have not been fully elucidated, they are believed to play important roles in receptor repression and transport (Pratt, 1992; Smith and Toft, 1992a). In addition, transient association of the molecular chaperone protein hsp70 with the receptor is thought to be important for the unfoldase activity allowing dissociation from hsp90 and transport to the nucleus. The ability of the receptor in its "transportosome" form to be translocated to the nucleus via cytoskeletal elements is also a critical aspect of receptor function and the physical basis for the "active cycling" model of receptor cycling in and out of the nucleus (Orti *et al*, 1989; Pratt, 1993). These are all potential targets for zinc that would have profound negative effects on nuclear localization yet cannot be excluded by *in vitro* transformation studies. The role of phosphorylation and dephosphorylation in ligand binding, transformation and translocation is at best still unclear, and it is also possible that added zinc could exert positive or negative effects on relevant kinases and phosphatases. For example, zinc has been found to regulate the activity of protein kinase C, which may phosphorylate glucocorticoid receptor. These and other aspects of GR signalling fall outside the scope of this project and remain to be investigated.

Effects of zinc on glucocorticoid receptor signalling: implications for the effects of zinc on glucocorticoid-induced apoptosis. The inhibitory effects of zinc on *in vivo* and *in vitro* glucocorticoid receptor-ligand binding ultimately lead back to the question of whether these results have any relevance to the inhibitory effects of zinc on glucocorticoid-induced apoptosis in mouse thymocytes. Successful ligand binding is necessary for the lytic action of glucocorticoids in thymocytes and other cell lines, as evidenced by the inhibitory action of antagonists such as RU486. Studies with tumor lines containing mutant receptors and transfection studies with genes encoding receptors with truncations or deletions have shown that receptors with truncated or nonfunctional steroid binding domains induce cell death constitutively in the absence of hormone. Cell death is therefore under strict negative control requiring the presence of successful hormone binding for induction. Inhibition of steroid binding would therefore almost certainly have the effect of inhibiting subsequent apoptosis.

Although the conditions of *in vivo* steroid binding are not entirely consistent with those observed for zinc-associated inhibition of glucocorticoid-induced apoptosis, these disrepancies can be explained by differences between the experimental systems. The dose-response curves for *in vivo* zinc inhibition of receptor-ligand binding, inhibition of nuclear localization and inhibition of apoptosis are almost identical, with ED_{50}s in the range of 200 to 300 μM. A discrepancy between these systems, however, is the requirement for zinc preincubation in *in vivo* receptor-ligand binding and nuclear localization. Zinc inhibited hormone-induced apoptosis almost entirely when added simultaneously with steroid, requiring no preincubation despite intracellular zinc concentration data suggesting that several hours were required for a significant amount of zinc to enter the cell (Figure 6-10).

This apparent disagreement can be explained by the fact that *in vivo* hormone binding assays measure all receptor-ligand interactions in the cytoplasm, while apoptosis

is a biological response to only a small percentage of those binding events. While specific cytoplasmic binding events plateau rapidly (within 60 minutes) as the receptor pool becomes saturated with ligand, thymocytes individually enter apoptosis for hours after apparent receptor saturation (Figure 5-5). Glucocorticoid-induced thymocyte apoptosis therefore occurs sequentially as has been discussed previously, with the mechanism for this "delay" factor being currently unknown. Steroid must also be present throughout the entire period in which all hormone-sensitive thymocytes are undergoing apoptosis (Figure 5-6). Incubating cells with hormone for a period sufficient to saturate all cytoplasmic receptors (about one hour) and then removing extracellular steroid only induces apoptosis in a fraction of the thymocytes that would die if cells were exposed to steroid for the entire period required for all hormone-sensitive thymocytes to die (about 8 to 12 hours).

These observations are consistent with the current nonequilibrium receptor cycling regulatory model for GR cycling from the non-hormone bound, inactive state to the hormone-bound, active state, and provide a speculative model for the mechanism by which zinc could inhibit apoptosis by affecting ligand binding to receptor (Munck and Holbrook, 1988; Orti *et al*, 1989; Orti *et al*, 1993). The nonequilibrium cycling model proposed by Munck and colleagues suggests that ligand-bound receptors are translocated to the nuclear membrane, where they "dock", with their nuclear localization signals and DNA binding domains repressed by hsp90. When an appropriate signal is given (such as phosphorylation or dephosphorylation), hsp90 dissociates, the nuclear localization signal is derepressed and the receptor enters the nucleus and activates transcription. A significant fraction of receptors do not release hsp90 or are transcriptionally inactive in the nucleus, and are eventually cycled back out into the cytoplasm. Steroid then dissociates from the receptor, and another hormone binding event is necessary for the receptor to begin the cycle again. This is consistent with the sequential nature of thymocyte apoptosis, since not all receptor-ligand binding events (as detected by an *in vivo*

binding assay) result immediately in cell death (as detected by the apoptosis assay). This also explains the apparent discrepancy between the effects of zinc on *in vivo* ligand binding and on apoptosis. While zinc does not appear to inhibit ligand binding until several hours after addition, the successful receptor-ligand interactions occuring during this time probably resulted in only a small percentage of the total hormone-induced apoptotic events, which occur sequentially over a longer period of time (8 to 12 hours). Zinc could therefore have inhibited a significant amount of total thymocyte apoptosis even though it might have little effect on receptor-ligand binding events occuring early in the incubation period. Zinc inhibition of glucocorticoid-induced apoptosis is therefore consistent with the observed ability of zinc to inhibit receptor-ligand binding *in vivo*.

Is the effect of zinc on glucocorticoid receptor signal transduction inhibiting apoptosis? These experiments support the notion that the effects of zinc on GR signalling may offer a viable mechanism for the observed effects on hormone-induced cell death. As discussed in Chapter 3, the potential targets for the inhibitory effects of zinc are vast. It is likely that no one mechanism is entirely correct, but that zinc may have multiple effects that can result in the inhibition of cell death. The observation that zinc can prevent cell death induced by stimuli other than hormones (such as irradiation) also supports the notion that zinc may have more than one site of action in the inhibition of cell death. Nevertheless, these results clearly implicate GR function as a potential target for the effects of zinc on glucocorticoid-induced apoptosis. In addition, the effects of zinc on GR signalling represent a model for other modes of apoptosis requiring induction through receptor-mediated transcriptional activation.

Recommendations for further study. The ability of zinc to reversibly inhibit GR-ligand binding and the inability of zinc to dissociate preformed GR-ligand complexes suggest that

zinc is acting directly at the steroid binding domain of GR. The ability of the reducing agent DTT to abolish the effects of zinc strongly suggests that thiol residues are involved. An obvious target for zinc is therefore the vicinal dithiols in the steroid binding domain, the redox status of which has been previously shown to affect the affinity of receptor-ligand binding. An obvious next step is to therefore determine if this actually is the site of zinc inhibition, or whether other zinc binding moieties in the steroid binding domain or in other parts of the receptor are involved. Rat HTC GR genes site-mutagenized at the vicinal dithiols and transfected into cells have been previously shown to retain ligand binding ability, but are no longer blocked by thiol crosslinking or modifying agents such as arsenite or MMTS (Simons *et al*, 1992). Transfection of GR genes site-mutagenized at the appropriate cysteine residues would therefore allow a precise determination of whether these residues are in fact responsible for the inhibitory activities of zinc on receptor-ligand binding, since mutants would presumably not be affected by zinc treatment. The next obvious course of action, directly proving that inhibition of receptor-ligand binding leads directly to inhibition of GR-inducible transcription and ultimately apoptotic death could be accomplished with this same system, using cell lines that have been transfected with GR-inducible reporter genes and cell lines that are sensitive to glucocorticoids.

The other necessary line of inquiry is other mechanisms in addition to GR signalling that may be involved in inhibition of apoptotic death. As discussed above and in Chapter 3, the number of potential mechanisms is vast. Nevertheless, determination of the mechanism of zinc inhibition of apoptotic death will shed considerable light on the biochemistry of the cell death process and may provide some insight into a possible physiological role for zinc in the regulation of this phenomenon.

APPENDIX 1

Paper: Telford, W.G. and Fraker, P.J. (1994) **Preferential induction of apoptosis in mouse $CD4^+CD8^+\alpha\beta TCR^{lo}CD3\epsilon^{lo}$ thymocytes by zinc** (in press, *Journal of Cellular Physiology*).

In Chapter 6, the intriguing observation was made that zinc at lower concentrations than those able to inhibit apoptosis (below 200 μM) could actually induce apoptosis in mouse thymocytes. In the following paper, the ability of zinc to induce apoptotic death was confirmed flow cytometrically (by reduced PI DNA fluorescence and forward scatter), by detection of DNA fragmentation using gel electrophoresis, by electron micrographic examination of morphology and by the inhibitory effects of transcriptional and translational inhibitors. In addition, zinc was shown to induce apoptosis in roughly the same subsets of thymocytes found in Chapter 5 to be sensitive to glucocorticoids (the $CD4^+CD8^+\alpha\beta TCR^{lo}CD3\epsilon^{lo}$ lineage). These results represent yet another modulatory effect of zinc on immune cell apoptosis.

Preferential induction of apoptosis in mouse $CD4^+CD8^+\alpha\beta TCR^{lo}CD3\epsilon^{lo}$ thymocytes by zinc.

William G. Telford[1] and Pamela J. Fraker[1,2]

Department of Microbiology[1]
Department of Biochemistry[2]
Michigan State University
East Lansing, MI 48824 USA

Send correspondence to:

Dr. Pamela J. Fraker, Ph.D.
215 Biochemistry
Michigan State University
East Lansing, MI 48824-1319 USA

Telephone: (517) 353-9585
FAX: (517) 353-9334

This work was supported by National Institutes of Health grant HD-10586 and the Michigan State University Biotechnology Research Program.

Running Title: Zinc induces thymocyte apoptosis

This paper contains 8 figures and 2 tables.

ABSTRACT

High concentrations of zinc salts (500 μM and greater) are known to inhibit apoptosis in a variety of systems. However, closer examination of dose effects revealed that lower concentrations of zinc (80 to 200 μM) could induce apoptosis in approximately 30 to 40% of mouse thymocytes following eight hours incubation. The ability of zinc to cause thymocyte apoptosis was detected flow cytometrically by reductions in propidium iodide DNA fluorescence and forward scatter, both quantitative indicators of apoptotic death. Zinc induced both internucleosomal DNA fragmentation and morphological changes characteristic of apoptosis as determined by gel electrophoresis and electron microscopy respectively. In addition, transcriptional and translational inhibitors prevented zinc-induced apoptosis indicating a requirement for *de novo* mRNA and protein synthesis, another characteristic of apoptotic death. Fluorescent immunophenotype-specific apoptotic analysis indicated that zinc-induced apoptosis occurred primarily in the less mature $CD4^+CD8^+\alpha\beta TCR^{lo}CD3\epsilon^{lo}$ thymocyte subset, with lower amounts of death occurring in the other subsets. This lineage specificity was shared with glucocorticoid-induced apoptosis. Taken together, these results indicate that zinc induces true apoptotic death in mouse thymocytes and suggests a role for zinc in the positive regulation of apoptosis.

INTRODUCTION

Apoptosis or programmed cell death is a phenomenon observed in a variety of cellular systems (Kerr and Harmon, 1991). It is characterized by several physiological and morphological changes in the cell, including membrane blebbing and the degradation of nuclear DNA into internucleosomal fragments via the activation of an endogenous endonuclease. Apoptosis in mouse thymocytes induced by glucocorticoids, ionizing radiation and other stimuli has been particularly well-characterized and is currently the subject of intense inquiry (Wyllie, 1980; Cohen *et al*, 1992)

Previous work demonstrated that high concentrations of zinc salts (0.5 - 5 mM) inhibited glucocorticoid-induced apoptosis in mouse thymocytes (Cohen and Duke, 1984). This phenomenon has been observed with a wide variety of cell types as discussed in a recent review (Zalewski and Forbes, 1993). Several theories have been advanced to explain the inhibitory effect of zinc, including inactivation of endogenous endonuclease activity (Cohen and Duke, 1984; book chapter) and inhibition of poly(ADP-ribose) synthetase, which may play a role in the demise of apoptotic cells due to energy depletion resulting from costly DNA repair attempts (Shimuzu *et al*, 1990). High concentrations of zinc have also been shown to modulate the activity of protein kinase C (PKC) in lymphocytes, and it has been postulated that zinc may stimulate PKC activity with subsequent inhibitory effects on apoptosis (Csermely *et al*, 1988a; Zalewski *et al*, 1991; Zalewski and Forbes, 1993).

Despite considerable speculation in this area, a clearly defined mechanism to explain the ability of zinc to inhibit cell death or a physiological role for zinc in the

regulation of apoptosis has yet to be established. The extremely high concentrations of zinc required to inhibit apoptosis (generally greater than 0.5 mM) have also raised the question of whether these effects are physiologically relevant to the regulation of apoptosis or are only likely to be encountered *in vitro*. Lower concentrations of zinc (25 μM) inhibited apoptosis only in the presence of trace metal ionophores, which artificially elevate intracellular zinc levels (Zalewski *et al*, 1991). The effects of lower concentrations of zinc alone on thymocyte apoptosis have remained undetermined.

We have previously confirmed that high concentrations of zinc salts do inhibit glucocorticoid-induced apoptosis in mouse thymocytes (Telford *et al*, 1991). In this paper, we report that lower concentrations of zinc salts (in the range of 80 to 200 μM) can actually induce apoptosis in mouse thymocytes. The ability of zinc to cause apoptosis in mouse thymocytes has been confirmed flow cytometrically by reduced propidium iodide (PI) DNA fluorescence (a measure of chromatin degradation) and reduced forward light scatter (a measure of reduced cellular volume) in affected cells, both known indicators of apoptotic death in mouse thymocytes (Telford *et al*, 1991; Telford *et al*, 1992). In addition, fluorescent immunophenotyping for thymocyte surface markers associated with T lymphocyte differentiation has been combined with flow cytometric apoptotic analysis to demonstrate that zinc induces apoptosis in distinct developmental subsets of mouse thymocytes. These observations suggest a possible bifunctional role for zinc as an activator and inhibitor in thymocyte apoptosis.

MATERIALS AND METHODS

Materials. Male A/J mice were obtained from The Jackson Laboratory, Bar Harbor, ME and housed in the Department of Biochemistry animal facility. Histopaque 1083, RPMI-1640 culture media, corticosterone, ultrapure zinc sulfate heptahydrate and emetine HCl were obtained from Sigma Chemical Co., St. Louis, MO. Cycloheximide and actinomycin D were obtained from Boerhinger Mannheim, Indianapolis, IN. All antibodies were obtained from Pharmingen, San Diego, CA. Phycoerythrin (PE)-conjugated avidin was obtained from Vector Laboratories, Burlingame, CA. Propidium iodide (PI) and 4'-6-diaminido-2-phenylindole (DAPI) were obtained from Molecular Probes, Eugene, OR.

Cell culture. Whole thymuses were removed from young mice (6-12 weeks old) and passed through stainless steel 100 micron screens into 2% heat-inactivated fetal bovine serum in phosphate buffered saline (PBS/FBS). The resulting single cell suspensions were erythrocyte-depleted over Histopaque 1083 gradients and resuspended in RPMI-1640 supplemented with 10% FBS. Cells were then cultured in 24 well plates at 2×10^6 cells per ml per well for periods up to eight hours at 5% CO_2. Where applicable, corticosterone at 1 μM or zinc sulfate heptahydrate at concentrations indicated in the results were added at the beginning of the culture period. Cycloheximide, emetine HCl and actinomycin D were used where indicated at 50 μg/ml, 10 μM and 5 μg/ml respectively.

Fluorescent immunophenotyping. Following incubation, some samples were resuspended in PBS supplemented with 10% FBS and 0.1% sodium azide at 2 x 10^6 cells per ml per sample and immunophenotyped for T-lineage markers. Mouse $\alpha\beta$TCR and CD3ϵ on thymocytes were labeled with FITC-conjugated monoclonal antibodies to these markers (from H57-597 and 145-2C11 murine hybridomas) for two-color analysis with PI. Mouse CD4 α-chain on thymocytes was labeled with a FITC-conjugated monoclonal (GK1.5) and mouse CD8 with a biotin-conjugated monoclonal (53.2) followed by secondary labeling with PE-conjugated avidin for three-color analysis with DAPI. All labeling was carried out at 4°C.

Detection of apoptosis by flow cytometry. All cell samples (both with and without previous fluorescent immunophenotyping) were fixed using the method previously described by Garvy *et al* (1993). Briefly, cells were resuspended in one part cold 50% FBS in PBS. Three parts cold 70% EtOH were added dropwise with gentle mixing. Cells were incubated at 4°C for one hour, washed twice with cold PBS, and resuspended in either PI at 50 μg/ml (for unlabeled samples or those labeled with FITC-conjugated antibodies to $\alpha\beta$TCR or CD3ϵ) or DAPI at 1 μg/ml (for samples labeled with FITC- and PE-conjugated antibodies to both CD4 and CD8 respectively). Staining with PI required the addition of 50 - 100 units RNase, while DAPI required no such addition. Samples stained with PI only or with PI and a FITC-conjugated antibody (one- or two-color) were flow cytometrically analyzed on an Ortho Cytofluorograph 50-H fluorescence-activated cell sorter (Becton-Dickinson, San Jose, CA) with an Intel 80386 processor-based microcomputer using Acqcyte™ data acquisition and MultiPlus™ data analysis software

(Pheonix Flow Systems, Palo Alto, CA). Samples stained with DAPI, FITC and PE (three-color) were analyzed on a Vantage fluorescence activated cell sorter (Becton-Dickinson, San Jose, CA) using LYSYS-2™ data acquisition and analysis software. Fluorochrome excitation for one- and two-color analysis required single argon laser excitation at 488 nm. Three-color analysis required simultaneous argon laser excitation at 488 nm for FITC and PE and krypton laser excitation at 350 nm for DAPI. Quantitation of apoptosis was carried out by determining the percentage of cells in the apoptotic or hypodiploid region of the PI or DAPI DNA cell cycle as previously described, either directly or following gating for phenotype (Telford *et al*, 1991; Garvy *et al*, 1993). Initial gating through PI or DAPI DNA width versus area fluorescence with inclusion of cells in the apoptotic region excluded debris and doublets prior to cell cycle and immunophenotypic analysis.

Electron microscopy. Cells were pelleted by centrifugation, fixed with 4% gluteraldehyde, embedded, sectioned and examined by electron microscopy (Phillips 301 transmission).

Detection of apoptosis by gel electrophoresis. Genomic DNA from mouse thymocytes incubated with no added agents, corticosterone or zinc as described above was extracted and purified using a genomic DNA anion exchange purification kit (Qiagen, Germany). Purified DNA was subsequently electrophoresed on 1.8% agarose gels using λ phage HindIII digested DNA as a molecular weight marker. Gels were stained with ethidium bromide, photographed under ultraviolet light and analyzed by scanning densitometry to

generate tracings of the DNA fragmentation patterns.

RESULTS

Zinc induced apoptosis in mouse thymocytes. In the course of experiments aimed at determining the minimum zinc concentration required to inhibit apoptosis, the surprising observation was made that certain concentrations of zinc could actually induce thymocyte apoptosis. This is illustrated in Figures 1 and 2. Mouse thymocytes were incubated with zinc sulfate heptahydrate at 100 μM for 8 hours, fixed with ethanol, stained with propidium iodide (PI) and flow cytometrically analyzed for PI fluorescence (an indicator of DNA content) and forward and side light scatter (indicators of cell size and density respectively). Treatment of thymocytes with zinc was found to produce a significant subpopulation of cells with both reduced DNA content (Figure 1) and cell size (Figure 2) as evidenced by reductions in PI fluorescence and forward light scatter, both quantitative indicators of apoptotic death (Telford *et al*, 1991; Telford *et al*, 1992). Zinc-induced apoptosis of approximately 33% to 34% following eight hours incubation showed an almost 4-fold increase over backgrounds levels of approximately 9% to 14% with no treatment. Zinc-induced apoptosis did not increase significantly beyond eight hours incubation. Treatment of thymocytes with the glucocorticoid corticosterone as a positive control for apoptotic death showed that the loss of DNA fluorescence and forward light scatter following zinc treatment was almost identical in form to that observed for glucocorticoid treatment, strongly suggesting that zinc induced apoptosis (as opposed to necrosis) in these cells. Zinc did appear to be less potent than glucocorticoid as an apoptotic stimulus, however, since corticosterone treatment at 1 μM induced nearly twice the level of apoptotic death by eight hours (Figures 1 and 2).

A dose-response curve for zinc-induced apoptosis as measured by loss of PI fluorescence found the optimal zinc concentration was approximately 80 to 200 μM (Figure 3). This range was fairly narrow; concentrations higher than 200 μM and lower than 80 μM did not induce cell death. Viability of thymocytes following treatment with zinc at 100 μM as determined by trypan blue exclusion (a test of membrane integrity), fluorescein diacetate uptake (a measure of endogenous esterase activity) and rhodamine 123 fluorescence (an indicator of mitochrondrial function) gave viabilities comparable to untreated thymocytes (greater than 90%), indicating that zinc did not induce necrotic death in thymocytes (data not shown). Interestingly, other biologically relevant metals, including copper, iron and nickel did not induce apoptosis or necrosis in mouse thymocytes at equivalent concentrations, although copper did induce some thymocyte apoptosis at concentrations greater than 500 μM (data not shown). Cadmium and gold, metals that can substitute for zinc in some enzyme systems induced considerable necrotic death in mouse thymocytes as measured by trypan blue exclusion, making detection and quantitation of any accompanying apoptotic death impossible to determine (data not shown).

Zinc-induced apoptosis in mouse thymocytes was further confirmed by examination of cell morphology by electron microscopy and by the presence of DNA fragmentation as detected by gel electrophoresis. Figure 4 shows that cell samples incubated with zinc at 100 μM contained thymocytes with typical apoptotic morphology, including cytoplasmic condensation and nuclear compaction and margination. To detect the presence of internucleosomal DNA fragmentation, genomic DNA from zinc-treated thymocytes was electrophoresed on agarose gels. Scanning densitometry of the resulting

DNA fragment distribution revealed internucleosomal DNA fragmentation consistent with that observed with corticosterone-treated thymocytes run simultaneously as a positive control (Figure 5).

To further confirm that zinc was inducing classical apoptotic death, the transcriptional inhibitor actinomycin D or the translational inhibitors cycloheximide or emetine HCl were added simultaneously with zinc at the beginning of cell culture. Transcriptional and translational inhibitors have been previously found to prevent apoptosis in mouse thymocytes, reflecting the requirement for new mRNA and protein synthesis in apoptotic death (Cohen and Duke, 1984). All agents were found to completely inhibit zinc-induced apoptosis (Figure 6). These results appear to confirm that zinc induced apoptosis in mouse thymocytes, since *de novo* mRNA and protein synthesis were required. Taken together, flow cytometric analysis of DNA content and forward scatter, cell morphology, the state of the genomic DNA and the apparent requirement for new gene expression demonstrated that zinc induced apoptotic death.

Mouse thymocyte subsets were differentially sensitive to zinc.

The discovery that zinc induces apoptosis in mouse thymocytes prompted the question of whether all thymocytes were equally sensitive to zinc, or if any developmental subsets of thymic T-lineage lymphocytes were differentially sensitive to zinc. Mouse thymocytes show varying degrees of lineage-specific sensitivity to *in vitro* glucocorticoid treatment that may bear functional relevance to *in vivo* mechanisms of thymic selection (MacDonald and Lees, 1990; Murphy *et al*, 1990; Vasquez *et al*, 1992). The ability of zinc to induce

subset-specific apoptosis in mouse thymocytes might therefore reflect a functional significance for this apoptotic stimuli, as is probably the case for glucocorticoids.

To determine whether zinc-induced apoptosis displayed lineage-specific selectivity, mouse thymocytes were incubated for 8 hours with zinc sulfate at 100 uM or corticosterone at 1 μM as a positive control. Apoptotic analysis by reduced DNA dye fluorescence was then combined with fluorescent immunophenophenotyping using antibodies against mouse CD4, CD8, $\alpha\beta$TCR and CD3ϵ. Thymocyte sensitivity to zinc was analyzed in the $CD4^+CD8^+$, $CD4^+CD8^-$ and $CD4^-CD8^+$ subsets using simultaneous three color flow cytometric analysis with DAPI as the DNA dye. Cell death in thymocytes bearing varying levels of the $\alpha\beta$TCR/CD3 complex was measured using PI as the DNA binding dye.

The results for CD4/CD8 are shown in Figure 7 and Table 1. $CD4^+$ or $CD8^+$ thymocytes (shown in the top row of CD4 versus CD8 cytograms) were gated into $CD8^+$ or $CD4^+$ versus DNA content cytograms (middle and bottom rows) and the percentage of apoptotic cells in the double positive and single positive subsets determined directly from the cytograms. Table 1 gives the percentage apoptotic cells for untreated, corticosterone-treated and zinc-treated thymocytes for the total population, the $CD4^+CD8^+$, $CD4^+CD8^-$ and $CD4^-CD8^+$ subsets. Analysis of the zinc-treated thymocytes indicated that the greatest amount of apoptotic death occurred in the $CD4^+CD8^+$ subset (47.1%) relative to background apoptosis (16.0%). The $CD4^+CD8^-$ and $CD4^-CD8^+$ subsets showed varing degrees of sensitivity to zinc treatment (18.0% and 21.0%) relative to background (15.2% and 8.0%), but were less sensitive than the double positive subset. This result was similar to that observed for corticosterone treatment, which also caused

the greatest amount of cell death in the double positive subset (78.0%) compared to the CD4 or CD8 single positive subsets (42.0% and 28.3%). Although the $CD4^+CD8^-$ subset appears more sensitive to corticosterone than the $CD4^-CD8^+$ subset in these results, the degree of single positive subset sensitivity for both corticosterone and zinc treatment were found to vary from experiment to experiment. Nevertheless, zinc was always found to induce the greatest levels of apoptosis in $CD4^+CD8^+$ thymocytes, a result similar to that found for corticosterone.

The ability of zinc to induce apoptosis in $\alpha\beta$TCR/CD3 subsets (low/intermediate/high) was also examined and compared to glucocorticoids. Cytograms for $\alpha\beta$TCR and CD3ϵ expression versus DNA content are shown in Figure 8, along with corresponding histograms for marker expression (FITC) and DNA content (PI) alone. The percentage of apoptotic cells for thymocytes expressing low, intermediate and high levels of $\alpha\beta$TCR and low or high levels of CD3ϵ were subsequently calculated from the cytograms. The results are shown in Table 2. Analysis of zinc-treated thymocytes indicated that the greatest amount of apoptotic death occurred in the $\alpha\beta TCR^{low}$ and $CD3\epsilon^{low}$ subpopulations (35.3% and 45.5%), with lesser degrees of cell death occurring in the $\alpha\beta TCR^{intermediate}$, $\alpha\beta TCR^{high}$ and $CD3\epsilon^{high}$ subpopulations (18.0%, 14.8% and 14.8%) compared to background levels. These results were consistent with corticosterone treatment, which also induced apoptosis preferentially in the $\alpha\beta TCR^{low}$ and $CD3\epsilon^{low}$ subsets (56.1% and 54.8%). Zinc and corticosterone were therefore both found to induce the greatest amount of apoptosis in the $\alpha\beta TCR^{lo}CD3\epsilon^{lo}$ thymocyte subset.

Taken together, these results demonstated that zinc preferentially induced apoptosis in the $CD4^+CD8^+\alpha\beta TCR^{low}CD3\epsilon^{low}$ thymocyte subset, with lower degrees of cell death

in the $CD4^+$ or $CD8^+$ single positive subsets or in thymocytes expressing higher levels of $\alpha\beta$TCR/CD3. The ability of zinc to preferentially induce apoptosis in the less mature, uncommitted double positive thymocyte compartment and the lesser sensitivity of the more highly differentiated single positive thymocyte subsets was consistent with the distribution of cell death observed for corticosterone treatment as well.

DISCUSSION

Zinc at high concentrations (500 μM and greater) has been previously shown to inhibit mouse lymphocyte apoptosis through an unknown mechanism (Zalewski and Forbes, 1993). In this paper, we demonstrated that zinc at lower concentrations (80 to 200 μM) could induce apoptosis in mouse thymocytes. Zinc-induced cell death has been demonstrated to be apoptotic death of the type induced by glucocorticoids as evidenced by flow cytometric reductions in chromatin stainability by PI and by reduced forward scatter, as well as by cell morphology and the presence of internucleosomal DNA fragmentation. In addition, transcriptional and translational inhibitors blocked zinc-induced apoptosis. These characteristics were all consistent with those observed for glucocorticoid-induced apoptosis in mouse thymocytes, leading to the conclusion that zinc was also inducing apoptotic death.

Zinc therefore appears to have a dual effect on *in vitro* thymocyte apoptosis, acting both as an inhibitor at higher concentrations and an activator at lower doses. It has been suggested that zinc may act as a negative regulator of apoptosis *in vivo*, presumably through the maintenance of intracellular zinc concentrations sufficiently large to prevent apoptosis (Zalewski *et al*, 1991; Zalewski and Forbes, 1993). While the ability of zinc to inhibit apoptosis *in vitro* supports this hypothesis, the concentrations of zinc necessary to effectively inhibit cell death in thymocytes and other cell types are extremely high, usually in the range of 500 to 5000 μM (Cohen and Duke, 1984). This range is well in excess of physiological concentrations of zinc generally found in cells and tissues, estimated to be less than 50 μM for most human tissues (Jackson, 1989). Lower

concentrations of zinc have been found to inhibit apoptosis only in the presence of trace metal ionophores such as pyrithione or diodoquinolone, which presumably increase the intracellular concentration of zinc to levels well above what zinc salts alone would produce (Forbes *et al*, 1989; Zalewski *et al*, 1991; Zalewski and Forbes, 1993). The ability of high concentrations of zinc to block apoptosis *in vitro* may therefore have questionable relevance to the normal regulation of thymocyte apoptosis. In fact, recent work suggests that high concentrations of zinc may only be inhibiting certain biochemical events of apoptosis such as internucleosomal DNA fragmentation, and may not prevent the ultimate demise of the cell after prolonged exposure (Barbieri *et al*, 1992). A physiological role for zinc as a positive rather than a negative regulator of apoptosis may therefore be more plausible, since the effective concentrations of zinc for apoptotic induction are closer to the normal physiological range than those necessary for inhibition.

Athough zinc was found to induce cell death to some degree in all thymocyte subsets, apoptosis was found to be predominantly induced in the less mature, uncommitted $CD4^+CD8^+\alpha\beta TCR^{lo}CD3\epsilon^{lo}$ thymocyte lineage. Thymocytes in the more mature $CD4^+CD8^-$ or $CD4^-CD8^+$ and $\alpha\beta TCR^{hi}/CD3\epsilon^{hi}$ subsets showed lesser degrees of sensitivity to zinc. It is of considerable significance that the thymocyte subsets found to be most sensitive to zinc *in vitro* were analogous with the populations found to be sensitive to glucocorticoids *in vitro*, both in this study and others (Lyons *et al*, 1992). In addition, transgenic mouse studies investigating the process of self antigen-induced selection in the thymus suggest that negative and positive selection in the thymus primarily occurs prior to CD4/CD8 single positive expression and increased TCR expression, in immature, uncommitted thymocytes that are predominantly $CD4^+CD8^+\alpha\beta TCR^{lo}$

(MacDonald and Lees, 1990; Murphy *et al*, 1990; Vasquez *et al*, 1992). Zinc and glucocorticoids therefore appear to induce apoptosis in thymocyte subsets that coincide with the thymocyte subsets susceptible to deletion during *in vivo* thymic selection.

One possible explanation for the coincidental specificity of glucocorticoid- and zinc-induced cell death could be induction of a similar spectrum of gene products following treatment. Heavy metals such as zinc and cadmium induce expression of a variety of genes in mammalian cells, including metallothionein-I and -II, heat shock protein 70 (hsp70) and the protooncogenes c-*jun*, c-*fos* and, c-*myc* (Karin et al, 1984; Richards *et al*, 1984; Mitani *et al*, 1990; Andrews *et al*, 1987; Jin and Ringhertz, 1990; Epner and Herschman, 1991). Glucocorticoids also induce expression of metallothioneins and hsp70 in hepatocytes (Vedeckis *et al*, 1987). It is believed that zinc and other metals induce gene expression by enhancing zinc finger transcription factor binding to metal responsive elements (MREs), which may share transcriptional control with glucocorticoid, phorbol ester and other enhancer regions (Karin *et al*, 1984; Anderson *et al*, 1987). It is therefore possible that zinc could be inducing apoptosis via positive or negative transcriptional regulation of genes also invoked during glucocorticoid-induced cell death. This is supported by the need for *de novo* transcription and translation in zinc-induced death. The similar subset specificities of hormone- and zinc-induced death also argues for coincidental expression of gene products that would only induce apoptosis in a restricted thymocyte lineage. Suppression of c-*myc*, c-*myb* and c-Ki-*ras* has been observed in glucocorticoid-induced lymphoid cell death, while upregulation of c-*myc*, c-*fos*, c-*jun* and hsp70 have been observed in other apoptotic systems (Vedeckis *et al*, 1987; Buttyan *et al*, 1988; Rubin *et al*, 1991). Apoptotis-associated gene expression may therefore be

coincidentally activated by both glucocorticoids and zinc. Interestingly, zinc and cadmium induce both *egr-1* and *nur77* expression in Swiss 3T3 cells, genes found to be expressed during TCR-mediated thymocyte apoptosis (Epner and Herchman, 1991; Dr. Barbara Osborne, personal communication).

Another mechanism by which zinc may induce apoptosis is by modulation of secondary signalling events associated with hormone-induced cell death. Although receptor-mediated gene expression is normally necessary for the hormone-induced apoptosis, secondary glucucorticoid-associated signalling events such as Ca^{2+} translocation and cAMP upregulation are also essential components of apoptotic signal transduction (Cohen *et al*, 1992). Induction of these signalling events even in the absence of receptor-mediated gene expression (such as Ca^{2+} flux with ionophores) can still result in apoptosis (McConkey *et al*, 1989b). Zinc may therefore be inducing apoptosis by modulation of one or more of these signalling events.

This notion is supported by considerable evidence that zinc can act directly at the level of signal transduction of lymphocytes and other cell types. Zinc is a necessary component in the structure of over 100 metalloenzymes, indicating that its presence or absence may exert considerable control over cellular processes (Chesters, 1992). At the level of signal transduction, zinc can substitute for and compete with calcium at a number of binding sites (Haberman and Richardt, 1987), an example being the inhibition of erythrocyte calmodulin activity both *in vivo* and *in vitro* (Brewer *et al*, 1980). Zinc can also modulate the activity of protein kinase C (PKC) both *in vitro* and *in vivo* (Murakami *et al*, 1987; Csermely *et al*, 1988a). PKC possesses a putative zinc binding domain (Parker *et al*, 1986) and recent work suggests that zinc is required for interaction of PKC

with diacylglycerol or phorbol ester and subsequent translocation to and interaction with the plasma membrane in mouse lymphocytes (Csermely *et al*, 1988b; Zalewski *et al*, 1990). Calcium flux, calmodulin activity and PKC activation have all been implicated in the regulation of thymocyte apoptosis (McConkey *et al*, 1989a; Ojeda *et al*, 1990; Dowd *et al*, 1991; Cohen *et al*, 1992), suggesting that zinc may be inducing apoptosis via one or more of these mechanisms. It should also be noted at this point that zinc at concentrations of 10 to 100 μM acts as a weak mitogen in mouse splenic T cells, both by itself and in synergy with mitogenic lectins such as phytohemagglutinin. It is not clear, however, whether this is the result of zinc-induced gene expression, secondary signalling events or both (Kirchner and Ruhl, 1970; Warner and Lawrence, 1986; Pocino *et al*, 1992). Zinc may therefore be able to induce cell death at the level of apoptosis-associated secondary signalling events.

The ability of zinc to induce apoptosis at concentrations approaching relevant physiological levels and the possibility of zinc interaction at the level of apoptotic signal transduction raises the question of whether *in vitro* treatment with zinc and subsequent induction of apoptosis is actually simulating biochemical event that might occur *in vivo*. Zinc influx (either from extracellular or intracellular sources) may be a glucocorticoid-mediated signalling event associated with the induction of apoptotic death, and incubation of thymocytes with zinc *in vitro* may mimic such an event. *In vivo*, this elevation in zinc concentration could either be the result of zinc influx from outside the cell or translocation of intracellular zinc to the appropriate cellular compartment. Glucocorticoids have been repeatedly shown to decrease plasma zinc levels in both rats and humans, a process closely coordinated with zinc influx into hepatocytes, lymphocytes and other cell types

(Cousins, 1989). Metallothionein expression in hepatocytes and lymphocytes is stimulated by glucocorticoids and may contribute to zinc influx and retention in these cells (Cousins *et al*, 1986). Glucocorticoids may therefore be inducing zinc influx from extracellular sources. Intracellular chelatable pools of zinc have been postulated to exist in lymphocytes (Forbes *et al*, 1990), and previous work has demonstrated translocation of zinc between the nucleus and the cytoplasm of mouse lymphocytes in response to phorbol ester treatment and other stimuli (Csermely *et al*, 1987; Csermely and Somogyi, 1989). Incubation of mouse lymphocytes with zinc *in vitro* may therefore be mimicking an *in vivo* positive regulatory event normally induced by glucocorticoids and possibly other apoptotic stimuli, making zinc an potentially important component in the signal transduction of apoptotic death.

Table 1. Corticosterone- and zinc-induced apoptosis in CD4/CD8 subsets of mouse thymocytes. The percentage of cells undergoing apoptosis in the total thymocyte population (TOTAL) and in the $CD4^+CD8^+$, $CD4^+CD8^-$ and $CD4^-CD8^+$ subpopulations was calculated from the CD4 versus CD8 and subsequently derived CD4- and CD8-gated cytograms illustrated in Figure 7. Values are expressed as the mean plus or minus standard deviation of duplicate samples. In a typical thymus the percentages of cells were 75%, 12% and 3% in the $CD4^+CD8^+$, $CD4^+CD8^-$ and $CD4^-CD8^+$ subpopulations respectively.

Treatment	Percentage apoptosis			
	TOTAL	$CD4^+CD8^+$	$CD4^+CD8^-$	$CD4^-CD8^+$
No treatment	16.0 ± 0.2%	15.4 ± 0.6%	15.2 ± 0.5%	8.0 ± 1.2%
CS 1 μM	71.6 ± 0.3%	78.0 ± 0.2%	42.0 ± 1.0%	28.3 ± 1.0%
Zn 100 μM	41.5 ± 1.2%	47.1 ± 1.8%	18.0 ± 0.3%	21.0 ± 0.4%

Table 2. Corticosterone- and zinc-induced apoptosis in $\alpha\beta$TCR and CD3ϵ subsets of mouse thymocytes. The percentage of cells undergoing apoptosis in the total population (TOTAL), the $\alpha\beta TCR^{lo}$ (low), $\alpha\beta TCR^{int}$ (intermediate), $\alpha\beta TCR^{hi}$ (high) or in the $CD3\epsilon^{lo}$ (low) or $CD3\epsilon^{hi}$ (high) subsets was calculated from the $\alpha\beta$TCR or CD3ϵ versus DNA content cytograms illustrated in Figure 8. Values are expressed as the mean plus or minus standard deviation of duplicate samples. In a typical thymus the percentages of cells were 23%, 19% and 8% in the $\alpha\beta TCR^{lo}$, $\alpha\beta TCR^{int}$ and $\alpha\beta TCR^{hi}$ subpopulations and 32% and 21% for the $CD3\epsilon^{lo}$ and $CD3\epsilon^{hi}$ subpopulations respectively.

Treatment	Percentage apoptosis			
	TOTAL	$\alpha\beta TCR^{lo}$	$\alpha\beta TCR^{int}$	$\alpha\beta TCR^{hi}$
No treatment	10.1 ± 0.3%	10.3 ± 0.2%	12.4 ± 0.4%	17.1 ± 0.4%
CS 1 μM	46.7 ± 0.1%	56.1 ± 1.3%	43.8 ± 0.4%	27.9 ± 0.3%
Zn 100 μM	29.4 ± 0.7%	35.3 ± 1.3%	18.0 ± 0.8%	14.8 ± 2.3%

Treatment	Percentage apoptosis		
	TOTAL	$CD3\epsilon^{lo}$	$CD3\epsilon^{hi}$
No treatment	10.3 ± 0.5%	12.4 ± 1.1%	9.4 ± 2.0%
CS 1 μM	44.8 ± 0.8%	54.8 ± 1.1%	30.4 ± 1.1%
Zn 100 μM	30.6 ± 0.4%	45.5 ± 0.5%	14.8 ± 0.1%

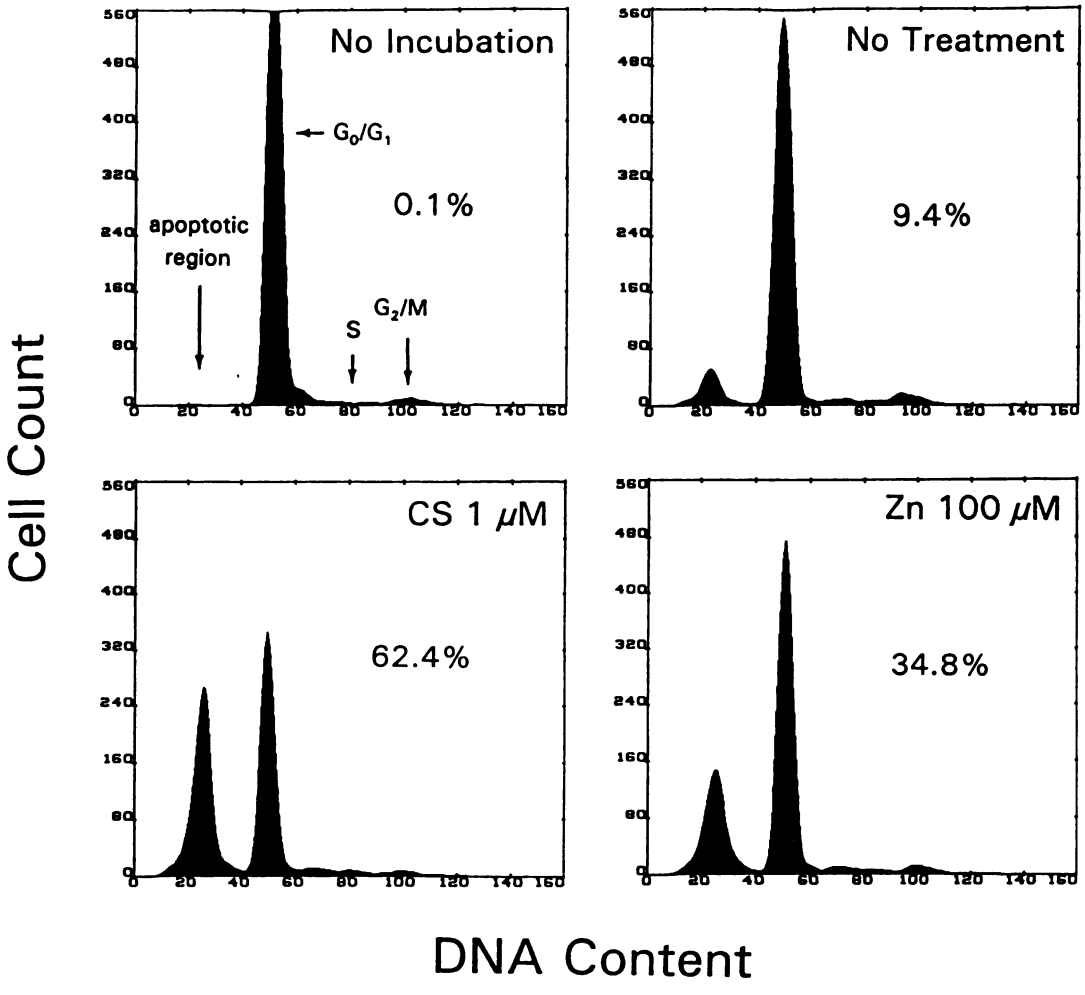

Figure 1. Zinc-induced apoptosis in mouse thymocytes as detected by flow cytometric cell cycle analysis. Fresh thymocytes (no incubation) or thymocytes incubated without (no treatment) or with corticosterone (CS 1 μM) or zinc sulfate (Zn 100 μM) for 8 hours were ethanol fixed, stained with PI and analyzed by flow cytometry as described in the text. Flow cytometric data are expressed as red fluorescence histograms (DNA content). Cell cycle regions and the apoptotic subpopulations are indicated with arrows. The percentage values represent the percentage of apoptotic cells in the total sample. Data are representative of five separate experiments.

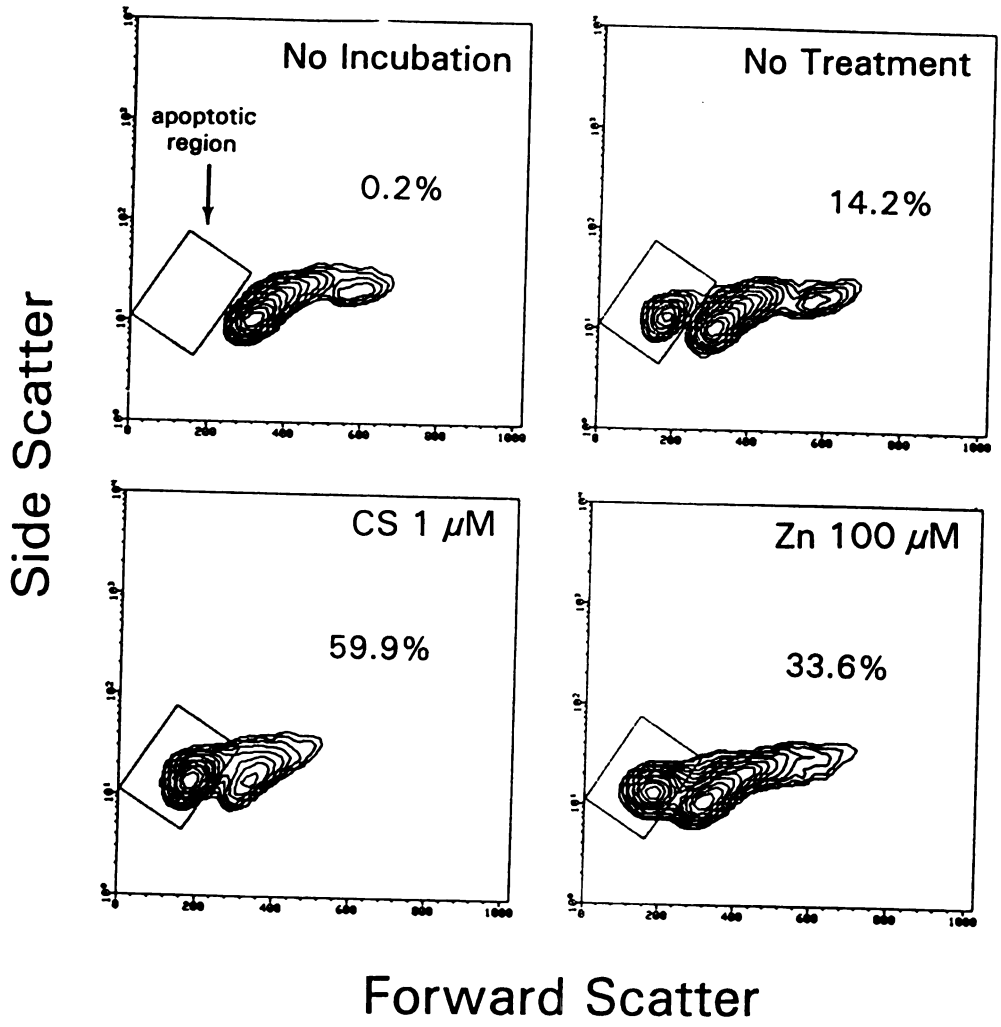

Figure 2. Zinc-induced apoptosis in mouse thymocytes as detected by flow cytometric light scatter analysis. The same samples described in Figure 1 were simultaneously analyzed by flow cytometry for forward versus side light scatter and are expressed as cytograms. The apoptotic subpopulations are indicated by the outlined regions. The percentage of apoptotic cells in each sample are given. Data are representative of five separate experiments.

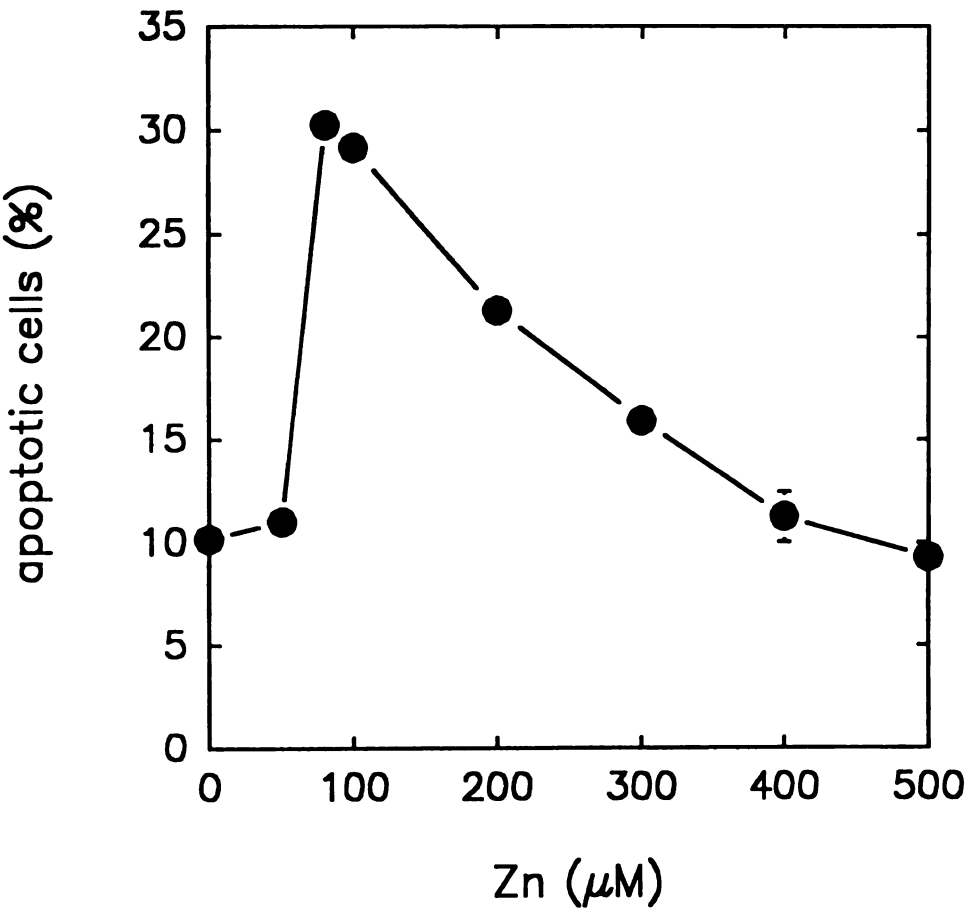

Figure 3. Dose-response curve for the induction of apoptosis in mouse thymocytes by zinc measured by reduced PI fluorescence as analyzed by flow cytometry. Mouse thymocytes were incubated with the indicated concentrations of zinc sulfate for 8 hours, fixed, stained with PI and analyzed. Values are expressed as plus or minus standard deviation of duplicate samples. For some data points error bars are not visible. Data is representative of three separate experiments.

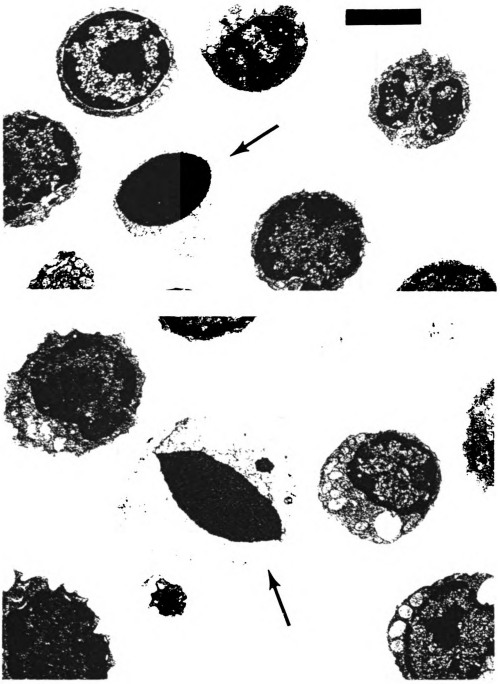

Figure 4. Electron micrographs of mouse thymocytes treated with zinc sulfate at 100 μM for 8 hours. Apoptotic thymocytes are indicated with arrows. Other thymocytes show normal morphology. Bar equals 5 μm.

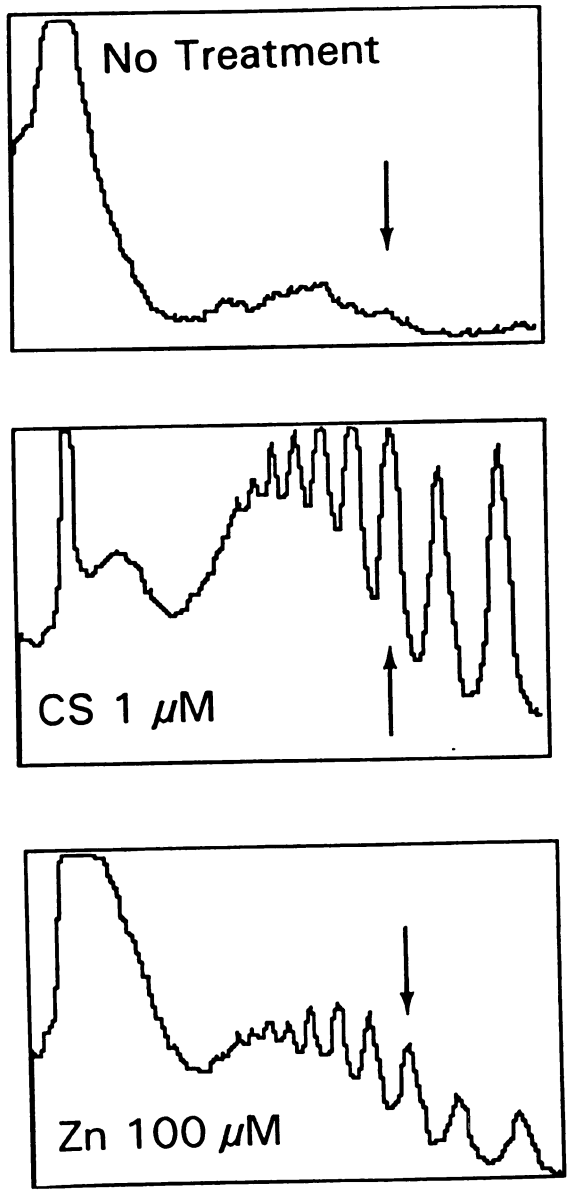

Figure 5. Densitometric tracings of purified mouse thymocyte DNA electrophoretic fragmentation patterns from fresh thymocytes (no incubation) or thymocytes incubated without (no treatment) or with corticosterone (CS 1 μM) or zinc sulfate (Zn 100 μM) for 8 hours. Photographs of ethidium bromide-stained gels were analyzed by scanning densitometry to obtain fragmentation pattern tracings. Arrows indicate the location of the 600 bp fragment based on λ HindIII molecular weight markers. Data are representative of two separate experiments.

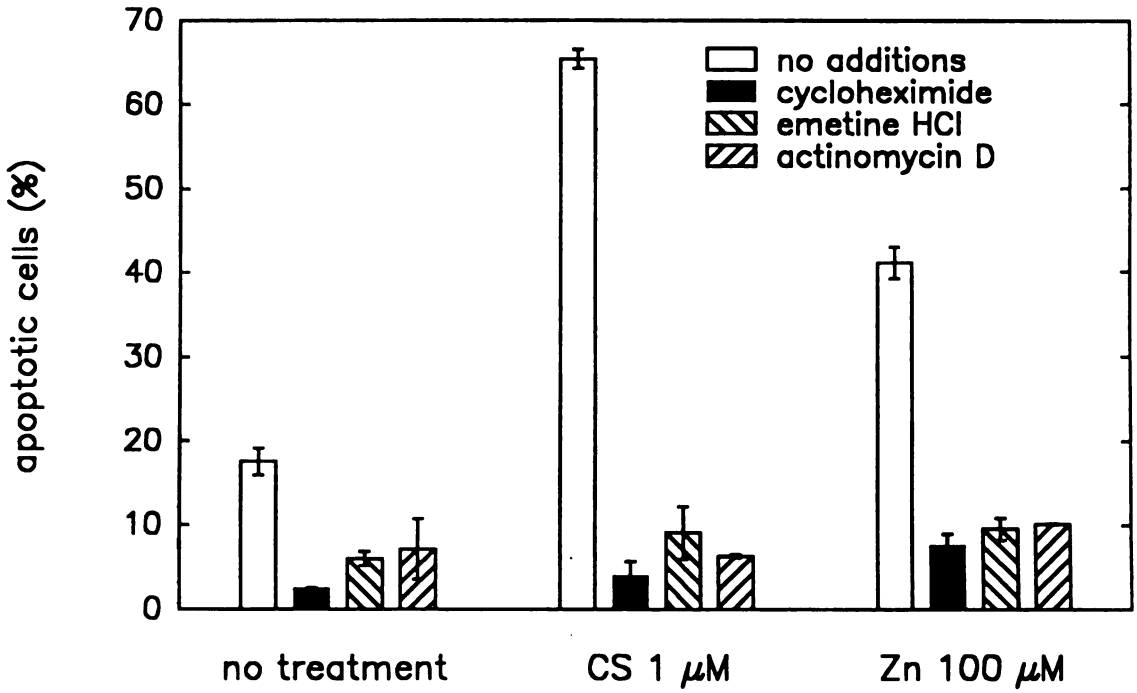

Figure 6. Inhibition of zinc-induced apoptosis in mouse thymocytes by transcriptional and translational inhibitors. Cycloheximide at 50 μg/ml, emetine HCl at 10 μM or actinomycin D at 5 μg/ml were added to mouse thymocytes simultaneously incubated without (no treatment) or with corticosterone (CS 1 μM) or zinc sulfate (Zn 100 μM) for 8 hours. Percentage apoptosis was measured by reduced PI fluorescence analyzed by flow cytometry. Values are expressed as plus or minus standard deviation of duplicate samples. Data are representative of three separate experiments.

Figure 7. Corticosterone- and zinc-induced apoptosis in CD4/CD8 subsets of thymocytes. Fresh thymocytes (no incubation) or thymocytes incubated with treatment) or with corticosterone (CS 1 μM), or zinc sulfate (Zn 100 μM) for eigh were immunophenotypically labeled for CD4 and CD8 expression (FITC a respectively), ethanol fixed, stained for cell cycle with DAPI, and flow cytome analyzed for all three fluorochromes as described in the text. Top panels show cyt for FITC-CD4 versus PE-CD8. Arrows mark the division between negative and p staining for both CD4 and CD8. Negative control fluorescence in fresh thymoc illustrated in the upper right corner of the no incubation cytogram. $CD4^+$ and subpopulations were then gated into CD8 or CD4 versus DNA content (DAPI) cyt (middle and bottom rows respectively). Percentage apoptotic cells was then calcula the total population and $CD4^+CD8^+$, $CD4^+CD8^-$ and $CD4^-CD8^+$ subsets directly fr cytograms based on the percentage of cells in the apoptotic region of the phe specific cell cycles (marked with arrows as in the top panels). Apoptotic percenta the total population and three subpopulations are given in Table 1. Data are represe of two separate experiments.

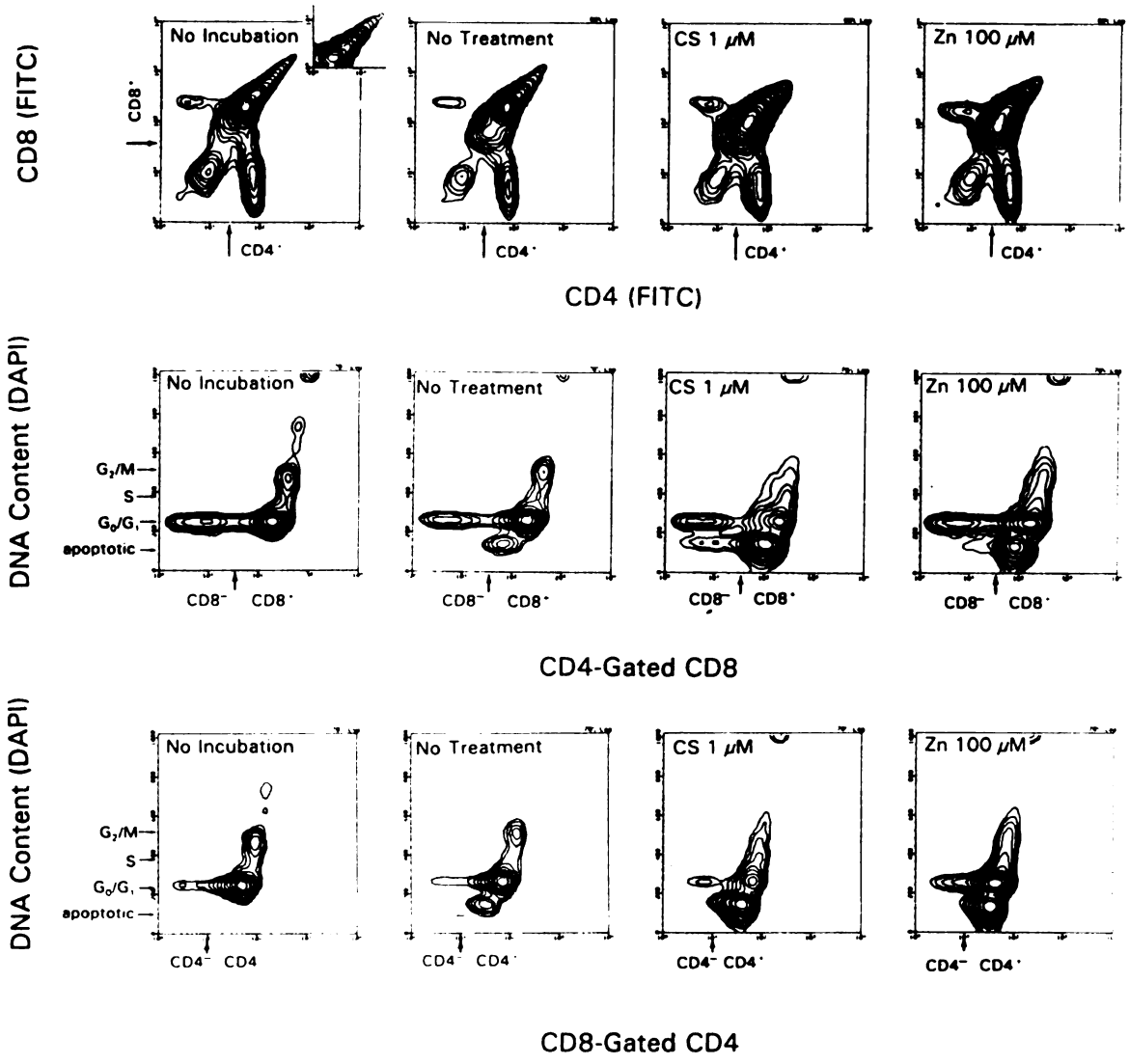
CD8 (FITC)
No Incubation
No Treatment
CS 1 μM
Zn 100 μM
CD8+
CD4+
CD4 (FITC)
DNA Content (DAPI)
G2/M
S
G0/G1
apoptotic
CD8- CD8+
CD4-Gated CD8
CD4- CD4+
CD8-Gated CD4

Figure 8. Corticosterone- and zinc-induced apoptosis in $\alpha\beta$TCR or CD3ϵ subsets of mouse thymocytes. Thymocytes were incubated without (no treatment) or with corticosterone (CS 1 μM) or zinc sulfate (Zn 100 μM) for eight hours. Cells were then immunophenotypically labeled for either $\alpha\beta$TCR or CD3ϵ (FITC), ethanol-fixed, stained for DNA content with PI as described in the text and flow cytometrically analyzed for both fluorochromes as described in the text. Top and bottom panels show $\alpha\beta$TCR or CD3ϵ expression versus DNA content (PI) cytograms respectively, with corresponding histograms showing distribution of $\alpha\beta$TCR or CD3ϵ expression subsets and DNA content (including the apoptotic region as indicated). Negative control fluorescence in untreated samples is shown in the no treatment phenotypic labeling histograms. Percentage apoptotic cells in the $\alpha\beta$TCR^{lo} (low), $\alpha\beta$TCR^{int} (intermediate), $\alpha\beta$TCR^{hi} (high) and the CD3ϵ^{lo} and CD3ϵ^{hi} subsets were calculated directly from marker expression versus DNA content cytograms based on the percentage of cells in the apoptotic region of each phenotype-specific cell cycle (marked with arrows). Apoptotic percentages for the total population and three subpopulations are given in Table 2. Data are representative of two experiments.

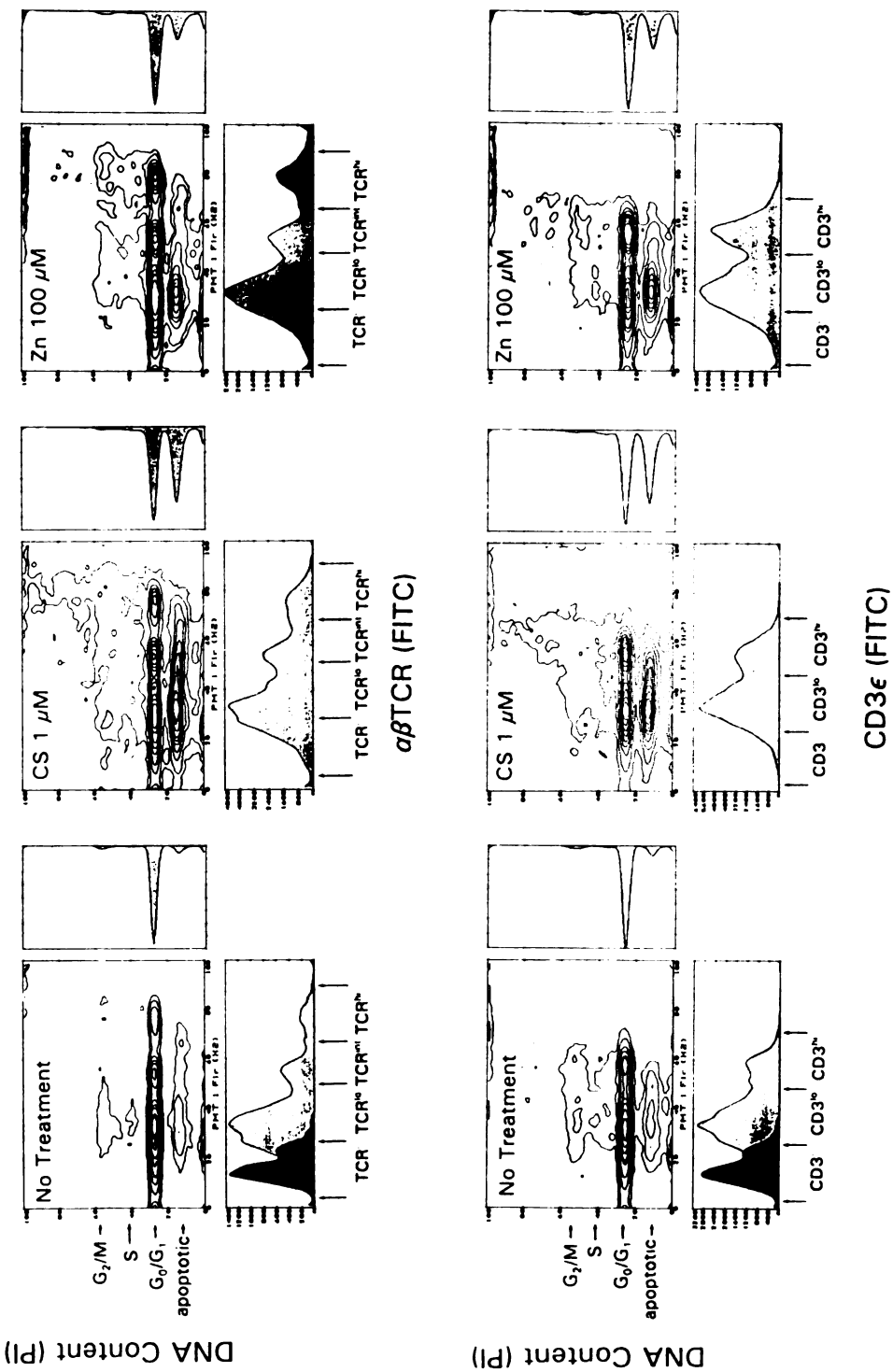
No Treatment
CS 1 μM
Zn 100 μM
G2/M
S
G0/G1
apoptotic
DNA Content (PI)
TCR TCR0 TCRint TCRhi
αβTCR (FITC)
CD3 CD30 CD3hi
CD3ε (FITC)

LITERATURE CITED

Alnemeri, E.S. and Litwack, G. (1989) Glucocorticoid-induced lymphocytolysis is not mediated by an induced endonuclease. *J. Biol. Chem.* 264, 4104-4111.

Alnemeri, E.S. and Litwack, G. (1990) Activation of internucleosomal DNA cleavage in human CEM lymphocytes by glucocorticoid and novobiocin. Evidence for non-Ca^{2+}-requiring mechanism(s). *J. Biol. Chem.* 265, 17323-17333.

Alnemeri, E.S., Fernandes, T.F., Haldar, S., Croce, C.M. and Litwack, G. (1992) Involvement of BCL-2 in glucocorticoid-induced apoptosis of human pre-B-leukemias. *Cancer Res.* 52, 491-495.

Alnemeri, E.S. and Litwack, G. (1993) Glucocorticoid-induced programmed cell death (apoptosis) in leukemia and pre-B cells. In *Programmed Cell Death: The Cellular and Molecular Biology of Apoptosis*, M. Lavin and D. Watters, eds., Harwood Academic Publishers, Switzerland, pp. 99-110.

Andersen, R.D., Taplitz, S.J., Wong, S., Bristol, G., Larkin, B. and Herschman, H.R. (1987) Metal-dependent binding of a nuclear factor to the rat metallothionein 1 gene promoter. *Mol. Cell. Biol.* 7, 3574-3581.

Andrews, G.K., Harding, M.A., Calvet, J.P. and Adamson, E.D. (1987) The heat shock response in HeLa cells is accompanied by elevated expression of the c-*fos* proto-oncogene. *Mol. Cell Biol.* 7, 3452-3458.

Antakly, T., Thompson, E.B. and O'Donnell, D. (1989) Demonstration of the intracellular localization and up-regulation of glucocorticoid receptor by *in situ* hybridization and immunocytochemistry. *Cancer Res.* 49, 2230s-2234s.

Archer, T.K., Hager, G.L. and Omichinski, J.G. (1990) Sequence-specific DNA binding by glucocorticoid receptor "zinc finger peptides". *Proc. Natl. Acad. Sci. USA* 87, 7560-7564.

Auricchio, F. (1989) Phosphorylation of steroid receptors. *J. Steroid Biochem.* 32, 613-622.

Bansal, N., Houle, A.G. and Melnykovych, G. (1990) Dexamethasone-induced killing of neoplastic cells of lymphoid derivation: lack of early calcium involvement. *J. Cell. Physiol.* 143, 105-109.

Bansal, N., Houle, A.G. and Melnykovych, G. (1991) Apoptosis: mode of cell death induced in T cell leukemia lines by dexamethasone and other agents. *Fed. Proc.* 5, 211-216.

Barbieri, D., Troiano, L., Grassilli, E., Agnesini, C., Cristofal, E.A., Monti, D., Capri, M., Cossarizza, A. and Franceschi, C. (1992) Inhibition of apoptosis by zinc: a reappraisal. *Biochem. Biophys. Res. Comm.* 187, 1256-1261.

Barnett, C.A., Schmidt, T.J. and Litwack, G. (1980) Effects of calf intestinal alkaline phosphatase, phosphatase inhibitors and phosphorylated compounds on the rate of activation of glucocorticoid-receptor complexes. *Biochemistry* 19, 5446-5455.

Baxter, J.D., Santi, D.V. and Rousseau, G.G. (1975) A filter technique for measurement of steroid-receptor binding. In *Methods in Enzymology* 36, B.W. O'Malley and J.G. Hardman, eds., Academic Press, New York, pp. 234-239.

Beato, M. And Feigelson, P. (1972) Characteristics of the glucocorticoid-receptor protein in rat liver cytosol. *J. Biol. Chem.* 247, 7890-7898.

Beato, M. (1989) Gene regulation by steroid hormones. *Cell* 56, 335-344.

Becker, P.B., Gloss, B., Schmid, W., Strahle, U. and Schutz, G. (1986) In vivo protein-DNA interactions in a glucocorticoid response element require the presence of hormone. *Nature* (London) 324, 686-688.

Berger, N.A. and Skinner, A.M. (1974) Characterization of lymphocyte transformation induced by zinc ions. *J. Cell Biol.* 61, 45-54.

Bettger, W.J. and O'Dell, B.L. (1981) Minireview: a critical physiological role of zinc in the structure and function of biomembranes. *Life Sci.* 28, 1425-1438.

Bettuzzi, S., Troiano, L., Davilli, P., Tropea, F., Ingletti, M.C., Grassilli, E., Monti, D., Corti, A. and Francheschi, C. (1991) *In vivo* accumulation of sulfonated glycoprotein 2 mRNA in rat thymocytes upon dexamethasone-induced cell death. *Biochem. Biophys. Res. Comm.* 175, 810-815.

Bodine, P.V. and Litwack, G. (1988a) Purification and structural analysis of the modulator of the glucocorticoid-receptor complex. *J. Biol. Chem.* 263, 3501-3512.

Bodine, P.V. and Litwack, G. (1988b) Evidence that the modulator of the glucocorticoid-receptor complex is the endogenous molybdate factor. *Proc. Natl. Acad. Sci. USA* 85, 1462-1466.

Bodwell, J.E., Orti, E., Coull, J.M., Pappin, D.J.C., Mendel, D.B., Smith, L.I. and Swift, F. (1991) Identification of phosphorylated sites in the mouse glucocorticoid receptor. *J. Biol. Chem.* 266, 7549-7555.

Borochov, N., Ausio, J. and Eisenberg, H. (1984) Interaction and conformational changes of chromatin with divalent cations. *Nucleic Acids Res.* 12, 3089-3096.

Borovansky, J. and Riley, P.A. (1983) The effect of divalent cations on Cloudman melanoma cells. *Eur. J. Cancer Clin. Oncol.* 19, 91-99.

Borovansky, J., Riley, P.A., Vrankova, E. and Necas, E. (1985) The effect of zinc on mouse melanoma growth *in vitro* and *in vivo*. *Neoplasma* 32, 401-406.

Borovansky, J. and Riley, P.A. (1989) Cytotoxicity of zinc *in vitro*. *Chem. Biol. Interactions* 69, 279-291.

Bremner, I. and Beatie, J.H. (1990) Metallothionein and the trace metals. *Ann. Rev. Nutr.* 10, 63-83.

Bresnick, E.H., Sanchez, E.R. and Pratt, W.B. (1988) Relationship between glucocorticoid receptor steroid-binding capacity and association of the Mr 90,000 heat shock protein with the unliganded receptor. *J. Steroid Biochem.* 30, 267-269.

Bresnick, E.H., Dalman, F.C., Sanchez, E.R. and Pratt, W.B. (1989) Evidence that the 90-kDa heat shock protein is necessary for the steroid binding conformation of the L cell glucocorticoid receptor. *J. Biol. Chem.* 264, 4992-4997.

Bresnick, E.H., Dalman, F.C. and Pratt, W.B. (1990) Direct stoichiometric evidence that the untransformed M_r 300 000, 9S glucocorticoid receptor is a core unit derived from a larger heteromeric complex. *Biochemistry* 29, 520-527.

Brewer, G.J. (1980) Calmodulin, zinc and calcium in cellular and membrane regulation: an interpretive review. *Amer. J. Hematol.* 8, 231-248.

Brune, B., Hartzell, P., Nicotera, P. and Orrenius, S. (1991) Spermine prevents endonuclease activation and apoptosis in thymocytes. *Exp. Cell. Res.* 195, 323-329.

Burnstein, K.L. and Cidlowski, J.A. (1989) Regulation of gene expression by glucocorticoids. *Ann. Rev. Physiol.* 51, 683-699.

Burnstein, K.L., Jewell, C.M. and Cidlowski, J.A. (1991) Evaluation of the role of ligand and thermal activation on specific DNA binding by *in vitro* synthesized human glucocorticoid receptor. *Mol. Endocrinol.* 5, 1013-1022.

Buttyan, R., Zakeri, Z., Lackshin, R. and Wolgemuth, D. (1988) Cascade induction of c-fos, c-myc and heat shock 70K transcripts during regression of the rat ventral prostate gland. *Mol. Endocrinol.* 2, 650-657.

Cadepond, F., Schweizer-Groyer, G., Segard-Maurel, I., Jibard, N., Hollenberg, S.M., Giguere, V., Evans, R.M. and Baulieu, E-E. (1991) Heat shock protein 90 as a critical factor in maintaining glucocorticosteroid receptor in a nonfunctional state. *J. Biol. Chem.* 266, 5834-5841.

Cairns, J.S., Mainwaring, M.S., Cacchione, R.N., Walker, J.A. and McCarthy, S.A. (1993) Regulation of apoptosis in thymocytes. *Thymus* 21, 177-193.

Carlstedt, J. and Gustafsson, J-A. (1988) Functional probing of glucocorticoid receptor structure. *J. Steroid Biochem.* 31, 593-597.

Caron-Leslie, L-A. and Cidlowski, J.A. (1991) Similar actions of glucocorticoids and calcium on the regulation of apoptosis in S49 cells. *Mol. Endocrinol.* 5, 1169-1179.

Carson-Jurica, M.A., Schrader, W.T. and O'Malley, B.W. (1990) Steroid receptor family: structure and functions. *Endocrine Rev.* 11, 201-220.

Catelli, M.G., Binart, N., Jung-Testas, I., Renoir, J.M., Baulieu, E.E., Feramisco, J.R. and Welch, W.J. (1985) The common 90-kd protein component of non-transformed '8S' steroid receptors is a heat shock protein. *EMBO J.* 4, 3131-3135.

Chakraborti, P.K., Hoeck, W., Groner, B. and Simons, S.S. (1990) Localization of the vicinal dithiols involved in steroid binding to the rat glucocorticoid receptor. *Endocrinology* 127, 2530-2539.

Chakraborti, P.K., Garabedian, M.J., Yamamoto, K.R. and Simons, S.S. (1992) Role of cysteines 640, 656 and 661 in steroid binding to rat glucocorticoid receptors. *J. Biol. Chem.* 267, 11366-11373.

Chesters, J.K. (1972) The role of zinc ions in the transformation of lymphocytes by phytohaemagglutinin. *Biochem. J.* 130, 133-139.

Chesters, J.K. (1992) Trace element-gene interactions. *Nutritional Rev.* 50, 217-223.

Chvapil, M., Ryan, J.N. and Zukoski, C.F. (1972) The effect of zinc and other metals on the stability of lysosomes. *Proc. Soc. Exp. Biol. Med.* 140, 642-646.

Chvapil, M. (1973) New aspects in the biological role of zinc: a stabilizer of macromolecules and biological membranes. *Life Sci.* 13, 1041-1049.

Cidlowski, J.A. (1982) Glucocorticoids stimulate ribonucleic acid degradation in isolated rat thymocytes *in vitro*. *Endocrinology* 111, 184-190.

Cidlowski, J.A., Bellingham, D.L., Powell-Oliver, F.E., Lubahn, D.B. and Sar, M. (1990) Novel antipeptide antibodies to the human glucocorticoid receptor: recognition of multiple receptor forms *in vitro* and distinct localization of cytoplasmic and nuclear receptors. *Mol. Endocrinol.* 4, 1427-1437.

Cohen, G.M., Sun, X-M., Snowden, R.T., Ormerod, M.G. and Dinsdale, D. (1993) Critical changes in apoptosis in thymocytes precede endonuclease activation. In *Programmed Cell Death: The Cellular and Molecular Biology of Apoptosis*, M. Lavin and D. Watters, Eds., Harwood Academic Publishers, Switzerland, pp. 123-132.

Cohen, J.J. and Duke, R.C. (1984) Glucocorticoid activation of a calcium-dependent endonuclease in thymocyte nuclei leads to cell death. *J. Immunol.* 132, 38-42.

Colbert, R.A. and Young, D.A. (1986) Glucocorticoid-induced messenger ribonucleic acids in rat thymic lymphocytes: rapid primary effects specific for glucocorticoids. *Endocrinology* 119, 2598-2605.

Compton, M.M. and Cidlowski, J.A. (1986) Rapid *in vivo* effects of glucocorticoids on the integrity of rat lymphocyte genomic deoxyribonucleic acid. *Endocrinology* 118, 38-45.

Compton, M.M. and Cidlowski, J.A. (1987) Identification of a glucocorticoid-induced nuclease in thymocytes. A potential "lysis gene" product. *J. Biol. Chem.* 262, 8288-8292.

Coppen, D.E., Cousins, R.J. and Richardson, D.E. (1985) Effect of zinc on chemically-induced peroxidation in rat liver parenchymal cells in primary culture. *Fed. Proc.* 44, 6404 (abstract).

Coppen, D.E., Richardson, D.E.and Cousins, R.J. (1986) Suppression of lipid peroxidation in rat hepatocytes in primary culture by supplemental zinc. *Fed. Proc.* 45, 1083 (abstract).

Cousins, R.J., Dunn, M.A., Leinart, A.S., Yedinak, K.C. and DiSilvestro, R.A. (1986) Coordinate regulation of zinc metabolism and metallothionein gene expression in rats. *Amer. J. Physiol.* 251, E688-E694.

Cousins, R.J. (1989) Systemic transport of zinc. In *Zinc in human biology*, C.F. Mills, ed., Springer-Verlag, London, pp. 79-93.

Cousins, R.J. and Lee-Ambrose, L.M. (1992) Nuclear zinc uptake and interactions and metallothionein gene expression are influenced by dietary zinc in rats. *J. Nutr.* 122, 56-64.

Crabtree, G.R., Munck, A. and Smith, K.A. (1980) Glucocorticoids and lymphocytes II. Cell cycle-dependent changes in glucocorticoid receptor content. *J. Immunol.* 132, 170-175.

Craig, E. (1985) The heat shock proteins. *CRC Crit. Rev. Biochem.* 18, 239-280.

Csermely, P., Gueth, S. and Somogyi, J. (1987) The tumor promoter tetradecanoyl-phorbol acetate (TPA) elicits the redistribution of zinc in subcelular fractions of rabbit thymocytes measured by X-ray fluorescence. *Biochem. Biophys. Res. Comm.* 144, 863-868.

Csermely, P., Szamel, M., Resch, K. and Somogyi, J. (1988a) Zinc increases the affinity of phorbol ester receptor in T lymphocytes. *Biochem. Biophys. Res. Comm.* 154, 578-583.

Csermely, P., Szamel, M., Resch, K. and Somogyi, J. (1988a) Zinc can increase the activity of protein kinase C and contributes to its binding to plasma membranes in T lymphocytes. *J. Biol. Chem.* 263, 6487-6490.

Csermely, P. and Somogyi, J. (1989) Zinc as a possible mediator of signal transduction in T lymphocytes. *Acta Physiol. Hung.* 74, 195-199.

Csmerely, P., Kajtar, J., Hollosi, M., Jalsovszky, G., Holy, S., Kahn, C.R., Gergely, P., Soti, C., Mihaly, K. and Somogyi, J. (1993) ATP induces a conformational change of the 90-kDa heat shock protein (hsp90). *J. Biol. Chem.* 268, 1901-1907.

Cullen, W.R., McBride, B.C. and Reglinski, J. (1984) The reaction of methylarsenicals with thiols: some biological implications. *J. Inorgan. Biochem.* 21, 179-194.

Cunningham-Rundles, S., Cunningham-Rundles, Dupont, B. and Good, R.A. (1980) Zinc-induced activation of human B lymphocytes. *Clin. Immunol. Immunopathol.* 16, 115-128.

Cuthill, S., Wilhelmsson, A., Mason, G.G.F., Gillner, M., Poellinger, L. and Gustafsson, J-A. (1988) The dioxin receptor: a comparison with the glucocorticoid receptor. *J. Steroid Biochem.* 30, 277-280.

Dahlman-Wright, K., Wright, A., Carlstedt-Duke, J. and Gustafsson, J-A. (1992) DNA-binding by the glucocorticoid receptor: a structural and functional analysis. *J. Steroid Biochem. Mol. Biol.* 41, 249-272.

Dahlman-Wright, K., Grandien, K., Nilsson, S., Gustaffson, J-A. and Carlstedt-Duke, J. (1993) Protein-protein interactions between the DNA-binding domains of nuclear receptors influence DNA-binding. *J. Steroid Biochem. Mol. Biol.* 45, 239-250.

Dahmer, M.K., Housely, P.R. and Pratt, W.B. (1984) Effects of molybdate and endogenous inhibitors on steroid-receptor inactivation, transformation, and translocation. *Ann. Rev. Physiol.* 46, 67-81.

Dalman, F.C., Sanchez, E.R., Lin, AL-Y., Perini, F. and Pratt, W.B. (1988) Localization of the phosphorylation sites with respect to the functional domains of the mouse L-cell glucocorticoid receptor. *J. Biol. Chem.* 263, 12259-12267.

Dalman, F.C., Bresnick, E.H., Patel, P.D., Perdew, G.H., Watson, S.J. and Pratt, W.B. (1989) Direct evidence that the glucocorticoid receptor binds to hsp90 at or near the termination of receptor translation *in vitro*. *J. Biol. Chem.* 264, 19815-19821.

Danielson, M., Northrop, J.P. and Ringold, G.M. (1986) The mouse glucocorticoid receptor: mapping of functional domains by cloning, sequencing and expression of wild-type and mutant receptor proteins. *EMBO J.* 5, 2513-2522.

Danielson, M., Hinck, L. and Ringold, G.M. (1989) Two amino acids within the knuckle of the first zinc finger specify response element activation by the glucocorticoid receptor. *Cell* 57, 1131-1138.

Darfler, F.J. and Insel, P.A. (1983) Clonal growth of lymphoid cells in serum-free media required elimination of H_2O_2 toxicity. *J. Cell. Physiol.* 115, 31-36.

Denis, M., Wikstrom, A-C. and Gustafsson, J-A. (1987) The molybdate-stabilized nonactivated glucocorticoid receptor contains a dimer of M_r 90,000 non-hormone-binding protein. *J. Biol. Chem.* 262, 11803-11809.

Denis, M., Wikstrom, A-C. and Gustafsson, J-A. (1988) Subunit composition of the molybdate-stabilized non-activated glucocorticoid receptor from rat liver. *J. Steroid Biochem.* 30, 271-276.

Denis, M. and Gustafsson, J-A. (1989a) The M_r 90.000 heat shock protein: an important modulator of ligand and DNA-binding properties of the glucocorticoid receptor. *Cancer Res.* 49, 2275s-2281s.

Denis, M. and Gustafsson, J-A. (1989b) Translation of glucocorticoid receptor MRNA *in vitro* yields a nonactivated protein. *J. Biol. Chem.* 264, 6005-6008.

DePasquale-Jardieu, P. and Fraker, P.J. (1979) The role of corticosterone in the loss in immune function in the zinc-deficient A/J mouse. *J. Nutr.* 109, 1847-1855.

Distelhorst, C.W. (1988) Glucocorticosteroids induce DNA fragmentation in human lymphoid leukemia cells. *Blood* 72, 1305-1309.

Domashenko, A.D., Nazarova, L.F. and Umansky, S.R. (1990) Comparison of the spectra of proteins synthesized in mouse thymocytes after irradiation or hydrocortisone treatment. *Int. J. Rad. Biol.* 57, 315-329.

Dong, Y., Cairns, W., Okret, S., and Gustafsson, J-A. (1990) A glucocorticoid-resistant rat hepatoma cell variant contains functional glucocorticoid receptor. *J. Biol. Chem.* 265, 7526-7531.

Dowd, D.R., MacDonald, P.N., Komm, B.S., Haussler, M.R. and Miesfeld, R. (1991) Evidence for early induction of calmodulin gene expression in lymphocytes undergoing glucocorticoid-mediated apoptosis. *J. Biol. Chem.* 266, 18423-18426.

Duke, R.C., Chervenak, R. and Cohen, J.J. (1983) Endogenous endonuclease-induced DNA fragmentation: an early event in cell-mediated cytolysis. *Proc. Natl. Acad. Sci. USA* 80, 6361-6365.

Durant, S. (1986) *In vivo* effects of catecholamines and glucocorticoid on mouse thymic cAMP content and thymolysis. *Cell. Immunol.* 102, 136-143.

Duvall, E., Wyllie, A.H. and Morris, R.G. (1985) Macrophage recognition of cells undergoing programmed cell death (apoptosis). *Immunology* 56, 351-358.

Eastman-Reks, S.B. and Vedeckis, W.V. (1986) Glucocorticoid inhibition of c-myc, c-myb and c-Ki-ras expression in a mouse lymphoma cell line. *Cancer Res.* 46, 2457-2462.

Epner, D.E. and Herschman, H.R. (1991) Heavy metals induce expression of the TPA-inducible sequence (TIS) genes. *J. Cell. Physiol.* 148, 68-74.

Etzel, K.R., Shapiro, S.G. and Cousins,R.J. (1979) Regulation of liver metallothionein and plasma zinc by the glucocorticoid dexamethasone. *Biochem. Biophys. Res. Comm.* 89, 1120-1126.

Fadok, V.A., Savill, J.S., Haslett, C., Bratton, D.L., Doherty, D.E., Campbell, P.A. and Henson, P.M. (1992) Different populations of macrophages use either the vitronectin receptor or the phosphatidylserine receptor to recognize and remove apoptotic cells. *J. Immunol.* 149, 4029-4035.

Falchuk, K.H., Hilt, K.L. and Vallee, B.L. (1988) Determination of zinc in biological samples by atomic absorption spectrometry. In *Methods in Enzymology* 158, J.F. Riordan and B.L. Vallee, eds., Academic Press, New York, pp. 422-434.

Fazakerly, G.V. (1984) Zinc Z-DNA. *Nucleic Acids Res.* 12, 3643-3648.

Fernandez-Ruiz, E., Rebollo, A., Nieto, M.A., Sanz, E., Somoza, C., Ramirez, F., Lopez-Rivas, A. and Silva, A. (1989) IL-2 protects T cell hybridomas from the cytolytic effect of glucocorticoids. *J. Immunol.* 143, 4146-4151.

Fesus, L., Thomazy, V. and Falus, A. (1987) Induction and activation of tissue transglutaminase during programmed cell death. *FEBS Lett.* 224, 104-108.

Flieger, D., Riethmuller, G. and Ziegler-Heitbrock, H.W.L. (1989) Zn^{++} inhibits both tumor necrosis factor-mediated DNA fragmentation and cytolysis. *Intl. J. Cancer* 44, 315-319.

Foekens, J.A., Portengen, H., van Driel, J., van Putten, W.L.J., Haije, W.G. and Klijn, J.G.M. (1988) Comparison of enzyme immunoassay and dextran-coated charcoal techniques for progesterone receptor determination in human breast cancer cytosols. *J. Steroid Biochem.* 29, 571-574.

Forbes, I.J., Zalewski, P.D., Hurst, N.P., Gainnakis, C. and Whitehouse, M.W. (1989) Zinc increases phorbol ester receptors in intact B-cells, neutrophil polymorphs and platelets. *FEBS Lett.* 247, 445-447.

Forbes, I.J., Zalewski, P.D., Giannakis, C., Petkoff, H.S. and Cowled, P.A. (1990) Interaction between protein kinase C and regulatory ligand is enhanced by a chelatable pool of cellular zinc. *Biochim. Biophy. Acta* 1053, 113-117.

Forbes, I.J., Zalewski, P.D. and Giannakis, C. (1991) Role for zinc in a cellular response mediated by protein kinase C in human B lymphocytes. *Exp. Cell. Res.* 195, 224-229.

Freedman, L.P., Luisi, B.F., Korszun, Z.R., Basavappa, R., Sigler, P.B. and Yamamoto, K.R. (1988) The function and structure of the metal coordination sites within the glucocorticoid receptor DNA binding domain. *Nature* (London) 334, 543-546.

Freedman, L.P. (1992) Anatomy of the steroid receptor zinc finger region. *Endocrine Rev.* 13, 129-145.

Gaido, M.L. and Cidlowski, J.A. (1991) Identification, purification and characterization of a calcium-dependent endonuclease (NUC18) from apoptotic rat thymocytes. NUC18 is not histone H2B. *J. Biol. Chem.* 266, 18580-18585.

Galili, U., Leizerowitz, R., Moreb, J., Gamliel, H., Gurfel, D. and Polliack, A. (1982) Metabolic and ultrastructural aspects of the in vitro lysis of chronic lymphocytic leukemia cells by glucocorticoids. *Cancer Res.* 42, 1433-1440.

Gametchu, B. and Harrison, R.W. (1984) Characterization of a monoclonal antibody to the rat liver glucocorticoid receptor. *Endocrinology* 114, 274-279.

Gametchu, B., Watson, C.S., Shih, C.C-Y. and Dashew, B. (1991) Studies on the arrangement of glucocorticoid receptors in the plasma membrane of S-49 lymphoma cells. *Steroids* 56, 411-419.

Garvy, B.A. and Fraker, P.J. (1991) Suppression of the antigenic response of murine bone marrow B cells by physiological concentrations of glucocorticoids. *Immunology* 74, 519-523.

Garvy, B.A., Telford, W.G., King, L.E. and Fraker, P.J. (1993) Glucocorticoids and irradiation induced apoptosis in normal murine bone marrow B-lineage lymphocytes as determined by flow cytometry. *Immunology* 79, 220-226.

Garvy, B.A., King, L.E., Telford, W.G., Morford, L.A. and Fraker, P.J. (1994) Chronic levels of corticosterone reduces the number of cycling cells of the B-lineage in murine bone marrow and induces apoptosis. *Immunology* (in press).

Gaskin, F.and Kress, Y. (1977) Zinc ion-induced assembly of tubulin. *J. Biol. Chem.* 252, 6918-6924.

Gasson, J.C. and Bourgeois, S. (1983) A new determinant of glucocorticoid sensitivity in lymphoid cell lines. *J. Cell Biol.* 96, 409-415.

Gehring, U. (1987) Wild-type and mutant glucocorticoid receptors of mouse lymphoma cells. In *Recent Advances in Steroid Hormone Action*, V.K. Moudgil, ed., Walter de Gruyter and Co., Berlin, Germany, pp. 427-442.

Giannakis, C., Forbes, I.J. and Zalewski, P.D. (1991) Ca^{2+}/Mg^{2+}-dependent nuclease: tissue distribution, relationship to inter-nucleosomal DNA fragmentation and inhibition by Zn^{2+}. *Biochem. Biophys. Res. Comm.* 181, 915-920.

Giguere, V., Hollenberg, S.M., Rosenfeld, M.G. and Evans, R.M. (1986) Functional domains of the human glucocorticoid receptor. *Cell* 46, 645-652.

Girotti, A.W., Thomas, J.P. and Jordan, J.E. (1985) Inhibitory effect of zinc(II) on free radical lipid peroxidation in erythrocyte membranes. *J. Free Radical Biol. Med.* 1, 395-401.

Goldstone, S.D. and Lavin, M.F. (1991) Isolation of a cDNA clone encoding a human β-galactoside binding protein overexpressed during glucocorticoid-induced cell death. *Biochem. Biophys. Res. Comm.* 178, 746-750.

Goldstone, S.D. and Lavin, M.F. (1993) Altered gene expression during apoptosis. In *Programmed Cell Death: The Cellular and Molecular Biology of Apoptosis.*, M. Lavin and D. Watters, eds., Harwood Academic Publishers, Switzerland, pp. 203-215.

Golstein, P., Ojcius, D.M. and Young, D-E. (1991) Cell death mechanisms and the immune system. *Immunol. Rev.* 121, 29-65.

Gomo, M., Moriwaki, K., Katagiri, S., Kurata, Y. and Thompson, E.B. (1990) Glucocorticoid effects on myeloma cells in culture: correlation of growth inhibition with induction of glucocorticoid receptor messenger RNA. *Cancer. Res.* 50, 1873-1878.

Govindan, M.V. (1980) Immunofluorescence microscopy of the intracellular translocation of glucocorticoid-receptor complexes in rat hepatoma (HTC) cells. *Exp. Cell Res.* 127, 293-297.

Govindan, M.V. (1987) The glucocorticoid receptor: purification, characterization and cloning of the cDNA. In *Recent Advances in Steroid Hormone Action*, V.K. Moudgil, ed., Walter de Gruyter and Co., Berlin, Germany, pp. 185-242.

Gradwohl, G., de Murcia, J.M., Molinete, M., Simonin, F. and de Murcia, G. (1989) Expression of functional zinc finger domain of human poly(ADP-ribose) polymerase in *E. coli*. *Nucleic Acids Res.* 17, 7112.

Grandics, P., Miller, A., Schmidt, T.J., Mittman, D. and Litwack, G. (1984a) Purification of the unactivated glucocorticoid receptor and its subsequent *in vitro* activation. *J. Biol. Chem.* 259, 3173-3180.

Grandics, P., Miller, A., Schmidt, T.J. and Litwack, G. (1984b) Phosphorylation *in vivo* of rat hepatic glucocorticoid receptor. *Biochem. Biophys. Res. Comm.* 120, 59-65.

Green, S. and CHambon, P. (1987) Oestradiol induction of a glucocorticoid-responsive gene by a chimaeric receptor. *Nature* (London) 325, 75-78.

Grippo, J.F., Tienrungroj, W., Dahmer, M.K., Housely, P.R. and Pratt, W.B. (1983) Evidence that the endogenous heat-stable glucocorticoid receptor-activating factor is thioredoxin. *J. Biol. Chem.* 258, 13658-13664.

Grummt, F., Weinmann-Dorsch, C., Schneider-Schaulies, J. and Lux, A. (1986) Zinc as a second messenger of mitogenic induction. Effects of diadenosine tetraphosphate (Ap_4A) and DNA synthesis. *Exp. Cell Res.* 163, 191-200.

Gruol, D.J., Campbell, N.F. and Bourgeois, S. (1986) Cyclic AMP-dependent protein kinase promotes glucocorticoid receptor function. *J. Biol. Chem.* 261, 4909-4914.

Gruol, D.J. and Bourgeois, S. (1987) Role of CAMP-dependent protein kinase in glucocorticoid receptor function. In *Recent Advances in Steroid Hormone Action*, Walter de Gruyter and Company, Berlin, pp. 315-335.

Gruol, D.J., Rajah, F.M. and Bourgeois, S. (1989a) Cyclic AMP-dependent protein kinase modulation of the glucocorticoid-induced cytolytic response in murine T-lymphoma cells. *Mol. Endocrinol.* 3, 2119-2127.

Gruol, D.J., Harrigan, M.T. and Bourgeois, S. (1989b) Modulation of glucocorticoid-induced responses by cyclic AMP in lymphoid cell lines. In *Gene Regulation by Steroid Hormones IV*, A.K. Roy and J.H. Clark, Eds., Springer-Verlag, New York, pp. 41-61.

Gruol, D.J., Wolfe, K.A. and Safarin, S. (1989c) Analysis of glucocorticoid receptor subspecies binding to DNA-cellulose and isolated nuclei. *J. Steroid Biochem.* 34, 319-323.

Gustafsson, J-A., Carlstedt-Duke, J., Wrange, O., Okret, S. and Wikstrom, A-C. (1986) Functional analysis of the purified glucocorticoid receptor. *J. Steroid Biochem.* 24, 63-68.

Gustafsson, J-A., Wikstrom, A-C. and Denis, M. (1989) The non-activated glucocorticoid receptor: structure and function. *J. Steroid Biochem.* 34, 53-62.

Gustafsson, J-A., Carlstedt-Duke, J., Stromstedt, P-E., Wikstrom, A-C., Denis, M., Okret, S. and Dong, Y. (1990) Structure, function and regulation of the glucocorticoid receptor. In *Molecular Endocrinolology and Steroid Hormone Action*, G.H. Sato and J.L. Stevens, eds., Alan R. Liss, Inc., New York, pp. 65-80.

Habermann, E. and Richardt, G. (1986) Intracellular calcium binding proteins as targets for heavy metal ions. *Trends in Pharm. Sci.* 7, 298-300.

Hammond, G.L. (1990) Molecular properties of corticosteroid binding globulin and the sex-steroid binding proteins. *Endocrine Rev.* 11, 65-79.

Hard, T., Kellenbach, E., Boelens, R., Maler, B.A., Dahlman, K., Freedman, L.P., Carlstedt-Duke, J., Yamamoto, K.R., Gustafsson, J-A. and Kaptein, R. (1991) Solution structure of the glucocorticoid receptor DNA-binding domain. *Science* (Wash., D.C.) 249, 157-160.

Harmon, J.M., Norman, M.R., Fowlkes, B.J. and Thompson, E.B. (1979) Dexamethasone induces irreversible G_1 arrest and death in a human lymphoid cell line. *J. Cell Physiol.* 98, 267-278.

Harrigan, M.T., Baughman, G., Campbell, N.F. and Bourgeois, S. (1989) Isolation and characterization of glucocorticoid- and cAMP-induced genes in T lymphocytes. *Mol. Cell. Biol.* 9, 3438-3446.

Harrison, R.W., Hendry, W.J., Turney, M., Kunkel, E., Thompson, E., Denton, R.A. and Gametchu, B. (1987) Immunochemical analysis of the glucocorticoid receptor. In *Recent Advances in Steroid Hormone Action*, V.K. Moudgil, ed., Walter de Gruyter, Berlin, pp. 467-475.

Hart, D.A. (1978) Effects of zinc chloride on hamster lymphoid cells: mitogenicity and differential enhancement of lipopolysaccharide stimulation of lymphocytes. *Infect. Immunol.* 19, 457-467.

Henninghausen, L. and Lubon, H. (1987) Interaction of protein with DNA *in vitro*. From *Methods in Enzymology*, Vol. 152, J.A. Abelson and M.I. Simon, eds., Academic Press, New York, pp. 721-735.

Hensketh, J.E. (1982) Zinc stimulated microtubule assembly and evidence of zinc binding to tubulin. *Intl. J. Biochem.* 14, 983-990.

Hensketh, J.E. (1984) Microtubule assembly in rat brain extracts. Further characterization of the effects of zinc on assembly and cold stability. *Int. J. Biochem.* 16, 1331-1339.

Hock, W., Martin, F., Jaggi, R. and Groner, B. (1989) Regulation of glucocorticoid receptor activity. *J. Steroid Biochem.* 34, 71-78.

Hockenbery, D., Nunez, G., Milliman, C., Schreiber, R.D. and Korsemeyer, S.J. (1990) Bcl-2 is an inner mitochrondrial membrane protein that blocks programmed cell death. *Nature* (London) 348, 334-336.

Hockenbery, D.M., Oltvai, Z.N., Yin, X-M., Milliman, C.L. and Korsemeyer, S.J. (1993) Bcl-2 functions in an antioxidant pathway to prevent apoptosis. *Cell* 75, 241-251.

Hoeck, W. and Groner, B. (1990) Hormone-dependent phosphorylation of the glucocorticoid receptor occurs mainly in the amino-terminal transactivation domain. *J. Biol. Chem.* 265, 5403-5408.

Hofert, J.F. and White, A. (1968) Effect of a single injection of cortisol on the incorporation of ^{3}H-thymidine and ^{3}H-deoxycytidine into lymphatic tissue DNA of adrenalectomized rats. *Endocrinology* 82, 767-776.

Holbrook, N.J., Bodwell, J.E., Jeffries, M. and Munck, A. (1982) Characterization of nonactivated and activated glucocorticoid-receptor complexes from intact rat thymus cells. *J. Biol. Chem.* 258, 6477-6485.

Hollenberg, S.M., Weinberger, C., Ong, E.S., Cerelli, G., Oro, A., Lebo, R., Thompson, E.B., Rosenfeld, M.G. and Evans, R.M. (1985) Primary structure and expression of a functional human glucocorticoid receptor cDNA. *Nature* (London) 318, 635-641.

Homo, F., Duval, D., Hatzfeld, J. and Evrard, C. (1980) Glucocorticoid sensitive and resistant cell populations in the mouse thymus. *J. Steroid Biochem.* 13, 135-143.

Housely, P.R., Dahmer, M.K. and Pratt, W.B. (1982) Inactivation of glucocorticoid-binding capacity by protein phosphatases in the presence of molybdate and complete reactivation by dithiothreitol. *J. Biol. Chem.* 257, 8615-8618.

Housely, P.R. and Pratt, W.B. (1983) Direct demonstration of glucocorticoid receptor phosphorylation by intact L-cells. *J. Biol. Chem.* 258, 4630-4635.

Housely, P.R., Grippo, J.F., Dahmer, M.K. and Pratt, W.B. (1984) Inactivation, activation and stabilization of glucocorticoid receptors. *Biochem. Actions Hormones* 11, 347-376.

Housely, P.R., Sanchez, E.R., Westphal, H.M., Beato, M. and Pratt, W.B. (1985) The molybdate-stabilized L-cell glucocorticoid receptor isolated by affinity chromatography or with a monoclonal antibody is associated with a 90-92-kDa nonsteroid-binding phosphoprotein. *J. Biol. Chem.* 260, 13810-13817.

Housely, P.R., Sanchez, E.R., Danielson, M., Ringold, G.M. and Pratt, W.B. (1990) Evidence that the conserved region in the steroid binding domain of the glucocorticoid receptor is required for both optimal binding of hsp90 and protection from proteolytic cleavage. *J. Biol. Chem.* 265, 12778-12781.

Howard, K.J. and Distelhorst, C.W. (1988) Evidence for intracellular association of the glucocorticoid receptor with the 90 kDa heat shock protein. *J. Biol. Chem.* 263, 3474-3481.

Hubbard, J. and Kalimi, M. (1983) Alteration of hepatic glucocorticoid receptor stability and nuclear binding *in vitro* by citrate. *Biochem. J.* 210, 259-263.

Hutchinson, K.A., Matic, G., Czar, M.J. and Pratt, W.B. (1992a) DNA-binding and non-DNA-binding forms of the transformed glucocorticoid receptor. *J. Steroid Biochem. Mol. Biol.* 41, 715-718.

Hutchinson, K.A., Czar, M.J. and Pratt, W.B. (1992b) Evidence that the hormone-binding domain of the mouse glucocorticoid receptor directly represses DNA binding activity in a major portion of receptors that are "misfolded" after removal of hsp90. *J. Biol. Chem.* 267, 3190-3195.

Hutchinson, K.A., Czar, M.J., Scherrer, L.C. and Pratt, W.B. (1992c) Monovalent cation selectivity for ATP-dependent association of the glucocorticoid receptor with hsp70 and hsp90. *J. Biol. Chem.* 267, 14047-14053.

Hutchinson, K.A., Dittmar, D.D., Czar, M.J. and Pratt, W.B. (1994) Proof that hsp70 is required for assembly of the glucocorticoid receptor into a heterocomplex with hsp90. *J. Biol. Chem.* 269, 5043-5049.

Idziorek, T., Formstecher, P., Danze, P-M., Sablonniere, N., Lustenberger, P., Richard, C., Dumur, V. and Dautrevaux, M. (1985) Characterization of the purified molybdate-stabilized glucocorticoid receptor from rat liver. *Eur. J. Biochem.* 153, 65-74.

Ip, M.M., Shea, W.K., Sykes, D. and Young, D.A. (1991) The truncated glucocorticoid receptor in the P1798 mouse lymphosarcoma is associated with resistance to glucocorticoid lysis but not to other glucocorticoid-associated functions. *Cancer Res.* 51, 2786-2796.

Iseki, R., Mukai, M. and Iwata, M. (1991) Regulation of T lymphocyte apoptosis. Signals for the antagonism between activation- and glucocorticoid-induced death. *J. Immunol.* 147, 4286-4292.

Ishida, R., Akiyoshi, H. and Takahashi, T. (1974) Isolation and purification of calcium and magnesium dependent endonuclease from rat liver nuclei. *Biochem. Biophys. Res. Comm.* 56, 703-710.

Iwata, M., Iseki, R. and Kudo, Y. (1993) Regulation of thymocyte apoptosis. Glucocorticoid-induced death and its inhibition by T-cell receptor/CD3 complex-mediated stimulation. In *Programmed Cell Death: The Cellular and Molecular Biology of Apoptosis.*, M. Lavin and D. Watters, eds., Harwood Academic Publishers, Switzerland, pp. 31-44.

Jackson, M.J. (1989) Physiology of zinc: general aspects. In *Zinc In Human Biology*, C.F. Mills, ed., Springer-Verlag, London, pp. 1-14.

Jin, P. and Ringhertz, N.R. (1990) Cadmium induces transcription of proto-oncogenes c-*jun* and c-*myc* in rat L6 myoblasts. *J. Biol. Chem.* 265, 14061-14064.

Ju, S-T. (1991) Distinct pathways of CD4 and CD8 cells induce rapid target DNA fragmentation. *J. Immunol.* 146, 812-818.

Kaiser, N. and Edelman, I.S. (1977) Calcium dependence of glucocorticoid-induced lymphocytolysis. *Proc. Natl. Acad. Sci. USA* 74, 638-642.

Kalimi, M., Colman, P. and Feigelson, P. (1975) The "activated" hepatic glucocorticoid-receptor complex. *J. Biol. Chem.* 250, 1080-1086.

Kalimi, M. and Love, K. (1980) Role of chemical reagents in the activation of rat hepatic glucocorticoid-receptor complex. *J. Biol. Chem.* 255, 4687-4690.

Karin, M., Haslinger, A., Holtgreve, H., Richards, R.I., Krauter, P., Westphal, H.M. and Beato, M. (1984) Characterization of DNA seqences through which cadmium and glucocorticoid hormones induce human metallothionein-II_A gene. *Nature* (London) 308, 513-519.

Kaufmann, S.H., Okret, S., Wikstrom, A-C., Gustaffson, J-A. and Shaper, J.H. (1986) Binding of the glucocorticoid receptor to the rat liver nuclear matrix. *J. Biol. Chem.* 261, 11962-11967.

Kerr, J.F.R., Wyllie, A.H. and Currie, A.R. (1972) Apoptosis: a basic biological phenomenon with wide-ranging implications in tissue kinetics. *Brit. J. Cancer* 26, 239-257.

Kerr, J.F.R. and Harmon, B.V. (1991) Definition and incidence of apoptosis: a historical perspective. In *Apoptosis: the molecular basis of cell death.* L. D. Tomei and F.O. Cope, eds., Cold Spring Harbor Laboratory Press, New York, pp. 5-30.

Kerr, J.F.R. (1993) Definition of apoptosis and overview of its significance. In *Programmed Cell Death: The Cellular and Molecular Biology of Apoptosis*, M. Lavin and D. Watters, Eds., Harwood Academic Publishers, Switzerland, pp. 123-132.

Kido, H., Fukusen, N. and Katunuma, N. (1987) Tumor-promoting phorbol ester amplifies the inductions of tyrosine aminotransferase and ornithine decarboxylase by glucocorticoid. *Mol. Endocrinol.* 3, 2119-2353.

Kirchner, H. and Ruhl, H. (1971) Stimulation of human peripheral lymphocytes by Zn^{2+} in vitro. *Exp. Cell Res.* 61, 229-232.

Kizaki, H., Shimada, H., Ohsaka, F. and Sakurada, J. (1988) Adenosine, deoxyadenosine and deoxyguanine induce DNA cleavage in mouse thymocytes. *J. Immunol.* 141, 1652-1657.

Kizaki, H., Tadakuma, T., Odaka, C., Muramatsu, J. and Ishimuru, Y. (1989) Activation of a suicide process of thymocytes through DNA fragmentation by calcium ionophores and phorbol esters. *J. Immunol.* 143, 1790-1794.

Kobusch, A-B. and Bock, K.W. (1990) Zinc increases EGF-stimulated DNA synthesis in primary mouse hepatocytes. *Biochem. Pharmacol.* 39, 555-558.

Kost, S.L., Smith, D.F., Sullivan, W.P., Welch, W.J. and Toft, D.O. (1989) Binding of heat shock proteins to the avian progesterone receptor. *Mol. Cell. Biol.* 9, 3829-3838.

Ku Tai, P-K., Albers, M.W., Chang, H., Faber, L.E. and Schrieber, S.L. (1992) Association of a 59-kilodalton immunophilin with the glucocorticoid receptor complex. *Science* (Wash., D.C.) 256, 1315-1318.

LaCasse, E.C. and Lefebvre, Y.A. (1991) Nuclear and nuclear envelope binding proteins of the glucocorticoid receptor nuclear localization peptide identified by crosslinking. *J. Steroid Biochem. Mol. Biol.* 40, 279-285.

LaFond, R.E., Kennedy, S.W., Harrison, R.W. and Villee, C.A. (1988) Immunocytochemical localization of glucocorticoid receptors in cells, cytoplasts and nucleoplasts. *Exp. Cell Res.* 175, 52-62.

Lazebnik, Y.A., Cole, S., Cooke, C.A., Nelson, W.G. and Earnshwa, W.C. (1993) Nuclear events of apoptosis *in vitro* in cell-free mitotic extracts: a model system for analysis of the active phase of apoptosis. *J. Cell Biol.* 123, 7-22.

Leach, K.L., Dahmer, M.K., Hammond, N.D., Sando, J.J. and Pratt, W.B. (1979) Molybdate inhibition of glucocorticoid receptor inactivation and transformation. *J. Biol. Chem.* 254, 11884-11890.

Leake, R.E. and Habib, F. (1987) Steroid hormone receptors: assay and characterization. In *Steroid Hormones: A practical approach*, Green, B. and Leake, R.E., eds., IRL Press, Washington, DC, pp.67-92.

Lebeau, M-C., Binart, N., Cadepond, F., Catelli, M-G., Chambraud, B., Massol, N., Radanyi, C., Redeuilh, C., Renoir, J-M., Sabbah, M., Schweizer-Groyer, G. and Baulieu, E-E. (1993) Steroid receptor associated proteins: heat shock protein 90 and p59 immunophilin. In Steroid Hormone Receptors: *Basic and Clinical Aspects*, V.K. Moudgil, ed., Birkhauser, Boston, pp. 261-280.

Lippman, M. and Barr, R. (1977) Glucocorticoid receptors in purified subpopulatons of human peripheral blood lymphocytes. *J. Immunol.* 118, 1977-1981.

Lohmann, R.D. and Beyersmann, D. (1993) Cadmium and zinc mediated changes of the Ca^{2+}-dependent endonuclease in apoptosis. *Biochem. Biophys. Res. Comm.* 190, 1097-1103.

Lyons, A.B., Samuel, K., Sanderson, A. and Maddy, A.H. (1992) Simultaneous analysis of immunophenotype and apoptosis of murine thymocytes by single laser flow cytometry. *Cytometry* 13, 809-821.

MacDonald, H.R. and Lees, R.K. (1990) Programmed death of autoreactive thymocytes. *Nature* (London) 343, 642-644.

MacDonald, R.G., Martin, T.P. and Cidlowski, J.A. (1980) Glucocorticoids stimulate protein degradation in lymphocytes: a possible mechanism of steroid-induced cell death. *Endocrinology* 107, 1512-1524.

MacDonald, R.G. and Cidlowski, J.A. (1982) Glucocorticoids inhibit precursor incorporation into protein in splenic lymphocytes by stimulating protein degradation and expanding intracellular amino acid pools. *Biochim. Biophys. Acta* 717, 236-247.

Madan, A.P. and DeFranco, D.B. (1993) Bidirectional transport of glucocorticoid receptors across the nuclear envelope. *Proc. Natl. Acad. Sci. USA* 90, 3588-3592.

Makman, M.H., Dvorkin, B. and White, A. (1968) Influence of cortisol on the utilization of nucleic acids and protein by lymphoid cells *in vitro*. *J. Biol. Chem.* 243, 1485-1497.

Martin, S.J. and Cotter, T.G. (1990) Disruption of microtubules induces an endogenous suicide pathway in human leukaemia HL-60 cells. *Cell Tissue. Kinet.* 23, 545-559.

Martin, S.J., Mazdai, G., Strain, J.J., Cotter, T.G. and Hannigan, B.M. (1991) Programmed cell death (apoptosis) in lymphoid and myeloid cell lines during zinc deficiency. *Clin. Exp. Immunol.* 83, 338-343.

Martin, S.J. and Cotter, T.G. (1994) Apoptosis in human leukemia: induction, morphology and molecular mechanisms. In *Apoptosis II: The Molecular Basis of Apoptosis in Disease*, L.D. Tomei and F.O. Cope, Eds., Cold Spring Harbor Laboratory Press, New York, pp. 185-229.

McConkey, D.J., Hartzell, P., Nicotera, P. and Orrenius, S. (1989a) Calcium-activated DNA fragmentation kills immature thymocytes. *Fed. Proc.* 3, 1843-1849.

McConkey, D.J., Nicotera, P., Hartzell, P., Bellomo, G., Wylie, A.H. and Orrenius, S. (1989b) Glucocorticoids activate a suicide process in thymocytes through an elevation of cytosolic Ca^{2+} concentration. *Arch. Biochem. Biophys.* 269, 365-370.

McConkey, D.J., Hartzell, P., Jondal, M. and Orrenius, S. (1989c) Inhibition of DNA fragmentation in thymocytes and isolated thymocyte nuclei by agents that stimulate protein kinase C. *J. Biol. Chem.* 264, 13399-13402.

McConkey, D.J., Hartzell, P., Chow, S.C., Orrenius, S. and Jondal, M. (1990a) Interleukin 1 inhibits T cell receptor-mediated apoptosis in mature thymocytes. *J. Biol. Chem.* 265, 3009-3011.

McConkey, D.J., Orrenius, S. and Jondal, M. (1990b) Agents that elevate cAMP stimulate DNA fragmentation in thymocytes. *J. Immunol.* 145, 1227-1230.

McConkey, D.J., Aguilar-Santelises, M., Hartzell, P., Eriksson, I., Mellstedt, H., Orrenius, S. and Jondal, M. (1991) Induction of DNA fragmentation in chromic B-lymphocytic leukemia cells. *J. Immunol.* 146, 1072-1076.

McConkey, D.J., Orrenius, S., Okret, S. and Jondal, M. (1993a) Cyclic AMP potentiates glucocorticoid-induced endogenous endonuclease activation in thymocytes. *Fed. Proc.* 7, 580-585.

McConkey, D.J., Orrenius, S. and Jondal, M. (1993b) Signal transduction in thymocyte apoptosis. In *Programmed Cell Death: The Cellular and Molecular Biology of Apoptosis.*, M. Lavin and D. Watters, eds., Harwood Academic Publishers, Switzerland, pp. 19-30.

McGhee, J.D. and Felsenfeld, G. (1980) Nucleosome structure. *Ann. Rev. Biochem.* 49, 1115-1156.

McGimsey, W.C., Cidlowsky, J.A., Stumpf, W.E. and Sar, M. (1991) Immunocytochemical localization of the glucocorticoid receptor in rat brain, pituitary, liver, and thymus with two new polyclonal antipeptide antibodies. *Endocrinology* 129, 3064-3072.

Mendel, D.B., Bodwell, J.E. and Munck, A. (1987) Activation of cytosolic glucocorticoid-receptor complexes in intact WEHI-7 cells does not phosphorylate the steroid-binding protein. *J. Biol. Chem.* 261, 3758-3763.

Mendel, D.B. and Orti, E. (1988) Isoform composition and stoichiometry of the 90-kDa heat shock protein associated with glucocorticoid receptors. *J. Biol. Chem.* 263, 6695-6702.

Mendel, D.B., Orti, E., Smith, L.I., Bodwell, J. and Munck, A. (1990) Evidence for a glucocorticoid receptor cycle and nuclear dephosphorylation of the steroid-binding protein. In *Molecular Endocrinology and Steroid Hormone Action*, G.H. Sato and J.L. Stevens, eds., Alan R. Liss, Inc., New York, pp. 97-117.

Meshinchi, S., Grippo, J.F., Sanchez, E.R., Bresnick, E.H. and Pratt, W.B. (1988) Evidence that the endogenous heat-stable glucocorticoid receptor stabilizing factor is a metal component of the untransformed receptor complex. *J. Biol. Chem.* 263, 16809-16817.

Meshinchi, S. and Pratt, W.B. (1989) Evidence that removal of an endogenous metal that stabilizes the untransformed glucocorticoid receptor in cytosol allows ligand-dependent receptor transformation. *J. Steroid Biochem.* 34, 315-317.

Miesfield, R., Rusconi, S., Godowski, P.J., Maler, B.A., Okret, S., Wikstrom, A-C., Gustaffson, J-A. and Yamamoto, K.R. (1986) Genetic complementation of a glucocorticoid receptor deficiency by expression of cloned receptor DNA. *Cell* 46, 389-399.

Miller-Diener, A., Schmidt, T.J. and Litwack, G. (1985) Protein kinase activity associated with the purified rat hepatic glucocorticoid receptor. *Proc. Natl. Acad. Sci. USA*, 82, 4003-4007.

Miller-Diener, A., Kirsch, T.M., Schmidt, T.J. and Litwack, G. (1987) Phosphorylation reactions associated with the glucocorticoid receptor. In *Steroid and Sterol Hormone Action*, T.C. Spelsberg and R. Kumar, eds., Martinus Nijhoff Publishing, Boston, pp. 149-174.

Mitani, K., Fujita, H., Sassa, S. and Kappas, A. (1990) Activation of heme oxygenase and heat shock protein 70 genes by stress in human hepatoma cells. *Biochem. Biophys. Res. Comm.* 166, 1429-1434.

Munck, A. and Brinck-Johnsen, T. (1968) Specific and non-specific physiochemical interactions of glucocorticoids and related steroids with rat thymus cells *in vitro*. *J. Biol. Chem.* 243, 5556-5565.

Munck, A. and Crabtree, G.R. (1981) Glucocorticoid-induced lymphocyte death. In *Cell Death in Biology and Pathology*, I.D. Bowen and R.A. Lockshin, Eds., Chapman and Hall, London, pp. 329-359.

Munck, A. and Holbrook, N.J. (1988) Cyclic, nonequilibrium models of glucocorticoid antagonism: role of activation, nuclear binding and receptor recycling. *J. Steroid Biochem.* 31, 599-606.

Munck, A. and Naray-Fejes-Toth, A. (1992) The ups and downs of glucocorticoid physiology: permissive and suppressive effects revisited. *Mol. Cell. Endocrinol.* 90, C1-C4.

Murakami, K., Whitely, M.K. and Routtenberg, A. (1987) Regulation of protein kinase C activity by cooperative interaction of Zn^{2+} and Ca^{2+}. *J. Biol. Chem.* 262, 13902-13906.

Murgia, M., Pizzo, P., Sandona, D., Zanovello, P., Rizzuto, R. and DiVirgilio, F. (1992) Mitochondrial DNA is not fragmented during apoptosis. *J. Biol. Chem.* 267, 10939-10941.

Murphy, K.M., Heimberger, A.B. and Loh, D.Y. (1990) Induction by antigen of intrathymic apoptosis of $CD4^+CD8^+$ TCR^{lo} thymocytes *in vivo*. *Science* (Wash., D.C.) 250, 1720-1722.

Nagle, W.A., Soloff, B.L., Moss, A.J. and Henle, K.J. (1990) Cultured chinese hamster cells undergo apoptosis after exposure to cold but nonfreezing temperatures. *Cryobiology* 27, 439-451.

Nakamuru, M., Sakaki, Y., Watanabe, N. and Takagi, Y. (1981) Purification and characterization of the Ca^{2+} plus Mg^{2+}-dependent endodeoxyribonuclease from calf thymus chromatin. *J. Biochem.* 89, 143-152.

Nazareth, L.V., Harbour, D.V. and Thompson, E.B. (1991) Mapping the human glucocorticoid receptor for leukemic cell death. *J. Biol. Chem.* 266, 12976-12980.

Nelipovich, P.A., Nikonova, L.V. and Umansky, S.R. (1988) Inhibition of poly(ADP-ribose) polymerase as a possible reason for activation of Ca^{2+}/Mg^{2+}-dependent endonuclease in thymocytes of irradiated rats. *Int. J. Rad. Biol.* 53, 749-765.

Nieto, M.A. and Lopez-Rivas, A. (1989) IL-2 protects T lymphocytes from glucocorticoid-induced DNA fragmentation and cell death. *J. Immunol.* 143, 4166-4170.

Ning, Y-M. and Sanchez, E. (1993) Potentiation of glucocorticoid receptor-mediated gene expression by the immunophilin ligands FK506 and rapamycin. *J. Biol. Chem.* 268, 6073-6076.

Norman, M.R. and Thompson, E.B. (1977) Characterization of a glucocorticoid-sensitive human lymphoid cell line. *Cancer Res.* 37, 3785-3791.

Norton, P.M. and Latchman, D.S. (1989) Levels of the 90kd heat shock protein and resistance to glucocorticoid-mediated cell killing in a range of human and murine lymphocyte cell lines. *J. Steroid Biochem.* 33, 149-154.

Ohara-Nemoto, Y., Stromstedt, P-E., Dahlman-Wright, K., Nemoto, Takayuki, Gustafsson, J-A., and Carlstedt-Duke, J. (1990) The steroid-binding properties of recombinant glucocorticoid receptor: a putative role for heat shock protein hsp90. *J. Steroid Biochem. Mol. Biol.* 37, 481-490.

Ojeda, F., Guarda, M.I., Maldonado, C. and Folch, H. (1990) Protein kinase-C involvement in thymocyte apoptosis induced by hydrocortisone. *Cell. Immunol.* 125, 535-539.

Okret, S., Dong, Y., Tanaka, H., Cairns, B. and Gustafsson, J-A. (1991) The mechanism for glucocorticoid-resistance in a rat hepatoma cell variant that contains functional glucocorticoid receptor. *J. Steroid Biochem. Mol. Biol.* 40, 353-361.

Onate, S.A., Estes, P.A., Welch, W.J., Nordeen, S.K. and Edwards, D.P. (1991) Evidence that heat shock protein-70 associated with progesterone receptors is not involved in receptor-DNA binding. *Mol. Endocrinol.* 5, 1993-2004.

Orti, E., Mendel, D.B., Smith, L.I., Bodwell, J.E. and Munck, A. (1989) A dynamic model of glucocorticoid receptor phosphorylation and cycling in intact cells. *J. Steroid Biochem.* 34, 85-96.

Orti, E., Bodwell, J.E. and Munck, A. (1992) Phosphorylation of steroid receptors. *Endocrine Rev.* 13, 105-127.

Orti, E., Hu, L-M. and Munck, A. (1993) Kinetics of glucocorticoid receptor phosphorylation in intact cells. *J. Biol. Chem.* 263, 7779-7784.

Owens, G.P., Hahn, W.E. and Cohen, J.J. (1991) Identification of mRNAs associated with programmed cell death in immature lymphocytes. *Mol. Cell. Biol.* 11, 4177-4188.

Pan, T., Freeman, L.P. and Coleman, J.E. (1990) Cadmium-113 NMR studies of the DNA binding domain of the mammalian glucocorticoid receptor. *Biochemistry* 29, 9218-9225.

Parker, P.J., Coussens, L., Totty, N., Rhee, L., Young, S., Chen, E., Stabel, S., Waterfield, M.D. and Ullrich, A. (1986) The complete primary structure of protein kinase C, the major phorbol ester receptor. *Science* (Wash., D.C.) 233, 853-859.

Perdew, G.H. and Whitelaw, M.I. (1991) Evidence that the 90-kDa heat shock protein (hsp90) exists in cytosol in heteromeric complexes containing hsp70 and three other proteins with M_r of 63,000, 56,000 and 50,000. *J. Biol. Chem.* 266, 6708-6713.

Picard, D. and Yamamoto, K.R. (1987) Two signals mediate hormone-dependent nuclear localization of the glucocorticoid receptor. *EMBO J.* 6, 3333-3340.

Picard, D., Salser, S.J. and Yamamoto, K.R. (1988) A movable and regulable inactivation function within the steroid binding domain of the glucocorticoid receptor. *Cell* 54, 1073-1080.

Picard, D., Kumar, V., Chambon, P. and Yamamoto, K.R. (1990a) Signal transduction by steroid hormones: nuclear localization is differentially regulated in estrogen and glucocorticoid receptors. *Cell Regulation* 1, 291-299.

Picard, D., Khursheed, B., Garabedian, M.J., Fortin, M.G., Lindquist, S. and Yamamoto, K.R. (1990b) Reduced levels of hsp90 compromise steroid receptor action *in vivo*. *Science* (Wash., D.C.) 348, 166-168.

Pocino, M., Malave, I. and Baute, L. (1992) Mitogenic effect of zinc on lymphocytes from strains of mice that are either high or low-responder to T-cell mitogens. *Immunopharmacol. Immunotoxicol.* 14, 295-321.

Pratt, W.B. (1987) Transformation of glucocorticoid and progesterone receptors to the DNA-binding state. *J. Cell. Biochem.* 35, 51-68.

Pratt, W.B., Jolly, D.J., Pratt, D.V., Hollenberg, S.M., Giguere, V., Cadepond, F.M., Schweizer-Groyer, G., Catelli, M.G., Evans, R.M. and Baulieu, E-E. (1988) A region of the steroid binding domain determines formation of the non-DNA-binding, 9S glucocorticoid receptor complex. *J. Biol. Chem.* 263, 267-273.

Pratt, W.B., Sanchez, E., Bresnick, E.H., Meshinchi, S., Scherrer, L.C., Dalman, F.C. and Welsh, M.J. (1989) Interaction of the glucocorticoid receptor with the M_r 90,000 heat shock protein: an evolving model of ligand-mediated receptor transformation and translocation. *Cancer Res.* 49, 2222s-2229s.

Pratt, W.B. (1990) Interaction of hsp90 with steroid receptors: organizing some diverse observations and presenting the newest concepts. *Mol. Cell Endocrinol.* 74, C69-C76.

Pratt, W.B. (1992) Control of steroid receptor function and cytoplasmic-nuclear transport by heat shock proteins. *BioEssays* 14, 841-848.

Pratt, W.B., Scherrer, L.C., Hutchinson, K.A. and Dalman, F.C. (1992) A model of glucocorticoid receptor unfolding and stabilization by a heat shock protein. *J. Steroid Biochem. Mol. Biol.* 41, 223-229.

Pratt, W.B. (1993) Role of heat shock proteins in steroid receptor function. In *Steroid Hormone Action: Frontiers in Molecular Biology*, M.G. Parker, Ed., Oxford University Press, London, pp. 188-145.

Pratt, W.B. and Scherrer, L.C. (1993) Heat shock proteins and the cytoplasmic-nuclear trafficking of steroid receptors. In *Steroid Hormone Receptors: Basic and Clinical Aspects*, W.K. Moudgil, ed., Birkhauser, Boston, pp. 215-260.

Raaka, B.M., Finnerty, M., Sun, E. and Samuels, H.H. (1985) Effects of molybdate on steroid receptors in intact GH_1 cells. *J. Biol. Chem.* 260, 14009-14015.

Ranelletti, F.O., Piantelli, M., Iacobelli, S., Musiani, P., Longo, P., Lauriola, L. and Marchetti, P. (1981) Glucocorticoid receptors and *in vitro* corticosensitivity of peanut-positive and peanut-negative human thymocyte subpopulations. *J. Immunol.* 127, 849-855.

Reardon, C.L. and Lucas, D.O. (1981) Zinc and mercury activate different mouse T cells and macrophage function is required. *Fed. Proc.* 40, 1130 (abstract).

Reardon, C.L. and Lucas, D.O. (1987) Heavy-metal mitogenesis: thymocyte activation by Zn^{2+} requires 2-mercaptoethanol and lipopolysaccharide as cofactors. *Immunobiol.* 174, 233-243.

Renoir, J-M., Buchou, T., Mester, J., Radanyi, C. and Baulieu, E-E. (1984) Oligomeric structure of molybdate-stabilized, nontransformed 8S progesterone receptor from chicken oviduct cytosol. *Biochemistry* 23, 6016-6023.

Renoir, J-M., Radanyi, C., Faber, L.E. and Baulieu, E-E. (1990) The non-DNA-binding heterooligomeric form of mammalian steroid hormone receptors contains a hsp90-bound 59-kilodalton protein. *J. Biol. Chem.* 265, 10740-10745.

Rexin, M., Busch, W. and Gehring, U. (1991a) Protein components of the nonactivated glucocorticoid receptor. *J. Biol. Chem.*, 266, 24601-24605.

Rexin, M., Busch, W., Segnitz, B. and Gehring, U. (1991b) Subunit structure of the glucocorticoid receptor and activation to the DNA-binding state. *J. Steroid Biochem. Mol. Biol.* 40, 287-299.

Rexin, M., Busch, W., Segnitz, B. and Gehring, U. (1992) Structure of the glucocorticoid receptor in intact cells in the absence of hormone. *J. Biol. Chem.* 267, 9619-9621.

Richards, R.I., Heguy, A. and Karin, M. (1984) Structure and functional analysis of the human metallothionein-I_A gene: differential induction by metal ions and glucocorticoids. *Cell* 37, 263-272.

Riehl, R.M., Sullivan, W.P., Vroman, B.T., Bauer, V.J., Pearson, G.R. and Toft, D.O. (1985) Immunological evidence that the nonhormone binding component of avian steroid receptors exists in a wide range of tissues and species. *Biochemistry* 24, 6586-6591.

Rosner, W. (1990) The functions of corticosteroid-binding globulin and sex hormone-binding globulin: recent advances. *Endocrine Rev.* 11, 80-91.

Rothenberg, E.V. (1990) Death and transfiguration of cortical thymocytes: a reconsideration. *Immunol. Today* 11, 116-119.

Ruhl, H. and Kirschner, H. (1978) Monocyte-dependent stimulation of human T cells by zinc. *Clin. Exp. Immunol.* 32, 484-498.

Russell, J.H., White, C.L., Loh, D.Y. and Meleedy-Rey, P. (1991) Receptor-stimulated death pathway is opened by antigen in mature T cells. *Proc. Natl. Acad. Sci. USA* 88, 2151-2155.

Sabbele, N.R., Van Oudenaren, A., Hooijkaas, H. and Benner, R. (1987) The effect of corticosteroids upon murine B cells *in vivo* and *in vitro* as determined in the LPS-culture system. *Immunology* 62, 285-290.

Sanchez, E.R., Toft, D.O., Schlesinger, M.J. and Pratt, W.B. (1985) Evidence that the 90-kDa phosphoprotein associated with the untransformed L-cell glucocorticoid receptor is a murine heat shock protein. *J. Biol. Chem.* 260, 12398-12401.

Sanchez, E.R., Housely, P.R. and Pratt, W.B. (1986) The molybdate-stabilized glucocorticoid binding complex of L-cells contains a 98-100 kDa steroid binding phosphoprotein and a 90 kDa non-steroid-binding phosphoprotein that is part of the murine heat-shock complex. *J. Steroid Biochem.* 24, 9-18.

Sanchez, E.R., Meshinchi, S., Schlesinger, M.J. and Pratt, W.B. (1987a) Demonstration that the 90-kilodalton heat shock protein is bound to the glucocorticoid receptor in its 9S nondeoxyribonucleic acid binding form. *Mol. Endocrinol.* 1, 908-912.

Sanchez, E.R., Meshinchi, S., Tienrungroj, W., Schlesinger, M.J., Toft, D.O. and Pratt, W.B. (1987b) Relationship of the 90-kDa murine heat shock protein to the untransformed and transformed states of the L cell glucocorticoid receptor. *J. Biol. Chem.* 262, 6986-6991.

Sanchez, E.R., Hirst, M., Scherrer, L.C., Tang, H-Y., Welsh, M.J., Harmon, J.M., Simons, S.S., Ringold, G.M. and Pratt, W.B. (1990a) Hormone-free mouse glucocorticoid receptors overexpressed in chinese hamster ovary cells are localized to the nucleus and are associated with both hsp70 and hsp90. *J. Biol. Chem.* 265, 20123-20130.

Sanchez, E.R., Faber, L.E., Henzel, W.J. and Pratt, W.B. (1990b) The 56-59 kilodalton protein identified in untransformed steroid receptor complexes is a unique protein that exists in cytosol in a complex with both the 70- and 90-kilodalton heat shock proteins. *Biochemistry* 29, 5145-5152.

Sanchez, E.R. (1992) Heat shock induces translocation to the nucleus of the unliganded glucocorticoid receptor. *J. Biol. Chem.* 267, 17-20.

Scatchard, G. (1949) The attractions of proteins for small molecules and ions. *Ann. N.Y. Acad. Sci.* 51, 660-672.

Schena, M. and Yamamoto, K.R. (1988) Mammalian glucocorticoid receptor derivatives enhance transcription in yeast. *Science* (Wash., D.C.) 241, 965-967.

Schena, M., Freedman, L.P. and Yamamoto, K.R. (1989) Mutations in the glucocorticoid receptor zinc finger region that distinguish interdigitated DNA binding and transcriptional enhancement activities. *Genes Dev.* 3, 1590-1601.

Scherrer, L.C., Dalman, F.C., Massa, E., Meshinchi, S. and Pratt, W.B. (1990) Structural and functional reconstitution of the glucocorticoid receptor-hsp90 complex. *J. Biol. Chem.* 265, 21397-21400.

Scherrer, L.C. and Pratt, W.B. (1992) Association of the transformed glucocorticoid receptor with a cytoskeletal protein complex. *J. Steroid Biochem. Mol. Biol.* 41, 719-721.

Schmid, W., Strahle, U., Schutz, G., Schmitt, J. and Stunnenberg, H. (1989) Glucocorticoid receptor binds cooperatively to adjacent recognition sites. *EMBO J.* 8, 2257-2263.

Schmidt, T.J., Miller-Diener, A., Webb, M.L. and Litwack, G. (1985) Thermal activation of the purified rat hepatic glucocorticoid receptor. *J. Biol. Chem.* 260, 16255-16262.

Schwartz, J.A., Mizukami, H. and Skafar, D.F. (1993) A metal-linked gapped zipper model is proposed for the hsp90-glucocorticoid receptor interaction. *FEBS* 315, 109-113.

Schwartzman, R.A. and Cidlowski, J.A. (1991) Internucleosomal deoxyribonucleic acid cleavage activity in apoptotic thymocytes: detection and endocrine regulation. *Endocrinology* 128, 1190-1197.

Schwartzman, R.A. and Cidlowski, J.A. (1993) Apoptosis: the biochemistry and molecular biology of programmed cell death. *Endocrine Rev.* 14, 133-151.

Segard-Maurel, I., Jibard, N., Schweizer-Groyer, G., Cadepond, F. and Baulieu, E-E. (1992) Mutations in the "zinc fingers" or in the n-terminal region of the DNA binding domain of the human glucocorticoid receptor facilitate its salt-induced transformation, but do not modify hormone binding. *J. Steroid Biochem. Mol. Biol.* 41, 727-732.

Sellins, K.S. and Cohen, J.J. (1987) Gene induction by gamma-irradiation leads to DNA fragmentation in lymphocytes. *J. Immunol.* 139, 3199-3206.

Sen, D. and Crothers, D.M. (1986) Condensation of chromatin: role of multivalent cations. *Biochemistry* 25, 1495-1503.

Sentman, C.L., Shutter, J.R., Hockenbery, D., Kanagwawa, O. and Korsemeyer, S.J. (1991) Bcl-2 inhibits multiple forms of apoptosis but not negative selection in thymocytes. *Cell* 67, 879-888.

Shimuzu, T., Kubota, M., Tanezawa, A., Sano, H., Kasai, Y., Hashimoto, H., Akiyama, Y. and Mikawa, H. (1990) Inhibition of both etoposide-induced DNA fragmentation and activation of poly(ADP)-ribose synthesis by zinc ion. *Biochem. Biophys. Res. Comm.* 169, 1172-1177.

Silva, C.M. and Cidlowski, J.A. (1992) The effect of oxidation/reduction on the charge heterogeneity of the human glucocorticoid receptor. *J. Steroid Biochem. Mol. Biol.* 41, 1-10.

Simons, S.S., and Thompson, E.B. (1981) Dexamethasone 21-mesylate: an affinity label of glucocorticoid receptors from rat hepatoma tissue culture cells. *Proc. Natl. Acad. Sci. USA* 78, 3541-3545.

Simons, S.S., Pumphrey, J.G., Rudikoff, S. and Eisen, H.J. (1987) Identification of cysteine 656 as the amino acid of hepatoma tissue culture cell glucocorticoid receptors that is covalently labeled by dexamethasone 21-mesylate. *J. Biol. Chem.* 262, 9676-9680.

Simons, S.S., Chakraborti, P.K. and Cavanaugh, A.H. (1990) Arsenite and Cadmium (II) as probes of glucocorticoid receptor structure and function. *J. Biol. Chem.* 265, 1938-1945.

Sloman, J.C. and Bell, P.A. (1976) The dependence of specific nuclear binding of glucocorticoids by rat thymus cells on cellular ATP levels. *Biochim. Biophys. Acta* 428, 403-413.

Smets, L., Metwally, E.A.G., Knol, E. and Martens, M. (1988) Potentiation of glucocorticoid-induced lysis in refractory and resistant leukemia cells by inhibitors of ADP-ribosylation. *Leukemia Res.* 12, 737-743.

Smets, L.A., Loesberg, C., Janssen, M. and Van Rooij, H. (1990) Intracellular inhibition of mono(ADP-ribosylation) by *meta*-iodobenzylguanidine: specificity, intracellular concentration and effects on glucocorticoid-mediated cell lysis. *Biochim. Biophys. Acta* 1054, 49-55.

Smith, D.F. and Toft, D.O. (1992a) Composition, assembly and activation of the avian progesterone receptor. *J. Steroid Biochem. Mol. Biol.* 41, 201-207.

Smith, D.F., Stensgard, B.A., Welch, W.J. and Toft, D.O. (1992b) Assembly of progesterone receptor with heat shock proteins and receptor activation are ATP mediated events. *J. Biol. Chem.* 267, 1350-1356.

Smith, L.I., Bodwell, J.E., Mendel, D.B., Ciardelli, T., North, W.G. and Munck, A. (1988) Identification of cysteine-644 as the covalent site of attachment of dexamethasone 21-mesylate to murine glucocorticoid receptors in WEHI-7 cells. *Biochemistry* 27, 3747-3753.

Smith, L.I., Mendel, D.B., Bodwell, J.E. and Munck, A. (1989) Phosphorylated sites within the functional domains of the 100-kDa steroid binding subunit of glucocorticoid receptors. *Biochemistry* 28, 4490-4498.

Stratling, W.H., Grade, C. and Horz, W. (1984) Ca/Mg-dependent endonuclease from porcine liver. Purification, properties and sequence specificity. *J. Biol. Chem.* 259, 5893-5898.

Sullivan, W.P., Vroman, B.T., Bauer, V.J., Puri, R.K., Riehl, R.M., Pearson, G.R. and Toft, D.O. (1985) Isolation of steroid receptor binding protein from chicken oviduct and production of monoclonal antibodies. *Biochemistry* 24, 4214-4222.

Sun, X-M., Dinsdale, D., Snowden, R.T., Cohen, G.M. and Skilleter, D.N. (1992) Characterization of apoptosis in thymocytes isolated from dexamethasone-treated rats. *Biochem. Pharmacol.* 44, 2131-2137.

Surks, M.I., Ramirez, I.J., Shapiro, L.E. and Kumare-Siri, M. (1989) Effect of zinc(II) and other divalent cations on binding of 3,5,3'-triiodo-L-thyronine to nuclear receptors from cultured GC cells. *J. Biol Chem.* 264, 9820-9826.

Swat, W., Ignatowicz, L. and Kisielow, P. (1991) Detection of apoptosis of immature $CD4^+CD8^+$ thymocytes by flow cytometry. *J. Immunol. Methods* 137, 79-87.

Tadakuma, T., Kizaki, H., Odaka, C., Kubota, R., Ishimura, Y., Yagita, H. and Okumura, K. (1990) $CD4^+CD8^+$ thymocytes are susceptible to DNA fragmentation induced by phorbol ester, calcium ionophore and anti-CD3 antibody. *Eur. J. Immunol.* 20, 779-784.

Takano, Y.S., Harmon, B.V. and Kerr, J.F.R. (1991) Apoptosis induced by mild hyperthermia in human and murine tumour cell lines: a study using electron microscopy and DNA gel electrophoresis. *J. Path.* 163, 329-336.

Tashima, Y., Terui, M., Itoh, H., Mizunuma, H., Kobayashi, R. and Marumo, F. (1989) Effect of selenite on glucocorticoid receptor. *J. Biochem.* 105, 358-361.

Telford, W.G., King, L.E. and Fraker, P.J. (1991) Evaluation of glucocorticoid-induced apoptosis in mouse thymocytes by flow cytometry. *Cell Prolif.* 24, 447-459.

Telford, W.G., King, L.E. and Fraker, P.J. (1992a) Comparative evaluation of several DNA binding dyes in the detection of apoptosis-associated chromatin degradation by flow cytometry. *Cytometry* 13, 137-143.

Telford, W.G., King, L.E. and Fraker, P.J. (1992b) Flow cytometric analysis of apoptosis: a review. *Appl. Fluorescence Technol.* 4, 12-17.

Telford, W.G. and Fraker, P.J. (1994a) Preferential induction of apoptosis in mouse $CD4^+CD8^+\alpha\beta TCR^{lo}CD3\epsilon^{lo}$ thymocytes by zinc. *J. Cell. Physiol.* (in press).

Telford, W.G., King. L.E. and Fraker, P.J. (1994b) Rapid quantitation of apoptosis in pure and heterogeneous cell populations using flow cytometry. *J. Immunol. Methods* (in press).

Tenniswood, M., Taillefer, D., Lakins, J., Guenett, R., Mooibroek, M., Daehlin, L. and Welsh, J. (1994) Control of gene expression during apoptosis in hormone-dependent tissues. In *Apoptosis II: The Molecular Basis of Apoptosis in Disease*, L.D. Tomei and F.O. Cope, Eds., Cold Spring Harbor Laboratory Press, New York, pp. 283-311.

Thomas, D.J. and Caffrey, T.C. (1991) Lipopolysacharide induced double-stranded DNA fragmentation in mouse thymus: protective effect of zinc pretreatment. *Toxicology* 68, 327-337.

Thompson, E.A. (1991) Glucocorticoid insensitivity of P1798 lymphoma cells is associated with production of a factor that attenuates the lytic response. *Cancer Res.* 51, 5551-5556.

Thompson, E.B., Yuh, Y-S., Ashraf, J., Gametchu, B., Johnson, B. and Harmon, J.M. (1988) Mechanisms of glucocorticoid function in human leukemic cells: analysis of receptor gene mutants of the activation-labile type using the covalent affinity ligand dexamethasone mesylate. *J. Steroid Biochem.* 30, 63-70.

Thompson, E.B. (1989) Glucocorticoid inhibition of gene expression and proliferation of murine lymphoid cells *in vitro*. *Cancer Res.* 49, 2259s-2265s.

Thompson, E.B., Nazareth, L.V., Thulasi, R., Ashraf, J., Harbour, D. and Johnson, B.H. (1992) Glucocorticoids in malignant lymphoid cells: gene regulation and the minimum receptor fragment for lysis. *J. Steroid Biochem. Mol. Biol.* 41, 273-282.

Tienrungroj, W., Sanchez, E.R., Housely, P.R., Harrison, R.W. and Pratt, W.B. (1987a) Glucocorticoid receptor phosphorylation, transformation, and DNA binding. *J. Biol. Chem.* 262, 17342-17349.

Vallee, B.L., Coleman, J.E. and Auld, D.S. (1991) Zinc fingers, zinc clusters and zinc twists in DNA-binding protein domains. *Proc. Natl. Acad. Sci. USA* 88, 999-1003.

Van, N.T., Rabek, M., Barrows, G.H. and Barlogie, B. (1984) Estrogen receptor analysis by flow cytometry. *Science* (Wash., D.C.) 224, 876-877.

Van den Bogert, C., Bakker, H.M., Kuzela, S., Melis, T.E. and Kroon, A.M. (1989) Changes in nuclear protein pattern by glucocorticoid treatment of lymphoid cells. *J. Steroid Biochem. Mol. Biol.* 33, 955-963.

Varshavsky, A. (1987) Electrophoretic assay for DNA-binding proteins. In *Methods in Enzymology*, Vol. 151, Gottesman, M.M., ed., Academic Press, New York, p. 551-565.

Vasquez, N.J., Kaye, J. and Hedrick, S.M. (1992) *In vivo* and *in vitro* clonal deletion of double-positive thymocytes. *J. Exp. Med.* 175, 1307-1316.

Vedeckis, W.V. and Bradshaw, H.D. (1983) DNA fragmentation in S49 lymphoma cells killed with glucocorticoids and other agents. *Mol. Cell Endocrinol.* 30, 215-227.

Vedeckis, W.V., Eastman-Reks, S.B., Lapointe, M.C. and Reker, C.E. (1987) Glucocorticoid regulation of protooncogene expression and cellular proliferation. In *Steroid and Sterol Hormone Action*, T.C. Spelsberg and R. Kumar, Eds., Martinus Nijhoff Publishing, Boston, pp. 213-226.

Vedeckis, W.V. (1992) Nuclear receptors, transcriptional regulation, and oncogenesis. *Endocrine Rev.* 13, 1-12.

Voris, B.P. and Young, D.A. (1981) Glucocorticoid-induced proteins in rat thymus cells. *J. Biol. Chem.* 256, 11319-11329.

Walker, P.R., Smith, C., Youdale, T., Leblanc, J., Whitfield, J.F. and Sikorska, M. (1991) Topoisomerase II-reactive chemotherapeutic drugs induce apoptosis in thymocytes. *Cancer Res.* 51, 1078-1085.

Walker, P.R., Kwast-Welfeld, J., Gourdeau, H., Leblanc, J., Neugebaur, W. and Sikorska, M. (1993a) Relationship between apoptosis and the cell cycle in lymphocytes: roles of protein kinase C, tyrosine phosphorylation and AP-1. *Exp. Cell Res.* 207, 142-151.

Walker, P.R., Kwast-Welfeld, J. and Sikorska, M. (1993b) Relationship between apoptosis and the cell cycle. In *Programmed Cell Death: The Cellular and Molecular Biology of Apoptosis*, M. Lavin and D. Watters., Eds., Harwood Academic Publishers, Switzerland, pp. 59-72.

Waring, P., Eichner, R.D., Mullbacher, A. and Sjaard, A.J. (1989) Gliotoxin induces apoptosis in macrophages unrelated to its anti-phagocytic properties. *J. Biol. Chem.* 263, 18493-18499.

Waring, P., Egan, M., Braithwaite, A., Mullbacher and Siaarda, A. (1990) Apoptosis induced in macrophages and T blasts by the mycotoxin sporodesmin and protection by Zn^{2+} salts. *Intl. J. Pharmacol.* 12, 445-457.

Warner, G.L. and Lawrence, D.A. (1986) Cell surface and cell cycle analysis of metal-induced murine T cell proliferation. *Eur. J. Immunol.* 16, 1337-1342.

Weatherill, P.J. and Bell, P.A. (1987) Identification of two forms of molybdate-stabilized, non-transformed glucocorticoid hormone-receptor complex by gel filtration chromatography. *J. Steroid Biochem.* 26, 463-466.

Weissman, I.L. (1973) Thymus cell maturation: studies on the origin of cortisone-resistant thymic lymphocytes. *J. Exp. Med.* 137, 504-510.

Westin, G. and Schaffner, W. (1988) Biochemistry of metallothionein. *Biochemistry* 27, 8509-8515.

Westphal, U., Burton, R.M. and Harding, G.B. (1975) Characterization of steroid-binding glycoproteins: methodological comments. In *Methods in Enzymology* vol. 36, O'Malley, B.W. and Hardman, J.G., eds., pp. 91-104.

Wielchens, K. and Delfs, T. (1986) Glucocorticoid-induced cell death and poly[adenosine diphosphate(ADP)-ribosylation: increased toxicity of dexamethasone on mouse S49.1 lymphoma cells with the poly(ADP-ribosyl)ation inhibitor benzamide. *Endocrinology* 119, 2383-2392.

Willmam, T. and Beato, M. (1986) Steroid-free glucocorticoid receptor binds specifically to mouse mammary tumour virus DNA. *Nature* (London) 324, 688-691.

Wrange, O. and Gustaffson, J-A. (1978) Separation of the hormone- and DNA binding sites of the hepatic glucocorticoid receptor by means of proteolysis. *J. Biol. Chem.* 253, 856-865.

Wrange, O., Carlstedt-Duke, J. and Gustafsson, J-A. (1986) Stoichiometric analysis of the specific interaction of the glucocorticoid receptor with DNA. *J. Biol. Chem.* 261, 11770-11778.

Wright, A.P.H. and Gustafsson, J-A. (1991) Mechanism of synergistic transcriptional transactivation by the human glucocorticoid receptor. *Proc. Natl. Acad. Sci. USA* 88, 8283-8287.

Wyllie, A.H. (1980a) Glucocorticoid-induced thymocyte apoptosis is associated with endogenous endonuclease activation. *Nature* (London) 284 555-556.

Wyllie, A.H., Kerr, J.F.R. and Currie, A.R. (1980b) Cell death: the significance of apoptosis. In *International Review of Cytology*, G.H. Bourne and J.F. Danielli, eds., Academic Press, New York, pp. 251-306.

Wyllie, A.H., Beattie, G.J. and Hargreaves, A.D. (1980c) Chromatin changes in apoptosis. *Histochem. J.* 13, 681-692.

Wyllie, A.H. and Morris, R.G. (1982) Hormone-induced cell death. Purification and properties of thymocytes undergoing apoptosis after glucocorticoid treatment. Am. J. Path. 109, 78-87.

Wyllie, A.H., Morris, R.G., Smith, A.L. and Dunlop, D. (1984) Chromatin cleavage in apoptosis: association with condensed chromatin morphology and dependence on macromolecular synthesis. *J. Path.* 142, 67-77.

Yamamoto, K.R., Stampfer, M.R. and Tomkins, G.M. (1974) Receptors from glucocorticoid-sensitive lymphoma cells and two classes of insensitive clones: physical and DNA binding properties. *Proc. Natl. Acad. Sci. USA* 21, 3901-3905.

Yuh, Y-S. and Thompson, E.B. (1989) Glucocorticoid effect on oncogene/growth gene expression in human T lymphoblastic leukemia cell line CCRF-CEM. *J. Biol. Chem.* 264, 10904-10910.

Zacharchuk, C.M., Mercep, M., Chakraborti, P.K., Simons, S.S. and Ashwell, J.D. (1990) Programmed T lymphocyte death. Cell activation- and steroid-induced pathways are mutually antagonistic. *J. Immunol.* 145, 4037-4045.

Zalewski, P.D., Forbes, I.J., Giannakis, C., Cowled, P.A. and Betts, W.H. (1990a) Synergy between zinc and phorbol ester in translocation of protein kinase C to cytoskeleton. *FEBS Lett.* 273, 131-134.

Zalewski, P.D., Forbes, I.J. and Giannakis, C. (1990b) Physiological role for zinc in prevention of apoptosis (gene-directed death). *Biochem. Intl.* 24, 1093-1101.

Zalewski, P.D., Forbes, I.J., Giannakis, C. and Betts, W.H. (1991) Regulation of protein kinase C by Zn^{2+}-dependent interaction with actin. *Biochem. Intl.* 24, 1103-1110.

Zalewski, P.D. and Forbes, I.J. (1993) Intracellular zinc and the regulation of apoptosis. In *Programmed Cell Death: The Cellular and Molecular Biology of Apoptosis*, M. Lavin and D. Watters, Eds., Harwood Academic Publishers, Switzerland, pp. 73-85.

Zeng, J., Heuchel, R., Schaffner, W. and Kagi, J.H.R. (1991) Thionein (apometallothionein) can modulate DNA binding and transcription activation by zinc finger containing factor Sp1. *FEBS Lett.* 279, 310-312.

Zheng, L.M., Zychlinsky, A., Liu, C.C., Ojcius, D.M. and Young, D.M. (1991) Extracellular ATP as a trigger for apoptosis in programmed cell death. *J. Cell Biol.* 1112, 279-288.

Zilliacus, J., Wright, A.P.H., Norinder, U., Gustafsson, J-A. and Carlstedt-Duke, J. (1992a) Determinants for DNA-binding site recognition by the glucocorticoid receptor. *J. Biol. Chem.* 267, 24941-24947.

Zilliacus, J., Dahlman-Wright, K., Carlstedt-Duke, J. and Gustafsson, J-A. (1992b) Zinc coordination scheme for the c-terminal zinc binding site of nuclear hormone receptors. *J. Steroid Biochem. Mol. Biol.* 42, 131-139.

Zubiaga, A.M., Munoz, E. and Huber, B.T. (1992) IL-4 and IL-2 selectively rescue Th cell subsets from glucocorticoid-induced apoptosis. *J. Immunol.* 149, 107-112.

Zychlinsky, A., Zheng, L-M., Liu, C-C. and Young, J.D-E. (1991) Cytolytic lymphocytes induce both apoptosis and necrosis in target cells. *J. Immunol.* 146, 393-400.

Zykowski, L.P. and Munck, A. (1979) Kinetic studies on the mechanism of glucocorticoid inhibition of hexose transport in rat thymocytes. *J. Steroid Biochem.* 10, 573-579.